Durham E-Theses

Plasma treatment of polysulfone gas separation membranes

Hopkins, Janet

PLASMA TREATMENT OF POLYSULFONE

GAS SEPARATION MEMBRANES

Ph. D. Thesis

by

Janet Hopkins

University of Durham

Chemistry Department

1995

For Margy and Georgie

Statement of Copyright

The copyright of this thesis rests with the author. No quotation from it should be published without prior written consent and information derived from it should be acknowledged.

Declaration

The work described in this thesis was carried out in the Chemistry Department at the University of Durham between October 1992 and September 1995. All the work is my own unless stated to the contrary, it has not been submitted previously for a degree at this or any other University.

The author would like to officially register that the AFM images in chapters 2, 5 and 6 were collected by Dr. J. P. S. Badyal. All data have been interpreted in collaboration with Dr. J. P. S. Badyal.

List of Publications

The results from this work have been published or will be submitted for publication as follows:-

1. "Plasma Modification of Polyethersulfone", J. Hopkins and J. P. S. Badyal, ISPC-11, **1993**, *3*, 1174.

2. "Plasma Modification of Polyethersulfone", J. Hopkins and J. P. S. Badyal, *Macromolecules*, **1994**, *27*, 5498.

3. "Plasma Modification of Polysulfone", J. Hopkins and J. P. S. Badyal, submitted for publication.

4. "Non Equilibrium Glow Discharge Fluorination of Polymer Surfaces", J. Hopkins and J. P. S. Badyal, *J. Phys. Chem.*, **1995**, *99*, 4621.

5. "Synergistic Oxidation at the Plasma/Polymer Interface", J. Hopkins and J. P. S. Badyal, submitted for publication.

6. "CF_4 Plasma Treatment of Asymmetric Polysulfone Membranes", J. Hopkins and J. P. S. Badyal, submitted for publication.

7. "CF_4 Glow Discharge Modification of CH_4 Plasma Polymer Layers Deposited onto Polysulfone Gas Separation Membranes", J. Hopkins and J. P. S. Badyal, submitted for publication.

Other Publications

1. "Plasma Assisted Decomposition of Titanium Tetraisopropoxide", P. J. Ratcliffe, J. Hopkins, A. D. Fitzpatrick, C. P. Barker and J. P. S. Badyal, ISPC-11, **1993**, *3*, 1154.

2. "Plasma Assisted Decomposition of Titanium Tetraisopropoxide", P. J. Ratcliffe, J. Hopkins, A. D. Fitzpatrick, C. P. Barker and J. P. S. Badyal, *J. Mater. Chem.*, **1994**, *4*, 1055.

3. "Plasma Fluorination Versus Oxygenation of Polypropylene", J. Hopkins, R. D. Boyd and J. P. S. Badyal, submitted for publication.

Acknowledgements

Abstract

The chemical and topographical nature of a polymer surface can be changed by non-equilibrium glow discharge treatment. Surface modification of polysulfone and polyethersulfone was examined using a variety of plasma treatments at a fixed power, pressure and treatment time. The modification observed was found to be dependent upon the type of feed gas employed.

Tetrafluoromethane plasmas fluorinate polymer surfaces. The influence of polymeric structure on the extent of modification was examined. Phenyl ring containing polymers experienced a greater extent of modification compared to saturated polymers. The extent of modification is dependent upon both the fluorination mechanism and the surface affinity.

Plasmas contain a variety of species accompanied by an electromagnetic spectrum. The role of vacuum ultraviolet radiation in a plasma was investigated as a function of feed gas (argon, krypton, xenon and oxygen) on polyethylene and polystyrene, in an oxygen atmosphere. The xenon vacuum ultraviolet treatment gave rise to the greatest oxidation whilst the O_2 vacuum ultraviolet treatment was found to result in the least oxidation. The activation mechanisms varied with the feed gas chosen for the experiment.

Non-equilibrium glow discharge treatment can alter the transport properties of gases permeating through an asymmetric polysulfone membrane. The selectivity and permeability alter as a function of the treatment. The deposition of a methane plasma polymer onto the surface of the membrane resulted in an increase in the gas flux. Similarly CF_4 plasma treatment also gave rise to an increase in the gas flux. The deposition of a methane plasma polymer followed by a CF_4 plasma treatment resulted in a decrease in gas flux and a small increase in the oxygen/nitrogen selectivity.

CONTENTS

Chapter One

An Introduction to Non-equilibrium Glow Discharges, Gas Separation Membranes and Characterization Techniques

1

Chapter One

An Introduction to Non-equilibrium Glow Discharges, Gas Separation Membranes and Characterization Techniques

1.1 INTRODUCTION

The impetus behind this work was to develop the gas separation properties of a polysulfone membrane for use in the gas industry. Natural gas is obtained from tapping into gas reservoirs beneath the ground at many sites around the world. Unfortunately the gas quality can vary enormously from site to site and it is necessary to treat the gas in order to remove impurities and to produce gas that meets the specified quality standards. Natural gas often has impurities such as CO_2, H_2O and H_2S present along with a proportion of hydrocarbons. If the gas reserve is especially high in hydrocarbons it may be commercially viable to extract them and sell them independently. Moreover, it may be necessary for them to be removed in order to meet quality standards. Gaseous impurities, for example CO_2, need to be removed as it is an acidic gas which can cause corrosion to pipelines.

Natural gas can be purified in a number of ways such as low temperature separation or adsorption processes using silica or liquids (e. g. diethylene glycol). The use of membranes to separate impurities is an alternative technique which offers the advantage of lower capital investment and maintenance costs in the long term. This thesis investigates the use of plasma modification to achieve this goal.

Chapter one summarizes the background knowledge required for the work entailed. It covers how permeation processes are influenced by different factors and the implications this has for the transport of gases through a membrane. This is followed by a brief description of plasmas;

what they are, their uses and the advantages they possess over other techniques used for modification. Finally, chapter one also describes some of the analytical techniques that are used to study modifications achieved through the use of plasmas.

Chapter two is concerned with how polysulfone and structurally related polyethersulfone react when subjected to different gas plasma treatments. Chapters three and four investigate further some of the results found in chapter two, namely the influence of chemical structure on the extent of fluorination and the role of the radiation component in a plasma.

Chapters five and six are concerned with plasma treatment of a membrane in order to improve its gas separation properties. The transport properties of N_2 and O_2 through a plasma treated membrane are examined.

1. 2 PERMEABILITY

1. 2. 1 Background

Permeation is the passage of species through a membrane via the influence of a pressure/concentration gradient. It is dependent on several factors such as diffusion, solubility, concentration, pressure, structure etc and therefore as a result permeation is a complex process. Figure 1 illustrates the process of permeation through a membrane[1]. The two different components in the feed are separated into the retenate, which is rich in one of the species and the permeate which is rich in the other species, by the membrane.

Figure 1: Function of a membrane[1].
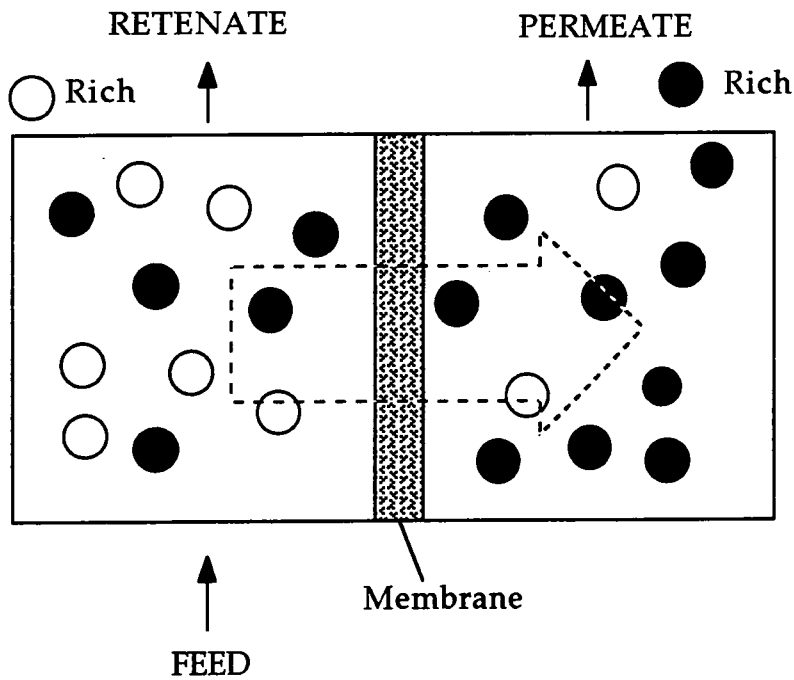
Permeability plays an important role in many areas. One example can be seen in the food and packaging industry where food preservation is dependent upon the barrier properties of the material. Permeation is also important for separation processes, for example in gas separation membranes or in controlled release devices which are used in medicine.

In order to develop efficient gas separation membranes, an extensive knowledge of how parameters such as the sorption gas, temperatures and the structure of the material affect the permeability is required.

Permeability is defined[2-4] by equation 1.

$$P = DS \qquad (1)$$

where P is the permeability, D is the diffusion coefficient and S is the solubility coefficient.

Since permeability is directly dependent on diffusion and solubility, then factors which influence these will influence permeability.

1. 2. 2 Factors Influencing Permeability

The permeation of gas molecules through a non porous membrane is generally regarded as a solution-diffusion process. This separation process is based upon both solubility and mobility factors. Diffusion selectivity favours the passage of the smallest molecule and solubility selectivity favours the passage of the most condensible molecule[5,6].

The diffusion of penetrant through a membrane is a process by which sorbed gas molecules are transported from one part of a polymeric membrane to another as a result of random motions of the molecules[4,7-9]. Diffusion is described by Fick's Law, equation 2[10,11].

$$J = -D \, (dc/dx) \qquad (2)$$

where J is the flux through the membrane, D is the diffusion coefficient and dc/dx is the concentration gradient through the membrane.

The cohesive energy density (CED) describes the forces between polymer chains. The greater the attractive forces between the chains the greater the expenditure of energy required to open a transient gap for the passage of a penetrant. Diffusivity is very sensitive to small changes in the parameters which affect the CED. The free volume of the polymer also affects the diffusion, since a large fractional free volume will enable easy passage of penetrants. A lower fractional free volume will reduce the available free volume required for the size of the penetrant[12]. The following paragraphs summarize how the membrane structure influences the permeability by affecting the solubility and diffusion coefficients.

The penetrant size and shape has a marked effect on the permeability. Small compact penetrants are more mobile than large bulky penetrants and are more likely to find a 'gap' in the polymer through which the molecule

can pass. Linear molecules are more flexible and have greater mobility to pass through the polymer[4,12].

The organisation of the polymer has great implications for the permeability. The packing of the polymer chains and therefore the density of the polymer will either enable or prevent penetrants passing through the membrane, depending on how tightly packed the structure is. The degree of crystallization is important as crystallites act as barriers to the transport of molecules creating a more tortuous path. This results in a decrease in permeability since the diffusion coefficient will be decreased. The amorphous regions are considered to be the transport pathways of the penetrants. Crosslinking has a similar effect as there will be a decrease in free volume through which the molecules can move. This is an especially important point for large molecules, for example N_2 compared to He[9,12].

Orientation of crystalline domains within the polymer will also alter the permeability. If the crystalline domains are parallel to the direction of diffusant then the permeability will be high. If the domains are perpendicular to the direction of diffusion molecules then the permeability will decrease since the domain now acts as a barrier[13-14].

Since diffusion and solubility are both temperature dependent then the permeability will also depend on temperature.

1. 2. 3 Membranes

There are many kinds of membranes which differ both in their structure and their function. Figure 2 illustrates the relationships between the type of membrane process, pore diameter and the penetrant size[9].

Figure 2: Relationship between pore diameter, separation process and penetrant size[9].
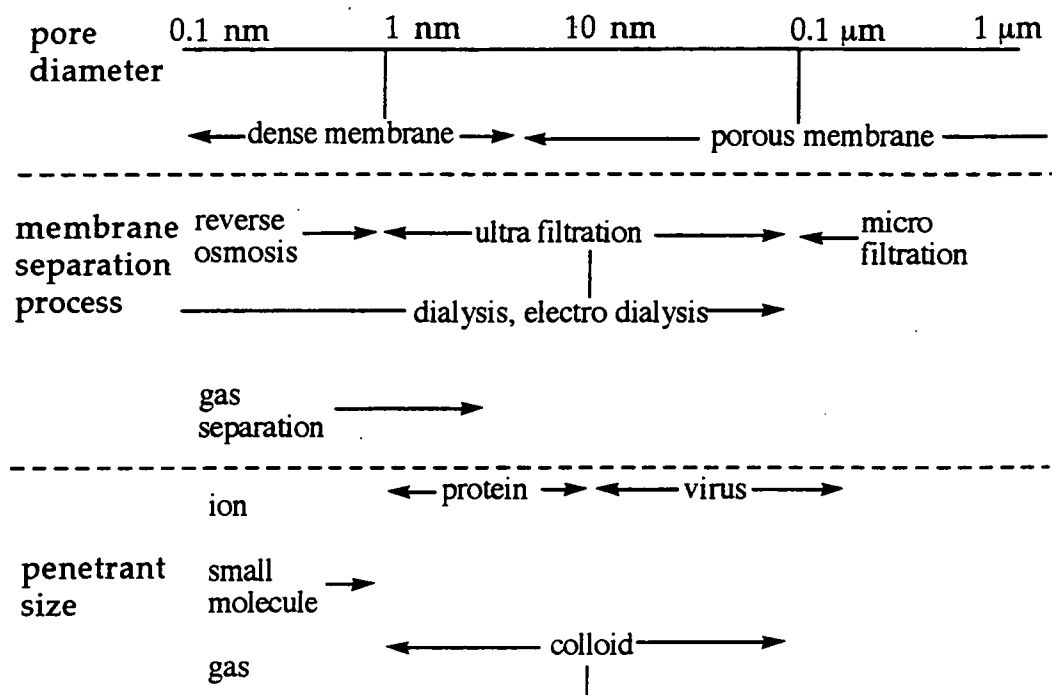
A membrane is a material which constitutes a physical barrier to a solution or gas. The extent to which the diffusing molecules permeate through the material is dependent, among many things, on the structure of the membrane. The permeation of an ideal polymer film (with no microvoids) involves three phenomena:-

1) Adsorption of gas at the film surface.

2) Diffusion of the dissolved gas towards the other surface of the membrane as a result of a pressure or concentration gradient.

3) Detachment from the film surface.

The sorption/desorption processes are rapid compared to diffusion.

Membranes are important for the selective permeation of molecules. The expression for the definition of the selectivity of a membrane is the ratio of the permeability coefficients, equation 3[15].

$$\alpha_{A/B} = P_A / P_B \qquad (3)$$

Where α is the selectivity of A and B, P_A is the permeability coefficient of A and P_B is the permeability coefficient of B.

The selectivity is characteristic of the membrane, which in turn is dependent upon the structure. The production of a membrane has a great influence on the performance of the membrane because the way in which it is formed relates to its' final structure. There are three types of membrane structure to be considered; dense, composite and asymmetric membranes[8,16].

Dense membranes, often referred to as polymeric films, are prepared by dissolution of a polymer substrate in a solvent medium followed by the application of the solution onto a substrate. The solvent then evaporates leaving behind a dense polymer film. The polymer and solvent determine the morphology of the film.

Composite membranes consist of two different materials. They are usually formed by depositing a thin film onto a microporous membrane. The selectivity of such membranes may be determined solely by the thin film.

Asymmetric membranes consist of a dense skin layer supported by a sponge-like matrix[1,6]. The porous underlayer and the thin dense skin are composed of the same material. Asymmetric membranes are formed by a phase inversion process which involves casting a polymer solution onto a substrate and immersing in non-solvent. Exchange between the solvent and non solvent occurs forming the membrane. The dense skin layer is a result of the faster exchange process at the surface where it is directly in contact with the non-solvent. There are many variables such as concentration of solution, choice of solvent, temperature, evaporation time and so on[17,18]. As a result it is difficult to achieve good membranes,

However asymmetric membranes have the advantage of good productivity, i.e high flux.

The criteria of a membrane are that it has high selectivity, high permeability and a long lifetime. For a membrane to have high selectivity it requires a material which is inflexible (so as to behave in a sieve-like manner), crystalline and highly crosslinked. High permeability requires a material which is amorphous with no crosslinking so that there are many available pathways for the penetrant to diffuse through. It can therefore be seen that there is a play off between permeability and selectivity and this has been a point of much research.

This aim of this thesis is to modify a polysulfone membrane so as to enhance the gas separation properties. There has been extensive research to find the "ideal membrane", that is one possessing both high selectivity and high permeability using a variety of methods. These methods broadly cover the search for new and better membrane materials[19-21] refining the preparation of a membrane[22,23] and the modification of existing membranes. Since polysulfone already possesses reasonable gas separation properties, modification of the polysulfone membrane itself may lead to an overall improvement in its gas transport properties. Modification of a membrane can be achieved in many ways such as chemical grafting of functionalities[24], irradiation with ion beams[25] and photooxidation[26]. In this thesis the method chosen to modify the polysulfone was by plasma treatment. Section 1. 3 briefly describes what plasmas are, their uses and some of the fundamental reactions that occur within plasmas.

1. 3 PLASMAS

A plasma[27] is a partially ionized gas consisting of many species such as ions, electrons and neutral species[28]. Plasmas are often referred to as the fourth state of matter. Figure 3 illustrates this idea. In the diagram the

temperature corresponds to the heavier particles only since the energy of the electrons is much higher in a non-equilibrium plasma. This will be explained in a subsequent section.

Figure 3: The states of matter[29].
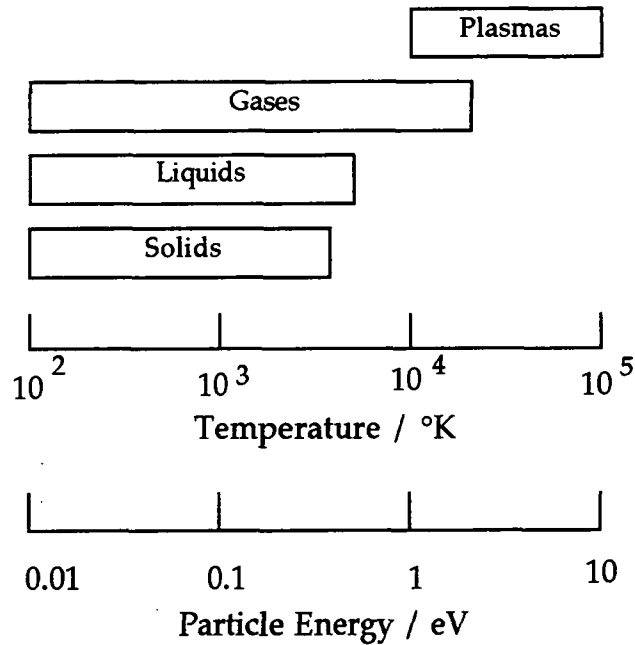
In order for a plasma to exist, the number of positive and negative charge carriers must be approximately equal, since this means that as a whole the plasma retains electrical neutrality. This criterion is satisfied when the dimensions of the discharged gas volume are much greater than the Debye length, equation 4 [29,30].

$$\lambda_D = (\varepsilon_0 k T_e / n e^2)^{1/2} \qquad (4)$$

where λ_D is the Debye length, ε_0 is the permittivity of free space, k is the Boltzmann constant, T_e is the electron temperature and n is the electron density. λ_D defines the distance over which a charge imbalance can exist, in other words although the plasma as a whole remains neutral, there will be perturbations (e. g point charges) over distances λ_D.

10

1. 3. 1 Types of Plasmas

There are two main types of plasma which can be considered, equilibrium and non-equilibrium.

1. 3. 1. 1 *Equilibrium Plasma*

In equilibrium or "hot" plasmas the electron and gas temperatures are approximately equal resulting in a high gas temperature[27]. Therefore equilibrium plasmas are unsuitable for treating polymers since processing would lead to degradation. Examples of equilibrium plasmas are arc and plasma torches which are, amongst other applications, used for melting, refining and other metallurgical applications[31]. Thermal plasmas are also used to produce controlled nuclear fusion[29].

1. 3. 1. 2 *Non-equilibrium Plasmas*

"Cold" or non-equilibrium plasmas are characterized by a low gas temperature and a high electron temperature. There are several different types of non-equilibrium discharges. They are described as[27,32,33]:-

1. 3. 1. 2. 1 *Silent Discharge*

This type of discharge is easily produced and can operate at pressures up to 1 atmosphere. High power dissipation can be achieved at lower voltages. The main disadvantage of a silent discharge is that the apparatus requires a small gap between the electrodes of large surface area. This often causes problems when dealing with organic reactants since the reactants can bridge the gap or accumulate on the walls of the reactor.

1. 3. 1. 2. 2 *Radio-frequency Discharge*

In radio-frequency discharges(>1MHz) there is no direct contact between the electrodes and the energy is fed into the plasma indirectly via capacitive or inductive coupling. Relatively homogeneous plasmas can be generated as the electric field wavelength is much larger than the vessel dimensions. Radio-frequency discharges work well at low pressures and are therefore a popular type of discharge used in the laboratory.

1. 3. 1. 2. 3 *Corona Discharge*

Corona discharges require extremely high pressures for production. At high pressures the discharge becomes unstable and is transformed into a high current arc discharge. However the discharge can be stabilised by the use of different sized electrodes e.g. a pointed electrode and a plane electrode. The volume of reactive species produced by the apparatus is very small and are therefore unsuitable for industrial applications since large quantities of active species is difficult.

1. 3. 2 Origin of a Glow Discharge

A small amount of free electrons is always present in a gas due to naturally occurring radioactivity or cosmic rays. If a voltage is applied to a gas then the available free electrons are accelerated by the electric field[29,30,34].

Initially the electrons will have insufficient energy to cause ionization or excitation because their collisions are elastic and transfer of energy between electrons and ions or neutrals is very small. As the electron continues to gain energy between collisions it causes ionization of the gas through inelastic collisions. Such collisions result in a large transfer of

energy between the electrons and the larger species within the plasma. Steady state is achieved when the rate of formation of ions is in equilibrium with the rate of recombination with electrons. The discharge is then self sustaining[29,34,35].

At a critical voltage there is an abrupt increase in current. This is known as the electric breakdown of the gas and occurs when the rate of ionization is sufficient to balance the loss of electrons by various processes. The breakdown of the gas depends on the parameters of the particular system e.g. gas pressure, and is determined experimentally. Paschen's law relates the breakdown velocity to the gas pressure and the distance between electrodes[29,30]. Equation 5 expresses the condition required for electric breakdown.

$$v_i = \lambda_D / \Lambda^2 \qquad (5)$$

v_i is the electron velocity, λ_D is the Debye length and Λ is the discharge gas volume.

The electron temperature[30,36] in a non-equilibrium plasma is much greater than the ion temperature. Typical values are $T_e \approx 3\text{-}30$ eV and $T_i \approx 0.5$ eV. Both of these values correspond to the bulk plasma. The difference in the temperatures is a consequence of the difference in mass of the two species, since electrons are much lighter than ions and therefore can attain more kinetic energy from the applied electric field, equation 6.

$$\text{Work done by field} = Eex = (Eet)^2 / 2m \qquad (6)$$

where E is the applied electric field, x is the distance travelled, t is the time, e is the elctronic charge and m is the mass of the particle being considered (electron or ion).

The characteristic "glow" of a non-equilibrium plasma corresponds to the relaxation of excited species to lower energy levels. This light spectrum contains components ranging from the infra-red to the ultraviolet regions. Once ionization of the gas has been achieved, a variety of reactive species are generated e.g. positive and negative ions, neutral species and radicals. There are many reactions which may occur between these species, which are discussed in section 1. 3. 4.

1. 3. 3 Basic Concepts of a Plasma

There are several terms which are used to describe the conditions within a plasma.

1. 3. 3. 1 Electron Energy Distribution Function (EEDF)

The electron velocity[27] distribution plays an important role in determining the physical properties of a plasma as it determines the electron energy distribution, average electron energy as well as the electron transport properties and reactions.

Electron energy[33] within a plasma is determined by the total field the electron is subjected to and their interactions with other particles. The Maxwell distribution describes the energy distribution of the electrons. Figure 4 demonstrates a typical distribution.

Figure 4: Maxwell energy distribution[27].
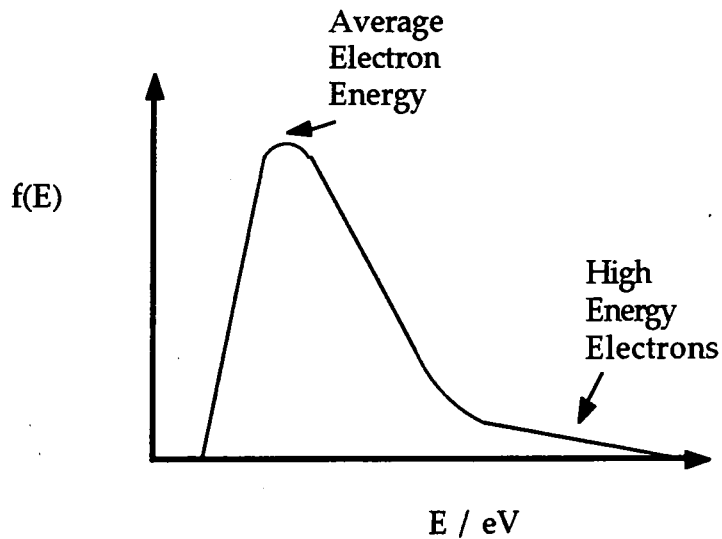
Note the existence of electrons with much higher energies (high energy tail) than the average electron energy. It is these electrons which are responsible for sustaining the plasma. The Maxwell distribution assumes that Te = Tg, which is not the situation within a non-equilibrium plasma. A better distribution of electron energies can be described using the Druyvesteyn distribution, although this is still only an approximation to the situation within a plasma. Similarly to the Maxwellian distribution, the Druyvesteyn distribution possesses a high energy tail, but the Druyvesteyn distribution predicts a larger number of high energy electrons.

1. 3. 3. 2 *Plasma Potential*

It has been found that the potential of a plasma is usually at least several volts more positive than the most positive surface in contact with the plasma[30,37]. This is because electrons usually have a higher mobility in plasmas than ions and will therefore reach the limits of the plasma much more quickly. If this process were sustained then the net result would be an increase in the positive charge since the electrons will leave the plasma at a

quicker rate than the ions. As the net charge increases, then it becomes energetically less favourable for the electrons to escape. However a steady state will be arrived at eventually if the plasma potential is high enough so that the rate loss of electrons is equal to the rate loss of ions. This is how a plasma retains its neutrality.

1. 3. 3. 3 *Floating Potential*

An electrically floating surface when placed in contact with a plasma becomes negatively charged as a consequence of the greater flux of electrons compared to ions[29,30,37]. The surface at a particular point becomes sufficiently negative to cause electrons to be repelled. When this occurs there is an equal flux of ions and electrons and the potential on the surface is said to have reached "floating potential".

1. 3. 3. 4 *Plasma Sheath*

There is a variation of electron density in a plasma where the edge of the plasma is in contact with a surface which is significantly different from the bulk plasma region. This region, known as the plasma sheath[37,38], has a much lower voltage accounting for the low electron density present there. Since the plasma has a uniform potential then most of the variation/drop in potential occurs at the sheath.

The plasma sheath is observable as a dark space adjacent to all surfaces in contact with the plasma. The darkness is the result of the low electron density in that region which leads to less excitation.

1. 3. 4 Chemistry of Non-equilibrium Discharges

Once a discharge has been ignited, there are numerous reactions which can occur between the species[39]. Complications arise because not only are there several distinct types of reaction but they can occur simultaneously[40]. Typical reactions are ion-molecule recombination, electron attachment, electron-ion recombination and ion-ion recombination[33]. As a result new species are generated which can also contribute to reactions within a plasma. There may be sufficient energy for excitation of atoms and molecules to higher energy levels and metastable states. The metastable can then transfer energy via a collision and result in ionization or dissociative ionization events. The schematic diagram, figure 5, shows some of the reactions taking place within a plasma.

Figure 5: Possible reactions within a plasma[27,33].
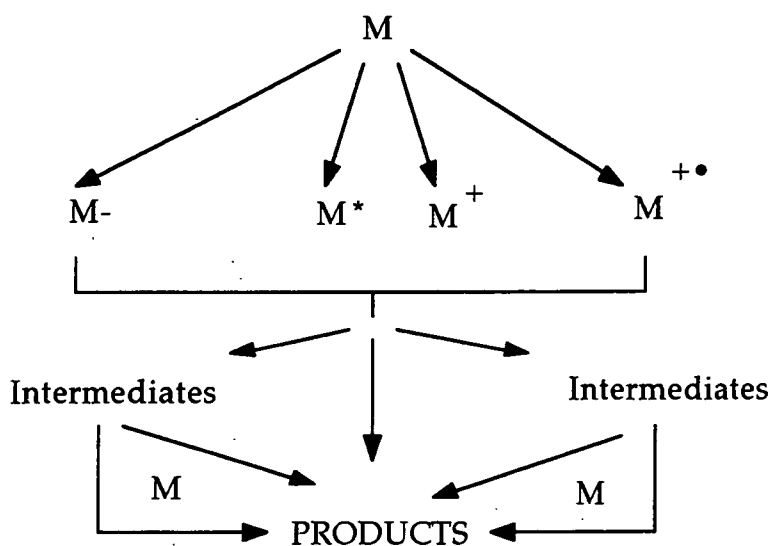
The existence of the many different species within the plasma together with a broad electromagnetic spectrum results in many different reactions occurring at a sample surface inside the plasma. Impacts from

neutrals, electrons, ions and photons result in numerous physical and chemical processes, figure 6 [28,29,41].

Figure 6: Interaction of species in a plasma with a surface[29].

Negative Ions

Positive Ions

Radicals

Electrons

Atoms

PLASMA

Photons

Metastables

Plasma Sheath

Solid
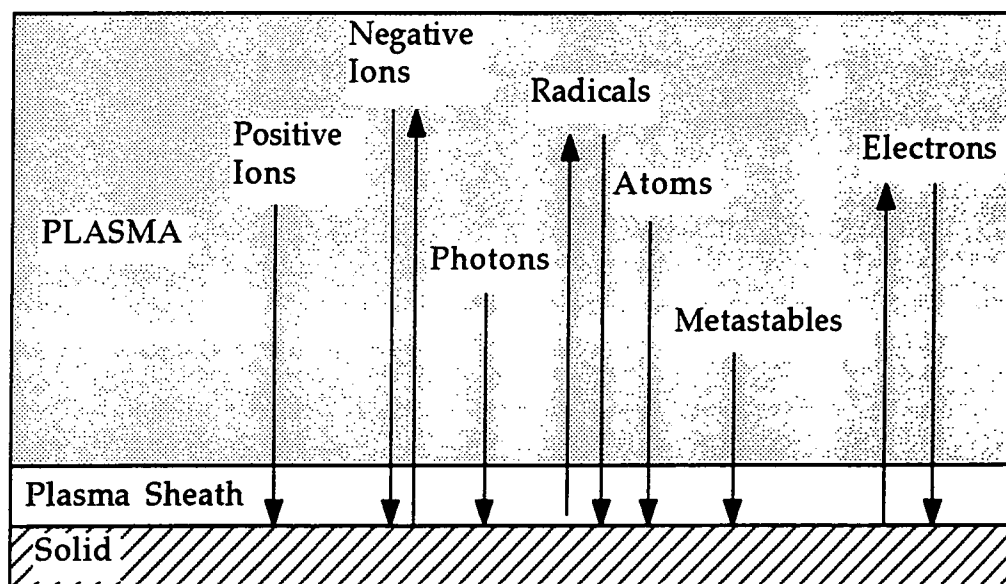
On impact with a surface, neutral particles transmit only small amounts of energy, resulting in the heating of the surface. If additional activation occurs, chemical reactions can occur, radicals can recombine and also react chemically by combining with radical sites. Electron impact can lead to desorption and/or dissociation of absorbed molecules. Due to the existence of the plasma sheath, positive ions are accelerated and gain energy which can lie in the region 10 - 500 eV depending on the plasma conditions. On impact this energy is released to the solid body. The UV radiation in a plasma can also impart energy to a surface. The actual energy will depend upon the type of plasma, however typical energies can be up to several eV. These photons have sufficient energy to produce radical sites on the surface, induce crosslinking and break chemical bonds. The depth of penetration of the radiation is greater than that found for other direct energy transfer processes[29,34,42,43].

1. 3. 5 The effect of Plasmas on Polymers

The use of plasmas to modify surfaces over recent years has become of great interest because of the technique's many advantages over the more conventional processes. One advantage of particular interest in industry is that the desirable properties of treated materials can be achieved in seconds rather than minutes or hours e.g. thermal pyrolysis used to obtain changes in wettability[27]. Not only does plasma surface modification increase efficiency, but it is often the only technique whereby a particular reactive pathway can be achieved.

Modification of a sample after plasma treatment can be observed experimentally via changes in the wettability, adhesion and chemical composition using techniques such as contact angle measurements, XPS and ATR-FTIR.

Plasma treatment modifies the surface to a layer of 50 Å - 10 μm[44] in depth. Since only the surface is modified, the bulk properties remain unchanged. This has obvious implications in industry as the surface of a material can be improved for a particular purpose whilst leaving the bulk properties e.g. strength unchanged.

The types of modification which a plasma can induce on a material can be split into three main groups[45]:-

1) Etching

2) Modification

3) Plasma polymerization

1. 3. 5. 1 *Etching*

Plasma etching is used extensively in the semiconductor industry. With the growing technological advances in the field, it has become

necessary for higher density of pattern transfer to be achieved[46,47]. Wet chemical etching is unable to produce the dimensional control needed for the minimum feature dimensions (<few μm)[28,47]. The use of plasmas for etching has the advantage of producing highly anisotropic etch features with less waste products. Figure 7 illustrates the difference between isotropic (no etch direction) and anisotropic (defined etch direction) etching.

Figure 7: Isotropic and anisotropic etching[36].
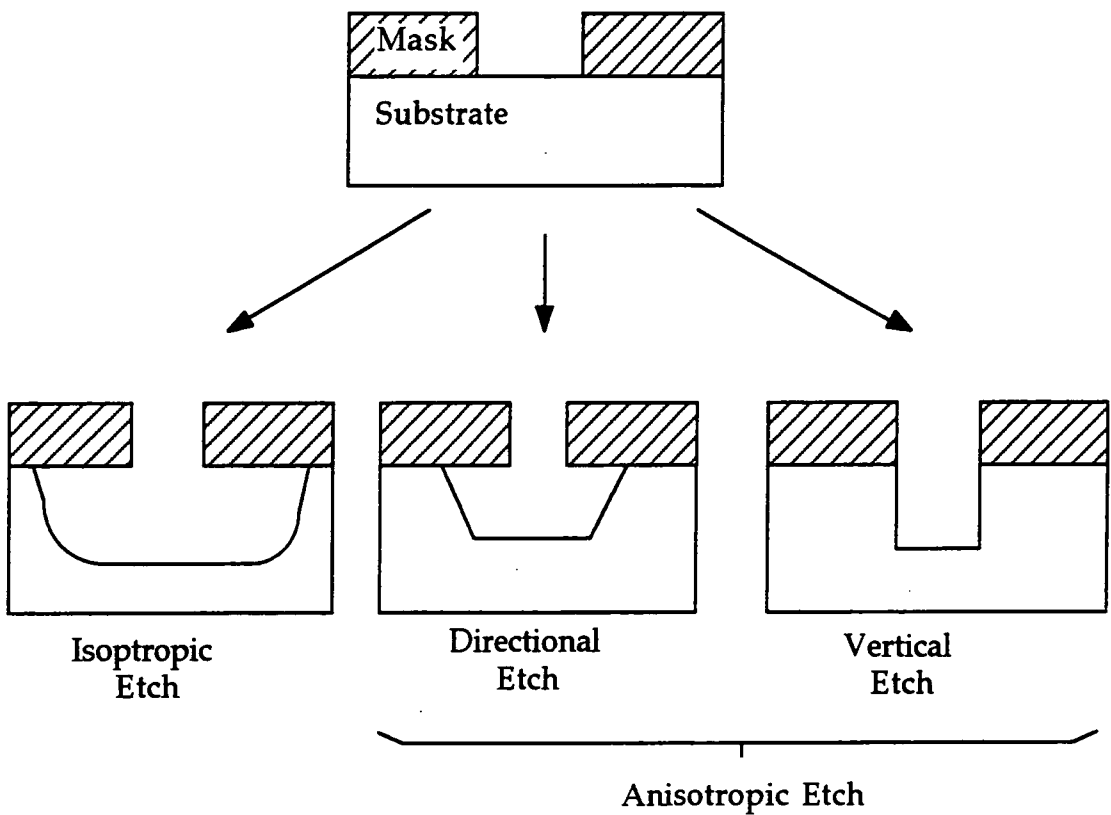
1. 3. 5. 2 *Modification*

Plasma treatment of a polymer can give rise to numerous surface modifications, such as incorporation of new groups, changes in wettability and adhesion and crosslinking.

1. 3. 5. 2. 1 *Molecular Weight Changes*

Plasma treatment of a polymer can result in molecular weight changes, the extent of which is dependent upon the plasma used[27]. Noble gases, N_2 and H_2 gas plasmas are more likely to result in crosslinking whilst oxygen containing plasmas more often than not favour chain scission. However molecular weight changes are also dependent upon the polymer[48].

It is thought that since noble gas plasmas[1] lead to crosslinking, then the explanation behind such behaviour is the presence of excited metastables transferring energy from the plasma to the polymer. This behaviour is called CASING (cross-linking by activated species of inert gases)[27]. The mechanism of energy transfer is shown in equation 7.

$$----------> RH^* + M \qquad (7a)$$
$$R\text{-}H + M^* ----------> R\bullet + H\bullet + M \qquad (7b)$$
$$----------> R1\bullet + R2\bullet + M \qquad (7c)$$

O_2 plasmas generally lead to a decrease in molecular weight at the surface probably as a result of chain scission. In oxygen atom reactions[49], abstraction does not lead to bond weakening in saturated or unsaturated molecules. It is only the addition of oxygen to an unsaturated molecule to form a saturated radical which results in a weakened C-C bond. Subsequent attack of the radical site results in bond breaking or chain scission and the production of low molecular weight volatile fragments. Obviously the susceptibility of attack of the polymer is dependent upon the polymer structure[50] e. g. the presence of polar functional groups and metallic atoms. One particular example of this is oxygen plasma treatment of polypropylene which leads to chain scission, whereas oxygen plasma treatment of polyethylene leads to crosslinking as a consequence of hydrogen abstraction[50].

Oxygen plasmas etch the surface of polymers, but the addition of another gas e. g. CF_4 can alter the etching rate. An optimum in fluorine atoms will yield a maximum in etching rate[51] but an excess of fluorine atoms will result in fluorination and inhibit etching through competition with oxygen atoms[52]. The critical parameter in determining whether etching , polymerization or fluorination occurs is the C/CF_x ratio[53].

Plasma treatment at higher powers leads to ablation. For a chemical group to be implanted, the particle responsible must possess a certain minimal amount of energy[54]. Below this level, there will be insufficient energy to trigger a specific reaction. However above a certain power level, there is an increase in the kinetic energy of the particle and therefore there will be an increase in the rate of surface bombardment. Newly grafted structures will have a greater probability of being pulled away from the surface and therefore less chance of being incorporated into the surface structure.

1. 3. 5. 2. 2 *Wettability*

Wettability is the extent to which a liquid spreads on the surface of a solid[55]. It is often measured using contact angles.

It has been reported that the effect of oxygen plasma treatment on various polymers generally increases the wettability[56,57]. It is thought that the improvement in wettability on a polymer's surface is brought about by the formation of C=O, OH, -COOH groups. Using depth profiling techniques, it has been found that the percentage of alcohol and ether species increase, suggesting the carbonyl and carboxyl groups are concentrated within the first monolayer of material[58,59]. In the case of polypropylene most of the oxygen introduced is in the form of hydroxyl groups which is shown by XPS. The bulk polymer essentially remains unaffected by plasma treatment.

22

Contact angle measurements carried out on aged plasma treated polymers have shown that there is a decay in wettability, or "hydrophobic recovery"[60,61]. This is thought to be a consequence of the evolution of a high free energy system towards a thermodynamically stable state, rather than a result of contaminant adsorption. The extent of hydrophobic recovery is dependent upon the amount of crosslinking in the polymer. For example it was found that in polyethylene[61], hydrophobic recovery was far less effective than in polypropylene. Results from XPS show that the the surface composition is unaffected by ageing therefore eliminating diffusion of untreated bulk polymer as a cause for hydrophobic recovery[61]. The explanation of such results suggests the motion of macromolecules within the plasma modified layer in order to minimize the number of polar groups at the surface. However many polymers do age after plasma treatment[62] and the hydrophobic recovery is dependent upon the substrate and the temperature. The segmental and macromolecular motions intervene with the hydrophobic recovery[63-65].

1. 3. 5. 2. 3 *Adhesion*

The adhesion of two materials is dependent upon the intermolecular attractions between the phases[58]. In order to obtain maximum joint strength, the adhesive of a given surface must possess optimum polarity (so as to maximize wetting). This is obtained when the polarities of the adhesive and substrate are exactly equal.

In the literature, it has been recorded that plasma treatment improves adhesion[66]. It is likely that the reason for the improvement in the adhesive properties is possibly due to:-

a) electrostatic interactions

b) elimination of weak boundary layers by ablation

c) cross linking

d) mechanical interlocking as a result of increase in surface roughness

e) chemical changes

It is unlikely that the formation of a weak boundary layer results in the improvement of adhesion as sufficient cleaning of the sample will remove any such layer. It is known that plasma treatment often crosslinks polymers and this may possibly be an important factor in improving the cohesive strength.

There are a number of mechanisms suggested for the increase of adhesion in treated materials which involve macromolecular motions[58]. In most cases reorganisation appears to be the more important mechanism. However, at high temperatures, polystyrene favours the diffusion model. In both mechanisms, the driving force is the minimization of surface tension and the optimization of intramolecular interactions.

1. 3. 5. 2. 4 *Incorporation of New Species*

It has been found that plasma treatment of a material leads to the incorporation of new species into the surface[67]. The mechanism involves free radical formation followed by the reaction of activated species in the plasma gas. Each type of plasma will react uniquely with the polymer[54]. An example of this is that O_2 plasma treatment of polyethylene results in the formation of carbonyl and carboxyl groups, however in a N_2 plasma, nitrogen complexes are formed resulting in the release of hydrogen cyanide, cyanogen etc. It is interesting to note that gas mixture plasmas behave as though each component acts as if it were occupying the chamber alone.

The degree of incorporation of new functionalities on the surface is dependent upon polymer structure[68]. The concentration of fluorine atoms in CF_4 plasmas is high and grafting of CF groups often occurs[69,70]. Surface fluorination can also be thought of as a substitution reaction of hydrogen in the polymer structure[71].

The addition of new functional groups on the surface can be monitored by surface sensitive techniques as it is only the extreme monolayers of the polymer which are affected. Changes of the surface composition are often carried out by varying the plasma parameters e. g. pressure, power, temperature and by monitoring particular peaks of a spectrum. This enables a more comprehensive idea of the reaction mechanism to be obtained.

1. 3. 5. 3 *Plasma Polymerization*

Plasma polymerization[72-74] is a process whereby high molecular weight products can be formed by passing an organic vapour through a plasma produced in a low pressure discharge. This process is applicable to a wide range of starting materials including those not normally considered to be monomers for conventional polymerisation. Plasma polymerization produces an irregular network-like material which is amorphous and highly cross-linked[75]. The material has high thermal stability, high melting point and low solubility. The stoichiometric composition of the plasma deposited film differs from that of the of the initial monomer[76-78].

The process of plasma polymerization is complex, involving a large number of both homogeneous and heterogeneous reactions. Although the overall polymer deposition mechanism is not understood, results from experiments suggest that free radicals are the primary species propagating chain growth in the gas phase and on the surface of the deposited polymer. These species are formed by collisions in the gas phase. The growth of the polymer film occurs by the reaction of surface-free radicals with either gas phase free radicals or unsaturated monomer, figure 8.

Figure 8: Bicyclic step growth mechanism of plasma polymerization[74].
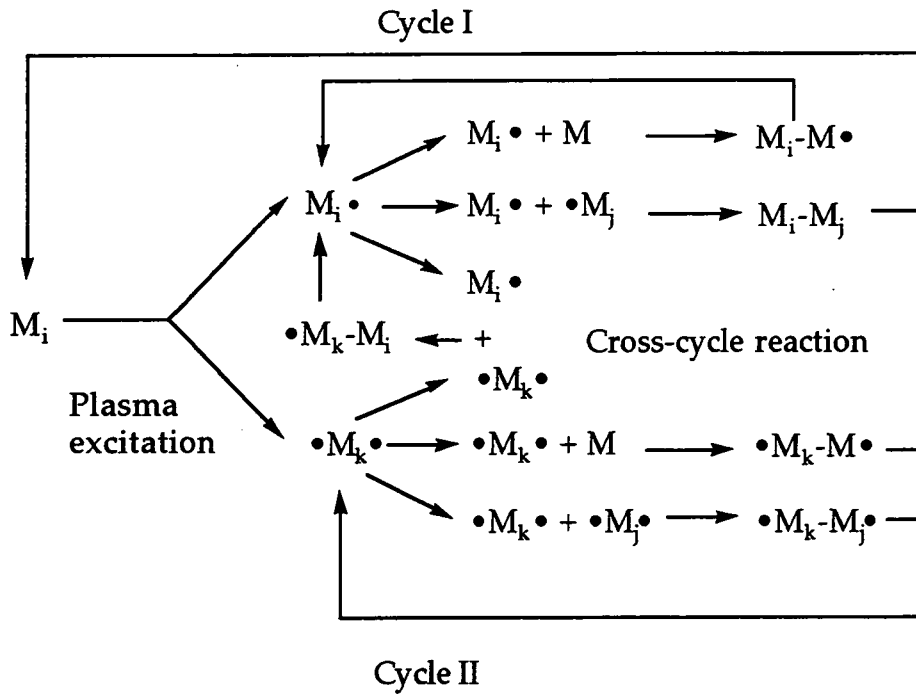
Cycle I

Figure 8 shows two major routes of step growth polymerization. Cycle I represents a repeated activation of the reaction products from monofunctional activated species. Cycle II represents pathways via difunctional/multifunctional activated species. Both cycles play a role[74] in plasma polymerization.

1. 3. 5. 3. 1 *Plasma Enhanced Chemical Vapour Deposition (PECVD)*

In conventional chemical vapour deposition, the substance to be deposited is vaporized and the vapour is decomposed or reacted with other gases on the substrate[47]. The film growth is determined by the slowest process. One of the major disadvantages of thermal CVD is the high temperature of the substrate required. The high temperature is often prohibitive in the growth of films, however in PECVD[79,80] the gas is excited to form reactive species which can adsorb to the substrate and undergo deposition to form thin films at lower substrate temperatures[81]. The use of

RF discharges causes partial ionisation of the gas producing ions and electrons whilst the temperature of the gas remains near room temperature. PECVD is advantageous as complex shaped parts can be treated as the gas penetrates into the smallest and most irregular areas.

1. 3. 6 Summary

Plasma treatment of a material leads to a variety of chemical and structural changes, altering the physical properties of the material. The use of plasmas enables the processing of materials in a most efficient way, possibly reducing the treatment time to minutes compared to other more conventional techniques. Only the first few monolayers of material are modified whilst leaving the bulk properties of the material unchanged, which therefore enables the possible uses of a particular material to be further increased.

1.4 ANALYTICAL TECHNIQUES

1. 4. 1 Photoelectron Spectroscopy

The surface sensitivity of any experimental technique is dependent on the probing depth of the technique used. In photoelectron methods[82], the surface sensitivity is not dependent upon the penetration depth of the incident radiation but upon the probability of an electron escaping without further loss of energy. The escape depth of an electron, figure 9, is dependent upon losses in energy due to phonons (lattice vibrations) and electron-electron excitations, so the mean free path of an electron before any inelastic scattering will vary with its kinetic energy[83]. That is, at very low energies there is insufficient energy for the excitation of the losses mentioned above so the mean free path will be long, butat very high

energies the mean free path is long because the probability for excitation decreases with increase of the kinetic energy. The mean free path passes through a minimum which is approximately 3 nm. Photoelectron spectroscopy is therefore a surface sensitive technique because it detects ejected electrons which have sufficient energy to escape from the first few monolayers of the sample.

Figure 9: The dependence of attenuation length, λ (in monolayers), on the emitted electron energy[84].
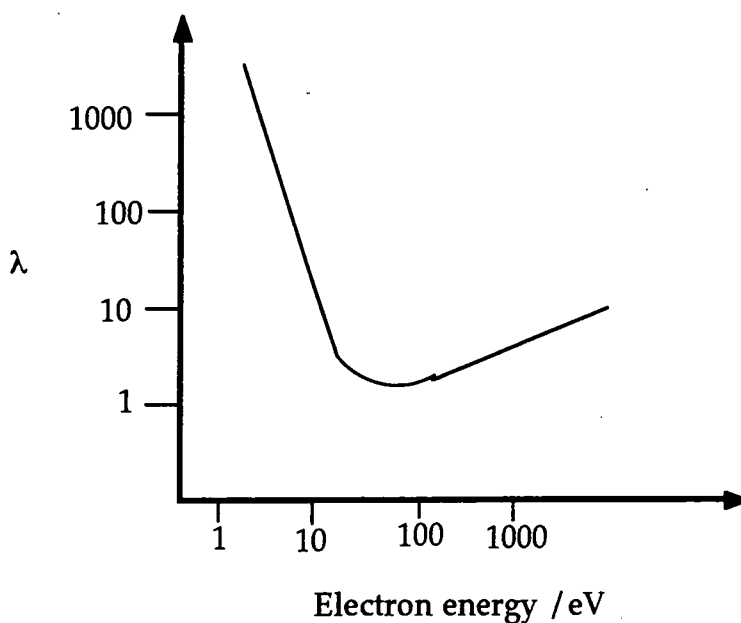
Photoelectron spectroscopy involves the ejection of electrons from atoms or molecules when they are bombarded with photons[84,85]. This can be related to the photoelectric effect i.e. electrons are ejected from the surface of an alkali metal at frequencies greater than the threshold frequency. As the frequency increases, the kinetic energy of the ejected electrons or photoelectrons increases linearly with frequency.

At the threshold frequency, the energy of the photon is sufficient to overcome the workfunction of the metal (∅ is the energy required to ionize electrons from the bulk to the vacuum level). At higher frequencies the

excess energy of the photons is converted into the kinetic energy of the emitted electrons (photoelectrons). From the conservation of energy, equation 8.

$$h\upsilon = \emptyset + 1/2m_e v^2 \qquad (8)$$

Where m_e is the mass of electron, v is the electron velocity, $h\upsilon$ is the photon energy and $\emptyset$ is the work function.

Photoelectron spectroscopy is a simple extension of the photoelectric effect. Since the energy of the photons bombarding the specimen is known and the kinetic energy of the electrons emitted are measured, then the binding energy of the specimen can be calculated, equation (9).

$$BE = h\upsilon - KE \qquad (9)$$

where BE is the binding energy of the core electron, $h\upsilon$ is the X-ray photon and KE is the kinetic energy of the emitted photoelectron. Photoionization of a core electron is shown in figure 10a[86].

The removal of a core electron in the photoionization process leaves a "vacancy". The filling of this vacancy by an electron from a higher energy shell can result in two different processes, x-ray fluorescence and the emission of an Auger electron, fig 10 b and c. X-ray fluorescence results in the emission of of an X-ray photon whereas the Auger process uses any excess energy from the relaxation process in the emission of an electron, an Auger electron. The energy of the Auger electron is dependent upon both the valence and core energy levels and Auger Electron Spectroscopy (AES) uses this to determine information about the energy levels of the sample. The emission of Auger electrons can complicate the XP spectrum, however, photoelectrons and Auger electrons can be distinguished by using a different ionization source. The KE of the photoelectrons will change (equation 9)

29

whilst the Auger electrons will remain unchanged simply because the energy of the Auger electron emitted is independent of the source and depends upon the energy levels of the process[86,87].

Figure 10: A schematic diagram of the photoionization process, x-ray fluorescence and Auger process[86].

a) Photoionization   b) X-ray fluorescence   c) Auger Process
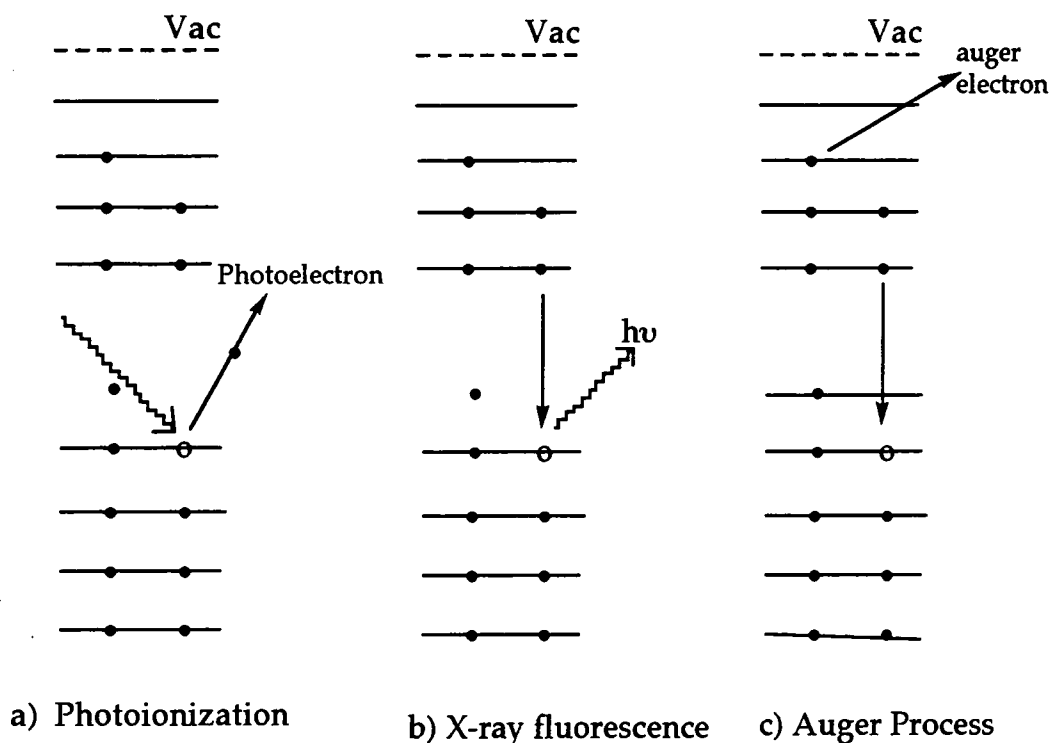
In XPS, the monochromatic source of photons is soft or low energy x-rays, which have sufficient energy to ionize electrons from core levels. By using the technique a variety of information can be obtained[84,88,89]:-

a) Absolute binding energies, which indicate the species present since the core levels are unique to a particular element and therefore elemental composition.

b) The ability to distinguish different oxidation states since the binding energy shifts upon change in valency.

c) To detect changes in the chemical environment.

1. 4. 1. 1 *Complications in Spectral Interpretation*

1. 4. 1. 1. 1 *X-ray Satellites*

X-rays are emitted when a beam of electrons produced by thermionic emission strikes a surface. The X-ray spectrum produced may be considered in two parts i.e. continuous radiation and the characteristic radiation, figure 11. The continuous spectrum has a well defined minimum wavelength corresponding to an electron losing all its energy in a single collision. The longer wavelengths correspond to electrons undergoing several collisions and deflections and therefore losing energy gradually. All or some of the kinetic energy of the electron is converted into the energy of the photon. This radiation is known as Bremsstrahlung radiation[82,84,87].

Figure 11: X-ray spectrum[82].
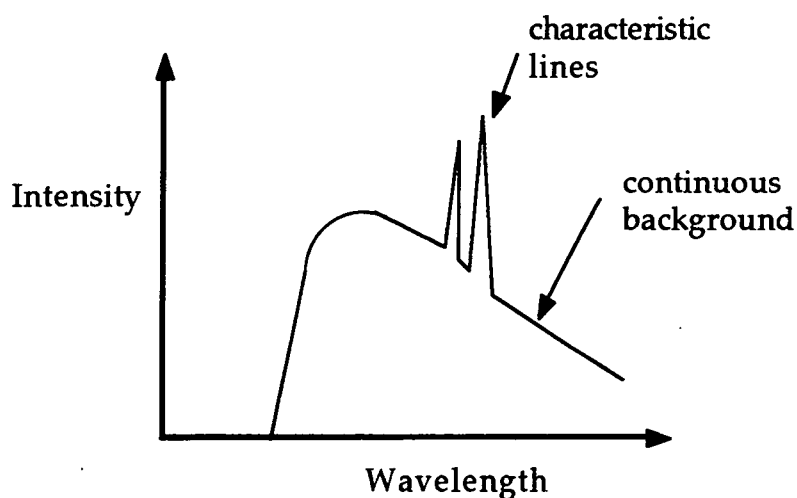
The sharp peaks or characteristic lines in the spectrum are due to one of the bombarding electrons in the beam knocking out one of the lightly bound electrons from the target element, leaving a vacancy in one of the lower energy levels. A transition of the electron from higher to lower energy level occurs resulting in the emission of a quantum of radiation.

Transitions are described by the particular energy levels concerned. A transition which ends at the K shell in the target atom is the K line and is classified in terms of the higher energy level e.g. L to K is a K_α line. K_α lines are generally more intense than K_β lines (M to K transition) and are usually selected for isolation when monochromatic X-ray radiation is required.

In most laboratory spectrometers, the x-ray sources are not usually monochromatic. Not only is Bremsstrahlung radiation (broad continuous distribution) produced upon which is superimposed the characteristic lines of the target material (anode), but a series of small intensity lines are also present, known as x-ray satellites. These satellites arise from less probable transitions (e.g. K_β) or transitions in a multiply ionized atom and are present as less intense peaks at known binding energy and FWHM.

1. 4. 1. 1. 2 *X-ray Ghosts*

These are due to excitations arising from impurity elements in an x-ray source, e. g. an Al $K_{\alpha1,2}$ ghost from a Mg K_α source[84,87]. The ghost is a consequence of the secondary electrons produced inside the source hitting the thin Al window which is present to prevent the secondary electrons hitting the sample. Dual x-ray sources are often used in spectrometers in order to differentiate between auger lines and peaks from XPS since auger electrons are independent of x-ray energy. Unfortunately if there is cross-talk between the filaments and anodes this can lead to ghost satellites.

1. 4. 1. 1. 3 *Multiplet Splitting*

This is important in systems with unpaired electrons in the valence levels e. g. transition metals. It is the exchange interaction which can occur between unpaired electrons which results in a lower energy than the anti parallel spin which is responsible for the phenomenon. Multiplet splitting[87] causes broadening in peaks and leads to a variation in the separation of the peak maxima.

1. 4. 1. 1. 4 *Shake-up Satellites*

Upon loss of a core electron by photoemission, the valence electrons associated have an apparent increase in nuclear charge. This results in a reorganisation of the valence electrons known as "relaxation"[84,87]. Relaxation may involve the excitation of a valence electron to a higher unfilled level which is referred to as shake-up . This gives rise to shake-up satellites on the low BE side of the photo-electron peaks.

In the C(1s) spectrum, shake-up satellites can give information about the unsaturated chemical bonds. In conjugated systems and in particular aromatics, the shake-up satellite can be 5-10 % of the main peak. In aromatic systems, the shake-up peak corresponds to a π-π^* transition, that is, a transition between the two highest filled orbitals and lowest unfilled orbitals. Monitoring of the peak in such cases can give an indication of the degree of aromaticity before and after modification of a surface.

Figure 12: Shake-up and shake-off processes[87].
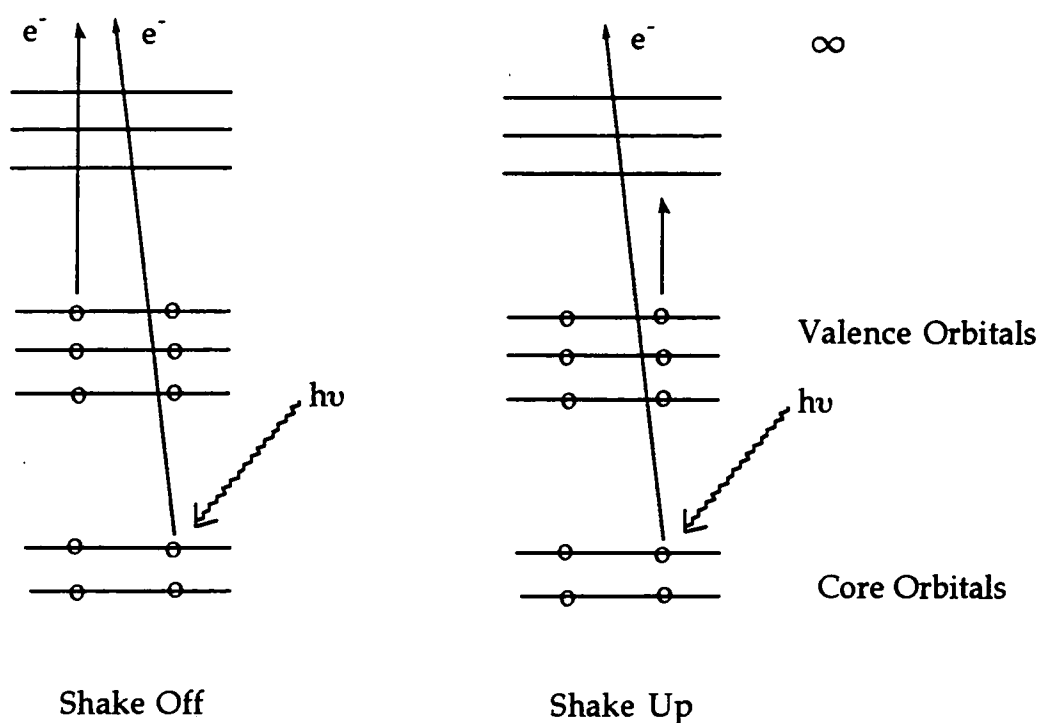
Shake Off   Shake Up

1. 4. 1. 1. 5 *Shake-off Satellites*

"Shake-off" is a process whereby a valence electron is completely ionized leaving an ion with vacancies in both core and valence levels. A diagram of the shake-up and shake-off processes is displayed in figure 12.

1. 4. 1. 1. 6 *Vibrational Broadening*

This effect gives rise to asymmetry in the peak which is due to vibrational fine structure[84,87]. There is a redistribution of electronic charge on core level ionization and this generally results in a decrease in bond length and a narrower molecular potential curve. Therefore core ionization is likely to result in vibrational excitation.

1. 4. 1. 2 *Experimental Methods in Electron Spectroscopy*

X-rays are produced by electrons (produced by thermionic emission) bombarding an aluminium or magnesium target giving rise to characteristic lines. The x-rays bombard the sample in the target chamber resulting in electrons being emitted in all directions. Some of the electrons emitted pass through the exit slit into the electron energy analyser onto an electron detector. The spectrum recorded is the number of electrons per unit time as a function of either ionization energy or kinetic energy of photoelectrons.

1. 4. 2 Infrared Spectroscopy

Infrared radiation lies in the electromagnetic spectrum between the visible and microwave regions, with wavelengths corresponding to 10^{-6}-10^{-3} m. The energy of most molecular vibrations corresponds to that of the IR region and the particular energy is characteristic of the molecule. Certain groups of atoms give rise to bands at, or near, the same frequency regardless of the structure of the rest of the molecule. The persistence of these characteristic bands enable structural information to be obtained.

Infrared[90,91,92] radiation promotes transitions in a molecule between rotational and vibrational energy levels of the ground electronic states. IR light is only absorbed when the oscillating dipole moment interacts with the oscillating electric field vector of the IR beam. Absorption only occurs if there is a change in the dipolar character of the molecule and this is determined by a selection rule.

An important result of the selection rules is that a molecule with a centre of symmetry is inactive in the IR whilst an unsymmetric molecule is active. The symmetry properties of a molecule in a solid can be different from those of an isolated molecule, therefore absorption bands are possible in the solid state which are forbidden in other phases.

A molecule can hold a large number of vibrational modes which can be the result of the vibrations of functional groups or individual bonds. Examples of molecular vibrations are; stretching where there are rhythmical movements along the bond axis therefore interatomic distance changes and bending where there is a change in bond angle between bonds with a common atom. The theoretical number of fundamental vibrations is usually never observed because overtones (multiples of a given frequency) and combinations (sum of two other vibrations) increase the number of bands. However, other phenomena decrease the number of bands.

IR has a number of applications. The spectrum of a compound is characteristic of the compound and can therefore be used for identification purposes. It can also be used for the determination of molecular structure and purity. IR can be used for both bulk and surface analysis depending on whether transmission or reflectance techniques are used.

ATR (Attenuated Total reflection)[86] is a technique used for obtaining the absorption spectra of thin films and opaque materials. In a single interference situation, radiation hits the sample and is reflected according to Snell's law, figure 14. The reflection or transmitted beams can be calculated using the Fresnel relations. In ATR, the sample is placed in contact with the reflecting face of a prism. The radiation is reflected along the prism by total internal reflection which gives rise to a standing wave due to the incident and reflected light beams coherently interfering at the interface. If the rarer medium is absorbing, then attenuated total reflection occurs. The energy that escapes temporarily from the prism is selectively absorbed and is independent of sample thickness.

Figure 13: Total reflection of radiation in a medium of refractive index n_2 by a thin film of refraction n_1 ($n_2 > n_1$)[86].
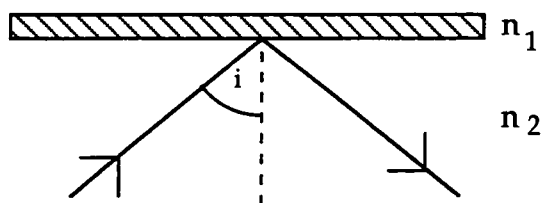
1. 4. 3 Mass Spectrometry

Electron impact mass spectrometry allows data about molecular weight and molecular formula to be obtained from a fragmentation pattern of ions separated by their mass to charge ratio (m/z). The technique involves molecules in the vapour phase being subjected to bombardment by a high energy electron beam resulting in ionization[88,93].

There are several types of mass spectrometer such as magnetic and time of flight (TOF). However in this section the quadrupole mass spectrometer is discussed since it is the most appropriate to this thesis.

A quadrupole mass spectrometer (QMS) consists of four parallel voltage carrying rods. An RF field exists between the rods and a varying DC field is superimposed on the the RF field, figure 14. Ions entering the the QMS will experience complex oscillations and only those ions with one particular m/z ratio at a given set of conditions will have a stable path and traverse the length of the rods through the filter. All the other ions will have unstable oscillations and will be defocussed and lost by collisions with either the rods or the casing of the spectrometer.

Figure 14: Schematic diagram of a quadrupole mass spectrometer[29].
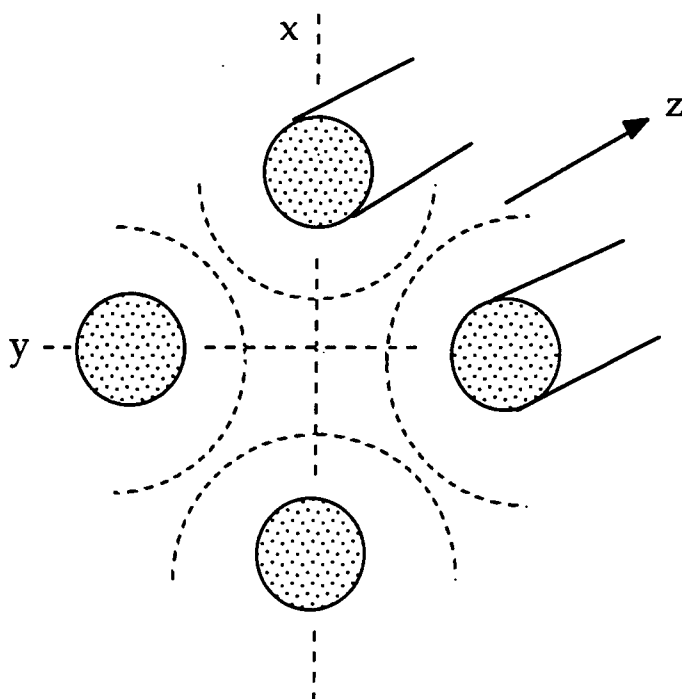
The QMS operates at low source voltages. The velocity of high mass ions is therefore slow and will experience few oscillations under the influence of the quadrupolar fields. This limits the performance of the mass spectrometer as high mass ions are less efficiently detected. The advantage of using a QMS is that the passage of positive and negative ions can occur simultaneously. It is also easier to enclose the system in UHV rather than to provide the pumping required for a magnetic mass spectrometer[94-96].

1. 4. 4 Atomic Force Microscopy

Atomic Force Microscopy (AFM) is a useful technique to "image" surfaces. It enables information about surface topography, molecular and atomic order, absolute feature dimensions, homogeneity of the surface and surface mechanical properties to be obtained. It has several advantages over other microscopy techniques since UHV is not a requirement (analysis can be obtained at ambient temperatures), high energy beams are not needed

(and therefore will not damage the sample) and special sample preparation is not necessary (e. g. metallization). The technique can be used on a variety of materials such as conductors, insulators and even liquids[97].

A schematic of an AFM is illustrated in figure 15.

Figure 15: Schematic diagram of an atomic force microscope[97].
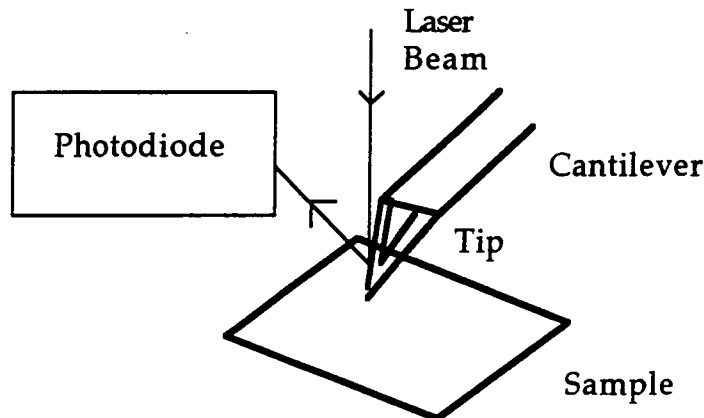
A sharp tip is mounted on a cantilever which is rastered across a sample surface[98-101]. The forces acting between the sample surface and stylus deflect the cantilever. The bending cantilever (vertical up direction) is proportional to the magnitude of the force. Measurement of the displacement gives a real 3D topographical representation of the surface. The cantilever deflections can be measured in two ways.

1) monitoring cantilever deflections as sample moved in plane (constant height mode).

2) monitoring cantilever deflection vertical displacements to maintain the cantilever deflection (constant force mode).

There is also the choice of two modes depending on the sample being analysed[102]. In contact mode, the tip is in close contact with the surface force. In non-contact mode (tapping mode), the tip hovers above the surface and is especially useful for the analysis of soft samples, e. g. polymers, where tip contact could produce artefacts / damage the surface.

1.5 REFERENCES

1.	Dorgan, J. R. *"Polymer Applications for Biotechnology"*, Chapter 3, Prentice Hall, 1992.

2.	Jia, L.; Xu, J. *Polymer Journal* , **1991**, 23, 5, 417.

3.	J. Crank, *"Mathematics of Diffusion"*. Oxford, 1956

4.	Comyn, J. Ed. *"Polymer Permeability"*, Elsevier Applied Science Publishers, 1985.

5.	Koros, W. J.; Fleming, G. K. *J. Memb. Sci.*, **1993**, , 831.

6.	Mazid, M. A.; Matsuura, T. *Sep. Sci. Technol.*, **1993**, 28, 2287.

7.	Wen, W. Y. *Chem. Soc. Rev.*, **1993**, 117.

8.	Kesting, R. E. *"Synthetic Polymeric Membranes. A Structural Perspective"*, 2nd Ed, Wiley, 1985.

9.	Osada, Y.; Nakagawa, T. Eds. *"Membrane Science and Technology"*, Dekker, 1992.

10.	P. S. Holden, G. A. Orchard & I. M. Ward, *J. Applied Polymer Science, Polymer Physics*, **1985**, 23, 709.

11.	Sanchez, I. C.; Rodgers, P. A. *Pur. Appl. Chem,*, **1990**, 62, 2107.

12.	Booth, C.; Price, C. Eds. *"Comprehensive Polymer Science, Volume Two"*, Chapter 20, Pergamon Press, 1989.

13.	Marton, C.; Marton, C. *"Methods of Experimental Physics, Polymers Volume 16, Part C: Physical Properties"*, Chapter 17, 315.

14.	Gearanite, G. B.; Markin, A. P.; Shlapinov, Y. A. *Polym. J.*, **1989**, 25, 39.

15.	Henema, E. R. *Adv. Mater.*, **1994**, 6, 264.

16.	Staude, E.; Bretback, L. *J. Appl. Polym. Sci.*, **1990**, 50, 229.

17.	Kesting, R. E.; Fritzsche, A. K.; Murphy, M. K.; Cruse, C. A.; Handerman, A. C.; Malon, M. K.; Moore, M. J.; *J. Appl. Polym.Sci.*, **1990**, 40, 1557.

18.	Lee, S. H.; Kim, S. S.; Kim, U. Y. *J. Appl. Polym. Sci.*, **1993**, 49, 539.

19. Shih, H. C.; Yeh, Y. S.; Yasuda, H. *J. Memb. Sci.*, **1990**, *50*, 229.

20. Zhou, W.; Gao, X.; Lu, F. *J. Appl. Polym. Sci.*, **1994**, *51*, 855.

21. Ghorsal, K.; Chern, R. T.; Freeman, B. D. *J. Polym. Sci. Phys. Ed.*, **1993**, *31*, 891.

22. Bottino, A.; Lanera-Roda, G.; Capenelli, G.; Munari, S. *J. Memb. Sci.*, **1991**, 557, 1.

23. Temoru, Y. *J. Polym. Sci. Phys. Ed.*, **1995**, *33*, 279.

24. Zhitaruck, N.; Kuznetsov, V. I. *Mackromol. Rap. Chem. Commun.*, **1989**, *10*, 613.

25. Xu, X. L.; Dolveck, J. Y.; Boiteaux, G.; Escoubes, M.; Monchain, M.; Dupin, J. P. *J. Appl. Polym. Sci.*, **1995**, *55*, 99.

26. Meier, I. K.; Langsam, M.; Klotz, H. C. *J. Memb. Sci.*, **1994**, *94*, 195.

27. Hollahan, J. R.; Bell, A. T. Eds. *"Techniques and Applications of Plasma Chemistry"*, Wiley-Interscience, 1974.

28. Coburn, J. W. *IEEE Trans. Plas. Sci.*, **1991**, *19*, 1048.

29. Grill, A. *"Cold Plasmas in Materials Technology"*, IEEE Press, 1994.

30. Chapman, B. "Glow Discharge Processes", Wiley, 1980.

31. Sholet, J. L. *IEEE Trans. Plas. Sci.*, **1991**, *19*, 725.

32. Shur, H. *Plas. Chem. Plas, Process.*, **1989**, *9*, 1.

33. Eliasson, B.; Kogelschatz, U. *IEEE Trans. Plas. Sci.*, **1991**, *19*, 6.

34. Grunwald, H. *Plasma Electronic*, 1.

35. National Academic Press, Washington, 1991.

36. Manos, D. M.; Flamm, D. L. *"Plasma Etching. An Introduction"*, Academic Press, 1989.

37. Vossen, J. L.; Ker, W. Eds. *"Thin Film Processes II"*, Academic Press, 1991.

38. Egitto, F. D.; Matienzo, L. J. *J. Vac. Sci. Technol.*, **1992**, *A10*, 3060.

39. Winter, H. F. *Top. Curr. Chem.*, **1980**, 94.

40. Smith, D.; Adams, N. G. *Pur. Appl. Chem.*, **1984**, *56*, 175.

41. Graves, D. B.; Jensen, K. F. *IEEE Trans. Plas. Sci.*, **1986**, *30*, 199.

42. Liston, E. M. *J. Adhesion,* **1989,** *30,* 199.

43. Clark, D. T.; Dilks, A. *J. Polym. Sci. Chem. Ed.,* **1977,** *15,* 2321.

44. Coopes, I.; Grifkins, K. *J. Macromol. Sci. Chem.,* **1982,** *17,* 217.

45. d' Agostino, R. Ed. *"Plasma Deposition, Treatment & Etching of Polymers",* Academic Press, 1990.

46. Lehma, H. W. *"Thin Solid Fims, V1",* Academic Press, 1991.

47. Grovenor, C. R. M. *"Microelectronic Materials",* IOP Publishing Ltd, 1989.

48. Wu, B. J.; Hess, D. W.; Soong, D. S.; Bell, A. T. *J. Appl. Phys.,* **1983,** *54,* 4, 1725.

49. Egitto, F. D. *J. Pur Appl. Chem,* **1990,** *62,* 1699.

50. Hand, B.; Long, T.; Dervis, D. C.; Rodriquez, F. *J. Appl. Polym. Sci.,* **1993,** *47,* 2135.

51. Emmi, F.; Egitto, F. D.; Matienzo, L. *J.Vac. Sci. Technol.,* **1991,** *A9,* 786.

52. Wu, S. Y.; Denton, D. D. *J. Vac. Sci. Technol.* **1993,** *A11,* 291.

53. Montazer-Rahmatic, P.; Areti, F.; Amouroux, J. A. *Surf. Coatings Technol.,* **1991,** *45,* 369.

54. Nguyen, L. T.; Hsung, N.; Suh, N. P. *J. Polym. Sci. Polym. Lett. Ed.,* **1980,** *18,* 541.

55. Cherry, B. W. *"Polymer Surfaces",* Cambridge Solid State Series, 1981.

56. Morra, M.; Ocheillo , E.; Garbassi, F. *Langmuir,* **1985,** *5,* 872.

57. Ochiello, E.; Morra, M.; Cinquina, P.; Garbassi, F. *Polymer Preparation,* **1990,** *31,* 308.

58. Ueno, T.; Shiraishi, H.; Iwayanagi, T.; Nongaki, S. *J. Electrochem. Soc. Sci. Technol.,* **1985,** *132,* 1168.

59. Foerch, R.; McIntyre, N. S.; Hunter, D. H. *J. Polym. Sci. Chem. Ed.,* **1990,** *28,* 193.

60. Garbassi, F.; Morra, M.; Ochiello, E.; Barino, L.; Scordamgha, R. *Surface Interface Analysis,* **1989,** *17,* 585.

61. Morra, M.; Ochiello, E.; Gila, L.; Garbassi, F. *J. Adhesion*, **1990**, *33*, 88.

62. Muttal, K. L. Ed. *"Metallized Plastics 2"*, Plenum Press, New York, 1991.

63. Ochiello, E.; Morra, M.; Cinquina, P.; Garbassi, F. *Polymer*, **1992**, *33*, 3007.

64. Yasuda, H.; Sharma, H. K.; Yasuda, T. *J. Polym. Sci. Phys. Ed.*, **1981**, *19*, 1285.

65. Hsuen, Y.; Chen, Y. *Ind. End. Prod. Res. Dev*, **1985**, *124*, 246,.

66. Gerenser, L. J. *J. Adhesion Science Technology*, **1987**, *4*, 303.

67. McTaggert, F. K. *"Plasma Chemistry in Electrical Discharges"*, Elsevier Publishing Company, 1967.

68. Scott, P. M.; Matienzo, L. J.; Babu, J. *J. Vac. Sci. Technol.*, **1990**, *A8*, 2382.

69. Strobel, M.; Corn, S.; Lyons, C. S.; Korba, G. A. *J. Polym. Sci. Chem. Ed.*, **1985**, *23*, 1125.

70. Lin, X.; Xiao, J.; Yu, Y.; Chen, J.; Zheng, G. *J. Appl. Polym. Sci.*, **1993**, *49*, 231.

71. Inagaki, N.; Tasaki, S.; Mori, K. *J. Appl. Polym. Sci.*, **1991**, *43*, 581.

72. Morita, S.; Hatton, S. *Pur. Appl. Chem.*, **1987**, *57*, 1177.

73. Well, A. T. *"Mechanisms and Kinetics of Plasma Polymerization"*.

74. Yasuda, H. *"Plasma Polymerization"*, Academic Press, 1985.

75. Haalan, D. D.; Clanson, S. J. *"Trends in Polymer Science"*, 1993.

76. Savage, C. R.; Timmons, R. B.; Lin, J. W. *Chem. Mat.*, **1991**, *3*, 575.

77. Inagaki, N.; Tasaka, S.; Murata, T. *J. Appl. Polym. Sci.*, **1989**, *38*, 1869.

78. Sakata, J.; Yamamoto, M.; Hirai, M. *J. Appl. Polym. Sci.*, **1986**, *31*, 1999.

79. Randhawa, H. *Thin Solid Films*, **1991**, *196*, 329.

80. Lucosvsky, G.; Tsu, D. V. *J. Non. Crys. Sol.*, **1987**, *97/98*, 265.

81. Wendel, H.; Suhr, H. *Appl. Phys.*, **1992**, *A54*, 389.

82. Smith, G. C. *"Surface Analysis by Electron Spectroscopy"*, Plenum Press, 1994.

83. M. Prutton, *"Surface Physics"* , Claredon Press, 1984.

84. Briggs, D.; Seah, M. P. Eds. *"Practical Surface Analysis: Volume 1"*, John Wiley & Sons,1990.

85. Woodruff, D. P.; Delchar, T. A. *"Modern Techniques of Surface Science"*, Cambridge University Press, 1990.

86. Hollas, J. *"Modern Spectroscopy"* ,John Wiley & Sons, 1988.

87. Gosh, P. K. *"Introduction to Photoelectron Spectroscopy"*, Wiley, 1983.

88. Walls, J. M. Ed. *"Methods of Surface Analysis: Techniques and Applications"*, Cambridge University Press, 2nd Edition, 1990.

89. Brundle, C. R.; Baker, A. D. Eds. *"Electron Spectroscopy: Theory, Techniques and Applications, Vol 1-4"*, Academic Press, 1978.

90. Cross, A. D. *"Introduction to Infra-Red Spectroscopy"*, Butterworths, 1964.

91. Cross, C. N. *"Chemical Applications of Infra-Red Spectroscopy"*, Academic Press, 1963.

92. Williams, D.; Fleming, I. *"Spectroscopic Methods in Organic Chemistry"*, McGraw Hill, 1966.

93. Briggs, D.; Brown, A.; Vickerman, J. C. *"Handbook of Static Secondary Ion Mass Spectrometry"*, John Wiley & Sons , 1989.

94. Briggs, D.; Seah, M. P. *"Practical Surface Analysis, Volume Two, Ion Neutral Spectroscopy"*, Wiley, 1990.

95. Silverstein, R. M.; Bassler, G. C.; Morrill, T. C. *"Spectrometric Identification of Organic Compunds"*, Fifth Ed., Wiley, 1991.

96. Chamber, A.; Fitch, R. K.; Halliday, B. S. *"Basic Vacuum Technology"*, Adam Higer, 1989.

97. Burnham, N. A.; Cotton, R. J. *J. Vac. Sci. Technol.* , **1989**, *A7*, 2906.

98. Drummond, C. J.; Sender, T. J. *Coll. Surf. A. Phys. Eng. Asp.*, **1994,** *87,* 217.

99. Goh, M. C.; Markievwivcz, P. *Chem. Ind.*, **1992,** 687.

100. Dietz, P.; Hansama, P. K.; Ihn, J.; Moteamedi, F.; Smith, P. *J. Mat. Sci.*, **1993,** *28,* 1372.

101. Magnov, S. N. *Appl. Spec. Rev.*, **1993,** *28,* 1.

102. Quate, C. F. *Surf. Sci.*, **1994,** *229/300,* 980.

Chapter Two

Plasma Modification of Polysulfone and

Polyethersulfone

Chapter Two

Plasma Modification of Polysulfone and Polyethersulfone

2. 1 INTRODUCTION

The aim of this chapter was to determine how the surface of polysulfone changed, chemically and topographically, when subjected to various gas plasma treatments. The work was carried out on dense polymer films so as to gain a fundamental understanding of the plasma reactions occurring at the surface. Polyethersulfone was also studied to compare how the slightly different chemical structure may affect the reactions at the surface.

2. 1. 1 Background

Polysulfones have a diverse range of applications such as connectors used in telecommunications, printed wiring substrates and as membranes. They holds many advantages over other materials for example high thermal resistance, flexibility yet toughness and good electrical properties. Many of these properties are derived from the rigidity of the polymer backbone[1] and the intersegmental chain packing.

In the bulk polymer[2], the presence of diarylsulfone grouping enhances stabilisation of S-C bonds via conjugation with aromatic groups resulting in a T_g greater than 200 °C. Such bonds are hydrolytically stable conferring strong resistance to attack by acids and alkalis.

The basic properties of polysulfones are favourable when compared to other high temperature plastics. They are generally transparent and exhibit high rigidity, low creep, good thermal stability and flame resistance. The

main disadvantage of the polymer is it's lack of chemical resistance to polar solvents.

2. 1. 2 Uses of Polysulfones

Polysulfone and its derivatives are versatile materials. They are used in the electronics industry for chip carriers, capacitor dielectrics and connectors. They are also used for printing wiring board fabrication[2,3,4]. Polysulfones can be used as a permselective separation barrier, with applications in both large scale production and on a laboratory scale[5].

Hydrodynamic sieving is an area where polysulfone membranes are particularly important[5]. Hydrodynamic sieving can be split into two main groups, ultrafiltration and microfiltration. Polysulfone is a popular material used for microfiltration, which has applications in biotechnology. The introduction of ionic groups[6] extends the application range as a separation membrane, for example neutral polysulfone can be prepared so that it sorbs oppositely charged particles. This is carried out by mixing the neutral polysulfone with an ion exchange polymer or by introducing ionic groups on the polymer. Other uses for polysulfone membranes include gas separation membranes[7], barrier packaging and in controlled release devices used in medicine and agriculture[7].

Its usage can be further increased by modifying the polymer chemically and physically, or by mixing it with other polymers to form composite structures[13].

2. 1. 3 Modification of Polysulfone

There are a number of ways to treat polysulfone chemically[8,9,10] but a far simpler method is by the use of plasmas, which is the area being studied in this chapter. By employing plasma treatment, the surface of polysulfone can be modified so as to alter the intrinsic properties of the polymer such as permeability, gas selectivity, adhesion and wettability.

The use of plasmas is an area of growing interest as a low temperature treatment which is applicable to a wide variety of materials. The disadvantages of using plasmas is that as yet there is not a good understanding of the interactions going on within the plasma and the reactions of the species with the sample surface. However with the use of diagnostic techniques such as UV emission spectroscopy and mass spectrometry, a more comprehensive idea of the reactions occurring within a plasma can be obtained.

It has been reported[11] that a plasma process (H_2O and He plasmas) has been optimized (pressure, power etc) to give maximum wettability, which is important in the fabrication of ultrafiltration and microfiltration membranes. XPS analysis[11] of the surface shows that treatment with the plasma increases the oxygen content at the surface.

Polysulfone has also been subjected to O_2, CF_4/O_2 and He plasma treatments in order to determine changes in wettability and adhesion[12]. All the plasma treatments gave rise to a decrease in the contact angle whilst giving rise to excellent adhesion to aluminium, even after sample ageing. It is thought that the formation of oxygen containing groups on the surface result in the formation of covalent bonds between oxygen and aluminium when metallized.

This chapter investigates the effect of a variety of plasma treatments on polysulfone and polyethersulfone. These two polymers were studied so as to compare and contrast how the polymeric structure was influenced by each plasma treatment. The structures are shown in figure 1.

Figure 1: Chemical Structure of Polysulfone (PSF) and Polyethersulfone (PES).

POLYETHERSULFONE (PES)

POLYSULFONE (PSF)
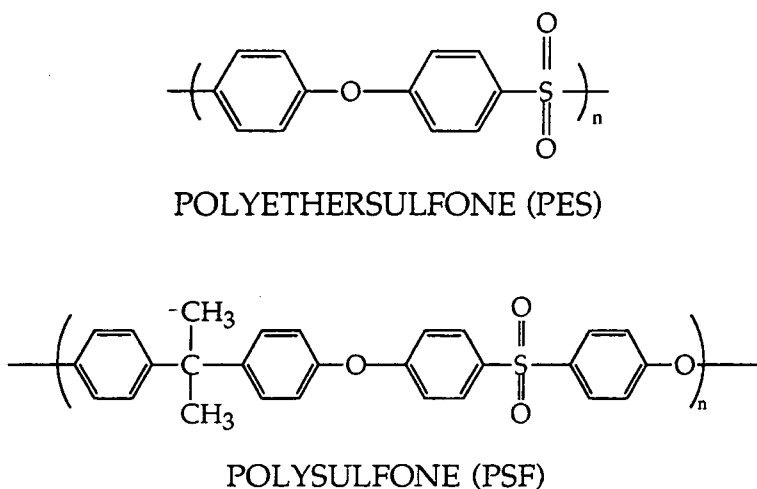
XPS and AFM have been used to probe the chemical and topographical changes encountered at the polymer surfaces during exposure to a variety of non-polymerizable glow discharge treatments.

## 2. 2 EXPERIMENTAL

2. 2. 1 Plasma Modification

Small strips of polysulfone (PSF) and polyethersulfone (PES) (Westlake Plastics Company) were ultrasonically washed in an isopropyl alcohol (BDH) / hexane (BDH) mixture for 30 seconds and dried in air. High purity oxygen (99.6%, BOC), hydrogen (99.99%, BOC), helium (99.995%, BOC), neon (99.999%, BOC), argon (99.999%, BOC), and carbon tetrafluoride

(99.7%, Air Products) gases were used for the various types of plasma treatment.

Glow discharge experiments were carried out in a cylindrical glass reactor (4.5 cm diameter, 515 cm^3 volume, base pressure of 1.5 x 10^{-3} Torr), enclosed in a Faraday cage[14], figure 2.

Figure 2: Schematic representation of the plasma rig.
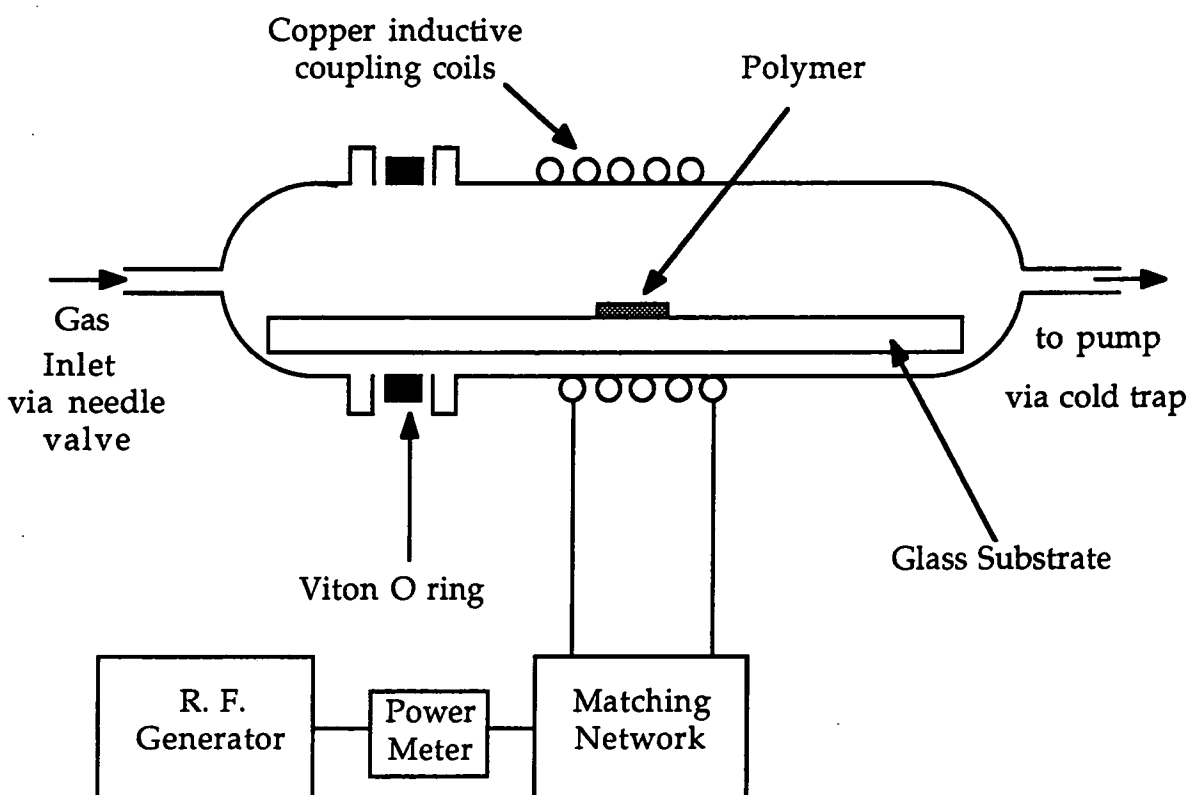
The reactor was fitted with a gas inlet Edwards LV10K needle valve, an Edwards PR-10K Pirani pressure gauge, and a Leybold 27 L min^{-1} two-stage rotary pump attached to a liquid nitrogen cold trap. Power from a Tegal Corporation 13.56 MHz radio frequency (RF) source was inductively coupled to the reactor via a copper coil (4 mm diameter, 13 turns, spanning 9 - 18 cm from the gas inlet) wound around the reactor. An RS SWR / power meter was used to gauge the input power into the plasma. After ignition of the plasma the system was balanced using the L-C matching network in

order to maximize the power input into the plasma. This was carried out by minimizing the standing wave ratio (SWR) (SWR= Total power generated/power transmitted to the plasma) of the forward power. All joints were grease-free.

A typical experimental run comprised initially scrubbing the reactor with detergent, rinsing with isopropyl alcohol, oven drying followed by a 60 min high power (50 W) air plasma cleaning treatment. Next, the reactor was opened up to atmosphere, a strip of polymer was inserted into the centre of the RF coils. The system was then evacuated back down to its original base pressure. At the beginning of each experiment the leak rate of the system was calculated (see section 2. 2. 3). This was carried out by isolating the pump from the reactor and measuring the increase in pressure over a given time. If an acceptable leak rate was determined, typically better than 2×10^{-3} cm^3 min^{-1}, then the gas of interest was introduced into the reaction chamber at 2×10^{-1} mbar pressure at a flow rate of approximately 1.9 cm^3 min^{-1} (i.e. at least 99.6% of the reactor contents). After allowing 10 min for purging, the glow discharge was ignited at 20 W for 5 min. Upon termination of treatment, the RF generator was switched off and the system was purged for a further 5 min before opening up the reactor to atmosphere. Each sample was characterized immediately after electrical discharge treatment by X-ray photoelectron spectroscopy (XPS) and atomic force microscopy (AFM).

2. 2. 2 Characterization of the treated samples

2. 2. 2. 1 *X-ray Photoelectron Spectroscopy (XPS)*

A Kratos ES300 electron spectrometer equipped with a Mg Kα X-ray source (1253.6 eV) and a hemispherical analyser was used for XPS surface analysis, figure 3.

Figure 3: Schematic representation of an electron spectrometer[70].
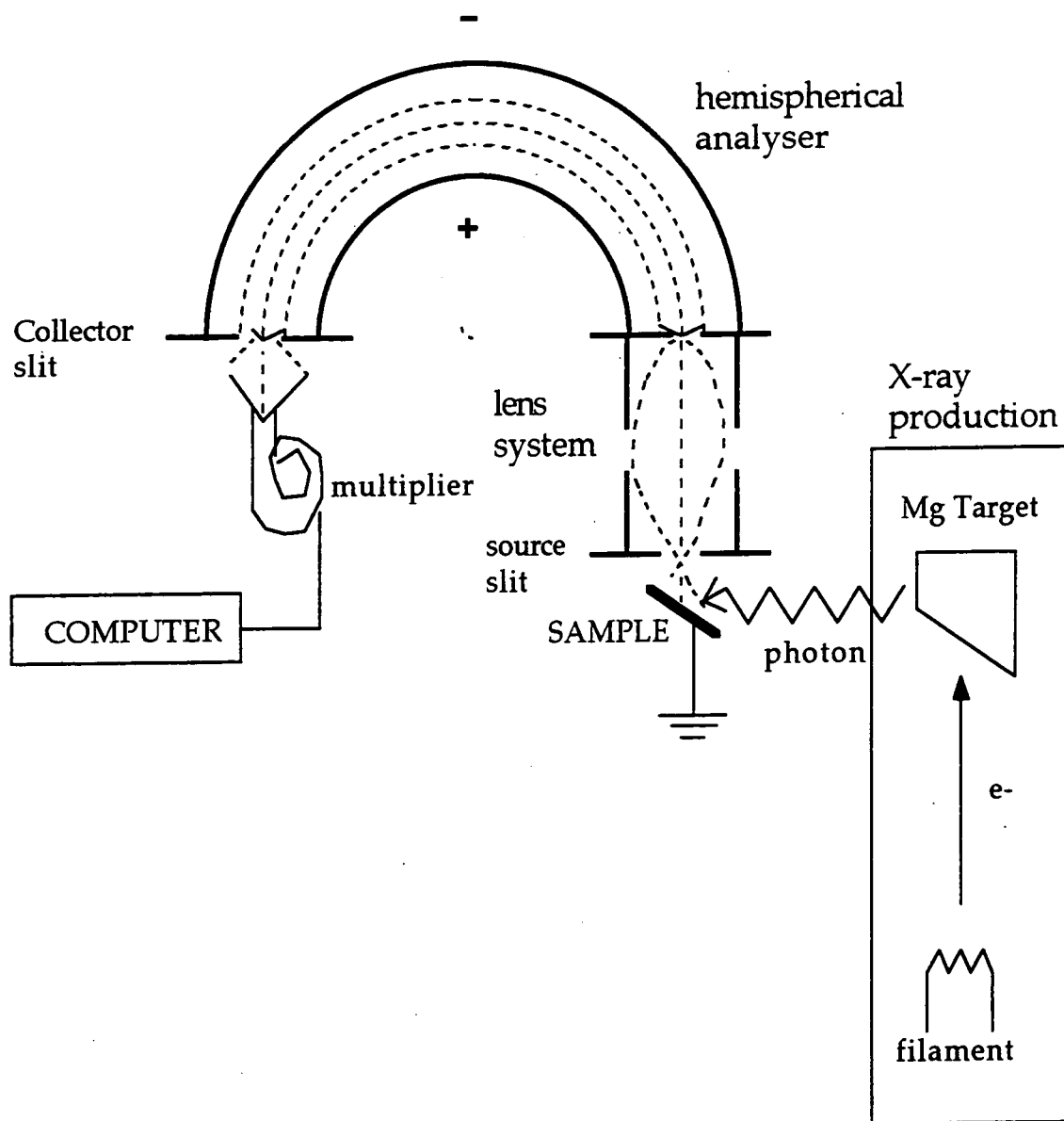
Photo-emitted core level electrons were collected at a take-off angle of 30° from the substrate normal, with electron detection in the fixed retarding ratio (FRR, 22:1) mode. XPS spectra were accumulated on an interfaced PC computer and curve fitted using a Marquardt minimization algorithm. Instrument performance was calibrated with respect to the gold $4f_{7/2}$ peak at 83.8 eV with a full width at half maximum (FWHM) of 1.2 eV. Instrumentally determined sensitivity factors for unit stoichiometry were taken as being C(1s) : O(1s) : S(2p) : N(1s) : F(1s) equals 1.00 : 0.55 : 0.54 : 0.74 :

0.53. XPS was used to check cleanliness of the polysulfone substrate and for the absence of any surface-active inorganic additives.

Samples were mounted on a stainless steel probe tip (2 cm x 0.7 cm) using Scotch adhesive tape. The probe was cleaned with analar isopropyl alcohol prior to insertion into the spectrometer.

2. 2. 2. 2 *Atomic Force Microscopy (AFM)*

Atomic force microscopy offers structural characterization of surfaces in the 10^{-4} - 10^{-10} m range without the prerequisite of special sample preparation, for example metallization as required for SEM. A Digital Instruments Nanoscope III atomic force microscope was used to examine the topographical nature of the polysulfone surface prior to and after electrical discharge exposure. All of the AFM images were acquired in air using the non-contact tapping mode[15], and are presented as unfiltered data. The technique employs a stiff silicon cantilever oscillating at a large amplitude near its resonance frequency (several hundred kHz).

The samples were mounted on magnetized stainless steel discs using Scotch adhesive tape.

2. 2. 3 Flow Rate Calculation

Gas flow and leak rates were calculated by assuming ideal gas behaviour[16].

$$PV = nRT \qquad (1)$$

where P is the pressure (atm), V is the volume of the reactor (l), n is the number of moles of gas, R is the universal gas constant (atm l K^{-1}) and T is the absolute temperature (K). At STP one mole of gas occupies 22414 cm^3.

The flow rate and leak rate can be calculated by measuring the increase in pressure over a given time, equation 2.

$$\text{Flow rate} = dn/dt = (dP/dt)\,(V/RT) \times 22414 \quad cm^3\ min^{-1} \quad (2)$$

where t is in minutes.

2. 3 RESULTS

2. 3. 1 Untreated Polymers

The C : O : S ratio for untreated PSF and PES films obtained from XPS is in resonable agreement with the theoretically predicted value of the sample, since the presence of impurities or additives is difficult to fully assess from commercially produced samples, tables 1 and 2. The slightly higher concentration of sulfur for PES can be attributed to preferential orientation of the sulfone group at the polymer surface[17,18]. C(1s) XPS spectra were fitted with Gaussian peaks of equal full width at half maximum (FWHM)[19], using a Marquardt minimisation computer program. This program minimizes the X^2 parameter using a least squares fit by linear regression. It is important to note that a good mathematical fit is not necessarily a curve fit with chemical meaning. The curve fits contained within this thesis were fitted using reference values from the literature in order to input the initial peak positions and chemical shifts. Values for peak amplitudes and widths were also input into the program. During the curve fitting process, values for peak positions, amplitudes and widths were limited to values which were chemically meaningfull.

Aromatic carbon atoms attached to hydrogen/carbon, sulfone, and ether groups exhibit C(1s) core level binding energies of 285.0 eV, 285.6 eV, and 286.6 eV respectively[17,18,20]. Low-energy π-π^* shake-up transitions

55

accompanying core level ionization around 291.7 eV were fitted with a Gaussian peak of different FWHM in order to assess the level of aromaticity present before and after glow discharge treatment[21,22], figures 4 and 5. The O(1s) peak of PSF is a 1:1 doublet with the peaks centred at 532.1 eV and 533.6 eV corresponding to oxygen bonded to sulfur (sulfone groups) and oxygen bonded to carbon in the backbone (ether linkage)[17,20]. A doublet structure was also noted in the O(1s) region of PES with a 2 : 1 intensity ratio, which corresponds to twice as many oxygen atoms attached to sulfur, sulfone groups (531.9 eV), as there are oxygen atoms located in ether environments (533.5 eV)[17,20]. The S(2p) peak for both PSF and PES was found to be an unresolved 2:1 doublet centred at 168.0 eV, this can be taken as being characteristic of a sulfone group, rather than a sulfide (163.6 eV), or sulfate (169.3 eV) environment[18,20,22,23]. The errors in the table refer to the reproducibility of the results from several independent experiments.

A very low level of surface roughness was measured for the clean polymer substrates by AFM with no indication of any ordered regions, which is agreement with the polymers being in an amorphous state[24], table 4 and figures 6 and 13.

2. 3. 2 Oxygen Plasma Treatment

The greatest degree of oxidation for PSF and PES occurs for the oxygen plasma treatment, tables 1 and 2. There was virtually no change in the S(2p) binding energy value, or in its FWHM. Munro found that sulfate species are generated during the UV photo-oxidation of PSF and PES[25,26] however these groups are absent following oxygen plasma treatment of the polymers. This difference in behaviour is most likely due to a less oxidized surface forming during the course of plasma oxidation as a consequence of simultaneous sputtering and UV photo-irradiation of the substrate[27].

Table 1: Summary of changes in elemental composition following plasma modification of polysulfone (20 W, 5 mins).

Treatment	%C	%S	%O	%N	%F
Theoretical	77.1	7.6	15.2	-	-
Untreated	82.4±0.1	4.1±0.4	13.6±0.2	-	-
O_2 plasma	59.1±3.2	4.9±0.6	32.2±2.6	2.9±0.1	-
H_2 plasma	89.2±2.4	1.4±0.02	9.1±2.0	-	-
He plasma	70.8±0.4	2.8±0.1	21.0±0.7	4.6±0.6	-
Ne plasma	70.2±0.2	3.1±0.3	23.2±0.7	3.3±0.5	-
Ar plasma	71.4±2.6	2.7±0.2	21.7±1.7	2.7±0.007	-
CF_4 plasma	41.1±0.2	0.5±0.6	6.9±0.8	-	51.5±1.4

Table 2: Summary of changes in elemental composition following plasma modification of polyethersulfone (20 W, 5 mins).

Treatment	%C	%S	%O	%N	%F
Theoretical	75.0	6.3	18.7	-	-
Untreated	76.3±1.5	7.9±0.8	15.9±0.8	-	-
O_2 plasma	55.6±3.2	7.2±0.4	34.4±0.04	2.7±0.2	-
H_2 plasma	84.9±1.5	3.2±0.3	10.9±0.2	2.2	-
He plasma	64.3±1.1	5.4±0.5	25.5±0.5	3.2±0.6	-
Ne plasma	64.0±0.5	6.6±0.3	24.7±0.4	3.9±0.2	-
Ar plasma	68.4±3.03	6.7±0.9	26.3±3.1	3.0±0.6	-
CF_4 plasma	40.9±0.8	1.2±0.1	10.3±0.1	-	47.5±1.1

The AFM figures of PSF (figure 7) and PES (figure 14) oxygen plasma treatments illustrate the severity of the treatment on the surface topography. A very uneven surface is generated exhibiting a globular texture.

All of the glow discharge treatments, of PSF and PES, undertaken in this study were found to result in complete disappearance of the C(1s) π-π^* shake-up satellite, and loss of the resolved O(1s) doublet into a broad single peak. A small amount of nitrogen was detected (approximately 2%) on some treated samples, the most likely origin for this being reaction between trapped free radical centres at the surface and the atmosphere during transport of the modified substrate from the glow discharge apparatus to the XPS spectrometer.

2. 3. 3 Hydrogen Plasma Treatment

Hydrogen glow discharge treatment of PSF and PES gave rise to an increase in the amount of surface carbon and a decrease in oxygen and sulfur content at the surface. There is a strong attenuation in the relative proportion of oxygenated carbon centres required to fit the C(1s) peak. The S(2p) peak displays an extra shoulder towards the low binding energy side of the sulfone peak (164.3 eV), which can be attributed to a -C-S-O- crosslinked environment[28], table 3. The corresponding C(1s) binding energy for this linkage is 285.6 eV[17,20]. From these experiments it can be concluded that hydrogen glow discharge treatment causes surface reduction. The constituent phenyl rings in the polymers probably undergo hydrogenation and crosslinking, whereas the ether and sulfone linkages are eliminated as gaseous H_2O and H_2S molecules respectively. Such species have been detected on heating polysulfone, where the breakdown of the sulfone linkages is postulated as being a result of hydrogen abstraction[29].

AFM figures of hydrogen plasma treated PSF and PES, figures 8 and 15 respectively, show a significant degree of disruption compared to the clean, untreated surface. There is a strong variation in the surface topography within the area sampled.

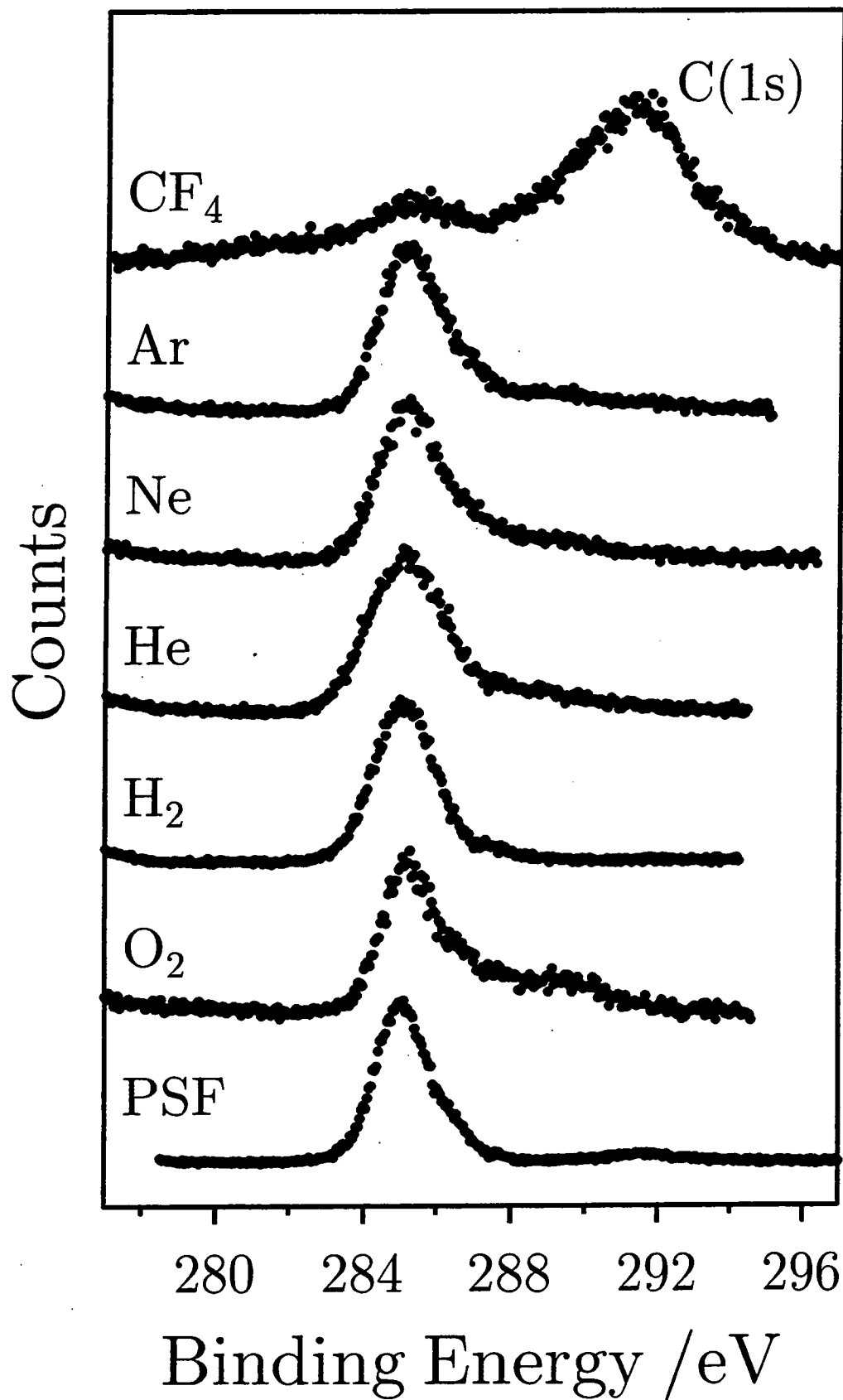Figure 4: C(1s) XP spectra of plasma treated PSF.

Figure 5: C(1s) XP spectra of plasma treated PES.

Figure 6: AFM micrograph of untreated PSF.
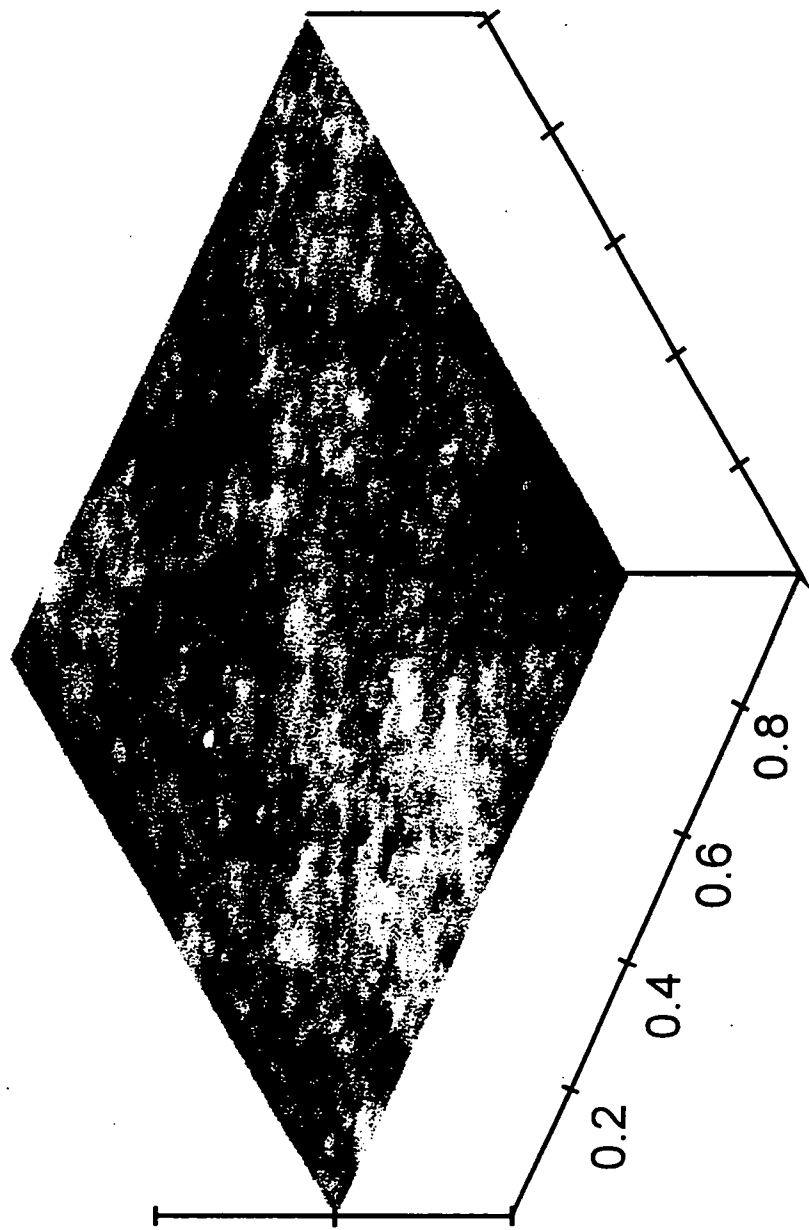
x = 0.2 μm / div
z = 200 nm / div

(a) CLEAN

61

Figure 7: AFM micrograph of oxygen plasma treated PSF.

(b) OXYGEN

x = 0.2 μm / div
z = 200 nm / div

62

Figure 8: AFM micrograph of hydrogen plasma treated PSF.

(c) HYDROGEN

x = 0.2 μm / div
z = 200 nm / div
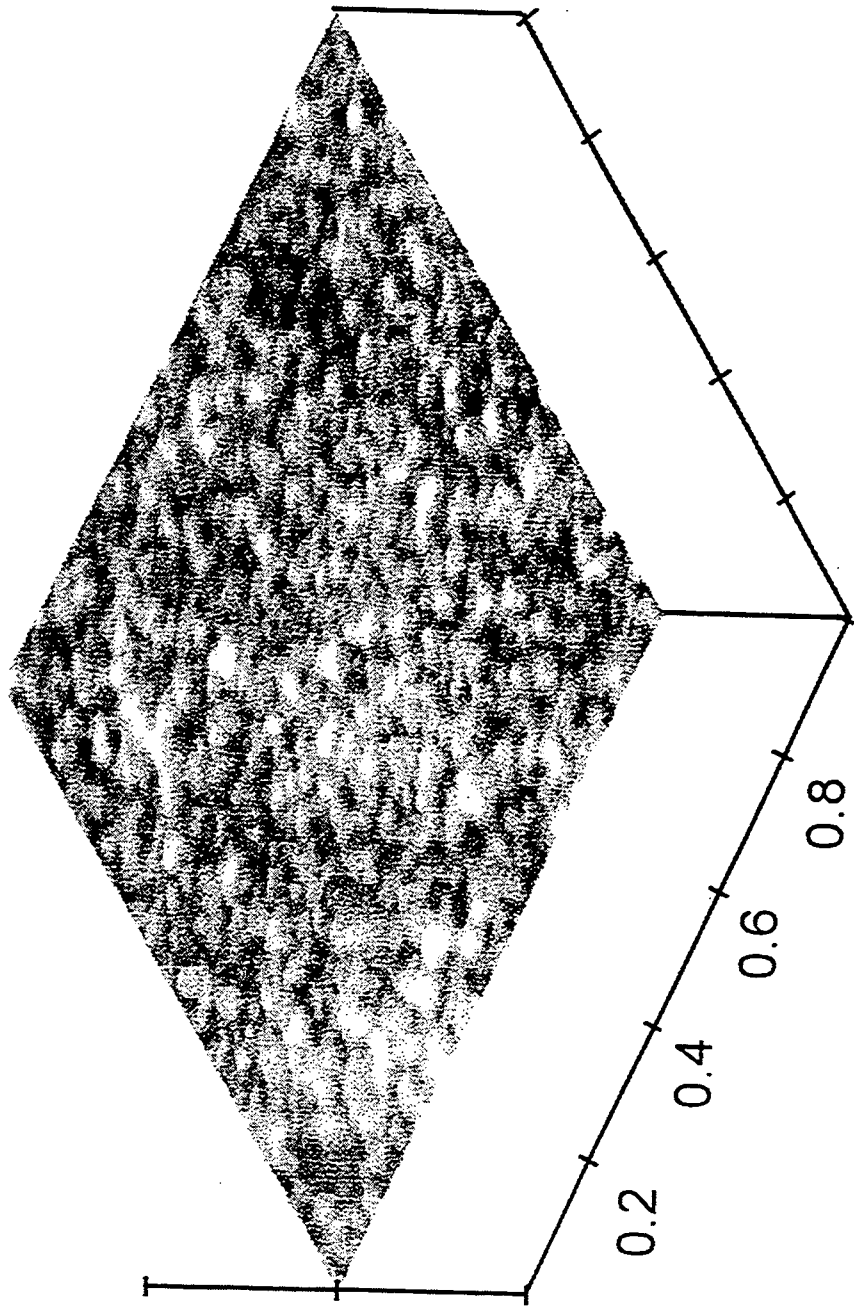
Figure 9: AFM micrograph of helium plasma treated PSF.

(d) HELIUM

x = 0.2 μm / div
z = 200 nm / div

64
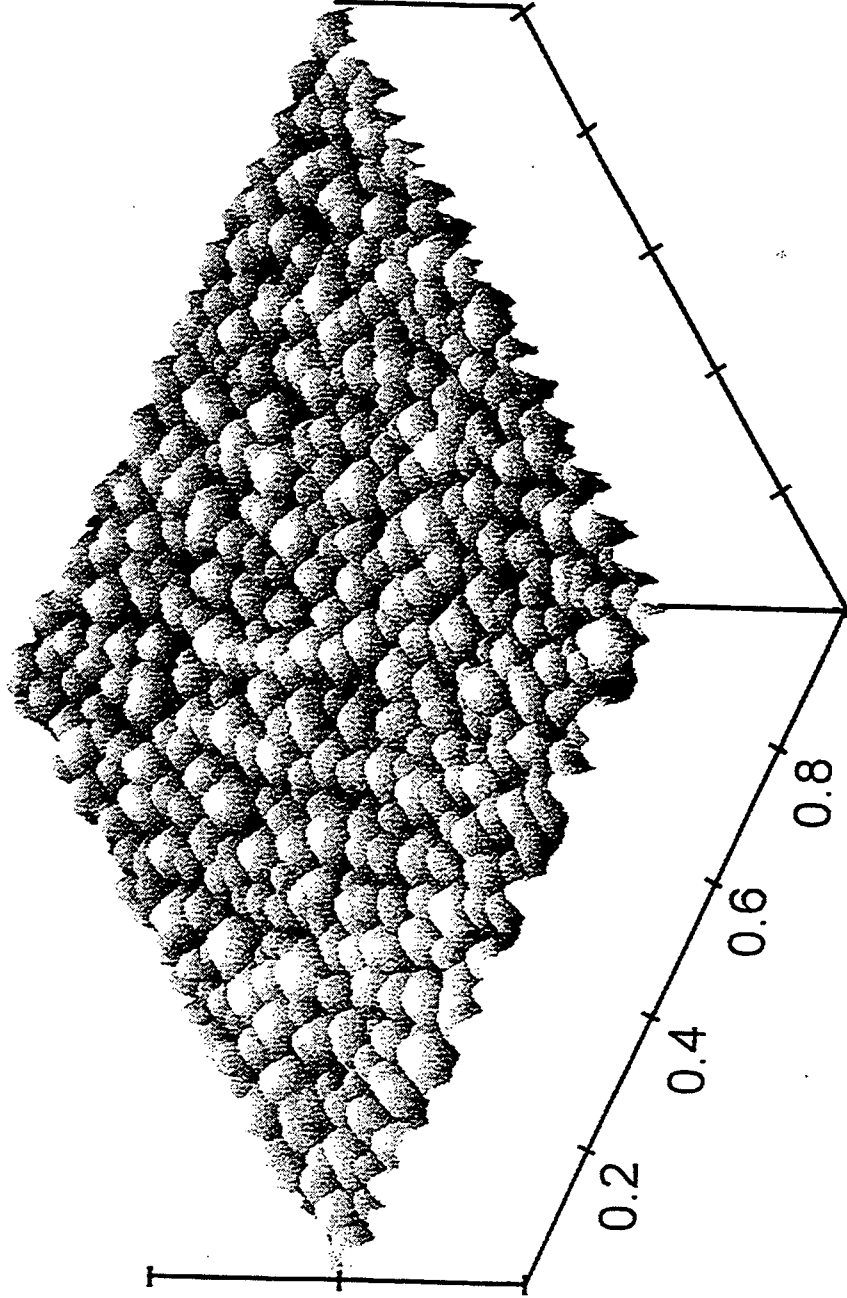
Figure 10: AFM micrograph of neon plasma treated PSF.
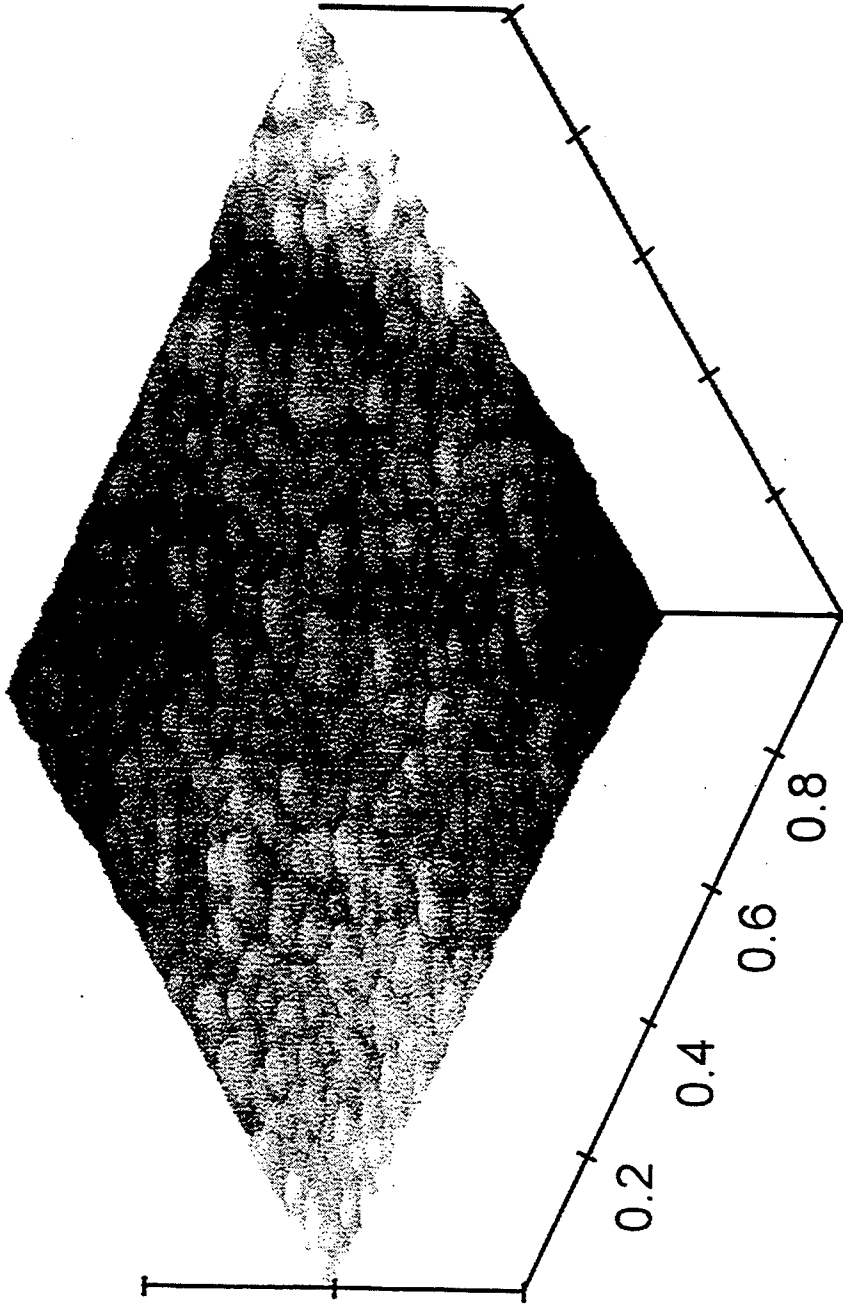
x = 0.2 μm / div
z = 200 nm / div

(e) NEON

65

Figure 11: AFM micrograph of argon plasma treated PSF.
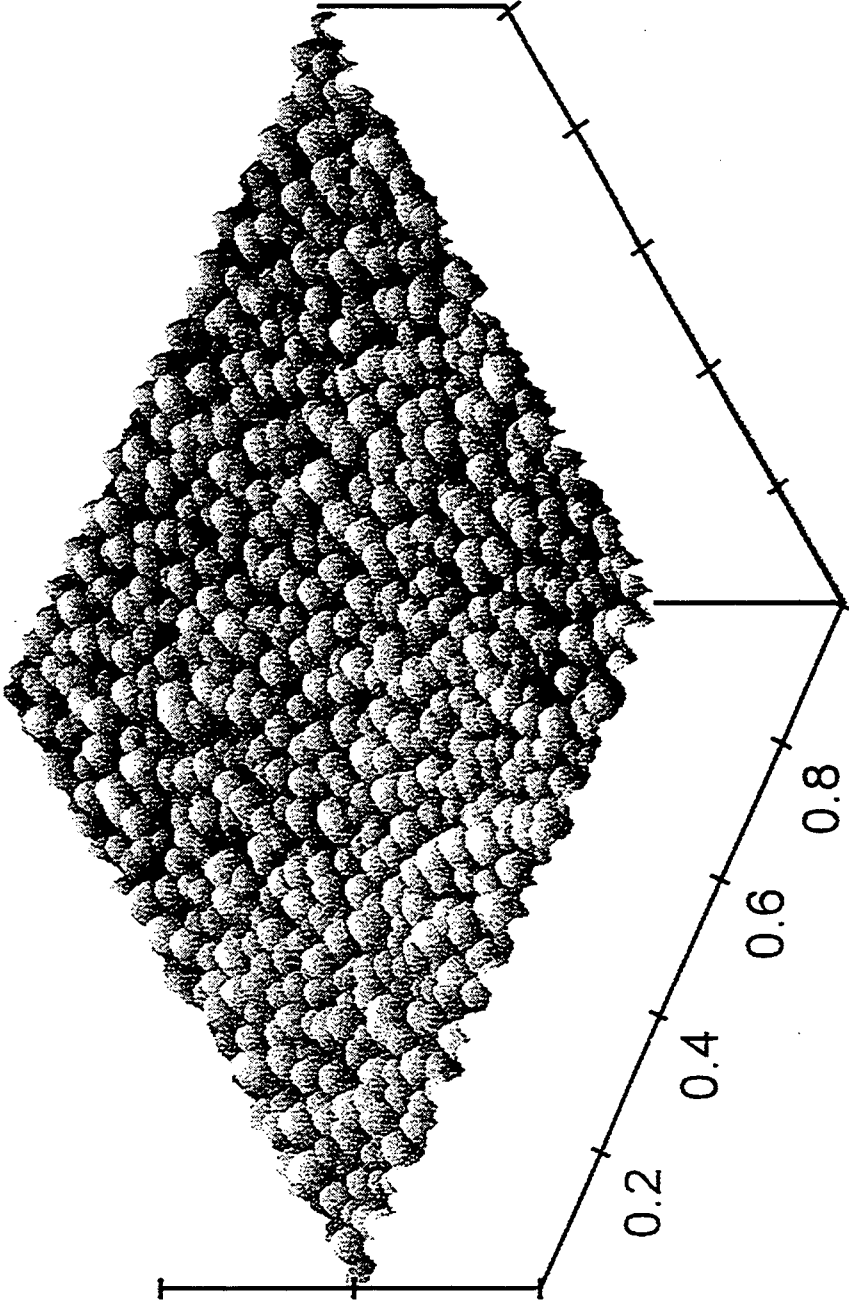
x = 0.2 μm / div
z = 200 nm / div

(f) ARGON

66

Figure 12: AFM micrograph of CF₄ plasma treated PSF.
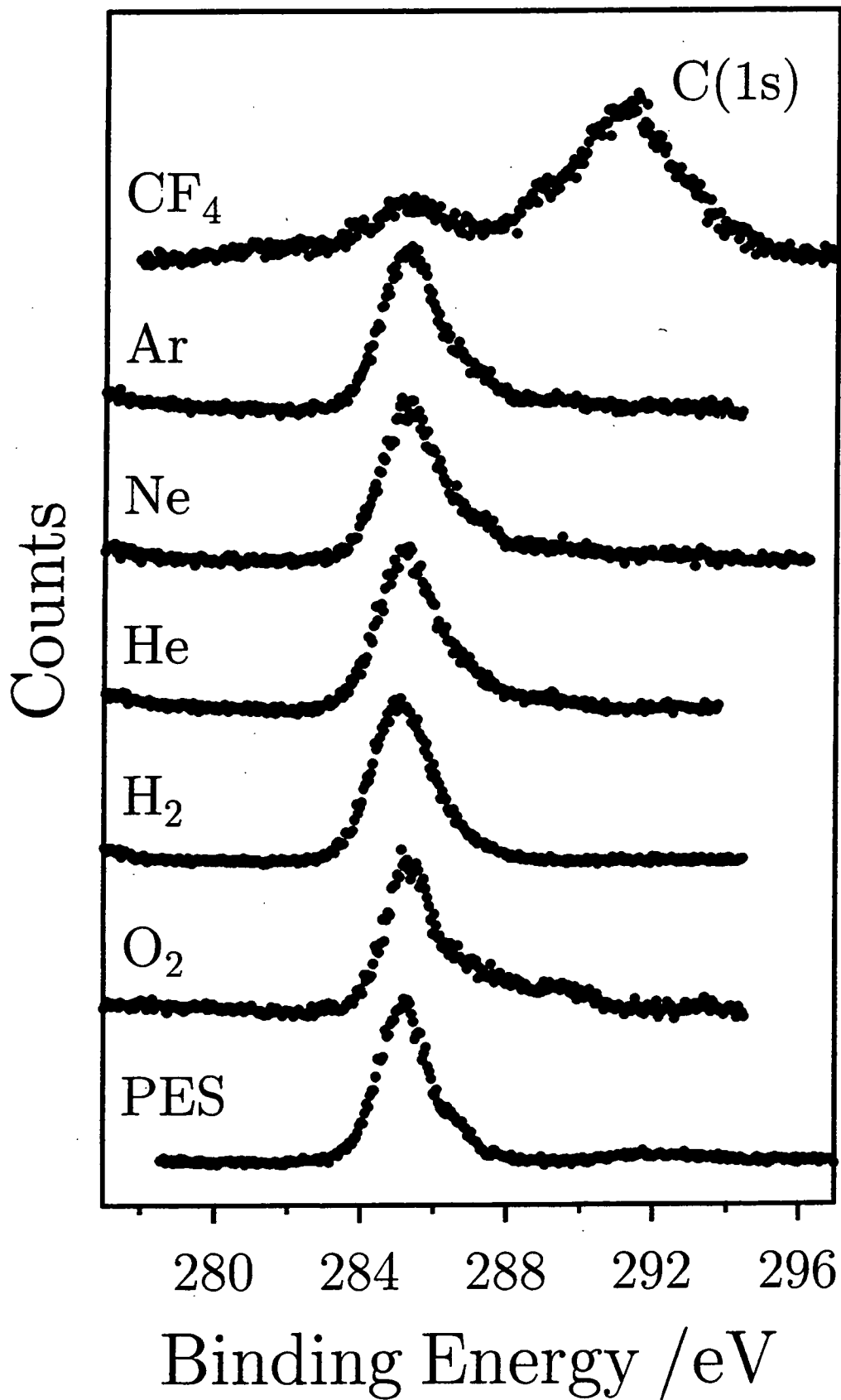

(g) CF$_4$

x = 0.2 μm / div
z = 200 nm / div
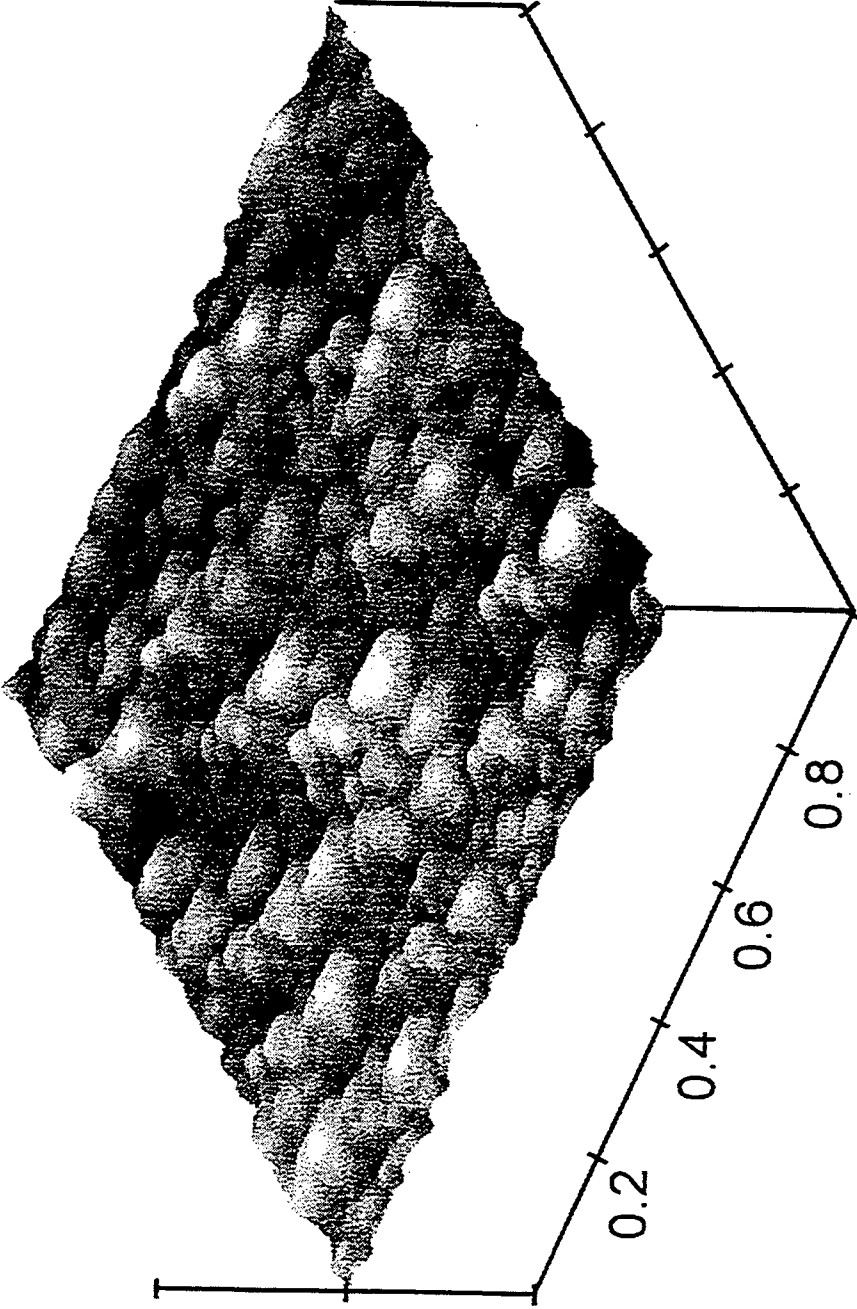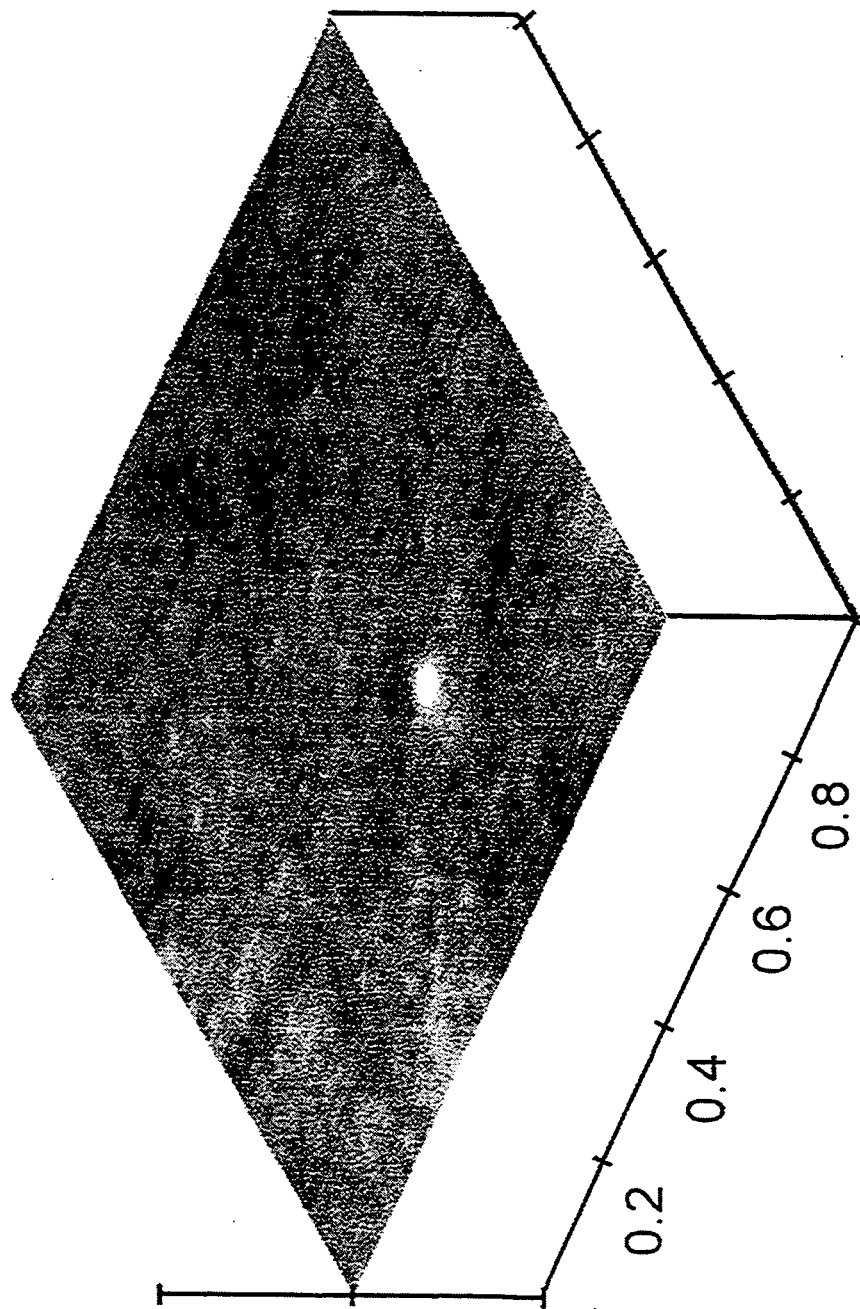
Figure 13: AFM micrograph of untreated PES.
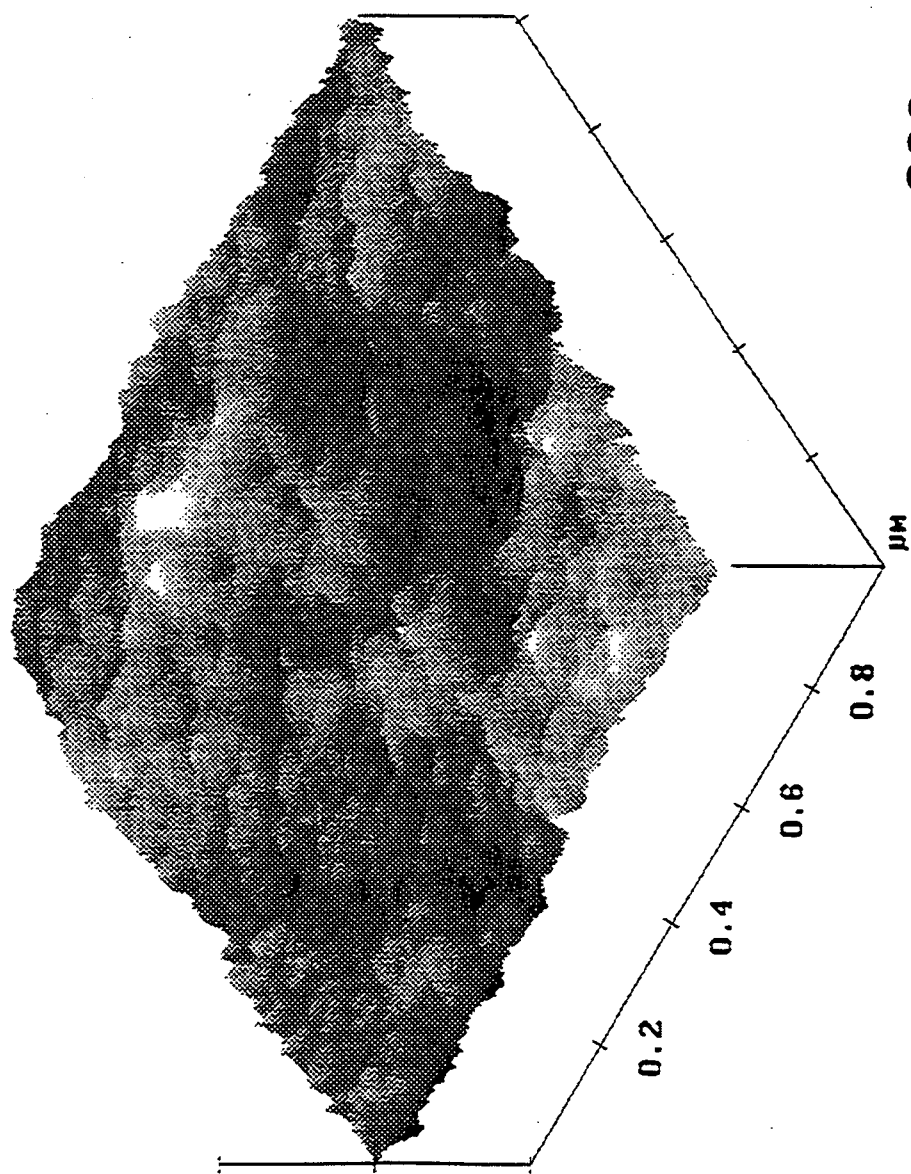
x = 200 nm / div
z = 5.0 nm / div

(a) Clean PES

Figure 14: AFM micrograph of oxygen plasma treated PES.

(b) O$_2$ PLASMA / PES

x = 200 nm / div
z = 200 nm / div
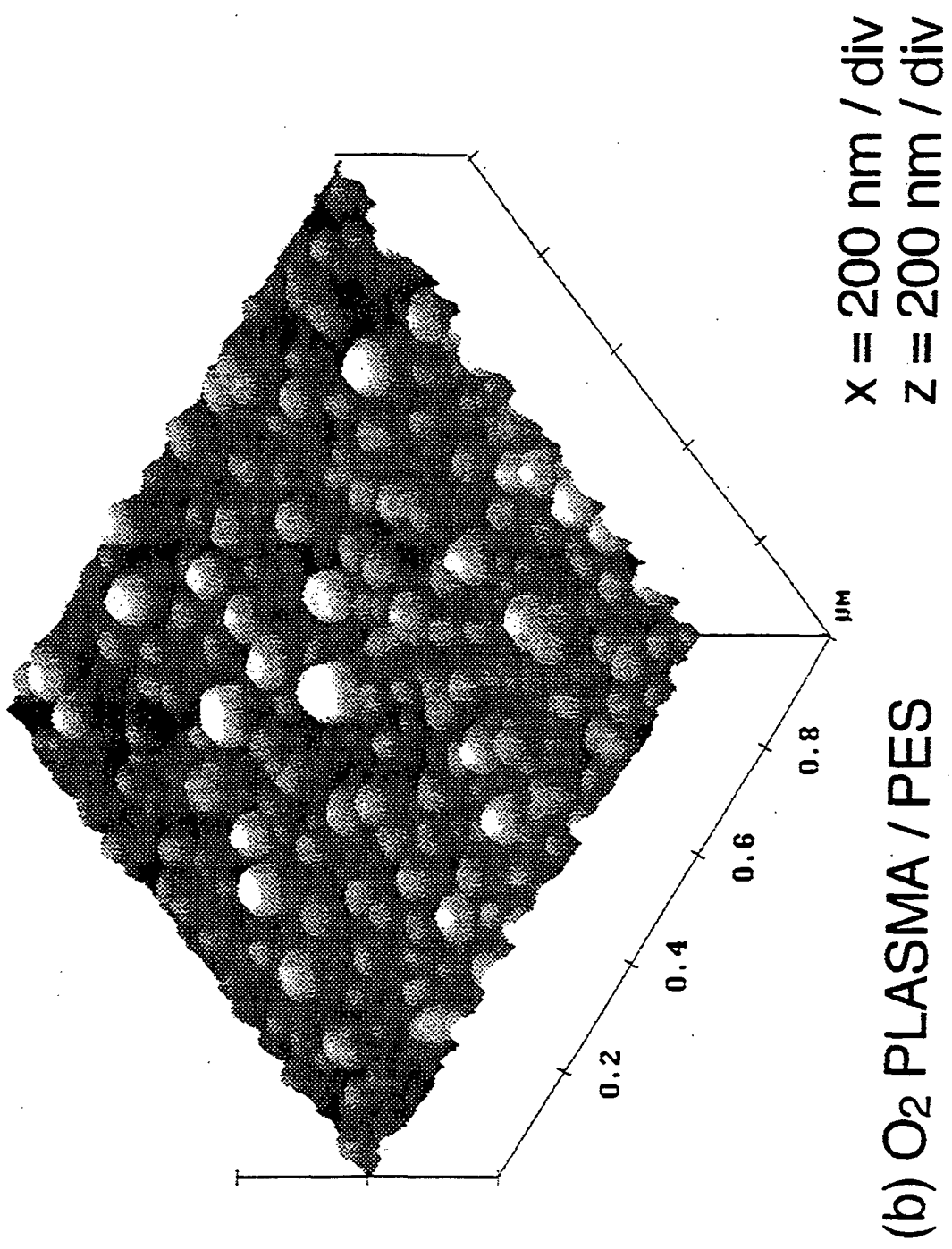
Figure 15: AFM micrograph of hydrogen plasma treated PES.
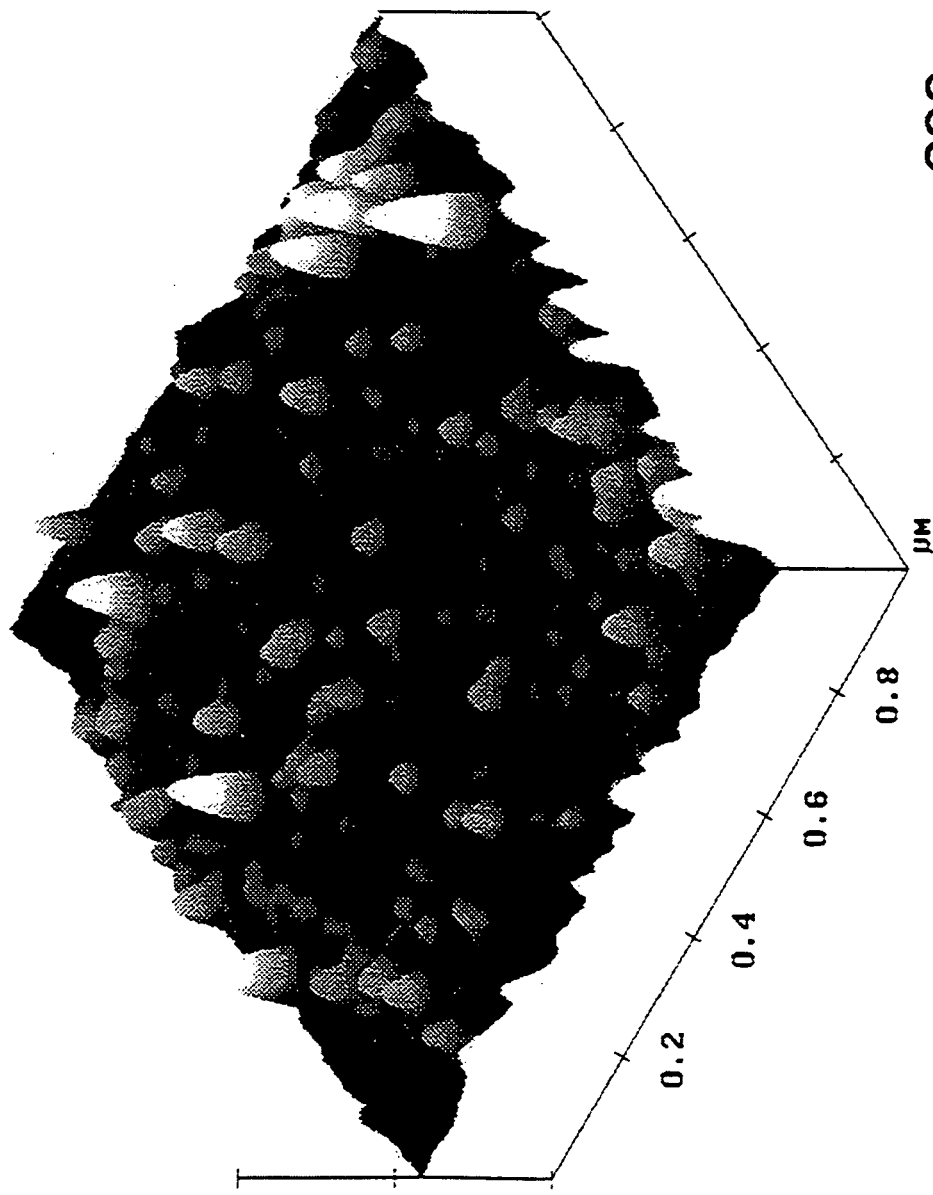
(c) H₂ PLASMA / PES

x = 200 nm / div
z = 50 nm / div

Figure 16: AFM micrograph of helium plasma treated PES.
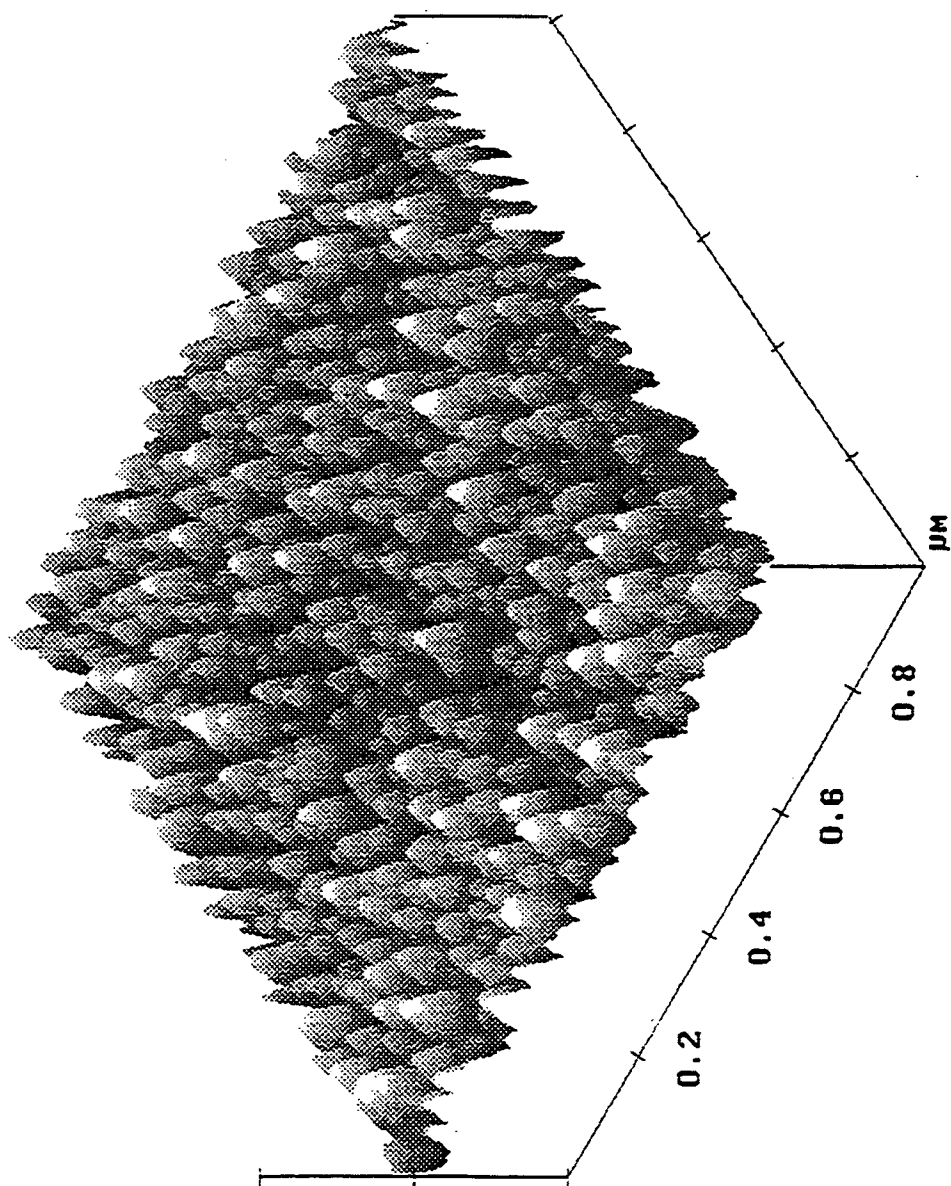
(d) He PLASMA / PES

x = 200 nm / div
z = 100 nm / div

Figure 17: AFM micrograph of neon plasma treated PES.

(e) Ne PLASMA / PES

x = 200 nm / div
z = 20 nm / div

72
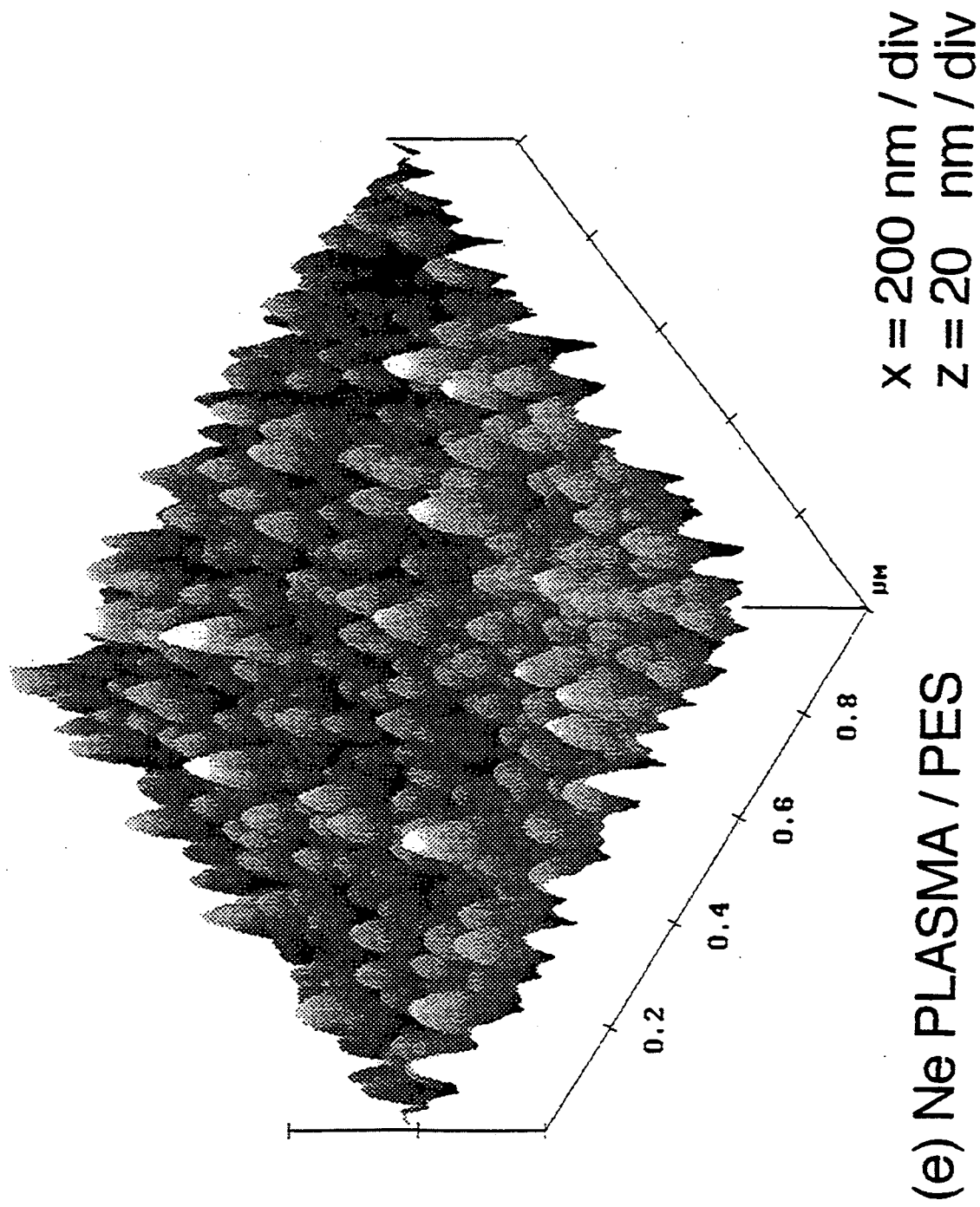
Figure 18: AFM micrograph of argon plasma treated PES.

x = 200 nm / div
z = 50 nm / div

(f) Ar PLASMA / PES

73
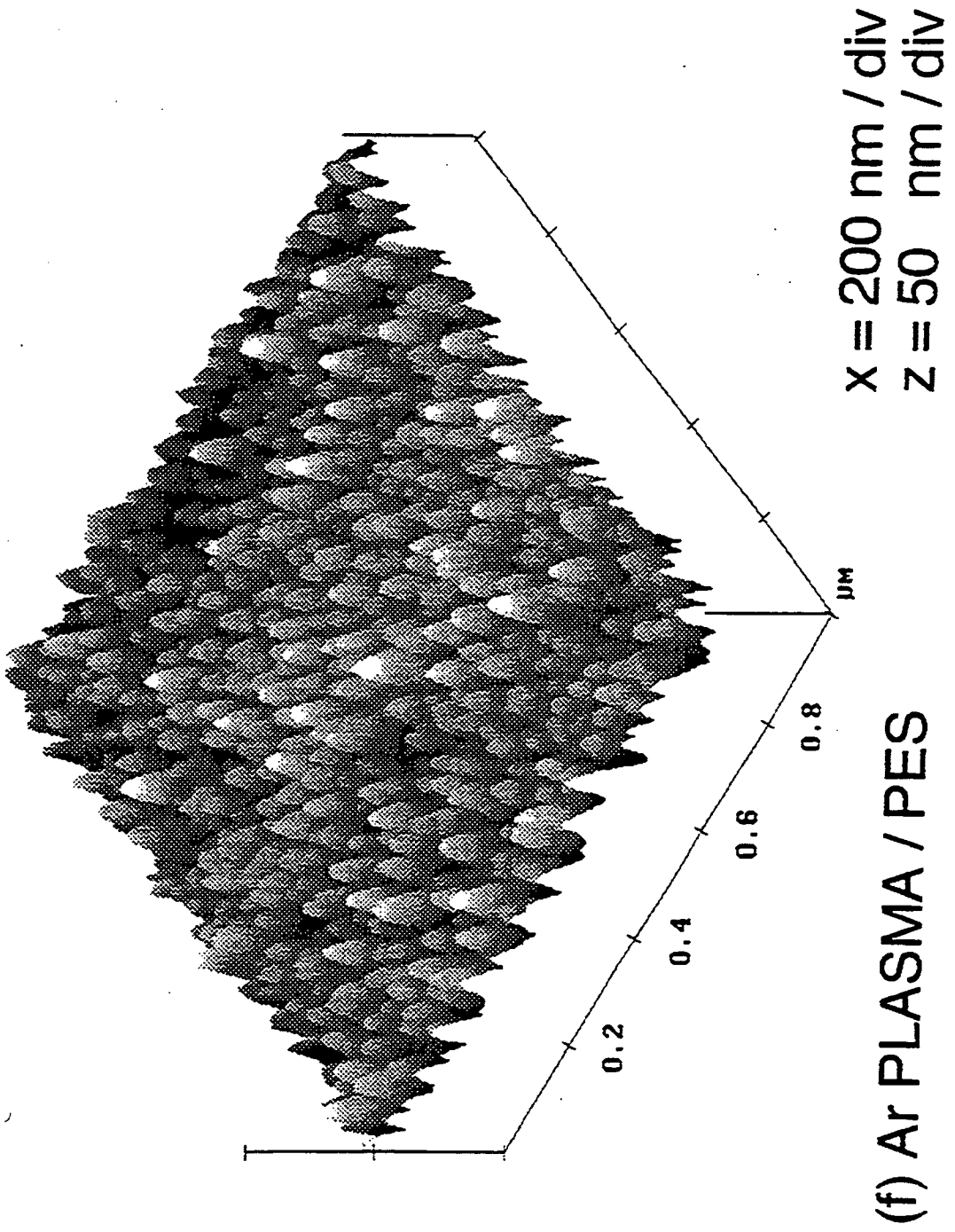
Figure 19: AFM micrograph of CF₄ plasma treated PES.
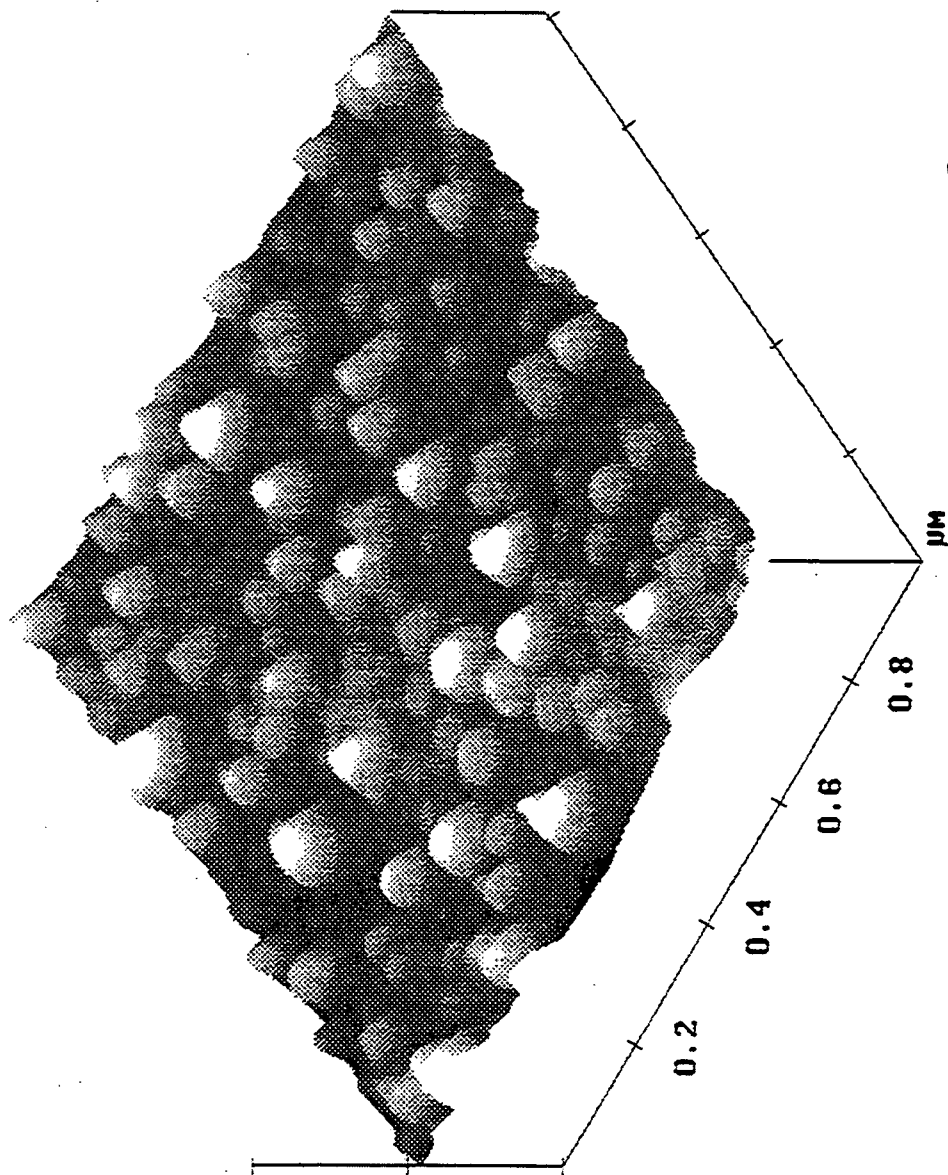
x = 200 nm / div
z = 100 nm / div

(g) CF₄ PLASMA / PES

74

Table 3: Summary of peak fits S(2p) spectra following plasma modification (20 W, 5 mins).

Plasma Treatment	PSF		PES	
	% -C-S-O-	% O=S=O	% -C-S-O-	% O=S=O
Theoretical	0.0	100.0	0.0	100.0
Untreated	0.0	100.0	0.0	100.0
O_2	0.0	100.0	0.0	100.0
H_2	28.9±2.8	71.1±2.8	12.8±0.1	87.2±0.1
He	11.0±0.1	89.0±0.1	5.6±0.6	94.4±0.6
Ne	8.6±2.9	91.4±2.9	3.2±1.1	96.8±1.1
Ar	5.9±0.4	94.1±0.4	3.4±0.6	96.7±0.6

2. 3. 4 Inert Gas Plasma Treatment (Helium, Neon, and Argon)

Modification of PSF and PES by helium, neon and argon glow discharges yield very similar chemical changes at the polymer surface, both polymers show an increase in the oxygen content and a reduction in both carbon and sulfur content for the inert gas plasma treatments. This behaviour is similar to that reported previously for the argon glow discharge treatment of polysulfone[22]. A slight shoulder towards lower binding energy is evident in the S(2p) spectra of the polymers, which can be attributed to the occurrence of a small level of sulfone reduction, table 3. It is interesting to note that an additional gaussian peak is required to fit the C(1s) envelope of PSF, corresponding to the carbonate functionality at 290.4 eV, compared to PES.

There are a number of plausible explanations for the observed increase in oxygen content during surface modification by these non-oxygen containing glow discharges:-

(i) reaction of the activated polymer surface with the atmosphere during sample transfer to the XPS spectrometer

(ii) main chain scission is known to occur photochemically[30], which could lead to preferential elimination of sulfone groups attached to chromophoric phenyl species

(iii) sputtered oxygen species may subsequently recombine with different sites at the polymer surface

(iv) surface rearrangement

The amount of sulfur retained at the polymer surface for PSF and PES follows the same trend , i. e., argon ~ neon > helium. This is not what might have been expected in terms of a simple momentum transfer sputtering model.

All three types of inert gas plasma treatments of PSF and PES result in the growth of a uniform columnar/globular surface topography, this effect being greatest with helium plasmas, figures 9-11, 16-18, table 4. Much larger globular features have been observed previously during corona treatment of polypropylene[31,32] which was attributed to the agglomeration of low-molecular-weight oxidized material[33] which could be washed off with solvent. This possibility of low molecular weight material was ascertained by comparing the AFM micrographs of noble gas plasma treated PSF, PES surfaces before and after washing with water, isopropyl alcohol, and hexane. No change in the surface texture was observed following rinsing in these solvents. Helium glow discharge causes the greatest chemical and physical disruption at the surface of PSF and PES, table 4.

Table 4 : AFM data of plasma treated PSF and PES.

Gas Treatment	PSF			PES		
	RMS Roughness/ nm	Particle Height/ nm	N° particles μm^2	RMS Roughness/ nm	Particle Height/ nm	N° particles μm^2
Clean	1.012	-	-	0.4	-	
O_2	6.6	-	-	9.8	-	
H_2	1.2	-	-	5.1	-	
He	11.0	32.6±5.4	388	11.0	31.5±5.4	445
Ne	4.0	6.0±1.6	295	3.0	6.6±1.7	380
Ar	7.8	23.6±3.2	492	5.5	15.5±2.0	452
CF_4	0.6	-	-	2.5	-	

2. 3. 5 CF_4 Plasma Treatment

CF_4 plasma treatment of PSF and PES results in a substantial amount of fluorination at the surface (approximately 50%), tables 1 and 2. This is accompanied by a dramatic change in the C(1s) XP spectrum with CF_2 functionalities being the predominant fluorine moiety[34]. The C(1s) peak was not fully deconvoluted due to overlapping peaks between carbon bonded to sulfur , oxygen and fluorine, however $\underline{C}F_2$ and $\underline{C}F_3$ peaks can be fitted since they appear at higher binding energies and do not overlap with the functionalities mentioned. For PSF these peaks were found to correspond to 13.6% $\underline{C}F_3$ (293.6 eV) and 34.6% $\underline{C}F_2$ (291.2 eV), $\underline{C}F$-CF_n (289.5 eV) functionalities were also present[20]. The 1:1 O(1s) doublet can no longer be resolved. Carbon bound to fluorine functionalities for PES were found to be 13.0% $\underline{C}F_3$ (293.6 eV), 40.9% $\underline{C}F_2$ (291.2 eV) accompanied by a degree of $\underline{C}F$-CF_n (289.5 eV) functionalities which overlap in binding energy with

oxygenated carbon centres[20]. The 2:1 O(1s) doublet can no longer be resolved. There was a strong attenuation of the S(2p) feature for both PSF and PES. The degree of fluorination of PES at the surface was greater than that for PSF.

Contrary to what might have been expected in terms of the highly reactive nature of CF_4 glow discharges, the treated PSF and PES surfaces (figures 12, 19 respectively) exhibit the smoothest texture amongst this series of feed gases, table 4. Similar behaviour has been previously reported using SEM characterization of polymer surfaces which have been exposed to pure CF_4 plasmas[35,36].

2.4 DISCUSSION

There are a range of energy transfer mechanisms in operation within a low pressure RF discharge, these include electron acceleration in the bulk of the plasma, electron deflection from sheath potentials, and ion and electron acceleration in the wall boundary sheaths[37]. For surface modification, the most important criteria of a glow discharge are the nature, the arrival rates, and the angular and energy distributions of the species impinging upon the surface[38]. Electron impact processes influence the density of ions, radicals, metastables, and photons contained within the plasma.

Inert gas plasmas interact with organic substrates via a direct energy transfer component arising from ions and metastables down to ~ 10 Å, and a radiative transfer component consisting of vacuum ultraviolet (VUV) photo-irradiation which can penetrate up to ~ 10 μm below a polymer surface[39-41]. The direct energy surface component is a consequence of species such as ions, neutrals and metastables bombarding the sample surface and transferring energy. The mean free path of an electron at near zero kinetic energy is small, therefore the contribution to the direct energy

78

component is small and is dominated by phonon excitation. In a radio-frequency discharge the output is mainly in the form of line spectra[34] (the transitions of atoms in the first excited state to the ground state, giving rise to a two line series designated I and II). In general, the M I emission lines are the most intense for low pressure noble gas plasmas (where M is the noble gas)[41,42], these are listed in table 5.

Table 5: Most intense vacuum UV emission lines for inert gas plasmas[41].

Noble Gas (M)	M I Emission Lines / nm	M II Emission Lines / nm	M_2* Continuum Emission / nm
He	58.4	30.4	58 - 110
Ne	73.3, 74.4	46.1, 46.2	74 - 100
Ar	104.8, 106.7	92.0, 93.2	105 - 155

On moving to heavier noble gas atoms (increasing atomic number), the observed trend in the level of surface roughening for PSF and PES is contrary to what might be expected in terms of a direct energy (momentum) transfer viewpoint[43]. It is however consistent with the radiative energy transfer model[41,44,45]. As the inert gas series is descended, the M I resonance lines become less energetic (wavelength increases), table 5, which will result in lower photochemical ablation. For heavier noble gas atoms, momentum transfer effects will make a greater contribution towards surface roughness. The competitive nature of these two effects is shown in table 4, Ne appears to have an intermediate roughness between the values obtained for

treatment with Ar and He plasmas for PSF and PES. He has the highest energy MI lines, however Ar has a greater mass therefore giving rise to a greater surface roughness value compared to Ne.

Oxygen plasmas contain a large number of different species such as atomic oxygen, metastables, singlet oxygen O_2 ($^1\Delta_g$) and a small concentration of ozone[46]. This can lead to a large number of chemical reactions, however, oxygen atoms are generally regarded as being the primary reactive species in conjunction with vacuum UV surface activation in an oxygen plasma[47,48,49]. This combination produces the most oxidized surface for both PS and PES in the experiments undertaken. Such a high level of surface oxidation during oxygen plasma treatment has been reported for a number of phenyl containing polymers, e.g. polyetherketone[50], polystyrene[51,52], polyetheretherketone[25], polyparaphenylene[53]. This can be attributed to the vacuum UV photoexcitation of the aromatic centres[27,52].

The extent of sulfone reduction of PSF in a hydrogen glow discharge is much greater than that found for the structurally related polyethersulfone. Such an observation can be attributed to the difference in the chemical structure. The pendant methyl groups in the bisphenol-A unit in polysulfone have an intrinsically lower chemical stability[30]. These aliphatic groups are much more reactive in hydrogen donation than the aromatic ring and can be readily explained in terms of the bond energies involved. To remove hydrogen from a phenyl ring requires 112 kcal/ mol, whereas to break C-H bond requires 104 kcal/mol[54]. Similar reasoning may be used to explain the greater sulfone reduction observed for the inert gas plasma treatment of PSF compared to PES.

A pure CF_4 glow discharge can be primarily regarded as a source of fluorine atoms with a low concentration of CF, CF_2, and CF_3 radicals[55-59]. This is supported by electron impact experiments with CF_4, which indicate that F atoms are the primary species[60]. Substitution of hydrogen atoms in C-

H bonds by fluorine to yield HF and fluorinated polymer is energetically favourable[61-63]. A pure CF_4 plasma displays poor etching behaviour[64] and it is generally considered to result in surface modification rather than plasma polymerization[63]. This is a consequence of the high F/C ratio in the gas which gives rise to many excited F* species in the plasma[65]. The fluorine gas is activated by UV light[61]. The extent of fluorine incorporation into the polymer surfaces is found to be greater than theoretically predicted on the basis of a straightforward exchange of hydrogen atoms for fluorine atoms, table 6. CF_4 glow discharges are also capable of imparting crosslinking[66] and the slightly higher carbon content compared to the expected theoretical value following substitution of hydrogen by fluorine is consistent with this. Hydrogen and sulfur atoms are probably removed from the polysulfone surface as HF and SF_6 respectively, however the reaction of fluorine atoms with oxygen will be energetically less favourable. This is consistent with fluorine atoms attacking the aromatic group in phenyl containing polymers[57,67,68].

Table 6: Comparison of the theoretical and experimental values for completely fluorinated PSF and PES (20 W, 5 min)

Elemental %	PSF		PES	
	Theoretical Fluorinated	Experimental Fluorinated	Theoretical Fluorinated	Experimental Fluorinated
C	39.4	41.1±0.1	38.3	40.9±0.8
O	5.8	6.9±0.8	12.8	10.3±0.1
S	3.9	0.3±0.1	8.5	1.2±0.1
F	50.9	51.5±1.0	40.4	47.5±1.1

The results for CF_4 treatment of polysulfone are very similar to those found for the direct fluorination of polysulfone by fluorine gas[69]. The experiments found that the aromatic rings became fully saturated after fluorination and that there was an attenuation in the sulfur content due to sulfur ejection accompanying fluorination. This suggests that a CF_4 glow discharge acts as a fluorinating agent by attacking the phenyl rings by substitution of the hydrogen atoms with fluorine atoms. The greater extent of fluorination of PES than PSF may be explained by this model.

The smoother surface of the CF_4 plasma treated polymers compared to the untreated surfaces suggests that the highly reactive F atoms etch the surface uniformly, giving rise to the surface topography observed.

2.5 CONCLUSIONS

Non-equilibrium glow discharge treatment of polysulfone using non-polymerizable gases results in surface modification. The type of modification depends upon the feed gas employed for the glow discharge. Oxygen plasma treatment gives rise to the highest level of oxidation. A hydrogen glow discharge treatment causes simultaneous loss of both oxygen and sulfur from the surface. Inert gas plasma treatment promotes the formation a uniform columnar texture accompanied by a small degree of oxidation at the surface. Extensive fluorination of PSF and PES occurs with CF_4 glow discharge treatment, which is thought to take place by substitution of C-H bonds by C-F bonds in the polymeric structure. There are slight differences in the extent of modification between the two polymers which can be explained in terms of the different chemical structure.

2. 6 REFERENCES

1.   Babari, T. A.; Koros, W. J.; Paul, D. R. *J. Polym. Sci. Phys. Ed.,* **1988,** *26,* 709.

2.   Goosey, M. T. Ed. *"Plastics for Electronics",* Elsevier Applied Science Publishers, 1985.

3.   MacDermott, C. P. *"Selecting Thermoplastics for Engineering Applications",* Dekker, 1984.

4.   Margolis, J. M. Ed. *"Engineering Thermoplastics for Engineering Applications",* Dekker, 1984.

5.   Staude, E.; Breitback, L. *J. App. Polym. Sci.,* **1991,** *43,* 559.

6.   Hinke, E.; Staude, E. *J. Appl. Polym. Sci.,* **1991,** *42,* 2951.

7.   Aminabhavi, T. M.; Aithal, U. S. *Rev. Macromol. Chem. Phys.,* **1991,** 117.

8.   Yau, W. W.; Jiang, Y. Q.; Jan, P. K. *Polym. Int.,* **1993,** *31,* 1631.

9.   Akzy, M.; Cracknell, J. G. *J. Appl. Polym. Sci.,* **1994,** *52,* 663.

10.   Maes, C.; Devaux, C.; Legras, R.; Passons, I. W.; McGrail, P. T. *J. Polym. Sci. Phys. Ed.,* **1994,** *32,* 3171.

11.   Asfarajau, K.; Segui, Y.; Aurelle, Y.; Abidine, N. *J. Appl. Polym. Sci.,* **1991,** *43,* 271.

12.   Wade, W. J.; Mammone, R. J.; Binder, M. *J. Appl. Polym. Sci.,* **1991,** *43,* 589.

13.   Huttinger, C. J.; Krekel, G.; Zielke, U. *J. Appl. Polym. Sci.,* **1994,** *51,* 737.

14.   Shard, A. G.; Munro, H. S.; Badyal, J. P. S. *Polym. Commun.,* **1991,** *32,* 152.

15.   Zhong, Q.; Inniss, D.; Kjoller, K.; Elings, V. B. *Surface Science.* **1993,** *290,* L688.

16.   Ehrlich, C. D.; Basford, J. A. *J. Vac. Sci. Technol.,* **1992,** *A10,* 1.

17. Clark, D. T.; Dilks, A.; Peeling, J.; Thomas, H. R. *Trans. Faraday Soc. Faraday Disc.,* **1975,** *60,* 183.

18. Clark, D. T.; Thomas, H. R. *J. Polym. Sci. Chem. Ed.,* **1978,** *16,* 791.

19. Evans, J. F.; Gibson, J. H.; Moulder, J. F.; Hammond, J. S.; Goretzki, H. *Fresenius Z. Anal. Chem.,* **1984,** *319,* 841.

20. Beamson, G.; Briggs, D. *"High Resolution XPS of Organic Polymers: The Scienta ESCA300 Database",* J. Wiley & Sons, Chichester, 1992.

21. Clark, D. T.; Adams, D. B.; Dilks, A.; Peeling, J.; Thomas, H. R. *J. Electron Spectrosc.,* **1976,** *8,* 51.

22. Yasuda, H.; Marsh, H. C.; Brandt, E. S.; Reilley, C. N. *Am. Chem. Soc. Polym. Pr.,* **1975,** *16,* 142.

23. Clark, D. T.; Feast, W. J.; Ritchie, I.; Musgrave, W. K. R.; Modena, M.; Ragazzini, M. *J. Polym. Sci. Polym. Chem. Ed.,* **1974,** *12,* 1049.

24. Clark, D. T., *Makromol. Chem., Macromol. Symp.,* **1993,** *75,* 1.

25. Munro, H. S.; Clark, D. T. *Polym. Deg. Stab.,* **1985,** *11,* 225.

26. Munro, H. S.; Clark, D. T. *Polym. Deg. Stab.,* **1985,** *11,* 211.

27. Wells, R. K.; Drummond, I. W.; Robinson, K. S.; Street, F. J; Badyal, J. P. S. *Polymer,* **1993,** *34,* 3611.

28. Brauman, S. K. *J. Polym. Sci. Polym. Chem. Ed.,* **1992,** *30,* 1247.

29. Ehlers, G. F. L.; Fisch, K. R.; Powell, W. R *J. Polym. Sci. Chem. Ed.,* **1969,** *A1, 7,* 2955.

30. Yamashita, T.; Tomitaka, H.; Kudo, T.; Horie, K.; Mita, I. *Polym. Degrad. Stab.,* **1993,** *39,* 47.

31. Kim, C.Y.; Goring, D.A.I., *J. Appl. Polym. Sci.,* **1971,** *15,* 1357.

32. Strobel, J.M.; Strobel, M.; Lyons, C.S.; Dunatov, C.; Perron, S. J. *J. Adhesion. Sci. Techol.* **1991,** *5,* 119.

33. Garbassi, F.; Morra, M.; Occhiello, E.; Barino L.; Scordamaglia, R., *Surf. Interface. Sci.,* **1989,** *14,* 585.

34. Poncin-Epaillard, F; Pompepui, B; Brosse, J *J. Polym. Sci. Chem. Ed.,* **1993,** *31,* 2671.

35. Kogoma, M., Kasai, H., Takahashi, K., Moriwaki, T., Okazaki, S. *J. Phys. D. Appl. Phys.*, **1987**, *20*, 147.

36. Sarmadi, A. M.; Kwon, Y. A. *Tex. Chem. Col.*, **1993**, *12*, 33.

37. Egitto, F. D., Matienzo, L. J. *Society of Vacuum Coaters, 36th Annual Technical Conference Proceedings,* 1993, 10.

38. Chapman, B. *"Glow Discharge Processes"*, Wiley, New York, 1980.

39. Clark, D. T.; Dilks, A. *J. Polym. Sci. Polym. Chem. Ed.*, **1977**, *15*, 2321.

40. Clark, D. T.; Dilks, A. *J. Polym. Sci. Polym. Chem. Ed.*, **1977**, *16*, 911.

41. Clark, D. T., Dilks, A. *J. Polym. Sci. Polym. Chem. Ed.*, **1980**, *18*, 1233.

43. Wells, R. K.; Ryan, M. E.; Badyal, J. P. S. *J. Phys. Chem.*, **1993**, *97*, 12879.

42. Samson, J. A. R. *"Techniques of Vacuum Ultraviolet Spectroscopy"*, Wiley, New York, 1967.

44. Liston, E. M. *Proc. IX Internat. Symp. on Plasma Chem.*, Pugnochiuso, Italy, 1989, L7.

45. Takacs, G. A.; Vukanovic, V.; Tracy, D.; Chen, J. X.; Egitto, F. D.; Matienzo, L. J.; Emmi, F. *Polym Degrad. and Stabil.*, **1993**, *40*, 73.

46. McTaggart, F. K. *"Plasma Chemistry in Electrical Discharges"*, Elvesier, 1967.

47. Hollahan, J. R.; Bell, A. T. Eds. *"Techniques and Applications of Plasma Chemistry"*, Wiley, New York, 1974, Chapter 1.

48. Shard, A. G.; Badyal, J. P. S. *J. Phys. Chem.* **1991**, *95*, 9436.

49. Joubert, O.; Pelletier, J.; Arnal, Y. *J. Appl. Phys.* **1989**, *65*, 5096.

50. Onyiriuka, E. C. *J. Vac. Sci. Technol.*, **1993**, *A11*, 2941.

51. Wells, R. K.; Drummond, I. W.; Robinson, K. S.; Street, F. J.; Badyal, J. P. S. *J. Adhes. Sci. Technol.*, **1993**, *7*, 1129.

52. Shard, A. G.; Badyal, J. P. S. *Macromolecules*, **1992**, *25*, 2053.

53. Tepermeister, I.; Swain, H. H. *J. Vac. Sci. Technol.*, **1992**, *A10*, 3149.

85

54. McMurray, J. *"Organic Chemistry"*, Brooks/Cole Publishing Company, 1988.

55. Zheng Jipuing Xu, *J. Appl. Polym. Sci.*, **1993**, *48*, 231.

56. Occhiello, E.; Morra, M.; Garbassi, F.; Bargon, J. *Appl. Surf. Sci.*, **1989**, *36*, 285.

57. d'Agostino, R.; Cramarossa, F.; DeBenedictis, S. *Plasma Chem. Plasma Processing*, **1982**, *2*, 213.

58. Truesdale, E. A.; Smolinsky, G. *J. Appl. Phys.*, **1979**, *50*, 6594.

59. Plumb, I. C.; Ryan, K. R. *Plasma Chem. Plasma Process*, **1986**, *6*, 205.

60. Kay, E. *Proceed. Internat. Ion Engineering Congress - ISIAT 83 & IPAT 83*, Kyoto, **1983**, 1657.

61. Inagaki, N.; Tasaka, S.; Mori, K. *J. Appl. Polymer Science.* **1991**, *43*, 581.

62. Strobel, M.; Corn, S.; Lyons, C. S.; Korba, G. A. *J. Polym. Sci. Chem. Ed.*, **1985**, *23*, 1125.

63. d'Agostino, R.; Cramarossa, F.; Fracassi, F.; Illuzzi, F. *in "Plasma Deposition, Treatment, and Etching of Polymers,"*, Academic Press Inc., San Diego, 1990, Chapter 2.

64. Egitto, D. F.; Vukanovic, V.; Taylor, G. N. *in "Plasma Deposition, Treatment, and Etching of Polymers"*, Academic Press Inc., San Diego, 1990, Chapter 5.

65. Iriyama, Y; Yasuda, H *J. Polym. Sci. Chem. Ed.*, **1992**, *30*, 1731.

66. Inagaki, N.; Kobayashi, N.; Matsushima, M. *J. Memb. Sci.*, **1988**, *38*, 85.

67. Strobel, M.; Lyons, C. S. *Polymeric Materials Science and Engineering, ACS Symposium Series No. 56,* , Amer. Chem. Soc. Washington D.C., 1987,p.232

68. Yasuda, T.; Okuno, T.; Yoshida, K.; Yasuda, H. *Polymeric Materials Science and Engineering, ACS Symposium Series No. 56*, Amer. Chem. Soc. Washington D.C., 1987, p. 240.

69. Mohr, J. M.; Paul, D. R.; Pinnau, I.; Koros, W. J. *J. Memb. Sci.*, **1991**, *56*, 77.

70. Dilks, A. *Ph.D. Thesis*, University of Durham, 1977.

Chapter Three

Non-equilibrium Glow Discharge Fluorination

of Polymer Surfaces

Chapter Three

Non-equilibrium Glow Discharge Fluorination of Polymer Surfaces

3.1 INTRODUCTION

Chapter two illustrated that two similar polymers, PES and PSF, react differently to an identical plasma treatment. The CF4 plasma treatment was particularly demonstrative of this result. This section further investigates how the chemical structure of the polymer substrate influences the extent of fluorination when subjected to a tetrafluoromethane non-equilibrium glow discharge.

3.1.1 Background

It is well documented that plasma treatment of polymers results in modification of the surface. The extent of modification depends partly upon the the gas used for the treatment. Gases used for plasma modification can be classified as follows:-

1) Chemically non-reactive plasma.

2) Chemically reactive plasma.

3) Polymer forming plasma.

Inert monatomic gases are examples of those which give rise to chemically non-reactive plasmas. Chemically reactive plasmas are formed from inorganic or organic molecular gases such as oxygen or nitrogen. Tetrafluoromethane results in such a plasma[1,2], thus in the plasma state there will be a reaction with the polymer sample but polymerization does not occur.

CF$_4$ plasmas[1,3,4,5] are often used as a source of atomic fluorine which can participate in chemical reactions. However a CF$_4$ plasma can also promote crosslinking[6] and be used as an etching enhancer[7].

3. 1. 2 Gas Mixtures

Development of the semiconductor industry over the past few decades has led to the requirement of techniques enabling higher circuit densities with low defect densities to be formed, in other words, precise process control. In the past chemical etching was used, however this method gave rise to no preferential etch direction and isotropic circular profiles. Plasma etching enables the vertical etch rate to exceed the horizontal etch rate allowing anisotropic etch profiles to be formed[8].

If a CF$_4$ plasma has a small amount of oxygen added, then the etch rate increases. This is due to shifts in the atomic concentration of the plasma. The oxygen atoms react with unsaturates, giving rise to F atoms and depleting polymer forming species, CF$_x$. The oxygen can be considered as burning the fluorocarbon radicals[9]. The essential reactions occurring in a CF$_4$/O$_2$ plasma are shown in figure 1.

Figure 1: Reactions occurring in a CF_4/O_2 plasma[8].
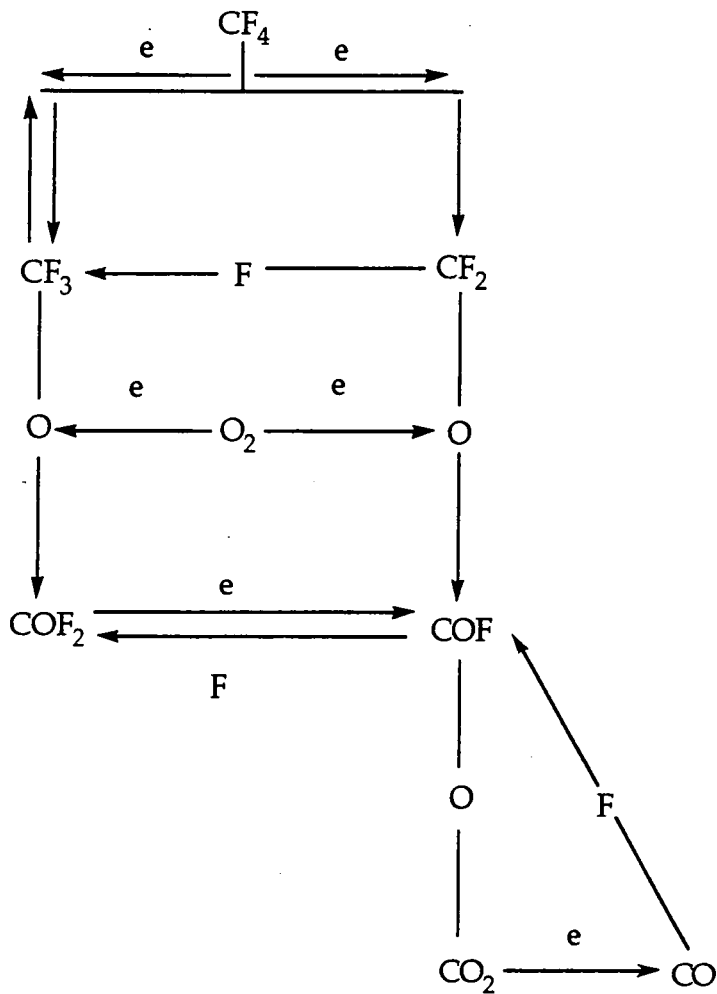
The selectivity of plasma etching can be enhanced by choosing an appropriate gas mixture. The gas mixture can be tailored for the particular application therefore achieving the selectivity required[10,11,12].

3. 1. 3 Pure CF_4 Gas Plasma Treatment

### 3. 1. 3. 1 *CF_4 Dissociation Mechanism*

Pure CF_4 plasma treatment of polymers often results in fluorination of the surface and is frequently used as a source of fluorine atoms. In general, fluorocarbon plasmas can result in two types of reaction:-

(i) Fluorination.

(ii) Plasma polymerization.

The reaction of a fluoroplasma has one main criterion which is the fluorinated carbon to atomic fluorine ratio, CF_x/F [13,14]. The CF_x radicals are responsible for the building blocks in plasma polymerization. The RF accelerates electrons by means of an oscillating field, which causes bond cleavage and ionization. The radicals are amongst the many species formed by ionization and account for the chemistry observed.[4] The dissociation of CF_4 gas in a plasma is as follows[15]

$$CF_4 \xrightarrow{\ e^- \ } F\cdot + CF_3 \xrightarrow{\ e^- \ } F\cdot + CF_2 \xrightarrow{\ e^- \ } F\cdot + CF$$
$$M \qquad\qquad M \qquad\qquad M$$
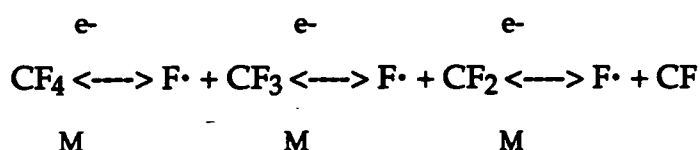
Species such as CF_2 and C_2F_2 have been detected in CF_4 plasmas by the use of absorption spectroscopy[16]. It was found that CF_2 species are present as approximately 1% of the source gas. These species were particularly enhanced in the plasma sheath region from direct dissociation of the source gas or by production through excited intermediate species.

Not only does the feed gas determine the plasma discharge but the experimental parameters such as electrode configuration and operating frequency are also important. Experiments[17] have shown that mechanisms of CF_4 decomposition and subsequent surface modification are closely dependent on the electrode geometry and excitation frequencies. Non-symmetrical configurations and low operating frequency result in the increase in the electron energy and enhance the dissociation of the plasma gas.

3. 1. 3. 2 *Surface Modification*

High CF_x/F ratios favour polymer formation[17] whilst low ratios favour etching and grafting. CF_4 plasmas tend to result in fluorination and grafting since there is a high concentration of fluorine atoms, ions and radicals relative to CF_x species. This can be observed in the CF_4 plasma treatment of polypropylene and polyethylene. Fluorine functionalities graft directly onto the surface of the polymers resulting in the formation of CF_3, CF_2 and CF species, which have been observed by XPS and IR spectroscopy.

A polymer surface can be made hydrophobic by the use of fluorocarbon plasmas[14]. Plasma treatment of nylon has shown that plasma treatment using fluorocarbon precursors results in a high contact angle regardless of the molecular size of the fluorocarbon used, i.e there is no dependence on the number of carbon atoms present in C_nF_{2n+2}. However, the durabililty of the plasma treated layer is dependent on the molecular size of the fluorocarbon. CF_4, although an efficient fluorination gas, resulted in poor durability of the plasma treated surface because of the short segment size implanted. The use of larger fluorocarbons[1] means that there are longer chains which can participate in greater and more complicated reactions. Regardless of the size of the fluorocarbon, at higher powers there is an increase in the active species and possible active surface sites. This is due to the higher energy input which results in possible crosslinking and ablation rather than simple fluorination.

It is thought that fluorination of polymer surfaces upon exposure to a CF_4 plasma proceeds via a substitution reaction[18,19]. Hydrogen is eliminated whilst fluorine or fluorocarbon groups are simultaneously activated by the plasma which can then fill the "vacancies". However the mechanism is as not as simple as it seems since fluorination by a CF_4 plasma depends not only on the feed gas but also on the polymer being treated[19]. The polymeric substrate complicates matters because elimination

of various species such as hydrogen and oxygen can take part in the reactions within the discharge resulting in the possible deposition of a plasma polymer.

3. 1. 4 Summary

Plasma treatment using CF_4 is a means of fluorinating the surface of a polymer without the utilisation of wet chemistry. It is a method which avoids the problem of toxic waste disposal. Not only is CF_4 used as a fluorinating reagent but it is often used in conjunction with oxygen in order to provide a way to maximize etching rates by increasing the atomic concentration. The ratio of carbon to fluorine atoms is fundamental in determining the type of reaction which occurs at the polymer-plasma interface, whether it is etching , fluorination or polymerization.

The influence of the chemical nature of a polymer substrate influences the level of surface fluorination during CF_4 non-equilibrium glow discharge treatment under comparable experimental conditions is examined in this chapter. A variety of polymers ranging from saturated to conjugated systems were chosen. The molecular structures of the various polymers employed in this study are summarised in figure 2.
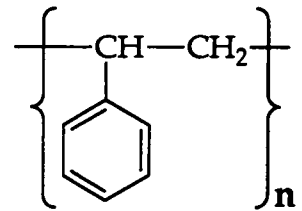
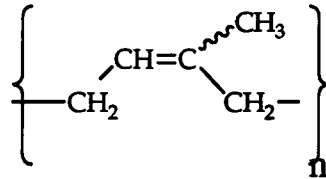Figure 2: Chemical structures of the polymeric substrates.
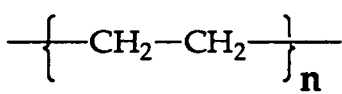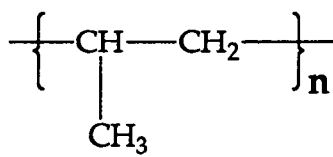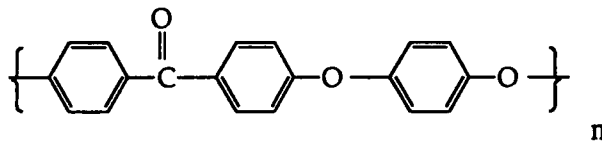

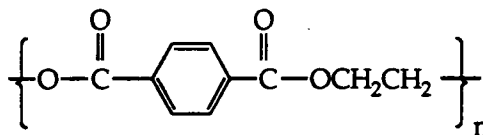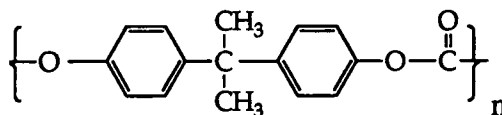POLYETHYLENE (PE)   POLYPROPYLENE (PP)   POLYSTYRENE (PS)

POLYISOPRENE (PIP)

POLYETHERETHERKETONE (PEEK)

POLYETHYLENE TEREPHTHALATE (PET)

POLYCARBONATE (PC)

The structures of PES and PSF are illustrated in Chapter 2, figure 1.

3. 2 EXPERIMENTAL

Small strips of additive-free low density polyethylene (ICI), polypropylene (ICI), polystyrene (Goodfellows), polyetheretherketone (ICI), polyethylene terephthalate (Hoechst), polycarbonate (General Electric Plastics), polyethersulfone (Westlake Plastics Company), and polysulfone (Westlake Plastics Company), were ultrasonically washed in a hexane / isopropyl alcohol mixture for 30 seconds and dried in air. Polyisoprene (Shell) was spin coated onto clean glass slides from 2% weight/volume toluene solution. High purity carbon tetrafluoride gas (99.7%, Air Products) was used for plasma treatment.

The plasma treatments were carried out as outlined in section 2. 2. The samples were analysed using XPS, the procedure is also decscribed in section 2. 2.

3. 3 RESULTS

XPS spectra of the clean saturated polyolefins (polyethylene and polypropylene) displayed a single C(1s) peak at 285.0 eV arising from $-\underline{C}_xH_y-$, Figure 3(a). Clean polystyrene exhibits a main C(1s) hydrocarbon peak at 285.0 eV and an additional high energy feature at ~291.6 eV (6% of the total C(1s) intensity) which is associated with low-energy π-π^* shake-up transitions that accompany core level ionization[20,21]. The C(1s) region of untreated polyisoprene comprises a main hydrocarbon peak, and a weak π-π^* shake-up feature (3% of the total C(1s) intensity) shifted by 6.5 eV towards higher binding energy. In the case of PET, polycarbonate, and polyetheretherketone, additional oxidised carbon centres were fitted[21], carbon adjacent to carboxylate ($>\underline{C}$-CO_2) at 285.7 eV, ether / alcohol / hydroperoxide linkage ($>\underline{C}$-O-) at 286.6 eV, carbonyl / double ether linkage ($>\underline{C}$=O / -O-$\underline{C}$-O-) at 287.9 eV, carboxylate (-O-$\underline{C}$=O) at 289.0 eV, and carbonate

(-O-$\underline{C}$O-O-) at 290.4 eV.   For polyethersulfone and polysulfone, carbon atoms attached to sulfone groups were also included at 285.6 eV[22,23].   In all cases, XPS peak fits for the untreated substrates were consistent with parent polymer structures[21].

Elemental concentrations following CF_4 plasma treatment of the various polymer substrates are compiled in table 1 (these are corrected for Mg K$\alpha_{3,4}$ satellites).   Experimentally measured F:C values are compared with the theoretically expected F:C ratios assuming a straightforward substitution of hydrogen by fluorine reaction pathway.   It is clearly evident that polymer substrates containing phenyl rings experience much greater fluorine incorporation compared to that found for the saturated polymers, figure 4 and table 1.   A small amount of oxygen incorporation was found in some cases, this is most likely to be due to reaction between trapped free radical sites at the surface with the laboratory atmosphere during sample transfer from the plasma chamber to the XPS spectrometer[24].

Table 1: Experimental and theoretical elemental percentages for various polymers after CF4 plasma treatment.

$$\Sigma = 100\%$$

Polymer	Type of Fluorination	%C	%O	%F	%S	Theoretical H:C (clean)	Experimental F:C
PE	Theoretical	33.3	-	66.7	-	2.00	1.18±0.03
	Experimental	44.3±0.2	3.1±2.1	52.6±1.9	-		
PP	Theoretical	33.3	-	66.7	-	2.00	1.11±0.08
	Experimental	45.0±1.7	5.5±0.1	49.5±1.6	-		
PIP	Theoretical	38.5	-	61.5	-	1.50	1.17±0.08
	Experimental	44.4±0.4	4.0±2.6	51.7±2.9	-		
PS	Theoretical	50.0	-	50.0	-	1.00	1.1±0.09
	Experimental	44.3±1.2	7.7±3.6	48.0±4.8	-		
PEEK	Theoretical	55.9	8.8	35.3	-	0.63	0.93±0.01
	Experimental	44.6±0.8	13.8±2.3	41.6±1.5	-		
PET	Theoretical	45.4	18.2	36.4	-	0.83	0.70±0.01
	Experimental	46.9±0.2	19.5±0.5	33.7±0.7	-		
PC	Theoretical	48.5	9.1	42.4	-	0.93	1.07±0.03
	Experimental	44.0±0.5	9.0±0.1	45.6±2.2	-		
PSF	Theoretical	50.0	7.4	40.7	1.9	0.81	1.26±0.04
	Experimental	41.1±0.1	6.9±0.8	51.5±1.0	0.3±0.2		
PES	Theoretical	50.0	12.5	33.3	4.2	0.67	1.21±0.04
	Experimental	40.9±0.8	10.3±0.1	47.5±0.8	1.2±0.1		

Figure 3 (a): C(1s) spectra of untreated polyethylene, polypropylene, polyisoprene, polystyrene, polyetheretherketone, polyethylene terephthalate, polycarbonate, polysulfone, and polyethersulfone.
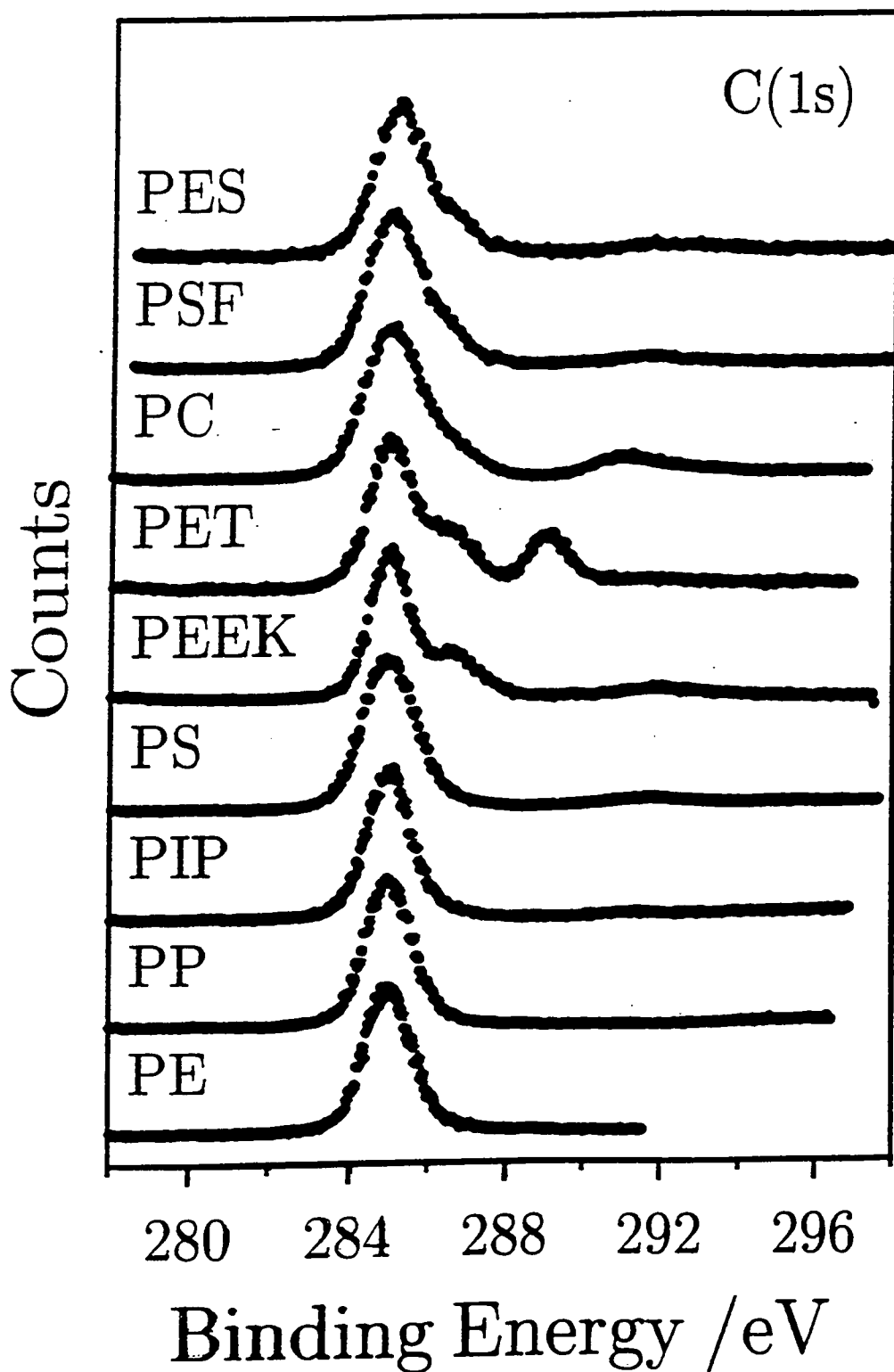
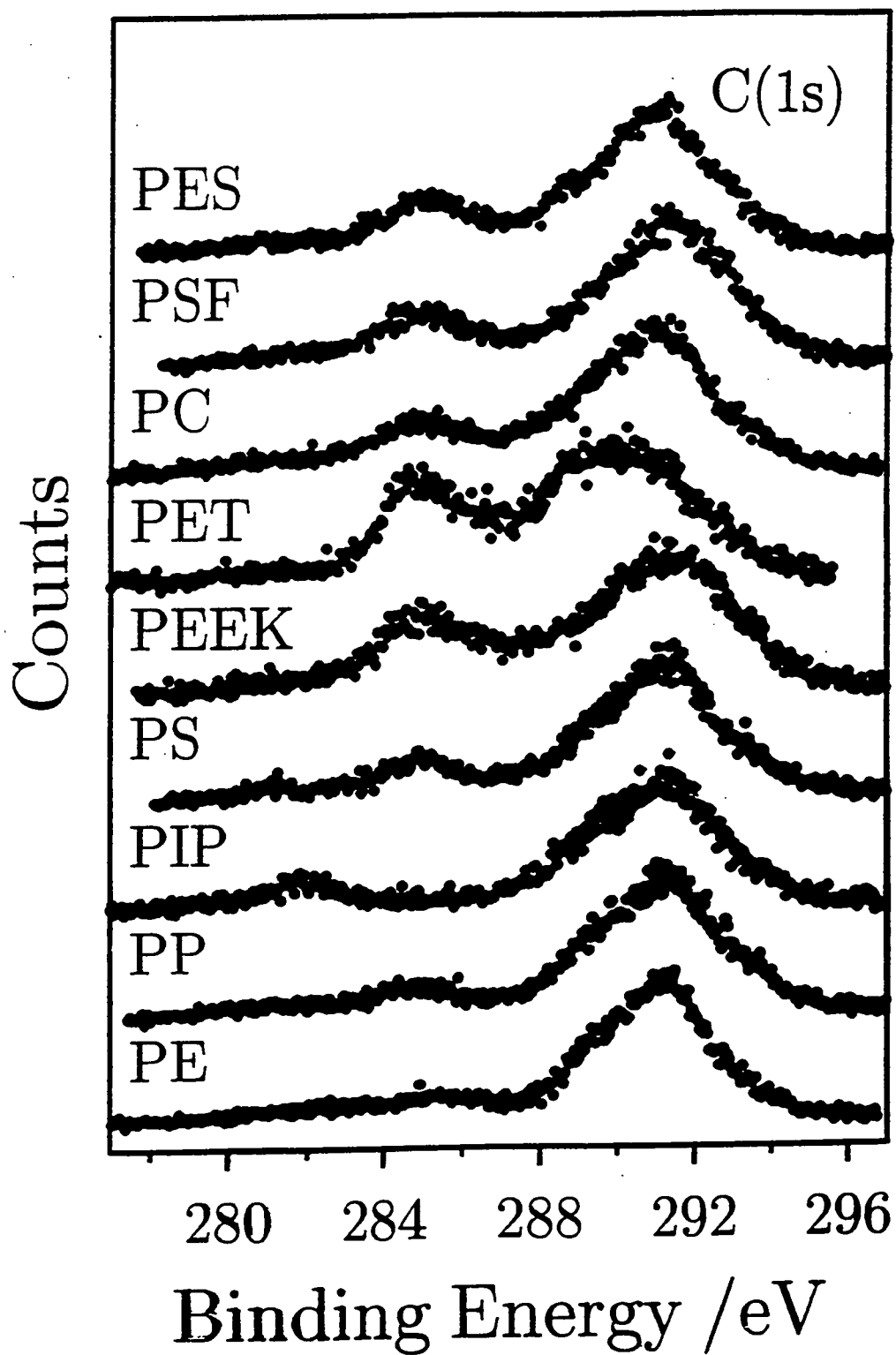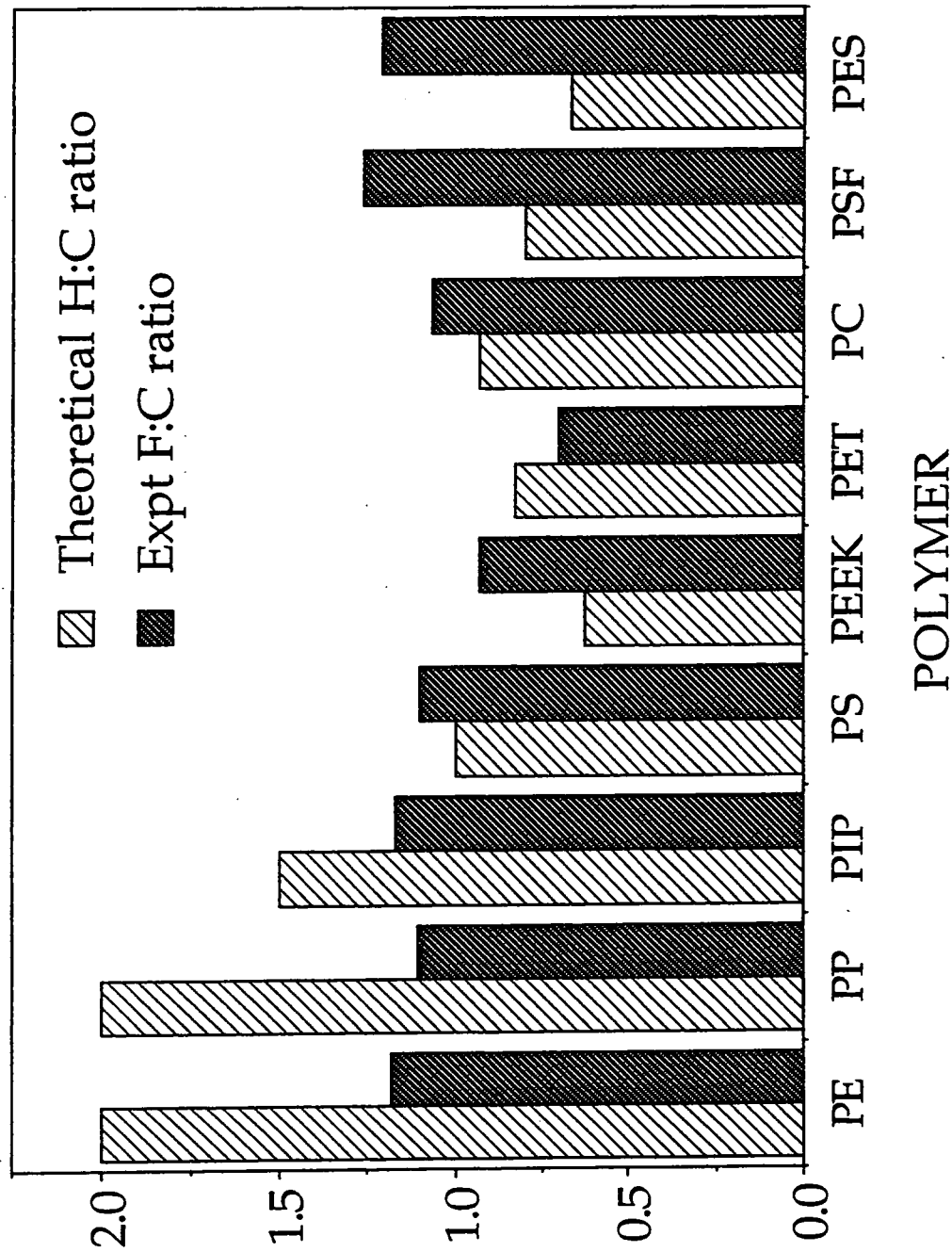Figure 3 (b): CF$_4$ plasma treated polymers (20 W, 5 min)

Figure 4: Comparison of theoretically calculated (assuming substitution of H atoms by F atoms) and experimentally measured levels of CF_4 plasma fluorination.

Deconvolution of the C(1s) envelopes following CF$_4$ electrical discharge modification indicates the presence of >$\underline{C}$F$_2$ and -$\underline{C}$F$_3$ groups at 291.2 eV and 293.6 eV respectively, figure 3(b). Such functionalities following fluorination have been observed by several workers[14,25-27]. No attempt has been made here to deconvolute the low binding energy side of the C(1s) peak, since there is overlap between partially fluorinated, oxygenated, and hydrogenated carbon functionalities[21].

3. 4 DISCUSSION

The presence of an alternating RF electromagnetic field across a CF$_4$ plasma causes electron acceleration, which in turn leads to bond cleavage and ionization of CF$_4$ molecules. The reactive component of a CF$_4$ plasma is reported to be fluorine atoms with a small concentration of CF, CF$_2$, and CF$_3$ radicals (all having vibrational and rotational temperatures approximately equal to room temperature)[15,28-31]. This is supported by electron impact experiments with CF$_4$, which indicate that fluorine atoms are the primary species[32]. This is a consequence of the high F/C ratio in CF$_4$ which gives rise to many excited F* species in the plasma[33]. The vacuum ultraviolet component of the glow discharge can also lead to electronic excitation of fluorine atoms[18]. This abundance of fluorine radicals can graft onto an organic surface[29] to yield >CF, >CF$_2$, and -CF$_3$ functionalities.

In the present study, it has been shown that the predominant reaction during CF$_4$ plasma treatment of polymeric substrates is surface fluorination, table 1, figure 3(b). For all the polymers studied, the degree of fluorination was found to be extensive. The F:C ratios obtained for polyethylene, polypropylene, and polystyrene are in agreement with previous reports[14,24]. Hydrogen abstraction by fluorine to form hydrogen fluoride is the initiation step for saturated polymers[34], although there is also likely to be some C-H bond rupture by the vacuum ultraviolet radiation component of the glow

discharge[35]. The formation of HF is thermodynamically favourable, since C-H bond strengths are in the 3-4 eV range[3,36] compared to 5.9 eV for H-F and 5.0 eV for C-F. Figure 5 illustrates the reaction pathway for the fluorination of a saturated polymer.

Figure 5: Mechanistic Pathway for the Surface Fluorination of Saturated Polymers.
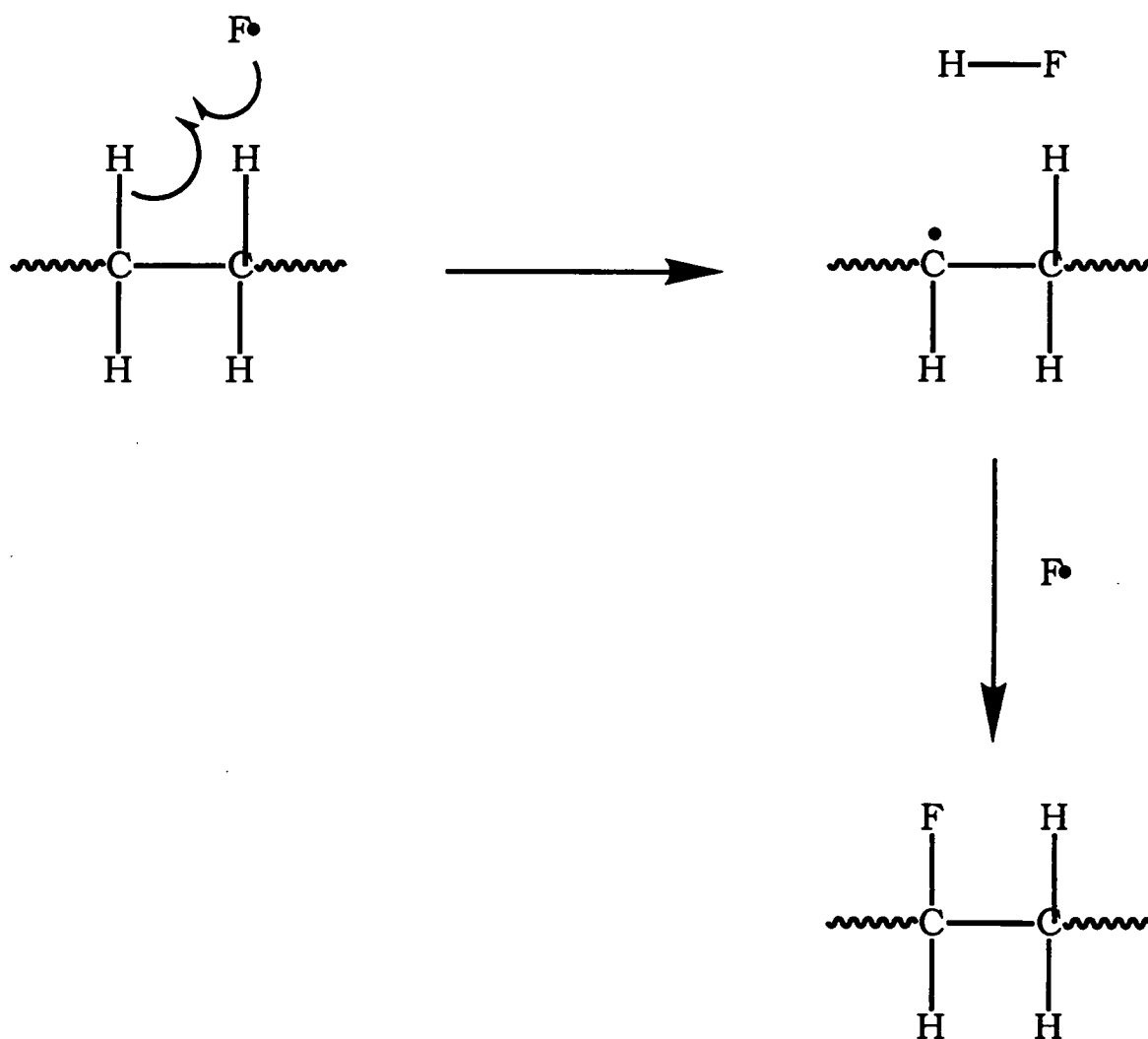
It is evident from the experimentally measured F:C ratios, that phenyl ring containing polymers are much more susceptible to plasma fluorination than might be expected on the basis of a hydrogen substitution reaction pathway, table 1. For example , the replacement of alternate H atoms by

phenyl groups along the polyethylene backbone in polystyrene significantly enhances the degree of fluorination. Phenyl-containing polymeric backbones with additional functionalities (e.g. polyethylene terephthalate[26], polyetherketone[25], polyetheretherketone, polycarbonate, polysulfone, polyethersulfone) also undergo extensive surface fluorination. A reaction pathway comprising fluorine addition at >C=C< double bond / aromatic carbon centres provides a viable explanation for the much higher levels of surface fluorination observed in the case of unsaturated polymers[34], figure 6.

Figure 6: Mechanistic Pathway for Surface Fluorination of Unsaturated Polymers.
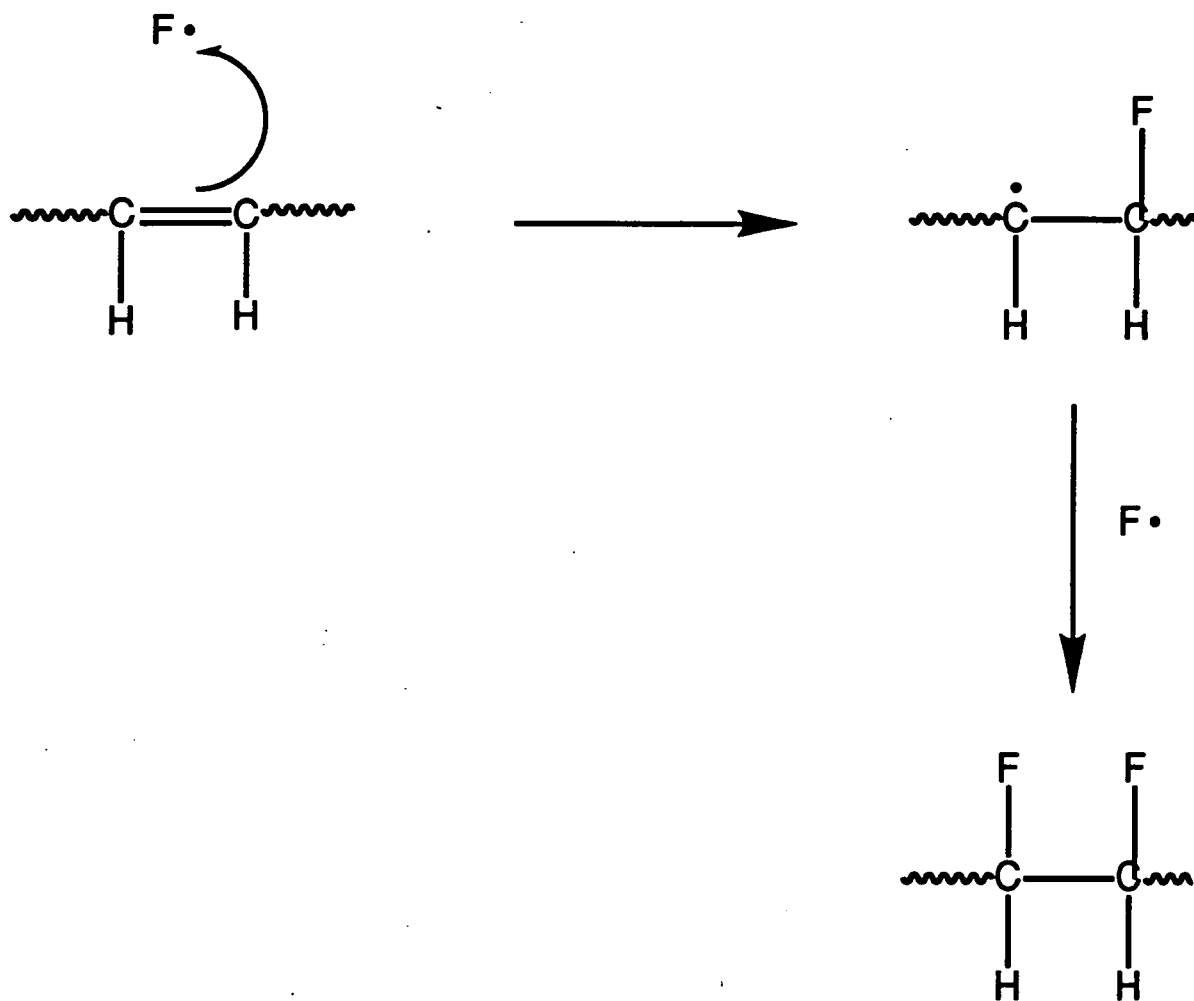
For both types of mechanism, the resultant free radical can be subsequently fluorinated to yield saturated >CHF functionalities. Repetition of the abstraction/fluorination mechanism at the >CHF moiety will eventually lead to the formation of >CF$_2$ groups. In the case of polysulfone and polyethersulfone, sulfur atoms are probably lost from the surface during CF$_4$ plasma treatment in a similar manner to that expected for hydrogen atoms, i.e. as SF$_6$ (instead of HF). However the reaction of fluorine atoms with oxygen will be energetically less favourable (OF$^\bullet$ bond strength = 2.4 eV)[5,37].

The overall trajectory of a fluorine atom incident upon a polymeric surface can be discussed in terms of its surface affinity[34]. This is the affinity that the reactants have for the polymer, or in other words the probability of finding the reactants in close proximity to the polymer surface. It is governed by the interactions between the valence p orbitals of fluorine with the highest occupied and the lowest unoccupied molecular orbitals of the polymer, figure 7.

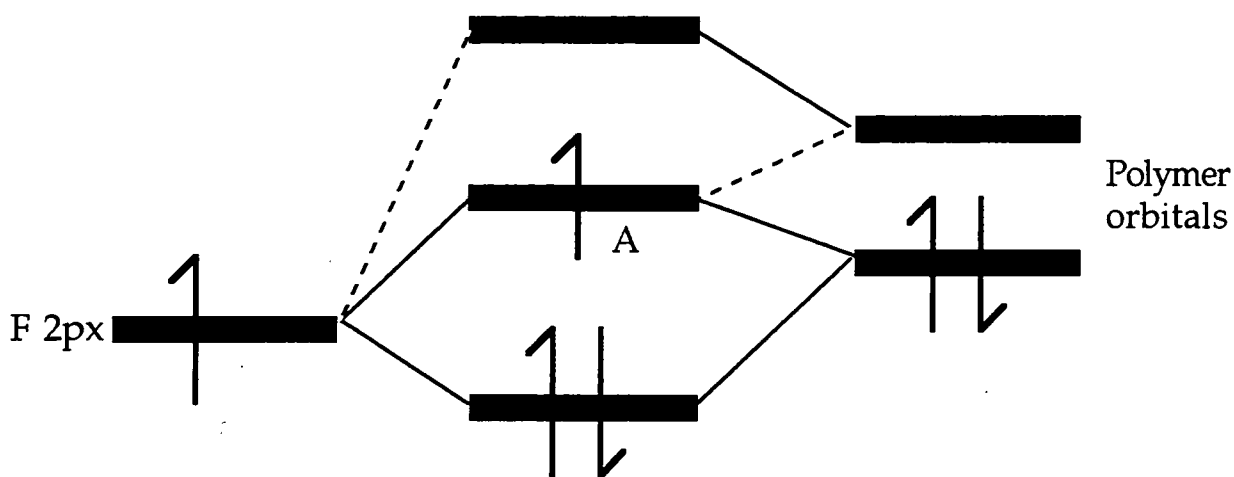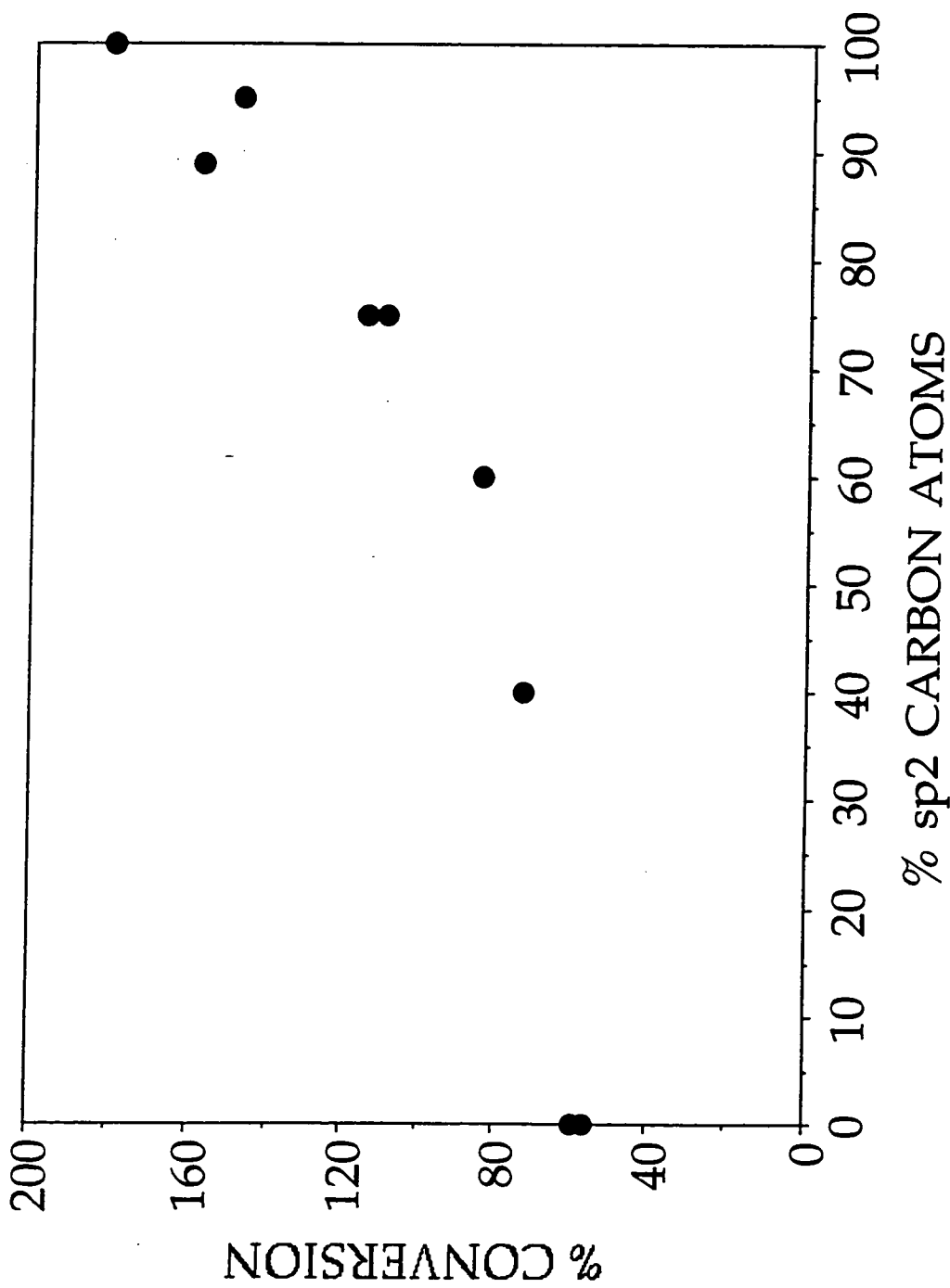Figure 7: Bonding interactions between F and polymer orbitals[39].

Figure 8: Experimentally observed F:C ratio divided by the theoretically expected values based upon hydrogen atom replacement by fluorine atoms (expressed as a percentage conversion) versus the percentage of >C=C< double bond / aromatic carbon centres in the parent polymer structure.

106

Approach of a fluorine group is governed by orbital A, figure 8. It can be considered as an antibonding interaction of F with the highest occupied molecular orbital of the polymer but is stabilized by a second order interaction with the lowest unoccupied orbital. Calculations based on a three orbital interaction model predict that the affinity of a fluorine atom towards a polymer surface is governed by the energy gap between the highest occupied and the lowest unoccupied molecular orbitals of the polymer[34]. Saturated polymers have a large energy gap, which leads to a high energy trajectory for fluorine atoms approaching saturated groups. The gap between the highest occupied and lowest unoccupied molecular orbitals is much smaller in unsaturated materials, and therefore incident fluorine atoms experience a greater surface affinity. Therefore the overall fluorine surface coverage measured for a given polymer following CF_4 plasma treatment is dependent upon its surface affinity and the dominant reaction mechanism.

The aforementioned description can be used to explain the observation made in this study that, in general, the experimental F:C ratios of phenyl containing polymers (polystyrene, polyetheretherketone, polycarbonate, polysulfone, and polyethersulfone), are found to be higher than the theoretically expected values for straightforward substitution of hydrogen atoms by fluorine atoms. In the case of saturated polymers (polyethylene and polypropylene), table 1 and figure 2, the F:C ratios are lower than predicted. This description is supported by results obtained from CF_4 or F_2 plasma treatment of several polymers where phenyl containing substrates were shown to be much more susceptible to fluorination[28-29,38-39]. Polyethylene terephthalate is an exception to this model. It is instructive to plot the observed F:C ratio divided by the theoretically expected values based upon hydrogen atom replacement by fluorine atoms (as a percentage conversion) versus the percentage of >C=C< double bond / aromatic carbon centres in the parent polymer structure,

figure 8. In this manner only the possible sites for fluorination are taken into account. As the %sp^2 or degree of unsaturation is increased, there is an increase in the %conversion. Clearly there is now a good correlation between the degree of unsaturation and the extent of fluorination observed for all of the polymers examined in this work.

3. 5 CONCLUSIONS

The higher level of fluorine incorporation at carbon centres observed for unsaturated polymers during CF_4 plasma treatment is consistent with atomic fluorine addition being the major reaction pathway. The lower levels of fluorine measured for the saturated polymer structures is in agreement with hydrogen substitution by atomic fluorine radicals being the dominant mechanism. The affinity of the fluorine atom approaching a surface must also be taken into account.

The overall extent of fluorination is dependent upon both the reaction mechanism and the surface affinity.

3. 6 REFERENCES

1. Iriyama, Y.; Yasuda, T.; Cho, D. L.; Yasuda, H. *J. Appl. Polym. Sci.,* **1990,** *39,* 249.

2. Xu, Z. J. *J. Appl. Polym. Sci.,* **1993,** *48,* 231.

3. d'Agostino, R. Ed.,*"Plasma Deposition, Treatment and Etching of Polymers"*, Academic Press, 1990, Chapter 2.

4. d'Agostino, R.,*"Plasma Deposition, Treatment and Etching of Polymers"*, Academic Press 1990, Chapter 1

5. Egitto, F. D.; Matienzo, L. J.; Schreyer, H. B. *J. Vac. Sci. Technol.,* **1992,** *A10,* 3060.

6. Inagaki, N.; Kobayashi, N.; Matsushima, M.; *J. Memb. Sci.*, **1988**, *38*, 85.

7. Pederson, L. A. *J. Electrochem. Soc.*, **1982**, *129*, 205.

8. Manos, D. M.; Flamm, D. L. Eds., *"Plasma Etching: An Introduction"*, Academic Press, 1989.

9. d'Agostino, R. Ed.,*"Plasma Deposition, Treatment and Etching of Polymers"*, Academic Press, 1990, Chapter 5.

10. Emmi, F.; Egitto, F. D.; Matienzo, L. J. *J. Vac. Sci. Technol.*, **1991**, *A9*, 786.

11. Win, S. Y.; Denton, D. D. *J. Vac. Sci. Technol.*, **1993**, *A11*, 291.

12. Grovenor, C. R. M., *"Microelectronics Materials"*, IOP Publishing, 1982.

13. Taylor, T.; Wolf, M. *Proc. Reg. Tech Conf. Photo Polymers*, **1979**, 175.

14. Strobel, M.; Corn, S.; Lyons, C. S.; Korba, G. A. *J. Polym. Sci. Polym. Chem. Ed.*, **1985**, *23*, 1125.

15. Truesdale, E. A.; Smolinsky, G. *J. Appl. Phys.*, **1979**, *50*, 6594.

16. Khairallah, Y.; Arefi, F.; Amouroux, J.; Leonard, D.; Bertrand, P. *ISPC-11.*, **1993**, 1224.

17. Haverlag, M.; Stoffels, E.; Stoffels, W. W.; Kroesen, G. M. W.; de Hoog, F. J. *ISPC-11*, **1993**, 1398.

18. Ingagaki, N.; Tasaka, S.; Mori, K. *J. Appl. Polym. Sci.*, **1991**, *43*, 581.

19. Iriyama, Y.; Yasuda, H. *J. Polym. Sci. Polym. Chem. Ed.*, **1992**, *30*, 1731.

20. Clark, D. T.; Adams, D. B.; Dilks, A.; Peeling, J.; Thomas, H. R. *J. Electron Spectrosc.*, **1976**, *8*, 51.

21. Beamson, G.; Briggs, D. *"High Resolution XPS of Organic Polymers: The Scienta ESCA300 Database"*, Wiley, New York, 1992.

22. Clark, D. T.; Dilks, A.; Peeling, J.; Thomas, H. R. *Trans. Faraday Soc. Faraday Disc.*, **1975**, *60*, 183.

23. Clark, D. T.; Thomas, H. R. *J. Polym. Sci. Polym. Chem. Ed.*, **1978**, *16*, 791.

24. Strobel, M.; Lyons, C. S. *Polymeric Materials Science and Engineering*, ACS, **1987**, *56*, 232.

25. Onyirinka, E. C. *J. Vac. Sci. Technol.*, **1993** , *A11*, 2941.

26. Yasuda, A.; Okuno, T.; Yoshido, K.; Yasuda, H. *J. Polym. Sci. Polym. Phys. Ed.*, **1988**, *26*, 1781.

27. Y. Momose, Y.; Takada, T.; Kazaki, S. *Polymeric Materials Science and Engineering* ACS, **1987**, 236.

28. d'Agostino, R.; Cramarossa, F.; DeBenedictis, S. *Plasma Chem. Plasma Process*, **1982**, *2*, 213.

29. Occhiello, E.; Morra, M.; Garbassi, F.; Bargon, J. *Appl. Surf. Sci.*, **1989** , *36*, 285.

30. Plumb, I. C.; Ryan, K. R. *Plasma Chem. Plasma Process.*, **1986**, *6*, 205.

31. Edelson, D.; Flamm, D. L. *J. Appl. Phys.*, **1984**, *56*, 1522.

32. Kay, E. *Proceed. Internat. Ion Engineering Congress - ISIAT 83 & IPAT 83*, Kyoto, **1983**, 1657.

33. Iriyama, Y.; Yasuda, H. *J. Polym. Sci. Chem. Ed.* **1992**, *30*, 1731.

34. Cain, S. R.; Egitto, F. D.; Emmi, F. *J. Vac. Sci. Technol.* **1987**, *A5*, 1578.

35. Hollander, A.; Klemberg-Sapieha, J.E.; Wertheimer, M.R. *Macromolecules*, **1994**, *27*, 2893.

36. Sheppard, W. A.; Sharts, C. M. *"Organic Fluorine Chemistry"*, Benjamin, New York, 1969.

37. Weast, R. C. Ed. *"CRC Handbook of Chemistry and Physics"*, CRC Press, 63rd Ed., 1982.

38. I. Tepermeister, I.; Swain, H. *J. Vac. Sci. Technol.*, **1992**, *A10*, 3149.

39. Yasuda, T.; Okuno, T.; Yoshida, K.; Yasuda, H. *Polymeric Materials Science and Engineering, ACS*, **1987**, *56*, 240.

Chapter Four

Synergistic Oxidation at the Plasma/Polymer

Interface

Chapter Four

Synergistic Oxidation at the Plasma/Polymer Interface

4. 1 INTRODUCTION

Results found in chapter two indicated that the vacuum ultraviolet (VUV) component in an inert gas plasma plays a vital role in the modification of polysulfone and polyethersulfone. The importance of the energy transfer mechanisms at a plasma/polymer interface is still under much debate and the aim of this study is to investigate the reaction pathways taking place . This work studies the effect of VUV radiation from the inert gases argon, krypton and xenon plasmas, on the surface modification of polyethylene and polystyrene in an oxygen atmosphere.

4. 1.1 Background

Electromagnetic Radiation output is largely dominated by characteristic line spectra originating from electronic transitions of neutral M(I) and singly ionized M^+(II)[1] to the ground state (where M is the element). The wavelengths of VUV radiation correspond to the region of the electromagnetic spectrum which is absorbed in air, hence experiments are carried out in a vacuum[2]. The wavelength range is generally considered to be 180-130 nm. The photon energies are approximately 6 eV which is sufficient for excitation of electronic transitions in many molecules[3].

The Rydberg transitions are used to describe electronic transitions in the UV region, described by equation 1.

$$T_n = I.P - u_n = R/(n-\delta)^2 \qquad (1)$$

where T_n is the Rydberg transition u_n is the frequency of absorbed photon, R is the Rydberg constant, n is an integer, I.P is the ionization potential and δ is a quantum defect.

4. 1. 2 Sources of VUV

VUV radiation spans a range of wavelengths and the choice of a VUV source is dependent upon its application. A few different types of sources are listed below.

4. 1. 2. 1 *Conventional VUV light source*[2,4]

VUV light sources are typically gas discharge lamps and their spectra depend upon the type of gas and the experimental conditions, for example pressure. An example of such a lamp is a low pressure He lamp which gives rise to specific emission lines at 58.4 nm (He(I) 2p->1s) and 30.4 nm (He (II) 2s->1s). The line spectra are produced by electronic transitions within atoms and molecules and are usually more intense than a continuum spectrum.

4. 1. 2. 2 *Synchrotron Radiation*[2,4]

Synchrotron radiation is produced as a consequence of accelerating electrons emitting radiation. The radiation emitted is a good light source and provides radiation at all wavelengths.
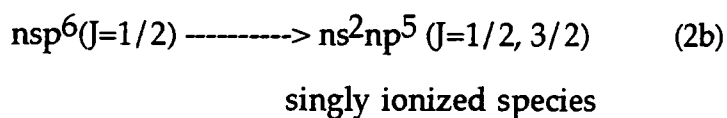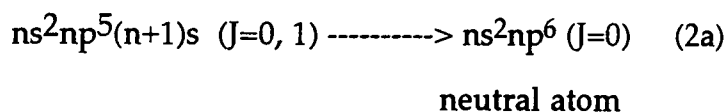
4. 1. 2. 3 *Plasmas*[4,5]

A plasma is a source of electromagnetic radiation extending from the VUV to the visible along with a number of different species such as positive and negative ions, atoms, metastables and electrons.

4. 1. 3 Plasmas and their Interaction with Polymers

All plasmas emit varying amounts of radiation in the VUV region depending on the type of discharge[1,4,6,7]. VUV cross-sections can be large and therefore surface reactions with a polymer contain a significant contribution arising from radiative transfer. The energy from VUV radiation can be absorbed in the first few monolayers of the surface and the energy is sufficient to break organic bonds.

Inert gas plasmas are considered to emit strongly in the VUV. The resonance lines (transitions between two levels permitted by selection rules) from an inert gas plasma arise from transitions from the excited state to the ground state, equation 2 (a) and 2 (b).

$$ns^2np^5(n+1)s \; (J=0, 1) \text{ ----------> } ns^2np^6 \; (J=0) \quad (2a)$$

<center>neutral atom</center>

$$nsp^6(J=1/2) \text{ ----------> } ns^2np^5 \; (J=1/2, 3/2) \quad (2b)$$

<center>singly ionized species</center>

Ne, Ar, Kr, Xe give rise to two component structures arising from the J splitting. He has only one component in each case[8].

The ionization process occurring to form the excited states in a plasma are shown in equations 3 (a) and 3 (b).

$$A + A \text{ ----------> } A + A^* \quad \text{excitation} \quad (3a)$$

$$A + A^* \text{ ----------> } A + A^+ \quad \text{ionization} \quad (3b)$$

<center>114</center>
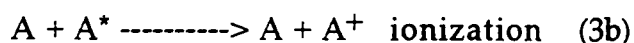
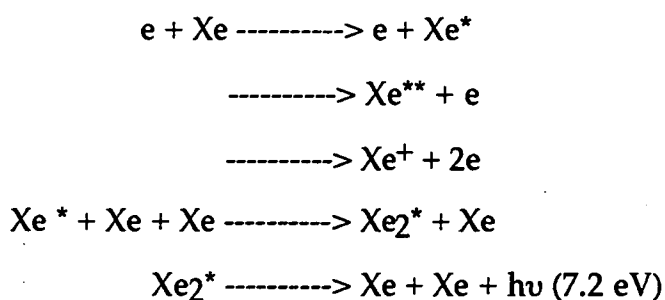If molecules are collisionally excited metastable states, then they can remain in excited states for long lifetimes due to their inability to radiate to the ground state[9].

The emission of VUV from an inert gas plasma may also be due to the formation of excimers. Excited dimers of Ar, Kr and Xe emit in the VUV region. Formation of dimers is shown in figure 1.

Figure 1: Excimer Formation.

$$e + Xe \text{----------} > e + Xe^*$$

$$\text{----------} > Xe^{**} + e$$

$$\text{----------} > Xe^+ + 2e$$

$$Xe^* + Xe + Xe \text{----------} > Xe_2^* + Xe$$

$$Xe_2^* \text{----------} > Xe + Xe + h\upsilon \text{ (7.2 eV)}$$

Excimer formation is a three body process and higher pressures are required[10]. Table 1 shows the ionization potential and metastable energies for the inert gases used in this set of experiments.

Table 1: Inert gas ionization potential and metastable energy data[8].

Atom	Ionization Potential		Metastable Energy	
	Designation	Energy (eV)	Designation	Energy (eV)
Ar	$^2P_{3/2}$	15.759	$^3P_0$	11.723
	$^2P_{1/2}$	15.937	$^3P_2$	11.548
Kr	$^2P_{3/2}$	13.999	$^3P_0$	10.562
	$^2P_{1/2}$	14.665	$^3P_2$	9.915
Xe	$^2P_{3/2}$	12.130	$^3P_0$	9.447
	$^2P_{1/2}$	13.436	$^3P_2$	8.315

In polymers, VUV radiation has been found to cause a number of reactions, from crosslinking of polymer surfaces, fluorination of polymers to initiation of photochemical modification. However, the importance of the role of VUV radiation in the modification of polymers is still much in debate.

4. 1. 3. 1 *Mechanism*

Clark and Dilks addressed[5] the question of whether direct energy transfer is competitive with radiative transfer, that is, polymer modification at the surface is either a result of modification of both radiative energy transfer (VUV) and/or direct energy transfer from species such as ions, schematically represented in figure 2.

Figure 2: Schematic representation of energy transfer to a polymer surface[5].
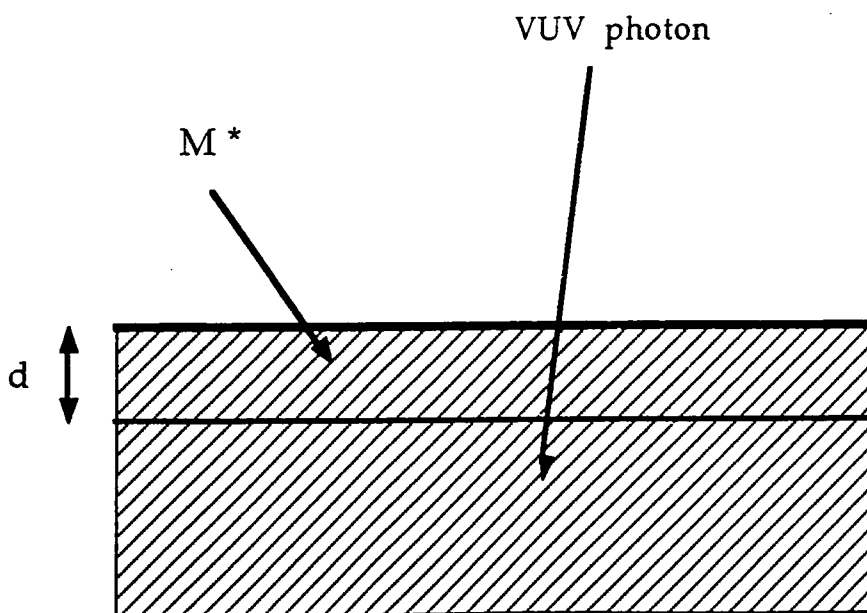
M* =metastable, ion species

d= depth to which metastables/ions penetrate in polymer

The attenuation coefficient for EM radiation arising from the photoionization from transitions to diffuse Rydberg states, is such that there will be little attenuation and therefore the surface reaction will be dominated mainly by ions and metastables. The contribution from radiative transfer is minor. The surface reactions in the first few monolayers are dominated by direct energy transfer, however the longer range radiative source will penetrate deeper into the sample.

Other work carried out by various authors[11,12,13,14] has also demonstrated that plasma treatment of polymers is a combination of rapid reaction due to direct energy transfer at the surface and a longer range radiative component due to UV and VUV radiation. Plasmas contain a number of different species such as electrons, ion, atoms and metastables, however vacuum ultraviolet radiation is an important component in glow discharges when treating polymers. At the surface, the ions, metastables and other species play an important role through direct energy transfer, radiative energy transfer becomes the more dominant mechanism for modification in the bulk, since it can penetrate further than ions/metastables which really only have a major part to play in modification at the first few monolayers.

In situ studies of argon plasma treatment of several polymers[15] showed that there were no new species incorporated. The π-π^* shake up transition, indicative of aromaticity, however did decrease compared to the untreated polymer and it was suggested that the argon plasma led to bond breaking and possible chain scission of the polymer. It is the aim of this study to determine whether it is the VUV radiation or the excited species within a plasma that lead to modification of polymer surfaces.

4. 2 EXPERIMENTAL

The experimental procedure followed for the VUV experiments was similar to the plasma experiments described in section 2. 2. Polyethylene (PE) film (ICI) was ultrasonically washed in a 1:1 mixture of iso-propanol alcohol and cyclohexane for 30 s, dried in air, then placed into the reactor vessel, figure 3. The system was evacuated and the reaction gases were let into the apparatus via needle valves to a pressure of 0.2mbar (plasma gas on the left hand side in the diagram and oxygen on the right hand side). The plasma was ignited at a power of 30 W and the ions and other such species were filtered out, allowing only the VUV radiation to pass to the reaction chamber, using a LiF crystal (cutoff wavelength 105 nm). After a treatment time of 30 minutes, the gases were purged for a further 5 minutes before opening up the chamber to atmosphere. The sample was then transferred to a Kratos ES300 X-ray spectrometer for analysis, as described in section 2. 2.

Figure 3. VUV experimental apparatus.
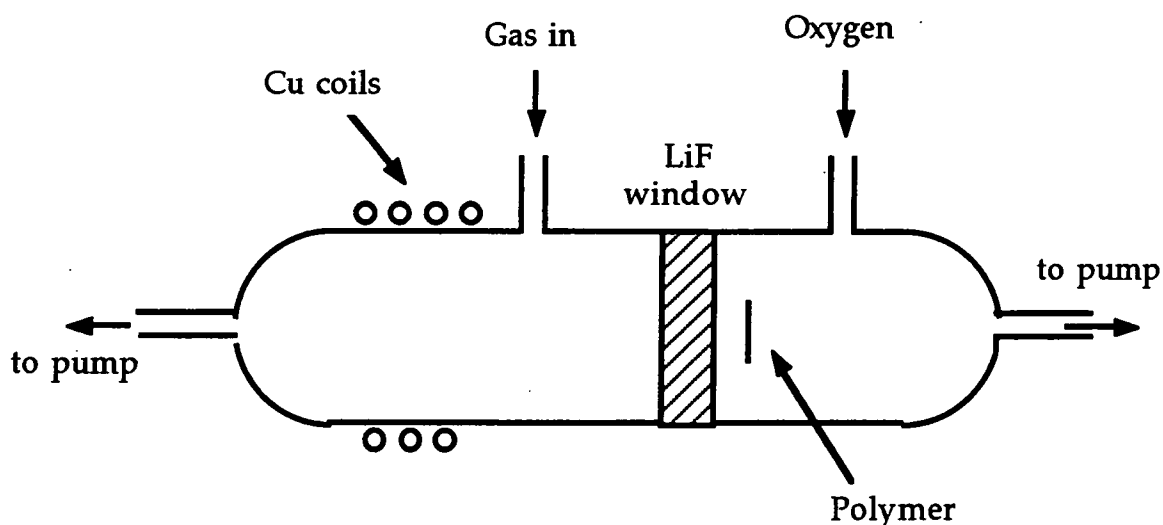
Nitrogen (99.995%, BOC), argon (99.999% BOC), krypton (99.997%, Spectra Gases) and xenon (99.999%, Spectra Gases) were used for the plasma,

sample side was oxygen (99.999%, BOC). The experiments were repeated using polystyrene (PS) (BP).

The plasma treatment of the polymers followed the procedure as recorded in section 2.2, at a power of 30 W.

The plasma/VUV treatments were run at steady state conditions, typically 30 min for a VUV treatment and 5 min for a plasma treatment.

4. 3 RESULTS

4. 3. 1 Polyethylene

XP spectra of the clean polyethylene displayed a single C(1s) peak at 285.0 eV arising from $-C_xH_y-$. Detailed chemical information about the modified polymer surfaces was obtained by peak fitting the C(1s) XPS spectra to a range of carbon functionalities[16,17]: carbon adjacent to a carboxylate group ($C-CO_2$ ~ 285.7 eV), carbon singly bonded to one oxygen atom ($C-O$ ~286.6 eV), carbon singly bound to two oxygen atoms or carbon doubly bonded to one oxygen atom ($O-C-O$ or $C=O$ ~287.9 eV), carboxylate groups ($O-C=O$ ~289.0 eV), and carbonate carbons ($O-CO-O$ ~290.4 eV), table 2. Errors within the tables refer to reproducibility results between independent experiments. $C-O$ groups were found to be the most prominent oxidised carbon species. Surprisingly, very little oxygen incorporation into the polyethylene surface was found during O_2/VUV exposure, figure 4.

Oxygen exposure to noble gas glow discharge treated polyethylene produced a lower level of surface oxidation compared to the corresponding VUV/O_2 experiments, with Xe-VUV/O_2 yielding a level of surface oxidation which is almost comparable to oxygen plasma treatment, figures 5, 6 and 7.

Table 2: Summary of oxidation treatments of polyethylene.

TREATMENT	% FUNCTIONALITIES					
	C-H	-C-CO$_2$	-C-O	>C=O	-C(O)=O	-O-C(O)=O
O$_2$ PLASMA	72.0±0.6	4.7±0.4	8.5±2.3	6.1±0.5	4.7±0.4	3.2±0.3
O$_2$ VUV	93.6±0.4	-	4.3±0.2	2.1±0.2	-	-
Ar PLASMA	77.4±0.04	4.57±0.25	8.67±0.65	4.31±0.47	4.57±0.3	0.5±0.7
Ar VUV	69.6±0.1	7.6±0	10.1±0.6	5.1±0.4	7.6±0	-
Kr PLASMA	76.5±2.6	5.1±1.2	9.2±1.0	4.12±0.9	5.08±1.2	-
Kr VUV	69.8±0.3	6.5±0.1	10.3±0.4	5.6±0.4	6.5±0.1	1.35±0.4
Xe PLASMA	79.9±0.7	4.3±0.6	8.3±3.8	3.1±1.2	4.3±0.6	1.1±1.1
Xe VUV	62.4±0.3	8.1±0.1	11.7±0.1	7.8±0.1	8.1±0.1	1.8±0.1

4. 3. 2 Polysytrene

Polystyrene consists of an alkyl chain polymeric backbone, to which phenyl rings are attached . Two peaks are observed in the C(1s) region of the XPS spectrum for the clean starting material: a hydrocarbon component (285.0 eV, 94% of total C(1s) signal) and a distinctive satellite structure at ~291.6 eV (6% of total C(1s) signal), which is associated with low-energy π --> π^* shake-up transitions that accompany core ionization[18]. Oxygen plasma treatment of polystyrene produced a range of oxygenated surface functionalities, table 3, however the extent of oxidation was found to be much greater than observed for polyethylene. Once again, very little oxygen incorporation into the polystyrene surface was found during O$_2$-VUV/O$_2$ exposure.

Reaction of ground state molecular oxygen following the various noble gas plasma treatments gave rise to a greater level of oxidation at the polystyrene surface compared to VUV/O$_2$ modification except for Xe-VUV/O$_2$ where in fact the reverse was found to be true, figures 8, 9 and 10.

Table 3: Summary of the oxidation treatments of polystyrene.

TREATMENT	% FUNCTIONALITIES						
	$\underline{C}$-H	$\underline{C}$-CO2	$\underline{C}$-O	>$\underline{C}$=O	$\underline{C}$(O)=O	-O-$\underline{C(O)}$=O	$\pi-\pi^*$
O$_2$ PLASMA	58.8±0.3	4.0±0.7	11.9±0.1	10.4±0.7	4.0±0.7	8.8±0.1	2.6±0.5
O$_2$ VUV	89.90.5	-	3.5±0.1	-	-	-	6.5±0.4
Ar PLASMA	71.4±2.3	3.0±0.7	10.4±0.1	5.9±0.4	3.0±0.7	4.4±0.4	2.0±0.1
Ar VUV	67.7±1.6	5.9±0.3	9.1±0.5	5.6±0.1	2.5±0.9	6	
Kr PLASMA	65.8±0.6	3.9±1.1	11.4±1.4	6.8±1.4	3.9±1.1	5.3±2.4	1.9±0.6
Kr VUV	71.7±3.1	1.9±0.3	10.7±0.2	5.5±1.7	1.9±0.3	5.7±1.4	2.7±0.8
Xe PLASMA	70.5±2.6	3.9±0.6	11.7±0.7	5.4±0.1	3.9±0.6	2.7±0.9	1.9±0.6
Xe VUV	63.4±2.5	3.6±0.7	10.5±0.5	8.1±0.3	3.6±0.7	8.0±0.2	2.7±0.2

Figure 4: O: C ratio of the PE treated by VUV and plasma.
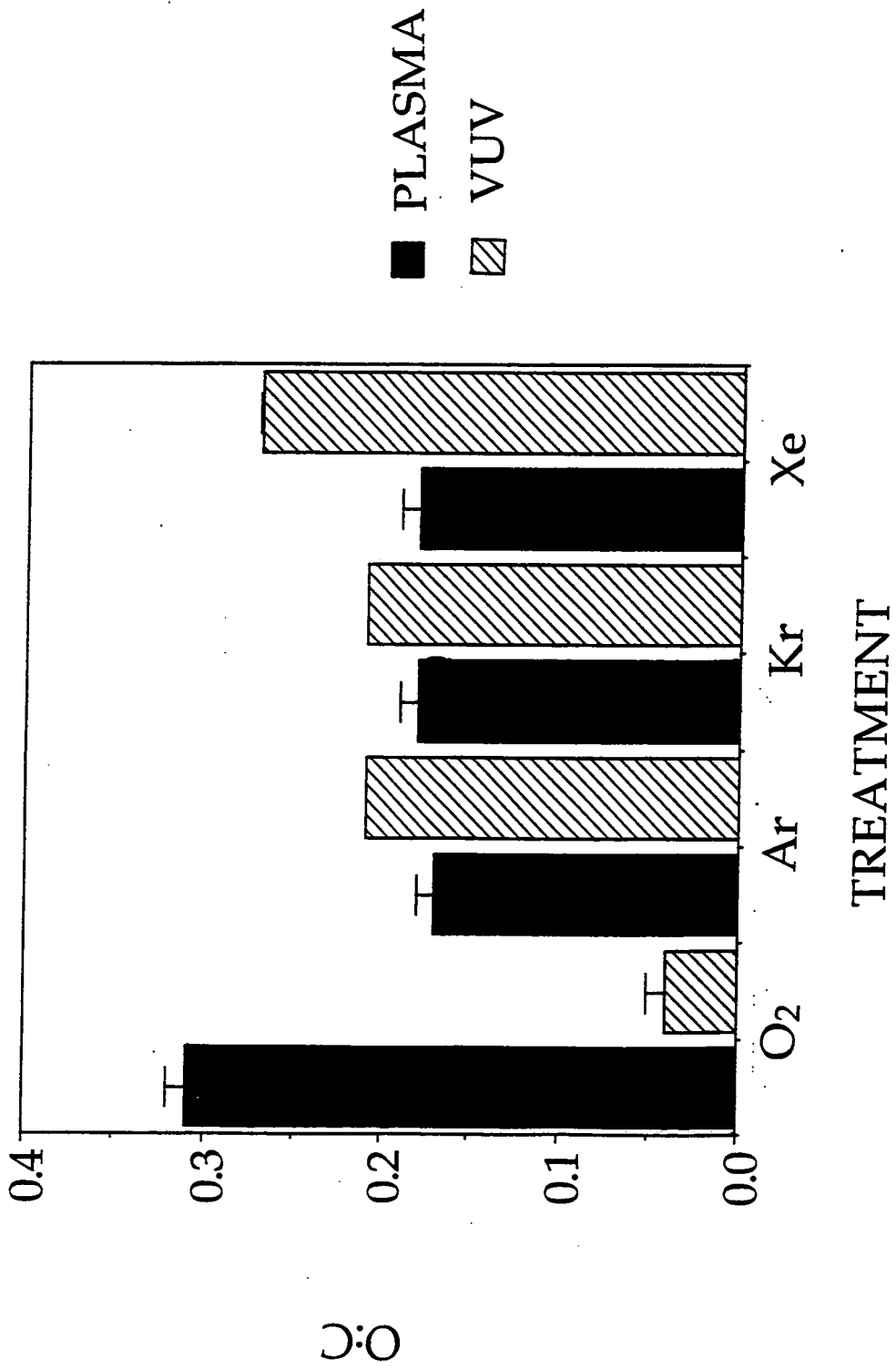
Figure 5: Typical C(1s) peak fit for Xe-VUV/O_2 treatment of polyethylene.

Figure 6: C(1s) XP spectrum of PE: (a) Untreated PE (b) O_2 plasma treatment (c) Ar plasma treatment (d) Kr plasma treatment (e) Xe plasma treatment.

Figure 7: C(1s) XP spectrum of PE: (a) Untreated PE (b) O_2 VUV (c) Ar VUV (d) Kr VUV (e) Xe VUV

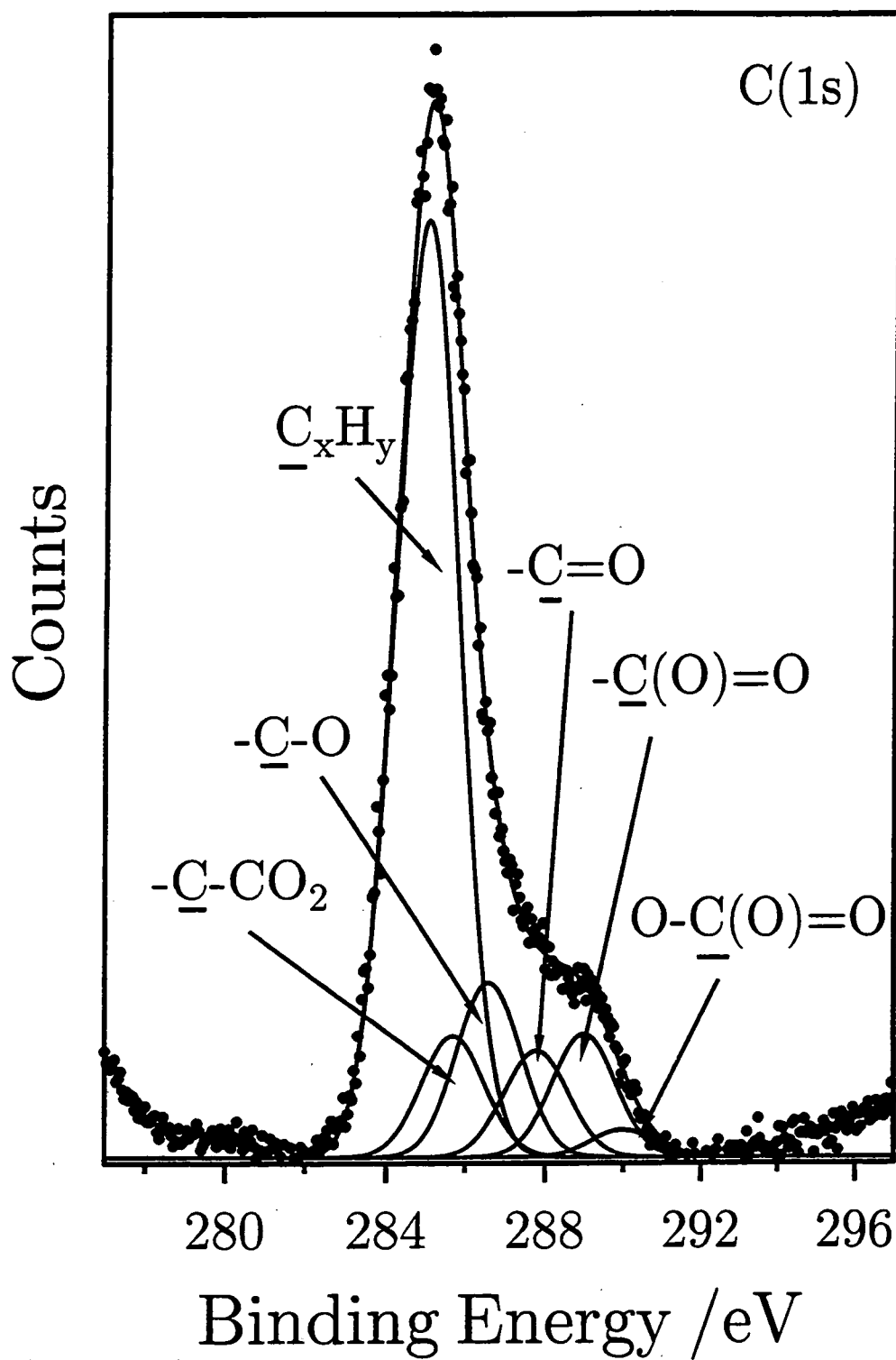Figure 8: O: C ratio of the PS treated by VUV and plasma.

126

Figure 9: C(1s) XP spectrum of PS: (a) Untreated PS (b) O_2 plasma treatment (c) Ar plasma treatment (d) Kr plasma treatment (e) Xe plasma treatment.
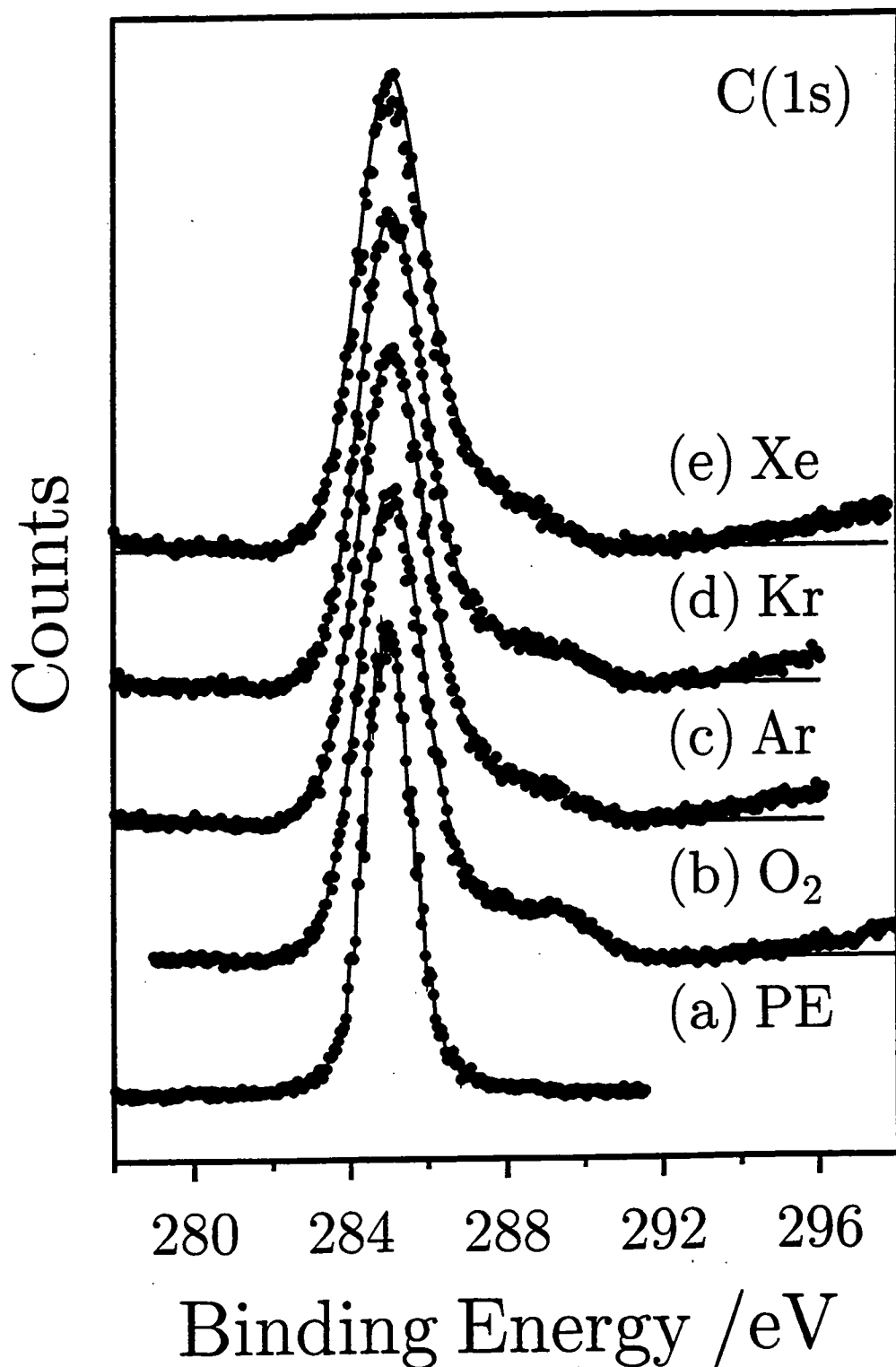
Figure 10: C(1s) XP spectrum of PS: (a) Untreated PS (b) O_2 VUV (c) Ar VUV (d) Kr VUV (e) Xe VUV.
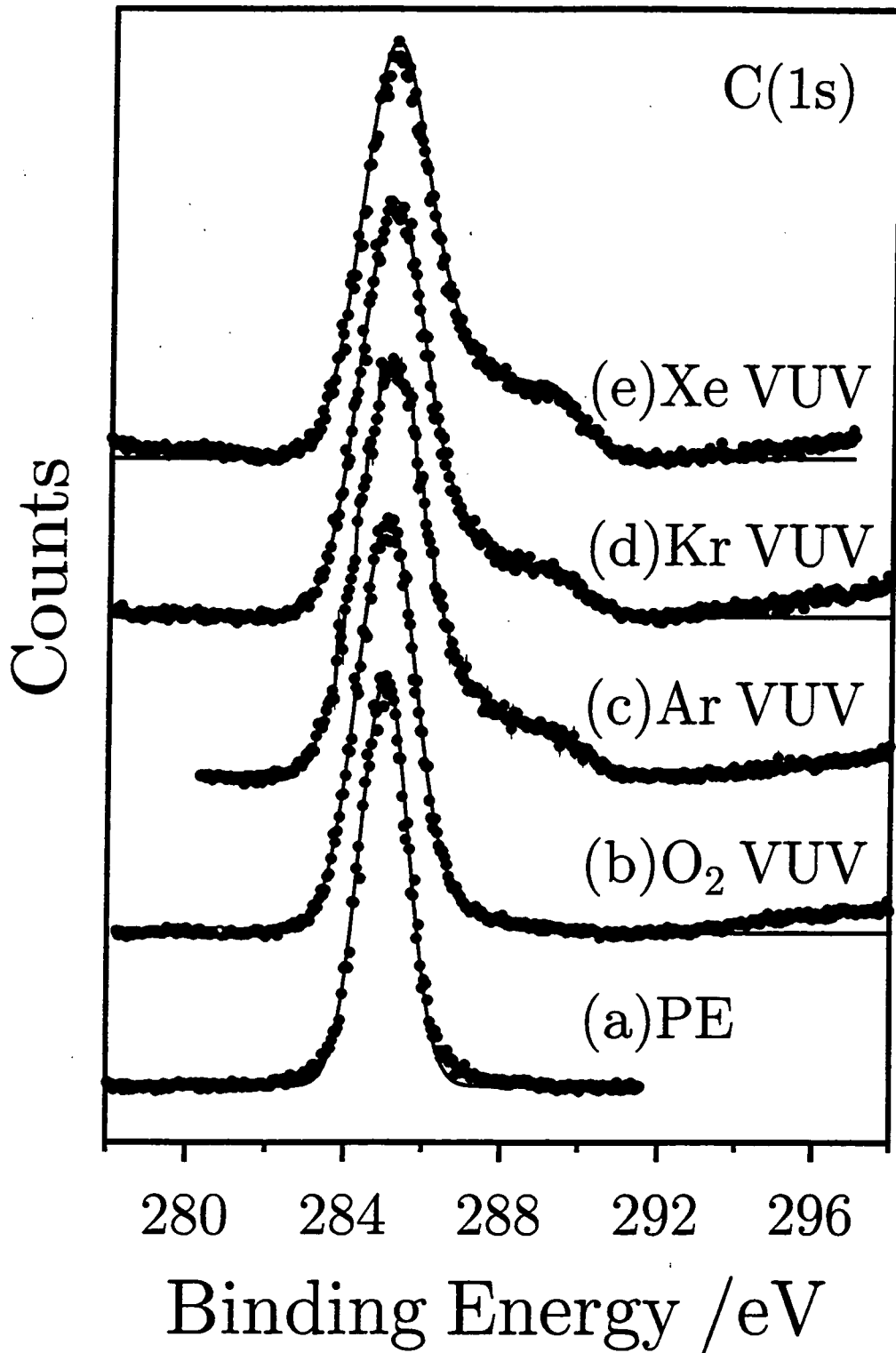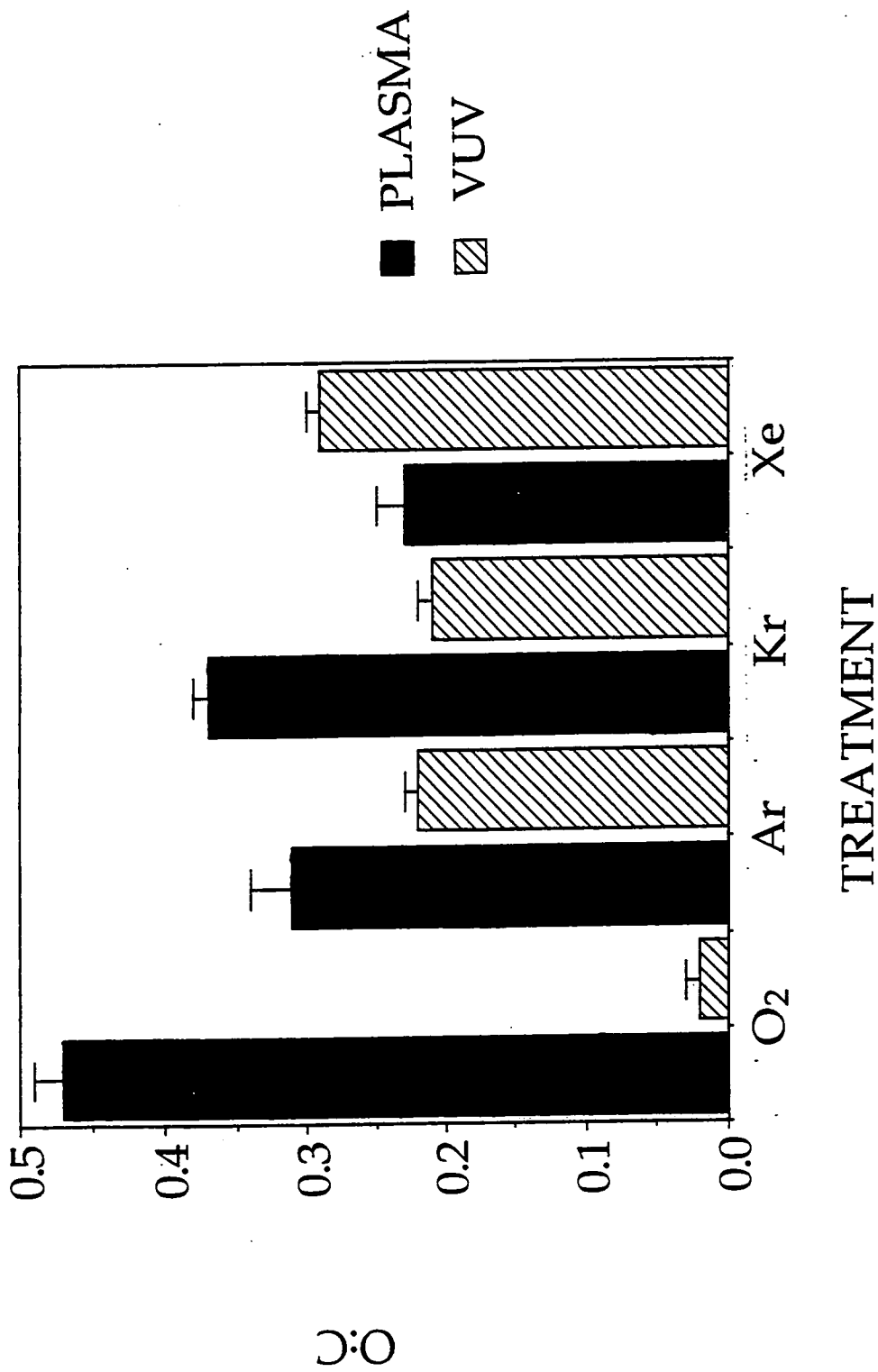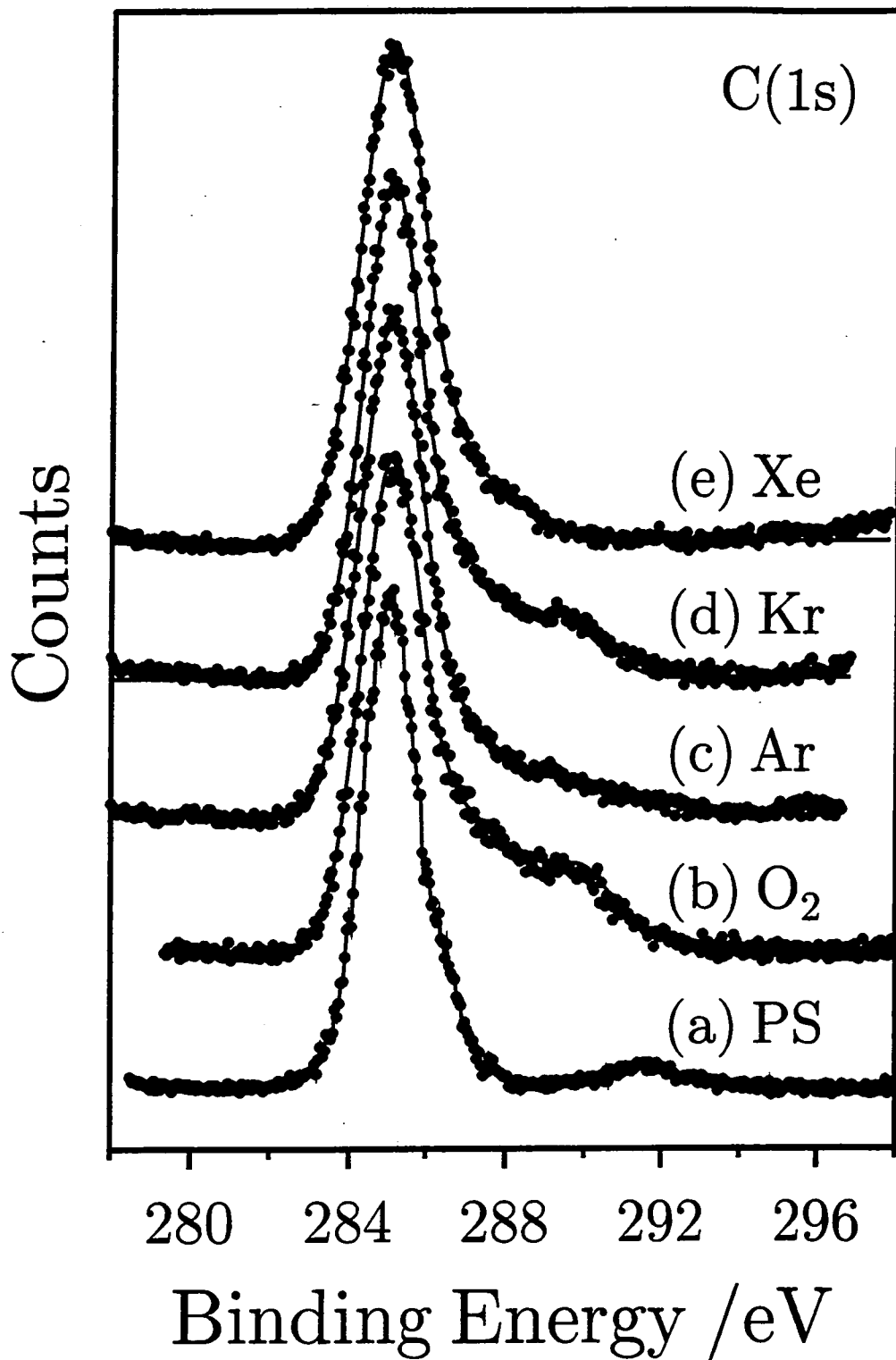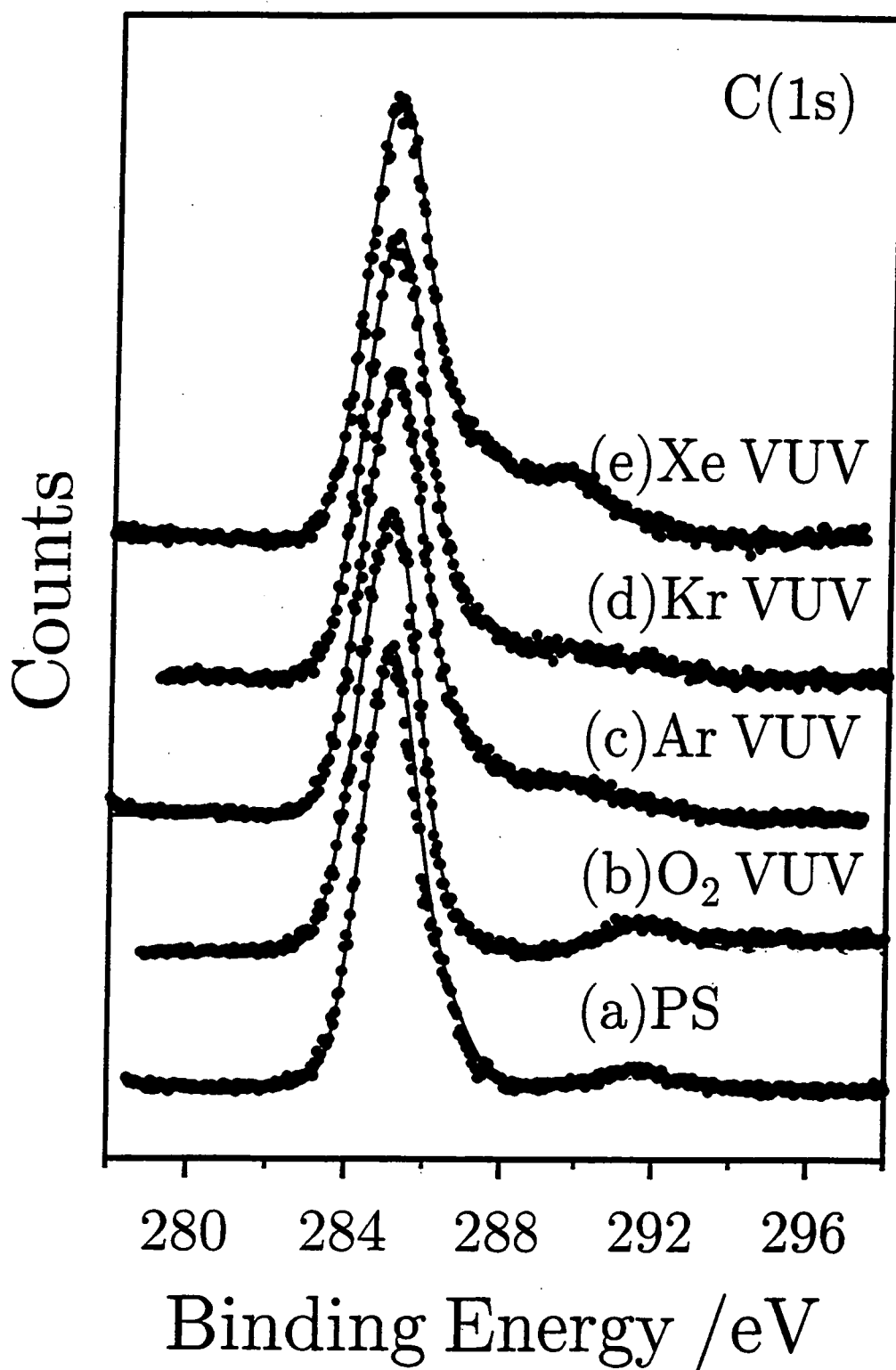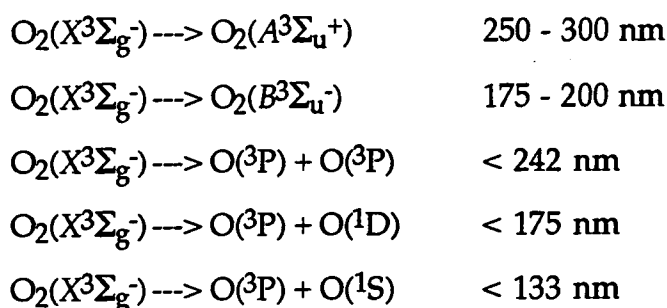
4. 4 DISCUSSION

Inert gas plasmas interact with organic substrates via a direct energy transfer component arising from ions and metastables down to ~ 10 Å, and a radiative transfer component consisting of vacuum ultraviolet (VUV) photo-irradiation which can penetrate up to ~ 10 μm below a polymer surface[5]. Typically, ion densities lie in the range of 10^8 - 10^{10} cm^{-3} with energies of 0 - 100 eV[19], whilst mean electron energies <e> span 0 - 20 eV with a high energy tail reaching out to 100 eV due to reflections at sheath boundaries[20].

Crossed-beam electron impact induced fluorescence studies with argon atoms have shown that the most intense VUV emission lines appear at 104.8 nm and 106.7 nm, these give rise to the Ar (I) transitions between the lowest lying electronically excited states and the ground state of the atom (i.e. $3s^23p^54s^1$ --> $3s^23p^6$)[21]. The excited ion Ar (II) resonance lines at 91.98 nm and 93.21 nm also emit strongly, and correspond to the $3s^13p^6$ --> $3s^23p^5$ transitions. The Ar (I) lines display a maximum excitation cross section at ~ 30 eV electron energies, whilst this occurs at ~ 50 eV for the Ar (II) lines. In general, the M (I) emission lines are the most intense for low pressure noble gas plasmas (where M is the noble gas)[4], these are 104.8, 106.7, 116.5, 123.6 and 131.2, 147 nm for Ar, Kr, and Xe respectively[1]. The background consists of a radiation continuum arising from excited inert gas molecules M_2^* and there is also emission in the UV/visible, but the intensity is at least two orders of magnitude lower than for the VUV region. A sample located in the centre of an inert glow discharge essentially receives irradiation from M(I) and M(II) resonance lines only[1,22] and it is these resonance lines which are considered as the main excitation energy. As mentioned in the introduction to this chapter, VUV wavelengths of the M(I) and M(II) resonance lines correspond to the region of the electromagnetic spectrum where radiation is absorbed by air (below 180 nm)[2] with photon energies

sufficiently high to induce electronic transitions and photoionization in many molecules[3].

A pure oxygen plasma contains many different species such as ions, atoms, ozone, and metastables of atomic and molecular oxygen, as well as electrons and a broad electromagnetic spectrum[23,24]. During plasma oxidation of a polymer surface, the observed incorporation of oxygenated functionalities is accompanied by the continual evolution of small volatile molecules (eg. CO, CO_2, H_2O, etc.)[25].

The photo-excitation of the oxygen molecule can be summarised in terms of the following threshold wavelengths:

$$O_2(X^3\Sigma_g^-) \longrightarrow O_2(A^3\Sigma_u^+) \qquad 250 - 300 \text{ nm}$$

$$O_2(X^3\Sigma_g^-) \longrightarrow O_2(B^3\Sigma_u^-) \qquad 175 - 200 \text{ nm}$$

$$O_2(X^3\Sigma_g^-) \longrightarrow O(^3P) + O(^3P) \qquad < 242 \text{ nm}$$

$$O_2(X^3\Sigma_g^-) \longrightarrow O(^3P) + O(^1D) \qquad < 175 \text{ nm}$$

$$O_2(X^3\Sigma_g^-) \longrightarrow O(^3P) + O(^1S) \qquad < 133 \text{ nm}$$

The molecular oxygen absorption cross-section passes through a maximum at approximately 145 nm and is very small below 130 nm (numerous Rydberg transitions[26]) and above 175 nm (the Schumann-Runge continuum[26,27]).

Vacuum UV photons typically possess energies corresponding to the order of electronic excitation and first ionization potentials for polymers[28]. Direct abstraction of hydrogen atoms from polymer molecules by oxygen is an endothermic reaction requiring 30 to 45 kcal/mol[29], therefore the attack by ground state atomic oxygen or molecular oxygen is thermodynamically unlikely with a ground state polymer[6]. However, reaction of oxygen at a generated polymer radical site by either direct attachment of atomic oxygen or addition of molecular oxygen followed by O-O bond rupture are possibilities[30].

130

Photons can create active sites in polymers if the radiation is sufficiently energetic, that is, the photon must be at least equal in energy to the first ionization potential of polymers for modification to occur. For example, saturated polymers require greater energy for active sites to be created, due to the strong coupling between atoms, polyethylene requires $\lambda < 145$nm, corresponding to 8.6 eV. The longest wavelength absorption band in polyethylene is associated to $\sigma \text{---} > \sigma^*$ transition and lies in the VUV region[31]. Unsaturated polymers require longer wavelengths and modification has been shown to occur at $\lambda > 200$nm[28]. Polystyrene contains phenyl rings which are chromophores[32], a specific group of atoms which absorb in a molecule giving rise to characteristic absorption bands, reducing the energy needed for modification of the surface to occur, since the difference between the HOMO and LUMO states is smaller for unsaturated than saturated polymers[33]. The longest wavelength for absorption is the $\pi \text{---} > \pi^*$ transition[31].

In order to activate polymers, there is an activation barrier to overcome before surface reactions can take place[34]. In the case of the O_2-VUV/O_2 experiments, the observed low levels of surface oxidation can be attributed to the absence of any σ bond photoionization (just σ-σ^* transitions) together with a very small molecular O_2 dissociation cross-section being coincident with the characteristic 130 nm emission line from the O_2 glow discharge.

Both the Ar (I) (104.8, 106.7 nm) and Kr (I) (116.5, 123.6 nm) emission lines overlap with a high photoionization cross-section for σ bonds[35,36] to create free radical centres which can undergo reaction with molecular O_2. The higher levels of oxidation observed for Xe-VUV/O_2 experiments can be attributed to the Xe(I) (147 nm) line coinciding with the peak of the molecular O_2 dissociation cross-section, i.e. attack by excited oxygen atoms.

In the case of polyethylene, molecular oxygen attack at the free radical centres generated following noble gas plasma treatment results in a lower

level of surface oxidation compared to the VUV/O_2 treatments. On consideration of the Xe VUV treatment, the generation of surface free radical sites will mainly be occurring by ion bombardment because the Xe (I) line wavelength is is not low enough to coincide with the photoionization cross-section of the polymer. The possibility of the Xe (II) line (110, 124.5 nm) simultaneously creating free radical centres, as in the Ar and Kr VUV treatment, would also contribute to the higher oxidation observed for the Xe VUV treatment.

For polystyrene, the higher levels of oxidation observed for the Ar and Kr plasma treatments imply that a greater concentration of surface free radicals are produced during glow discharge treatment, this can be attributed to ion bombardment of the phenyl rings being able to generate a significant number of extra free radical centres originating from their unsaturated nature, whereas this is not as important in the case of xenon.

Two important differences emerge between the two types of polymer substrate employed in this study: firstly polystyrene is far more susceptible to surface oxidation than polyethylene, and secondly, more highly oxidized functionalities are detected for the former. This can be attributed to the phenyl groups present in polystyrene, since photo-excitation readily generates unsaturated carbon centres at the polymer surface during VUV and plasma exposure.

Previous VUV studies using a N_2 glow discharge (strongest emission lines at 174 nm and 149 nm) in the presence of O_2 gas gave rise to significant amounts of surface oxidation for both polyethylene[37] and polystyrene[38] corresponding to O:C ratios of 1.25 and 1.11. These results are consistent with the present study, since the N_2 plasma emission lines coincide with the very high absorption cross-section of molecular O_2 leading to the formation of $O(^3P) + O(^1D)$.

Work carried out by Hollander *et al.*[39,40] on the role of VUV in a variety of plasmas found that the oxygen containing gas mixture (O_2-H_2) VUV experiments gave rise to the lowest level of oxidation which is consistent with the results found in this chapter. They concluded that atomic oxygen played a minor role in oxidation, since the wavelengths from a O_2-H_2 plasma enabled production of the atomic oxygen without activation of the PE surface. However in their discussion of how the polymer becomes activated, they fail to take into account the ionization potential of the polymer being treated and therefore only attribute modification to activation of the polymer by absorption of the VUV radiation.

4. 5 CONCLUSIONS

The experiments have shown that VUV irradiation of polyethylene and polystyrene will result in surface modification providing that the energy of the VUV is sufficiently energetic to cause ionization of the polymer. Oxidation occurs via the VUV radiation activating the polymer giving rise to radical sites which subsequently can react with atomic oxygen or molecular oxygen, resulting in oxidation. The two processes, polymer activation and oxidation of the sites can occur simultaneously during the reaction.

The extent of modification observed depends upon the polymeric substrate and the type of feed gas used for the experiment.

4. 6 REFERENCES

1.   Clark, D. T.; Dilks, A. *J. Polym. Sci. ,Chem. Ed.*, **1980**, *18*, 1233.

2.   Baer, T. *Annu. Rev. Phys. Chem.*, **1989**, *40*, 637.

3.   Asford, M. N.; Macpherson, M. T.; Simons, J. P. *"Photochemistry and Spectroscopy of Simple Polyatomic Molecules in the Vacuum Ultraviolet"*, Springer-Verlag, New York.

4.   Samson, J. A. R. *"Techniques of Vacuum Ultraviolet Spectroscopy"*, Wiley, 1967.

5.   Clark, D. T.; Dilks, A. *J. Polym. Sci. Polym. Chem. Ed.*, **1977**, *15*, 2321.

6.   Liston, E. M. *9 th ISPC*, **1989**, *3*, L7.

7.   Griem, H. R. *Mat. Sci. Engin.*, **1991**, *A 139*, 1.

8.   Dilks, A. *Ph. D. Thesis*, University of Durham, 1977.

9.   Kelly, A. J. *J. Chem. Phys*, **1966**, *45*, 1723.

10.   Kogelchatz, U. *Pure Appl. Chem.*, **1990**, *62*, 1667.

11.   Clark, D. T.; Hutton, D. R. *J. Polym. Sci. Polym. Chem. Ed.*, **1987**, *25*, 2643.

12.   Egitto, F. D. *Pure Appl. Chem.*, **1990**, *62*, 1699.

13.   Egitto, F. D.; Matienzo, L. J.; Schreyer, H. B. *J. Vac. Sci. Technol.*, **1992**, *A10*, 3060.

14.   Srinvasa, R.; Mayne Banton,V. *Appl. Phys. Lett.* , **1982**, *41* , 576.

15.   Mittal, K. L. Ed, *"Physicochemical Aspsects of Polymer Surfaces 2"*, Plenum, 1983, 749.

16.   Clark, D. T.; Adams, D. B.; Dilks, A.; Peeling, J.; Thomas, H. R. *J. Electron. Spec.*, **1976**, *8*, 51.

17.   Beamson, G.; Briggs, D. *"High Resolution XPS of Organic Polymers: The ESCA 300 Database"*, Wiley, N. Y., 1992.

18.   Clark, D. T.; Dilks, A. *J. Polym. Sci. Chem. Ed.*, **1977**, *15*, 15.

19. Seebok, R. J.; Kohler, W. E.; Romheld, M. *Contrib. Plasma. Phys.*, **1992**, *32*, 613.

20. Godyak, V. A.; Piejak, R. B. *Phys. Rev. Lett.*, **1990**, *65*, 996.

21. Ajello, J. M.; James, G. K.; Franklin, B.; Howell, S. *J. Phys. B. At. Opt. Phys.*, **1990**, *23*, 4355.

22. Stone, E. J.; Lawrence, G. M.; Fairchild, E. C., *J. Chem. Phys.*, **1976**, *65*, 5083.

23. Hollahan, J. R.; Bell, A. T. Eds. *"Techniques and Applications of Plasma Chemistry"*, Wiley, N. Y., 1974.

24. Hollahan, J. R. *J. Chem. Ed.*, **1966**, *43*, A401.

25. Mayoux, C.; Antoniou, A.; Ai, B.; Lacoste, R. *Eur. Polym. J.*, **1973**, *9*, 1069.

26. Okabe, H. *"Photochemistry of Small Molecules"*, Wiley Interscience, USA, 1978.

27. Landenburg, R.; Van Voorhis, C. C. *Phys. Rev.*, **1933**, *43*, 315.

29. Uri. N. *"Autooxidation and Antioxidants"*, Vol 2, Wiley, 1962.

28. Egitto, F. D. Pure Appl. Chem., **1990**, *62*, 1699.

30. Cain, S. R.; Egitto, F. D.; Emmi, F. *J. Vac. Sci. Technol.*, **1987**, *A5*, 1578.

31. McKellar, J. F.; Allen, N. S. *"Photochemistry of Manmade Polymers"*, Applied Science Publishers Ltd, 1979.

32. Calvert, J. G.; Pitts, J. N. Jr. *" Photochemistry"*, Wiley, 1966.

33. Matienzo, L. J.; Zimmerman, A.; Egitto, F. D. *J. Vac. Sci. Technol.*, **1994**, *A12*, 2662.

34. Takcas, G. A.; Vukanovic, V.; Tracy, D.; Chen, J. X.; Egitto, F. D.; Matienzo, L. J.; Emmi, F. *Polym. Degrad. Stabil.*, **1993**, *40*, 73.

35. Partridge, R. H. *J. Chem. Phys.*, **1966**, *45*, 5, 1685.

36. Clark, D. T.; Dilks, A. *J. Polm. Sci.. Polym. Chem. Ed.*, **1978**, *16*, 911.

37. Shard, A. G.; Badyal, J. P. S. *Polym. Commun.*, **1991**, *32*, 217.

38. Shard, A. G.; Badyal, J. P. S. J. Phys. Chem., **1991**, *95*, 9436.

39.   Hollander, A.; Klemberg-Sapieha, J. E.; Wertheimer, M. R. *Macromolecules*, **1994**, *27*, 2893.

40.   Hollander, A.; Kelmberg-Sapieha, J. E.; Wertheimer, M. R. *J. Polym. Sci. Chem. Ed.*, **1995**, *33*, 1013.

Chapter Five

CF$_4$ Plasma Treatment of

Asymmetric Polysulfone Membranes

Chapter Five

CF$_4$ Plasma Treatment of Asymmetric Polysulfone Membranes

5. 1 INTRODUCTION

This chapter investigates the effect a non-polymerizable, chemically reactive plasma has on the transport properties of an asymmetric polysulfone membrane. Results from chapter two and three show that a CF$_4$ plasma dramatically changes the surface properties both chemically and topographically. Transport properties of a permeant through a membrane are influenced by both chemical and physical properties and the aim of this chapter was to probe how plasma treatment affected such properties.

5. 1. 1 Background

Permeability plays an important role in many areas such as the food and packaging industry, gas separation membranes, filtration processes and in controlled release devices used in medicine. This work concentrates on gas separation membranes. The aim within this area is to produce membranes with high permeability and permselectivity (separation factor). There is usually a trade-off between these two properties since the factors which influence them conflict. High selectivity requires a material which is rigid, crystalline and highly crosslinked. High permeability requires a membrane which is amorphous because it is the amorphous regions in a polymer which the penetrants diffuse through. However materials can be produced where the traditional "trade-off" between these two properties is reduced and membranes can be prepared that possess both high selectivity and permeability. There are two general rules which are thought to explain

the structure/property relations. Structural changes in the membrane that inhibit packing such as the formation of relatively rigid chains can increase permeability whilst retaining selectivity. Alternatively, reduction of the rotational mobility about flexible linkages in the polymer backbone lead to higher permselectivities without losses in permeability, provided that the intersegmental packing is not significantly affected[1].

Research into achieving such a membrane is prolific and there are several methodologies:-

1. Development of new materials for gas separation.

2. Changing membrane structure.

3. Modifying membranes.

5. 1. 2 New Materials for Gas Separation

Several authors have achieved enhanced membrane properties by the preparation of new polymers for gas separation. A series of polycarbonates[2], with various substitutions on the aromatic ring, for example halogens, enabled the structure/property relationship to be investigated. It was found that Cl and Br resulted in a reduction in the permeability. This was attributed to the action of the cohesive forces due to the polarity of the halogens resulting in more densely packed chains. Fluorine substituted polycarbonates gave rise to high diffusivity coefficients due to fluorine hindering rotational movements about flexible linkages in the polymer backbone[3]. There has been similar work on polyimides[4] and polyacrylates[1].

5. 1. 3 Membrane Structure.

There are three main types of membrane structure, homogeneous (or dense), asymmetric and composite. A homogeneous membrane consists of one material with the same type of structure throughout. In contrast, an

139

asymmetric membrane consists of a dense skin layer supported by a porous matrix of the same material. Composite membranes are composed of materials of vastly different chemical structures[5].

The advantage of using an asymmetric membrane is that it allows high productivity, that is, the skin layer is the selective part of the membrane but it is very thin and therefore does not detrimentally alter the permeance. The "sponge-like" matrix acts as a mechanical support allowing gas to pass through with little resistance.

The phase inversion technique for the preparation of asymmetric membranes utilises a change in composition of initial polymer concentration for initiation of the phase separation. Preparation of an asymmetric membrane by concentration immersion involves three main steps[6,7,8,9]:-

1. Casting homogeneous film onto flat surface (typically a glass substrate).

2. Evaporation of casting film (evaporation step).

3. Immersion of evaporated film into nonsolvent/solvent bath or coagulation bath (quench step).

Figure 1: Schematic diagram of asymmetric membrane preparation.

Surrounding Medium

- -

Casting Film

Substrate Side
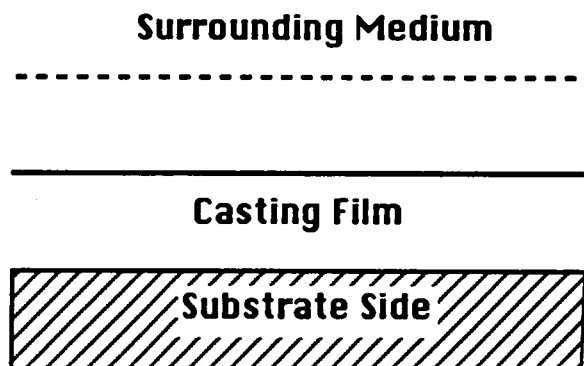
In the evaporation step the surrounding medium is air. In the quench step, the coagulation bath is the surrounding medium.

Each step involves many variables such as the solvent, quench medium, evaporation time, solvent concentration and so on. The final product is heavily dependent on the process of formation, leading to variations in the films even prepared from the same batch[10]. The ideal asymmetric membrane should comprise a very thin defect free skin layer and a substructure which does not contribute any resistance to gas transport[11].

5. 1. 4 Modification of Membranes.

Numerous different methods for the modification of membranes have been utilised including UV grafting of functionalities[12], fluorination[13], photooxidation[14], ion beam irradiation[15] and plasma treatment[16,17]. Modification via plasma treatment has been studied by depositing a thin layer of "plasma polymer" onto the membrane and by the grafting of functionalities onto the surface.

The deposition of an ultra-thin coating by plasma polymerization has been of interest in several areas of membrane technology from reverse osmosis membranes[18] to gas separation membranes[1]. The technique enables a permselective layer to be deposited on a highly permeable polymer. Matsuyama *et al.*[19] found that the performance of pervaporation membranes was improved by using siloxane monomers with long chains due to more continuous linking within the polymer structure. The deposition of a plasma polymer from fluorine containing monomers was found to improve the oxygen/nitrogen selectivity[20,21]. Plasma gas mixtures were also found to improve the hemocompatibility[22] of membranes.

Wang[23] modified polypropylene by using an ammonia plasma, which is considered to be a non-polymerizing gas but does chemically modify a surface in a glow discharge. Due to amination from the NH_3 plasma, the treated side becomes hydrophilic[23]. Ideally modification via

plasma treatment should utilise a gas treatment in a one step process, rather than the deposition of a plasma polymer, as this is more likely to reduce the flux through the membrane.

5. 2 EXPERIMENTAL

Asymmetric polysulfone membranes were prepared by casting polysulfone (Udel P3500, Union Carbide) 20% by weight dissolved in dimethylacetamide (99%+, Lancaster) onto a glass substrate at ambient temperature followed by immersion in deionized water. High purity carbon tetrafluoride (99.7%, Air Products) gas was used for the plasma treatments.

Figure 2: Experimental procedure for the formation of an asymmetric membrane.

CASTING　　　　　EVAPORATION　　　　　COAGULATION
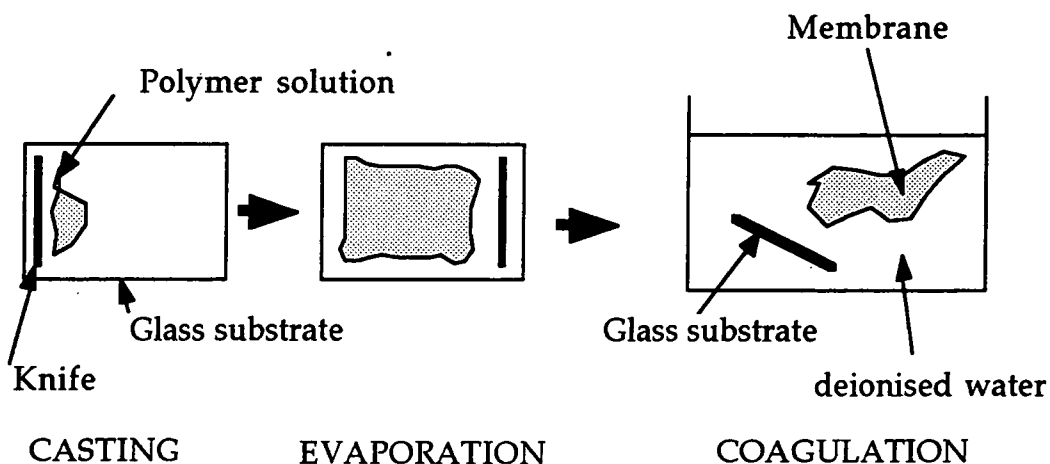
Discs (2.1 cm diameter) of the polysulfone asymmetric membranes (dense skin side) were plasma treated in accordance with the experimental outline described in section 2.2. The samples were analysed immediately by XPS and AFM (section 2.2).

Mass spectrometric sampling devices[24] have been previously used to evaluate the permeability of common elastomers[25,26]. In this study,

methane plasma polymer was deposited onto the dense side of the asymmetric polysulfone membrane and placed into a permeability probe[27], figures 3 and 4, which consisted of two drilled-out stainless steel flanges. A copper gasket was used to ensure a leak-tight seal and an electron microscope grid provided mechanical support to the membrane.

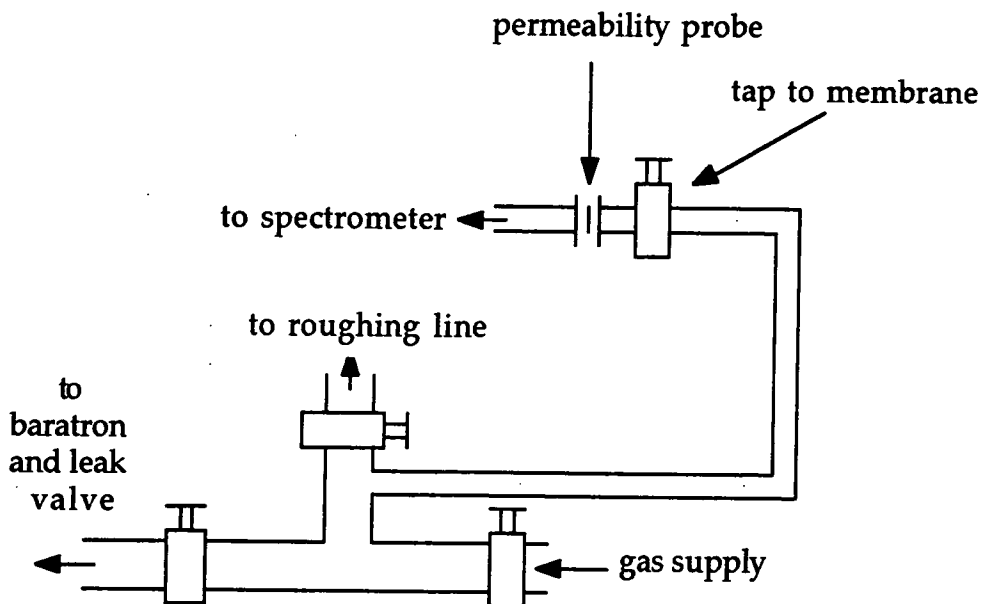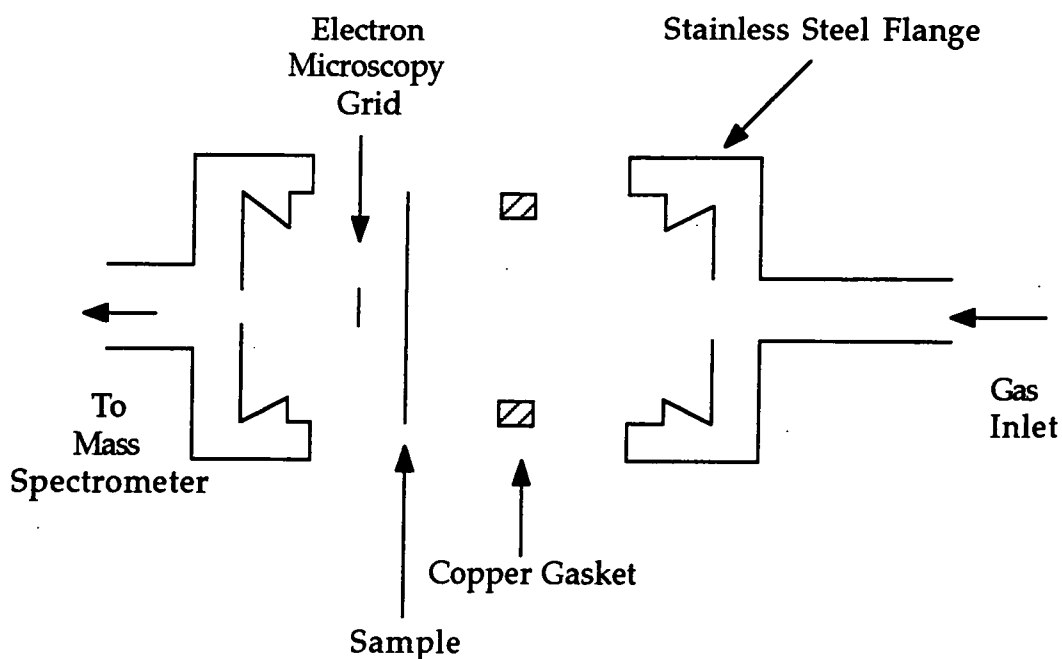Figure 3: Schematic diagram of the permeability apparatus.

Figure 4: Cross section of permeability probe.

The probe was coupled to the sample preparation chamber of a Kratos ES300 X-ray photoelectron spectrometer (base pressure of 2×10^{-10} mbar) by means of a stainless steel tube inserted through a ball valve. The coated side of each sample film was exposed to a gas pressure of 800 mbar. Permeant pressure was monitored with a UHV ion gauge (Vacuum Generators, VIG 24). A quadrupole mass spectrometer (Vacuum Generators SX200) interfaced to a PC computer was used to follow compositional analysis of the permeant species. High purity nitrogen (BOC, 99.995%) and oxygen (BOC, 99.6 %) gases were used. The quadrupole mass spectrometer's response per unit pressure was calculated by introducing each gas in turn into the chamber and recording the corresponding mass spectrum intensity at a predetermined pressure of 5×10^{-6} mbar (taking into account ion gauge sensitivity factors[28]). The mean equilibrium permeant partial pressure of each gas was measured in the steady-state flow regime[29].

5. 3 RESULTS

5. 3. 1 XPS

The chemical structure of clean untreated polysulfone was found to be consistent with the known structure (figure 1, section 2.2)[30], figure 5(a). The XP spectra of C(1s), O(1s) and S(2p) regions of untreated polysulfone have been discussed in section 2.3.1.

CF_4 plasma treatment of the asymmetric polysulfone membrane results in a substantial amount of fluorination at the surface. This is accompanied by a dramatic change in the C(1s) XPS spectrum with $>\underline{C}F_2$ functionalities being the predominant fluorine moiety. Fluorinated functionalities corresponding to $\underline{C}F_3$ at 293.6 eV and $\underline{C}F_2$ at 291.2 eV[30] can be assigned, as described in Chapter 2(section 2. 3), figure 5(b). The 1:1 O(1s) doublet could no longer be resolved and the S(2p) feature was found to be strongly attenuated.

The elemental ratio varied as a function of plasma duration and power, figure 6 and 7, approaching limiting values of approximately 48%C, 48%F, 0.8%S and 4%O at greater than powers of 5 W (15 minute treatment time) and no longer than a 5 minute treatment time (for a fixed power of 10 W) consistent with results found by a 5 minute fluorination (2% F_2 in He) treatment of poly(4-methyl-1-pentene)[31].

Figure 5: C(1s) XP spectrum of (a) untreated polysulfone, (b) CF$_4$ plasma treated polysulfone (20 W, 15 min).
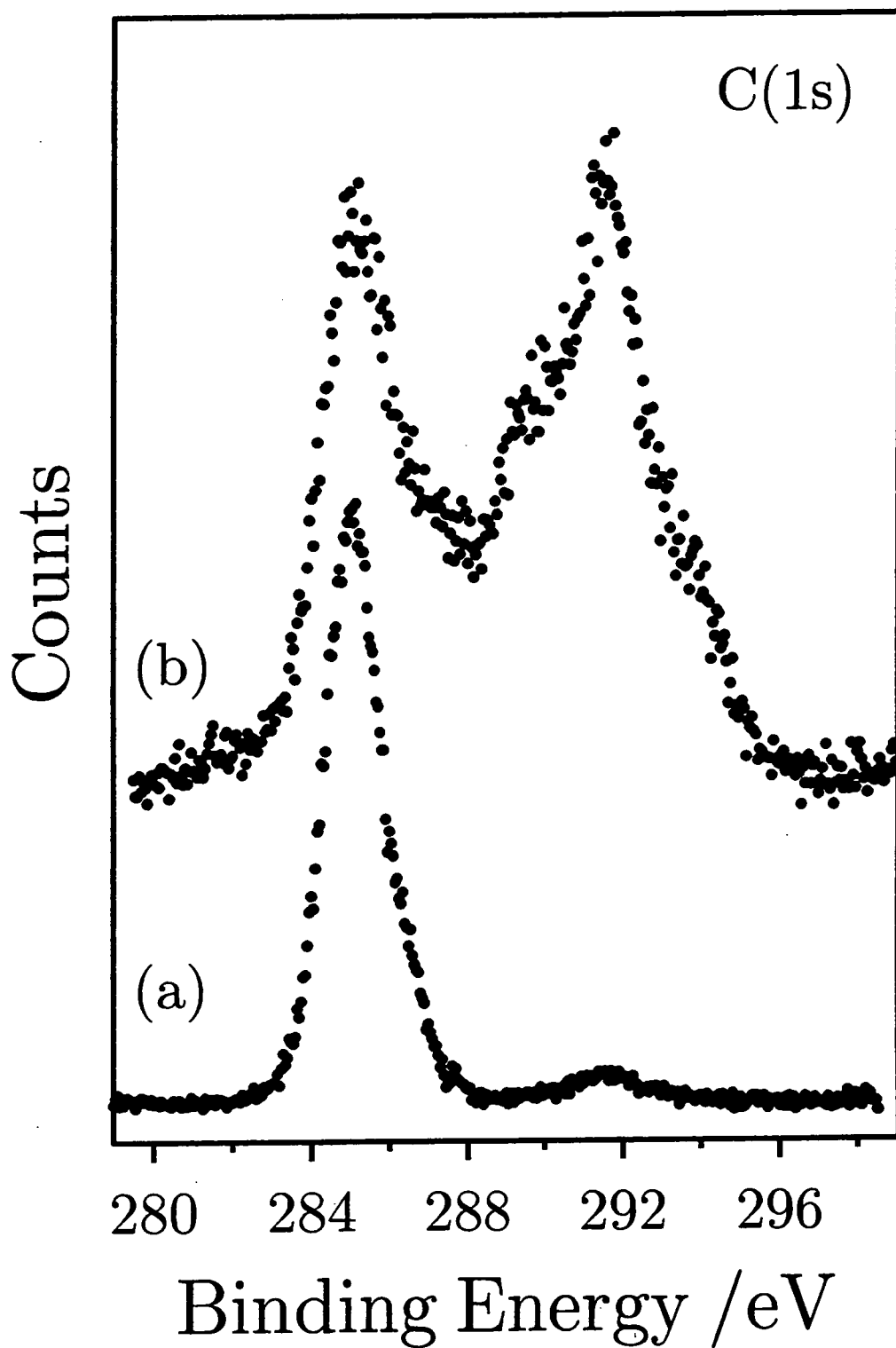
Figure 6: Elemental composition as a function of CF$_4$ plasma treatment time.
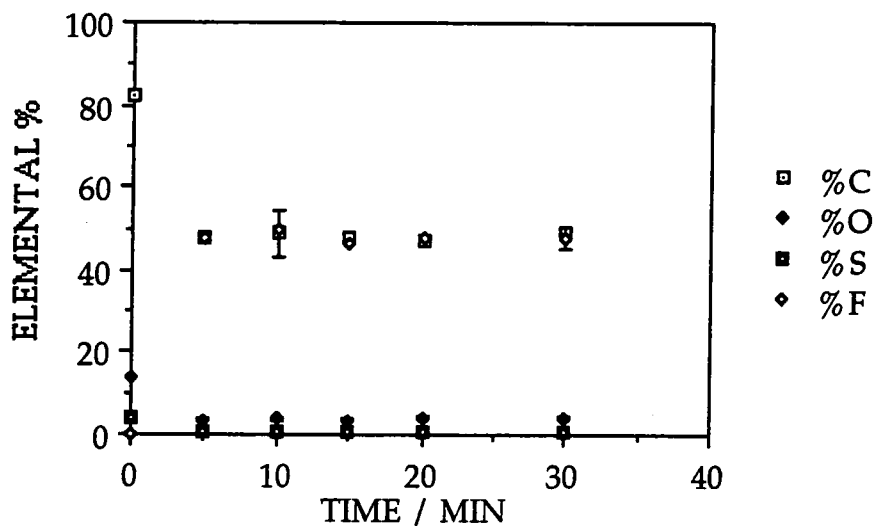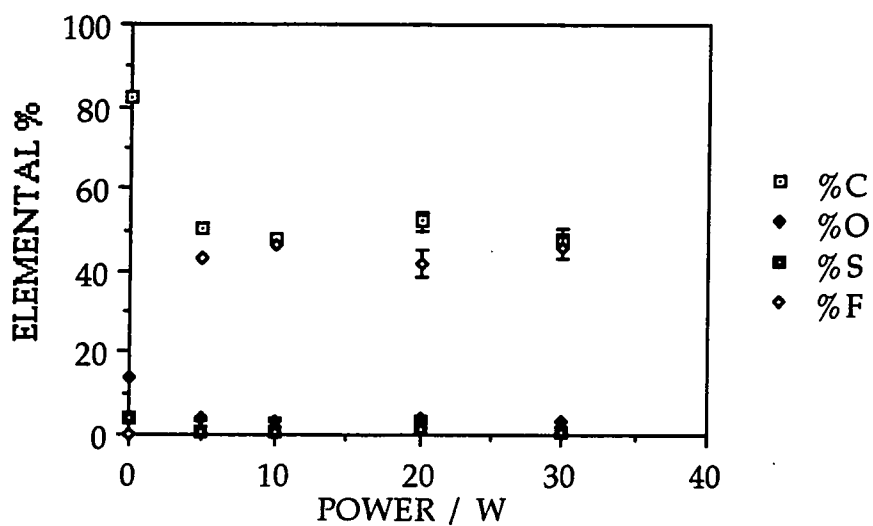

Figure 7: Elemental composition as a function of CF$_4$ plasma power.

5. 3. 2 AFM

The untreated dense skin side of the asymmetric polysulfone membrane has a compact structure, figure 8(a), whilst 1.27 ± 0.16 μm pores apertures are evident on the opposite face, figure 8(b).

A gradual roughening of the surface was observed during CF_4 plasma treatment of the dense skin side of the asymmetric membrane with increasing input powers and exposure times, figures 9 (a and b) and 10 (a and b) which eventually leads to small holes in the surface.

5. 3. 3 Permeability Measurements

Figure 11 shows the changes in permeant pressure with the power variation of a 15 minute CF_4 plasma treatment. There is initially a drop in permeant pressure for the 5 W treatment relative to the untreated membrane. As the power is increased, the permeant pressure rises with the greatest change observed at 30 W. O_2/N_2 selectivity is shown in figure 12. A similar trend was observed when the power was maintained at 10 W, whilst the treatment time was increased, as shown in figure 13. Such trends are consistent with the results found for fluorination of various polymers with fluorine gas[13,32].

Examining the selectivity (represented as α) of O_2/N_2, there appears to be slightly improved, at short treatment time (e.g. 5 min) or low powers (5 W). The $\alpha(O_2/N_2)$ of the 5 W, 15 min CF_4 plasma treated sample increased by to 1.38 ± 0.11, figure 12, and the $\alpha(O_2/N_2)$ of the 10 W, 5 min CF_4 plasma treated sample increased to 2.670 ± 0.34, figure 14. The errors refer to repetition of the permeability measurement on the same sample.

Figure 8 (a): AFM micrograph of the dense skin side of a polysulfone asymmetric membrane.

x = 2 µm / div
z = 2 µm / div

µm

2   4   6   8

(a)

149
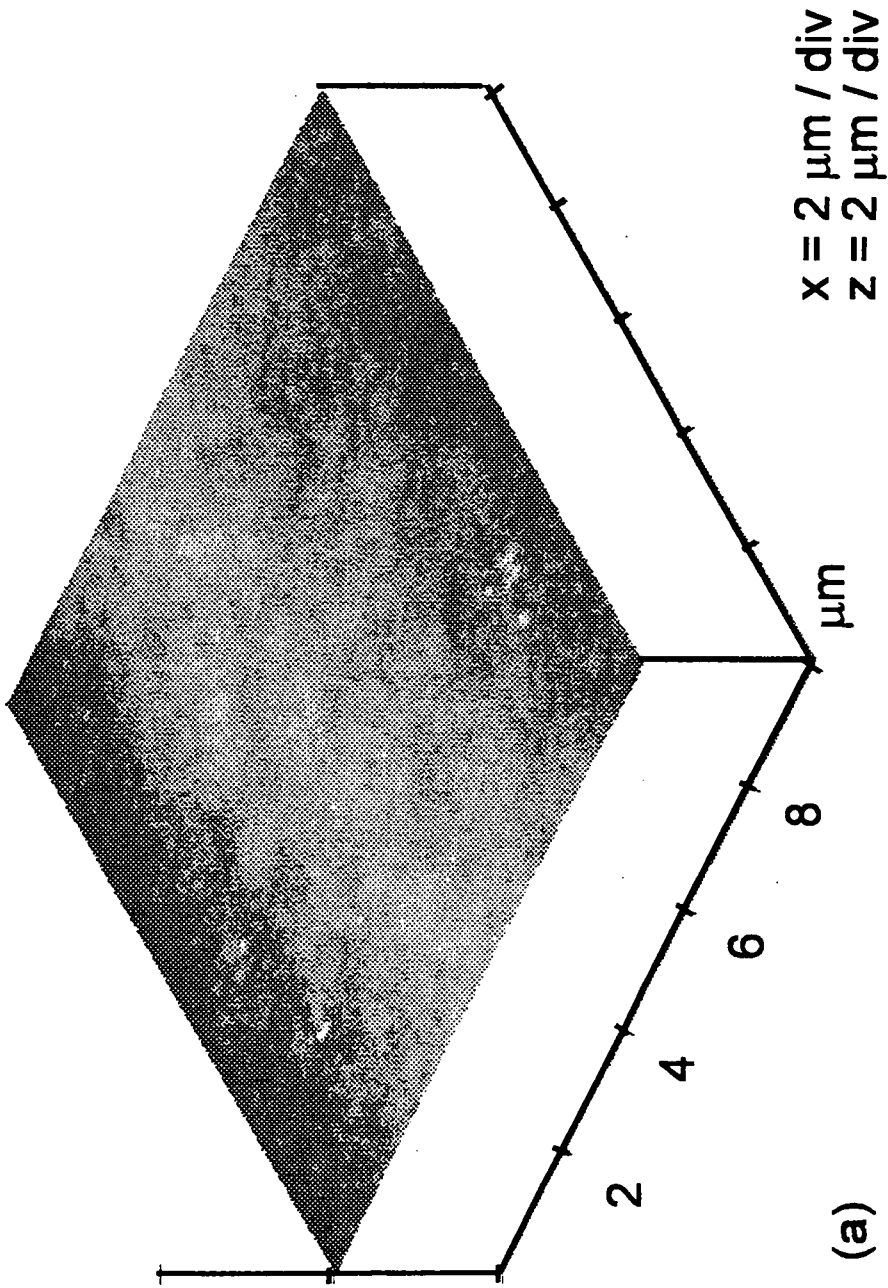
Figure 8 (b): AFM micrograph of the porous side of a polysulfone asymmetric membrane

x = 2 μm / div
z = 2 μm / div

μm

2   4   6   8

(b)
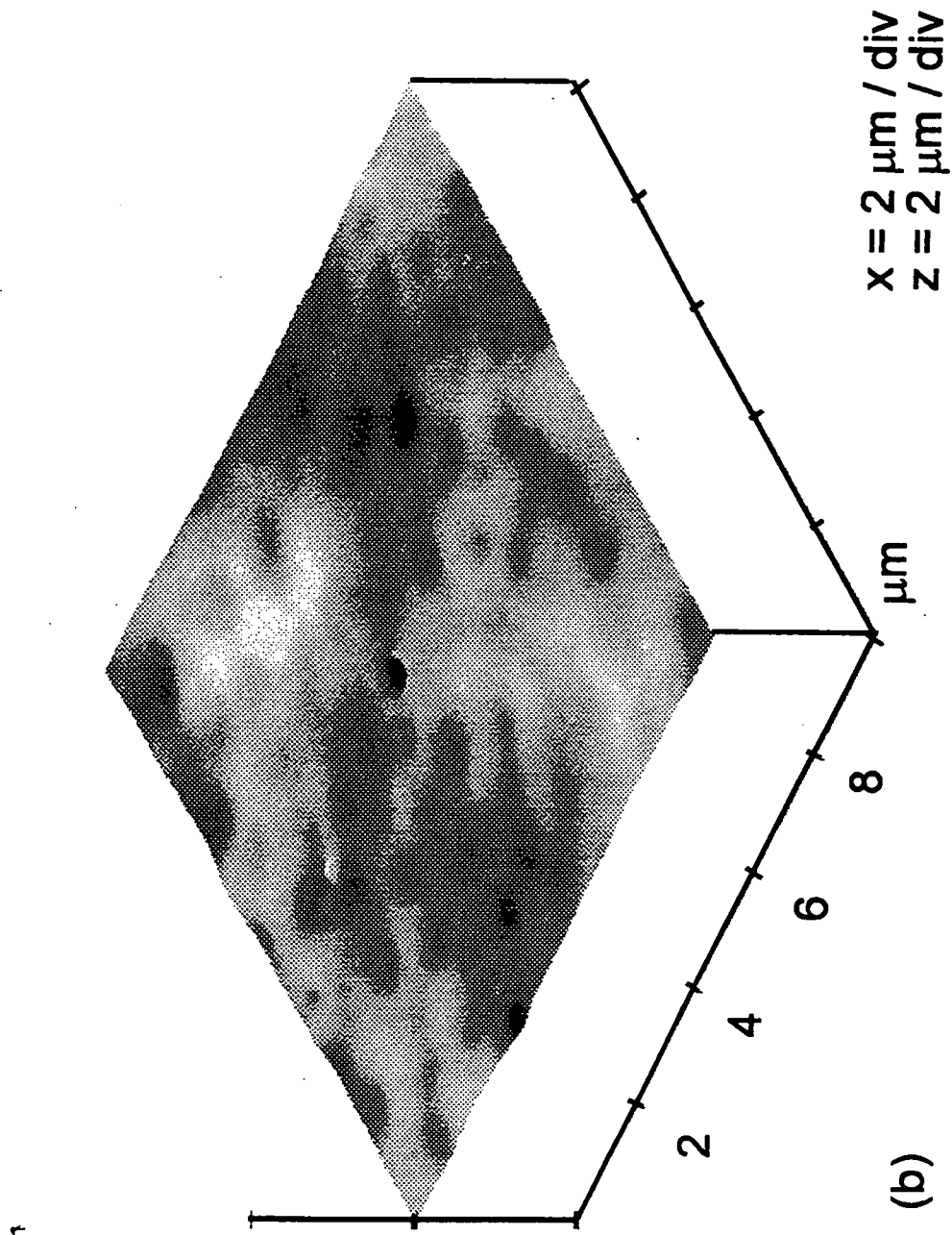
Figure 9 (a): AFM micrograph of a CF4 plasma treated asymmetric polysulfone membrane (5 W, 15 minutes).

x = 0.2 μm / div
z = 200 nm / div

μm

0.2   0.4   0.6   0.8

(a)

151
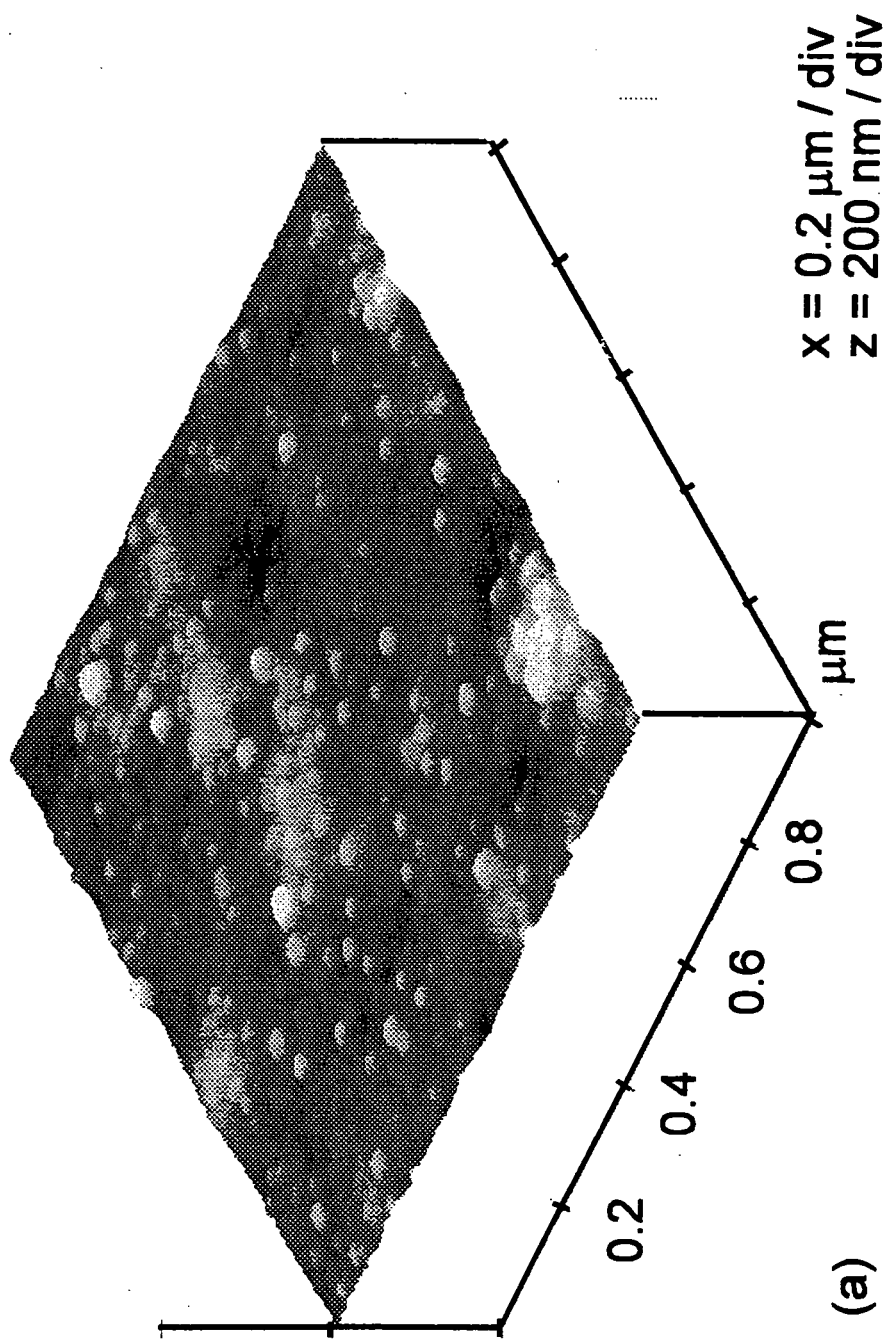
Figure 9 (b): AFM micrograph of a CF$_4$ plasma treated asymmetric polysulfone membrane (30 W, 15 minutes).

x = 0.2 μm / div
z = 200 nm / div

(b)

152
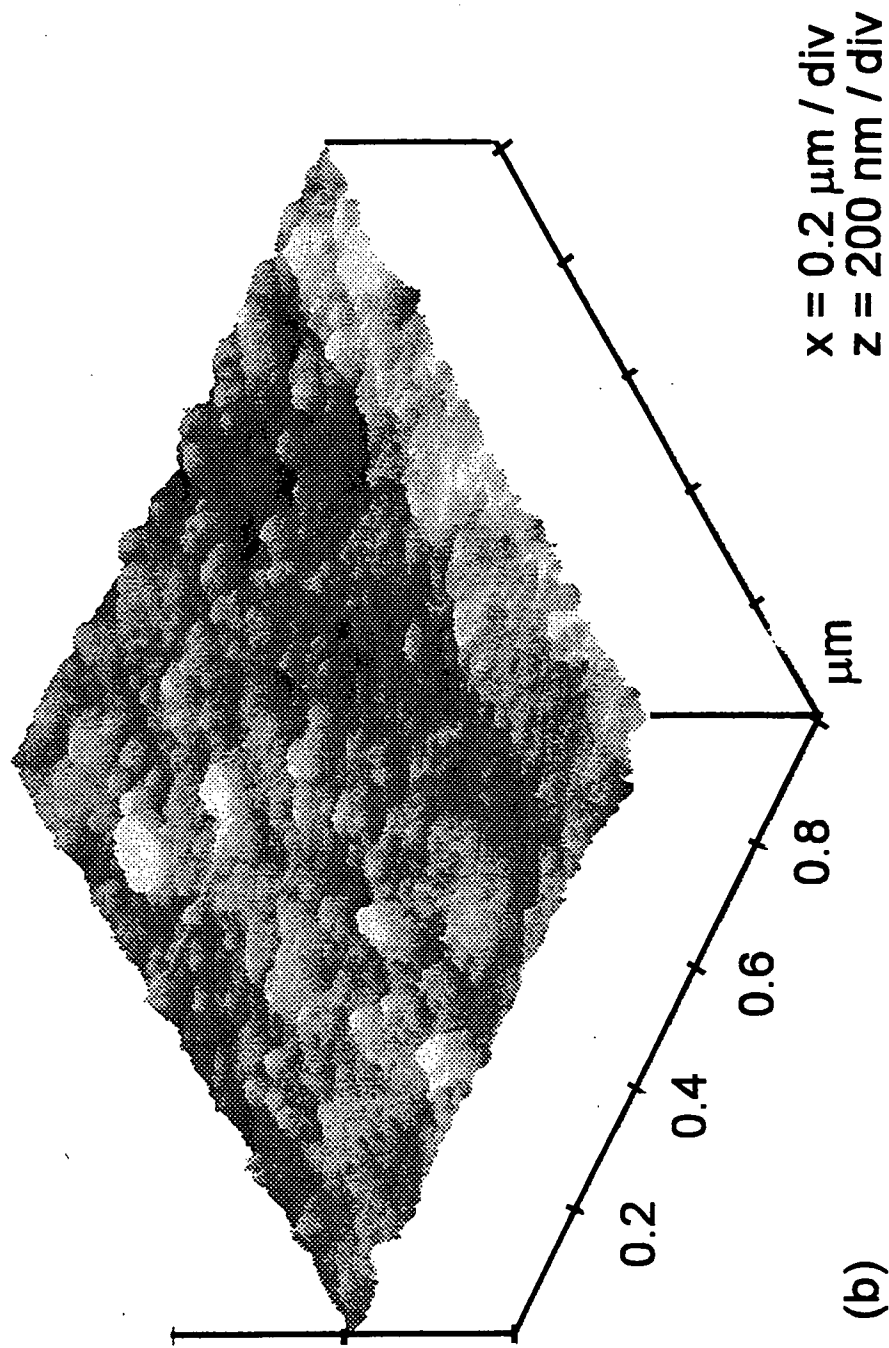
Figure 10 (a): AFM micrograph of a CF$_4$ plasma treated asymmetric polysulfone membrane (5 minutes, 10 W).

x = 0.2 μm / div
z = 200 nm / div

0.2   0.4   0.6   0.8   μm

(a)

153
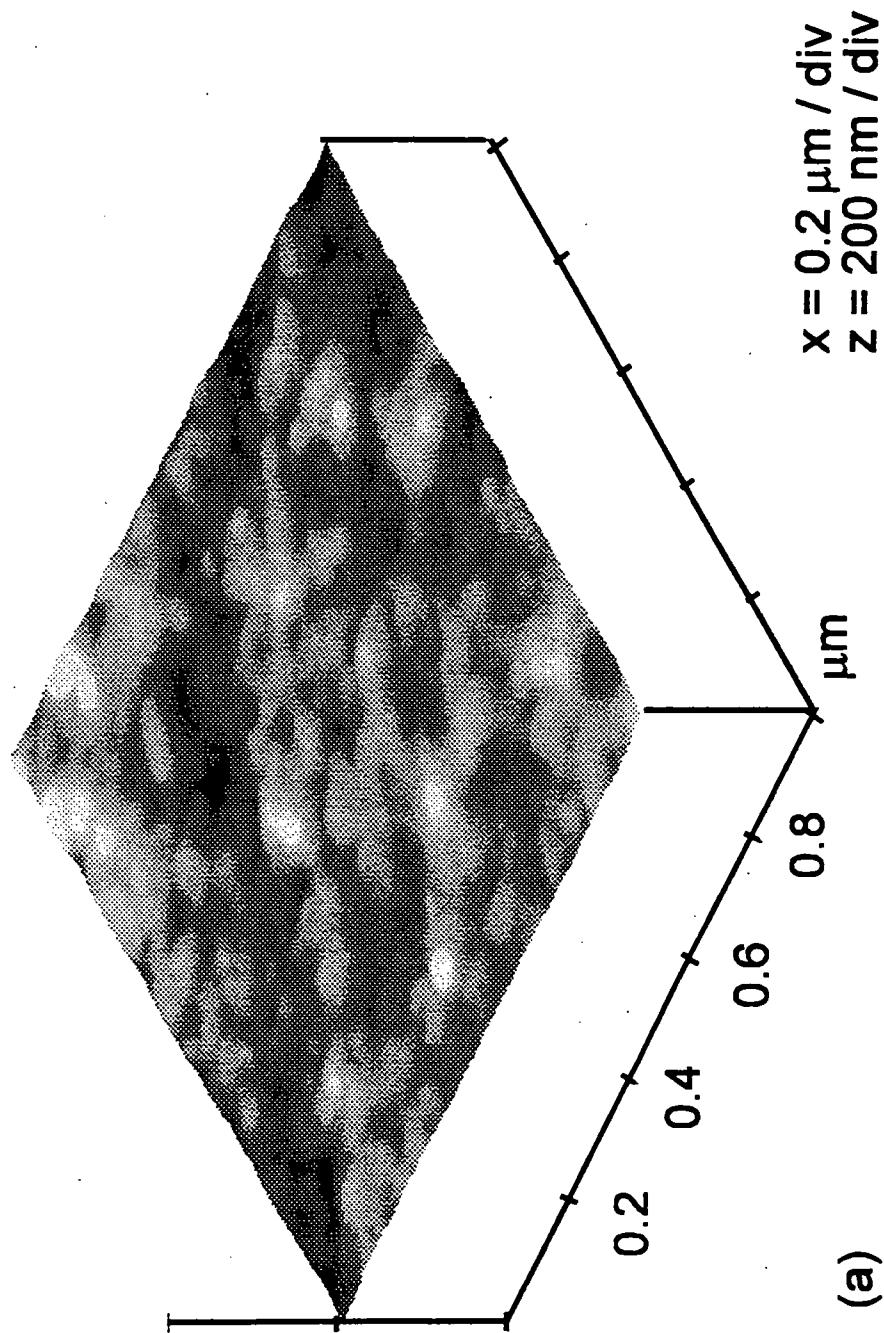
Figure 10 (b): AFM micrograph of a CF$_4$ plasma treated asymmetric polysulfone membrane (30 minutes, 10 W).

x = 0.2 μm / div
z = 200 nm / div

μm

0.2   0.4   0.6   0.8

(b)

154
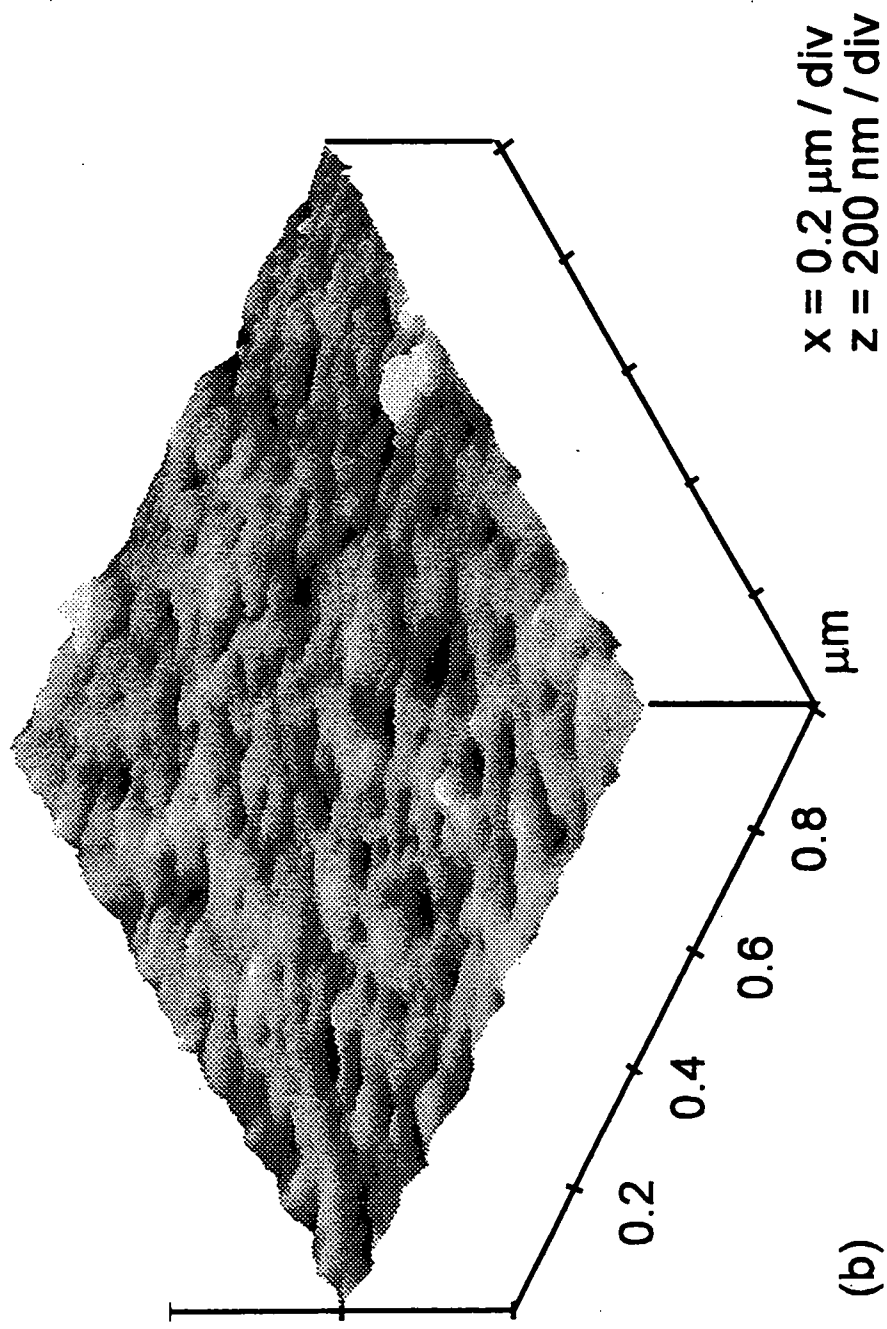
Figure 11: Pressure of permeant versus power of CF4 plasma treatment of an asymmetric polysulfone membrane.

155

Figure 12: Oxygen/Nitrogen selectivity of CF$_4$ plasma treated asymmetric polysulfone membrane as a function of plasma power.

156

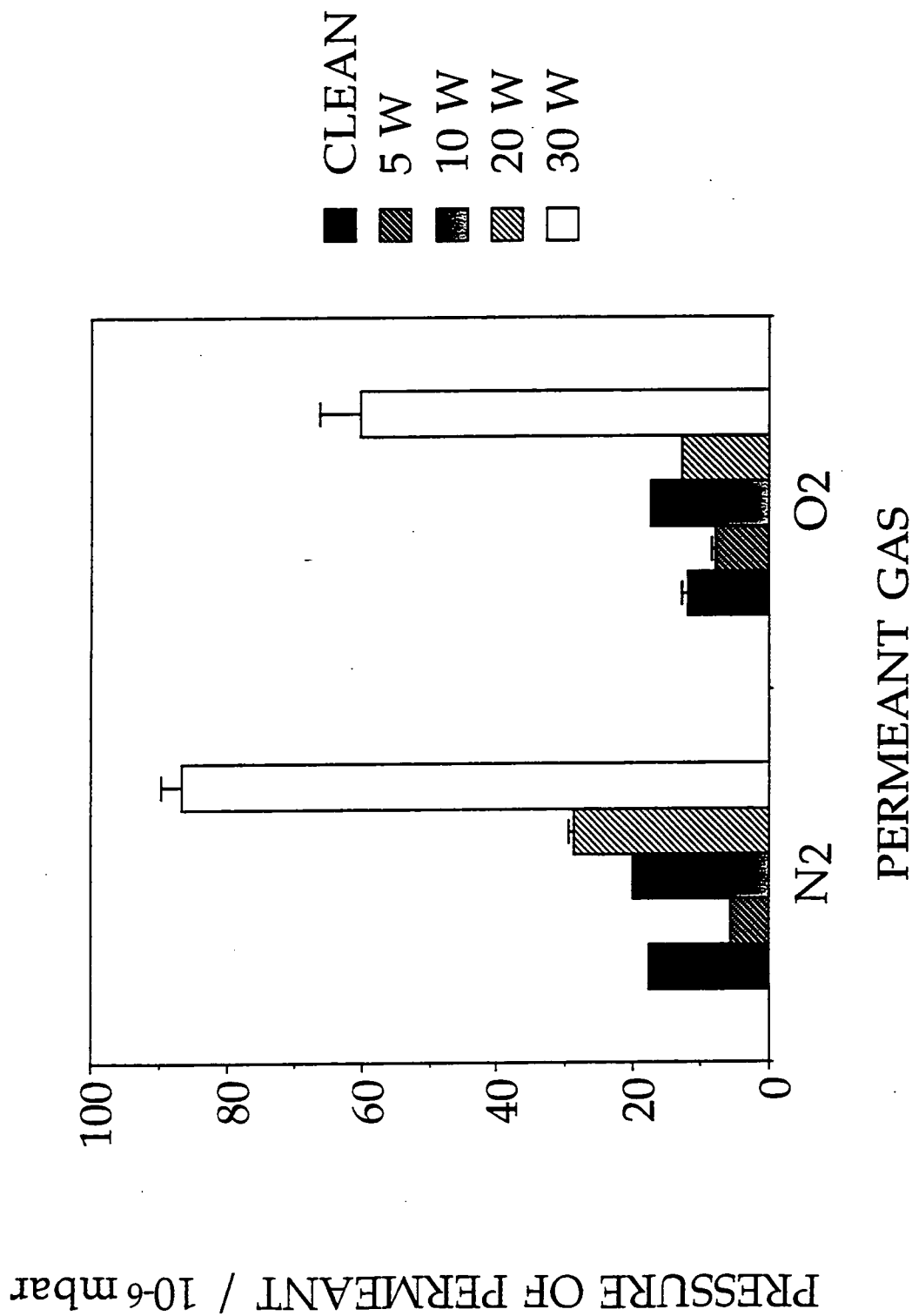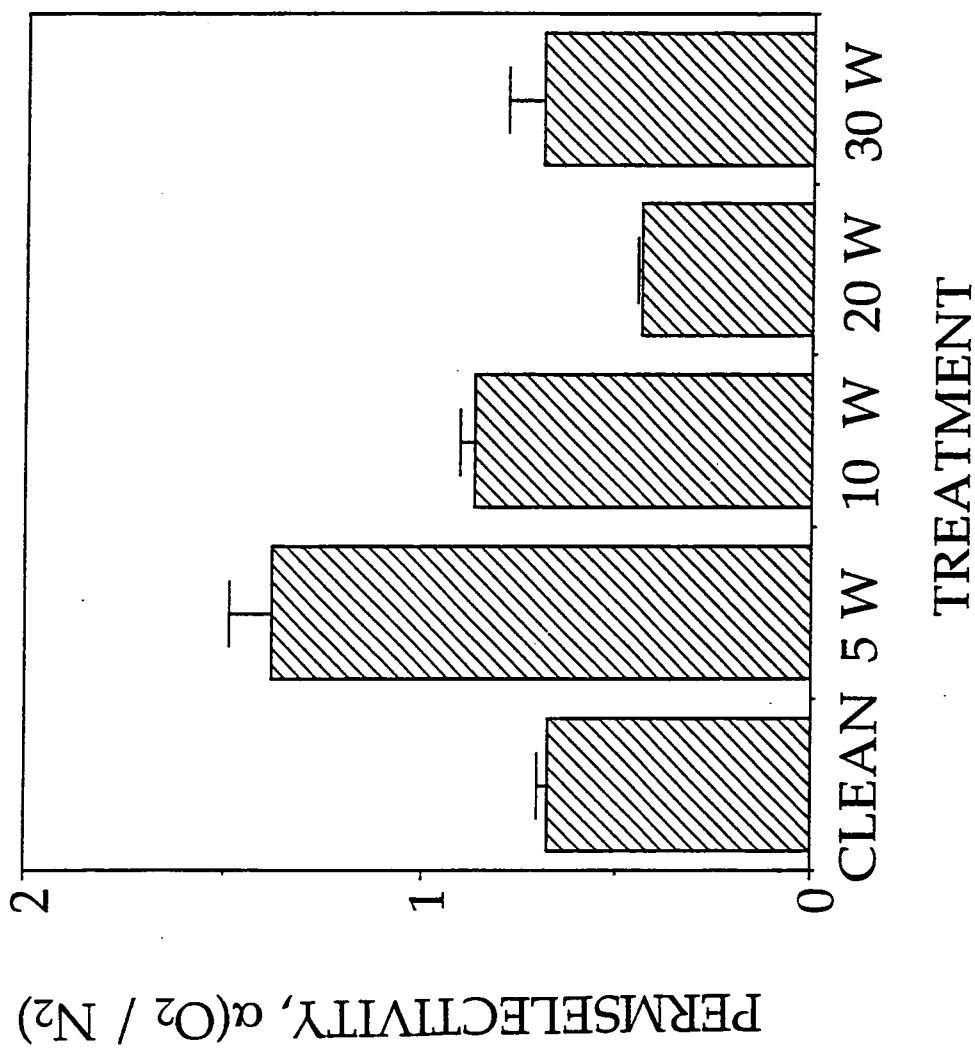Figure 13: Pressure of permeant versus duration of CF4 plasma treatment of an asymmetric polysulfone membrane.
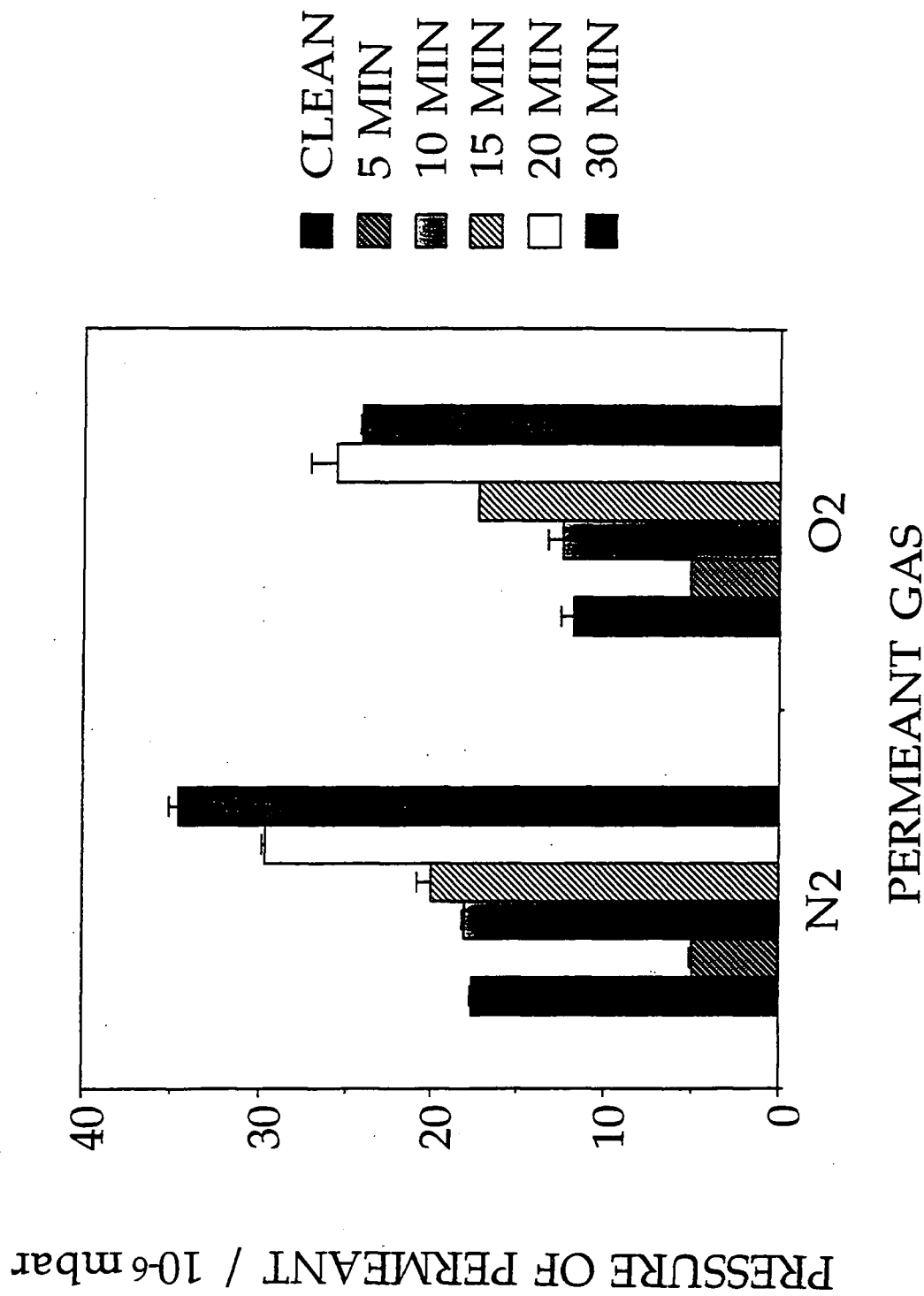
Figure 14: Oxygen/Nitrogen selectivity of 10W CF_4 plasma treated asymmetric polysulfone membrane as a function of plasma treatment time.

158
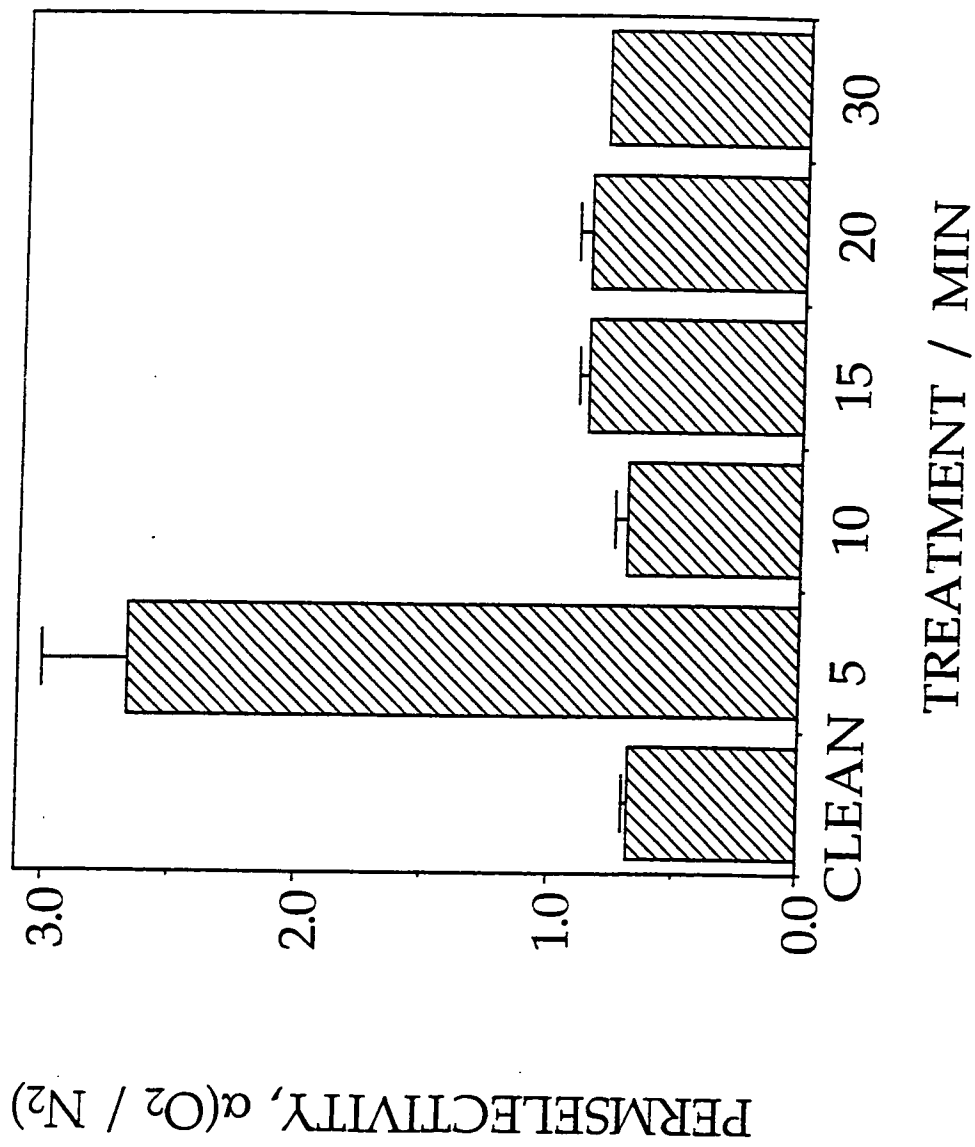
5. 4 DISCUSSION

Fluorination of a membrane surface has been studied by several workers[13,32-34] who found that the gas separation properties can be improved. Their work involved fluorination of dense and asymmetric polymer films by using a small percentage of fluorine gas in an inert gas, typically He. In this work, a CF_4 plasma was employed to fluorinate the surface which has the advantage of being an efficient, "clean" technique.

CF_4 plasma treatment of the asymmetric structure can be thought of as resulting in a composite structure, figure 15.

Figure 15: Schematic diagram of CF_4 plasma treatment of an asymmetric polysulfone membrane.

Asymmetric Polysulfone Membrane   Fluorinated Membrane
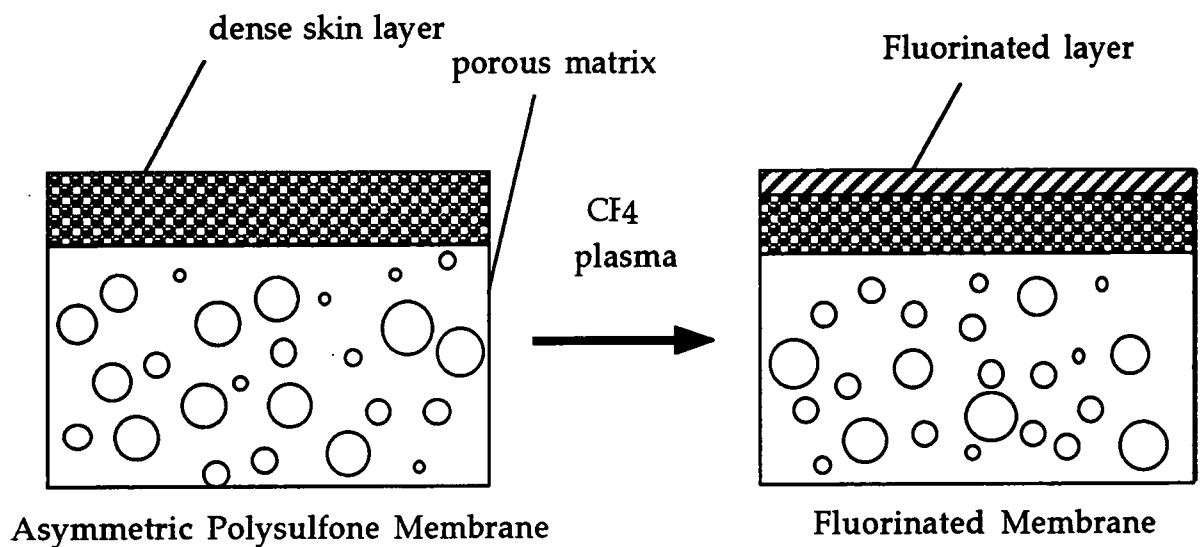
Since the dense skin layer and the fluorinated layer will have different permeation properties, a series resistance model can be used to describe the transport properties[35]. This model shows that the permeation of the gases will depend on both the depth and composition of the fluorinated layer, equation 1.

159

$$(P/l)_i = [(l_a/P_a)_i + (l_b/P_b)_i]^{-1} \qquad (1)$$

where (P/l) is the permeance through the membrane, P_a is the permeability through the unfluorinated layer, P_b is the permeability through the fluorinated layer and l_a, l_b are the thicknesses of the unfluorinated and fluorinated layers respectively. The porous substructure has not been included in the equation since, in theory, it should not contribute to the permeation properties[32,33]. The solubility, diffusivity and permeability of the gases studied may also be different in the fluorinated layer than for the untreated layer.

Fluorination of poly(4-methyl-1-pentene), PMP, produces a material which is insoluble in cyclohexane or chloroform[31], indicating that the surface was crosslinked since the solvents are used to make PMP. The VUV component in a CF_4 plasma will give rise to crosslinking in the subsurface of the polysulfone membrane. This may account for the observed decreases in permeant pressure for the gas molecules because a closed, rigid structure will present a more tortuous pathway to the permeant gas[36] than in the untreated membrane at low powers and short treatment times. The effect of crosslinking upon the passage of small molecules will be less effective[33], however since N_2 and O_2 are of comparable size (gas diameter 3.75, 3.61 Å respectively)[37], the attenuation in permeant pressure is similar.

Diffusivity selectivity is based upon the ability of polymer matrices to operate as size and shape selectivity through chain mobility and packing[34,38]. Fluorination of a polysulfone membrane by CF_4 plasma treatment will not only give rise to crosslinking at the surface but also rotational hindrance (since the F atom is bigger than the hydrogen atom it is replacing). This is likely to result in a more rigid structure due to the restriction of mobility of the molecular chains after fluorination. Since O_2 and N_2 are of a similar size then the change in permselectivity must depend upon changes in the solubility selectivity (dependent upon the solubility of

160

the permeating gases in the fluorinated structure) rather than the diffusivity selectivity.

The increase in O_2/N_2 selectivity is consistent with the greater affinity of fluorine functionalities to molecular oxygen in fluorocarbon bilayer films [39,40] compared to nitrogen, explaining the change in selectivity for short treatment time and low power CF_4 plasma treated samples.

Fluorination of asymmetric polysulfone by 2%F_2 in He gave rise to better gas transport characteristics at shorter exposure times[13] than the untreated polymer. It was suggested that at longer times the entire or a significant amount of the skin layer was fluorinated and since this was not the optimum value, then a decline in permselectivity is observed[13]. Similar results were found for polyphenyleneoxide and composite membranes[31,32].

In CF_4 plasmas the depth of fluorination is controlled by a balance between fluorination and ablation. The F atoms can etch/ablate the polymer whilst a combination of F atoms and CF_x radicals can contribute to the formation of the fluorinated layer[41]. The skin layer of an asymmetric membrane is very thin, 500-1000 Å[13] and the plasma treatment could result in damage of the skin at very thin or weak regions[32,33]. At higher powers, the extent of degradation due to "physical" etching by the CF_4 plasma as a result of increased ion flux[32,42] may lead to the destruction of the delicate skin layer leading to the observed increase in permeability. Beyond a critical power level the CF_4 plasma begins to result in more etching/degradation at the membrane surface than fluorination.

This can clearly be seen in the AFM micrographs where higher input powers and longer treatment times give rise to holes appearing in the dense skin surface to reveal the underlying "sponge-like" matrix of the asymmetric membrane. This leads to increases in gas permeability and a loss of any enhancement of permselectivity due to the rupture of the fluorinated skin.

It is interesting to note that the fluorination of an aysmmetric polysulfone membrane by exposure to F_2 gas does not show any change in the surface topography upon treatment[9], therefore the CF_4 plasma is a much more reactive medium compared to F_2 gas exposure.

5.5 CONCLUSIONS

CF_4 plasma treatment of an asymmetric membrane changes the permeation of gases through the membrane. Longer treatment times and higher powers of the plasma lead to higher permeant pressures as a consequence of damage of the thin skin layer by the action of the CF_4 plasma. The 5 W, 15 minute and the 10 W, 5 minute samples both gave rise to a reduction in permeant pressure and an increase in the $\alpha(O2/N2)$. The properties of these samples can be attributed to a number of possibilities predominantly that the action of the plasma is sufficient to cause fluorination of the skin layer without causing detrimental etching or damage to the permselective layer. The fluorinated layer itself will have different properties than the unfluorinated polysulfone, that is, the layer may be crosslinked resulting in a more rigid structure giving rises in the diffusion of the permeant gases. There may also be an interaction between the molecular oxygen and polar fluorine moieties.

Higher powers and longer plasma treatment times result in increases in the permeant pressure and decrease in oxygen/nitrogen selectivity due to damage of the dense selective layer of the polysulfone asymmetric membrane. The appearance of holes in the skin layer, reinforce the suggestion that more aggressive plasma treatment results in surface damage. The exposed underlying "sponge-like matrix" offers little resistance to the permeation of gases, hence the observed increase in permeant pressure accompanied by a decrease in the permselectivity with long/high power plasma treatments.

In conclusion there appears to be an optimum fluorination depth and composition for CF4 plasma treatment after which, the selective skin layer becomes damaged resulting in increased permeability and a decrease in pemselectivity of oxygen and nitrogen. Using the oxygen/nitrogen selectivity as a gauge to the behaviour of CH_4/CO_2 within a sample, membranes with enhanced gas separation properties will be able to be formed, through optimization of the experimental plasma parameters such as the power and length of treatment.

5. 6 REFERENCES

1.	Pixton, M. R.; Paul, D. R. *J. Polym. Sci. Phys. Ed.*, **1995**, *33*, 1135.

2.	Murganandam, N.; Koros, W. J.; Paul, D. R. *J. Polym. Sci. Phys. Ed.*, **1987**, *25*, **1999**.

3.	Costello, L. M.; Koros, W. J. *J. Polym. Sci. Phys. Ed.*, **1994**, *32*, 701.

4.	Yamamoto, Y.; Mi, Y.; Stern, S. A. *J. Polym. Sci. Phys. Ed.*, **1990**, *28*, 2291.

5.	Staude, E.; Breitbach, L. *J. Appl. Polym. Sci.*, **1991**, *43*, 559.

6.	Soane, D. S. Ed. *"Polymer Applications for Biotechnology"*, Prentice Hall, 1991, Chapter 3.

7.	McHugh, A. J.; Tsay, C. S. *J. Appl. Polym. Sci.*, **1992**, *46*, 2011.

8.	Tsay, C. S.; McHugh, A. J. *J. Polym. Sci. Phys. Ed.*, **1974**, *12*, 1667.

9.	Tsay, C. S.; McHugh, A. J. *J. Polym. Sci. Phys. Ed.*, **1991**, *29*, 1261.

10.	Pinnau, I.; Hellums, M. W., Koros, W. J. *Polymer*, **1991**, *32*, 14, 2612.

11.	Pinnau, I.; Koros, W. J. *J. Polym. Sci. Phys. Ed.*, **1993**, *31*, 419.

12.	Nystrom, N.; Jarveien, P. *J. Memb. Sci.*, **1991**, *60*, 275.

13.	Mohr, J. M.; Paul, D. R.; Pinnau, I.; Koros, W. K. *J. Memb. Sci.*, **1991**, *56*, 77.

14.	Meier, I. K.; Langsam, M.; Cklotz, H. *J. Memb. Sci.*, **1994**, *94*, 195.

15. Lin, X.; Dolveck, Y.; Boiteaux, G.; Escoubes, M.; Monchanin, M.; Dupin, J. P.; Davenas, J. *J. Appl. Polym. Sci.*, **1995**, *55*, 99.

16. Stancell, A. F.; Spencer, A. T. *J. Appl. Polym. Sci.*, **1972**, *16*, 1505.

17. Masouoka, T.; Iwatsubo, T.; Mizoguchi. *J. Appl. Polym., Sci.*, **1992**, *46*, 311.

18. Yasuda, H. *Appl. Polym. Sym.*, **1973**, *22*, 241.

19. Matsuyama, H.; Kanya, A., Teramaoto; M. *J. Appl. Polym. Sci.*, **1994**, *51*, 689.

20. Lin, X.; Chen, J.; Xu, J. *J. Memb. Sci.*, **1994**, *90*, 81.

21. Inagaki, N.; Tasaka, S.; Murata, T. *J. Appl. Polym. Sci.*, **1989**, *38*, 1869.

22. Clarotti, G.; Schue, F.; Sledtz, J.; Geckeler, K. E.; Gopel, W.; Orsetti, A. *J. Memb. Sci.*, **1991**, 61, 289.

23. Wang, Y. J.; Chen, C. H.; Yeh, M.; Suie, G. H.; Yu, B. C. *J. Memb. Sci.*, **1990**, *53*, 275.

24. Westover, L. B.; Tou, J. C.; Mark, J. H. *Anal. Chem.*, **1974**, *46* , 568.

25. Laurenson, L.; Dennis, N. T. M. *J. Vac. Sci. Technol.*, **1985**, *A3* , 1707.

26. Tou, J. C.; Rulf, D. C; DeLassus, P. T. *Anal. Chem.*, **1990**, *62* , 592.

27. Barker, C. P.; Kochem, K. -H.; Revell, K. M.; Kelly, R. S. A.; Badyal, J. P. S. *Thin Solid Films*, **1995**, *259*, 46.

28. Pressure measurement technical information, Vacuum Generators Limited.

29. Crank, J.; Park, G. S. Ed. *"Difusion in Polymers"*, Academic Press, London, 1968, Chapter 1.

30. Beamson, G.; Briggs, D. Eds. *"High Resolution XPS of Organic Polymers: The Scienta ESCA300 Database"*, Wiley, 1992.

31. Mohr, J. M.; Paul, D. R.; Taru, Y.; Mlsna, T. E.; Lagow, R. J *J. Memb. Sci.*, **1991**, *55*, 149.

32. Le Roux, J. D.; Paul, D. R.; Kampa, J.; Lagow, R. J. *J. Memb. Sci.*, **1994**, *90*, 21.

33. Le Roux, J. D.; Paul, D. R.; Kampa, J.; Lagow, R. J. *J. Memb. Sci.*, **1994**, *90*, 121.

34. Le Roux, J. D.; Teplyakov, V.; Paul, D. R. *J. Memb. Sci.*, **1994**, *90*, 55.

35. Henis, J. M. S.; Tripodi, M. K. *J. Memb. Sci.*, **1991**, *8*, 233.

36. Aroantskii, A. E.; Vakar, A. K.; Goluber, A. V.; Kraasheninner, E. G.; Liventsov, V. V.; Macherel, S. O.; Rusanor, V. D.; Fridman, A. A. *High Energy Chemistry*, **1990**, *24*, 223.

37. Yasuda, H. *"Plasma Polymerization"*, Academic Press, 1985.

38. Hellums, M. W.; Koros, W. J.; Husk, G. R.; Paul, D. R. *J. Memb. Sci.*, **1989**, *46*, 93.

39. Koros, W. J.; Fleming, G. K. *J. Memb. Sci.*, **1993**, *83*, 1.

40. Toshima, N. Ed. *"Polymers for Gas Separation"*, VCH Publishers, 1992.

41. Strobel, M.; Corn, S.; Lyons, C. S.; Korba, G. A. *J. Polym. Sci. Chem. Ed.*, **1987**, *25*, 1295.

42. Langotagne, B.; Kuttel, O. M.; Wertheimer, M. R. *Can. J. Phys*, **1991**, *69*, 202.

Chapter Six

CF_4 Plasma Treatment of Methane Plasma Polymer Layers Deposited on Asymmetric Polysulfone Membranes

Chapter Six

CF₄ Plasma Treatment of Methane Plasma Polymer Layers Deposited on Asymmetric Polysulfone Membranes

6.1 INTRODUCTION

Chapter five investigated the effect of CF_4 plasma modification on the permeation properties of an asymmetric polysulfone membrane. This chapter makes use of another area of plasma treatment, plasma polymerization, in order to deposit a methane plasma polymer onto the membrane surface. The surface composition and permeation properties are analysed and the effect of a post CF_4 plasma treatment is also investigated.

6. 1. 1 Background

The utilisation of plasma polymerization for the preparation of permselective membranes is a growing area. The technique enables the deposition of ultra-thin, uniform, pinhole free films[1,2,3,4] with applications in reverse osmosis, ion-exchange and gas separation membranes[5].

Plasma polymerization essentially involves the deposition of an organic (or organometallic) film through the excitation of a monomer by an electrical discharge. The precursor is dissociated and excited in the plasma resulting in the subsequent polymerization and deposition of a film[6,7]. It is a different type of process compared to conventional polymerization and the differences of plasma polymerization can be characterized in several ways. Firstly, for plasma polymerization of a monomer to occur, the monomer does not have to contain a functional group such as a double/triple bond or a cyclic group as with conventional polymerization.

The resultant polymer does not have a discernible repeat unit and is characterized by the plasma parameters rather than the monomer itself[8].

Plasma polymerization is thought to occur by a rapid step growth mechanism, where free radicals are the dominant reactive species. It is a complex process where not only are reactive species formed but the formation of non-reactive species and reaction of the plasma with the substrate can also occur. Figure 1 illustrates some of the reaction pathways which can occur during plasma polymerization[9].

Figure 1: Reaction pathways occurring during plasma polymerization[9].
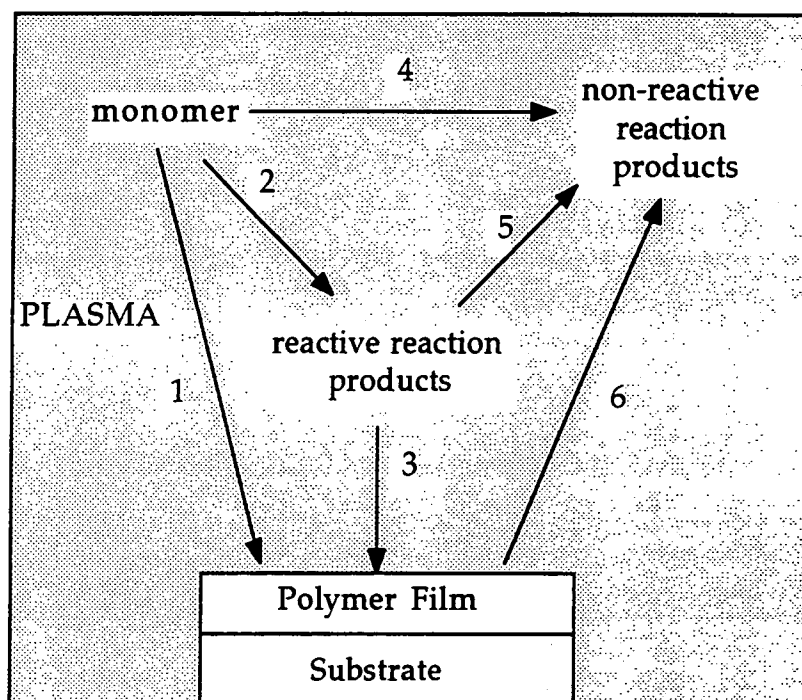
The monomer can polymerize and deposit a film (pathway 1) or be converted into reactive products (2) or form non-reactive products (4). Reactive products can convert to form polymer film (3) or be converted into non-reactive products (5). Alternatively degradation of the polymer film can occur (6). Reaction pathway 1 is known as plasma induced polymerization. Reaction pathways 2 and 3 are plasma polymerization.

The intermediate reactive products can be ions, excited molecules or free radicals.

Gas permeation through plasma polymers does not follow the conventional "solution-diffusion" mechanism as found with polymer films but follows a molecular-sieve type model[2] which is especially noticeable for small gas molecules. The difference in behaviour observed for diffusion in plasma polymers is a consequence of the absence of large scale segmental mobility and the high degree of cross-linking[7]. As a consequence of the nature of the films, plasma polymers can, in theory, make excellent gas separation membranes.

The characteristics of a plasma polymerized membrane depend upon many variables, such as the choice of monomer, substrate and plasma parameters[4,10,11]. Careful choice of the monomer is very important as the plasma polymerized membrane produced is dependent upon the monomer used for the deposition. Halogen containing monomers have shown to be potentially good membranes for gas separation or barrier properties[1], whilst monomer mixtures containing sulfonic groups have been linked to increased ionic conductivity and are therefore useful for areas of electrolytic activity e. g. batteries and ion-exchange membranes[12].

Glow discharge polymerization of methane results in crosslinked, pinhole-free films[13-15]. Methane plasma polymer films are used as barrier coatings in biomedical applications[13]. They also possess excellent adhesion properties, sufficiently good to improve the adhesive bonding of inert surfaces such as PTFE and stainless steel[14] for adhesive bonding. As a result of the compact network of a methane plasma polymer, it is of potential interest in the the field of gas separation[13]. Often a mixture of methane in conjunction with a fluoromonomer can be used to deposit plasma polymer coatings which can improve the gas separation performance of polymer membranes[16]. In this study, rather than taking a fluoromonomer/methane gas mixture, a pure methane plasma polymer is post-treated with a CF_4

169

plasma with a view to enhancing the O_2/N_2 gas separation characteristics of the underlying substrate, since CF_4 glow discharges can be regarded as a source of atomic fluorine which can participate in chemical reactions[17-21]. The CF_4 glow discharge treated methane plasma polymer films have been characterised by XPS, transmission FT-IR, AFM and permeability measurements as a function of glow discharge power.

6. 2 EXPERIMENTAL

Small strips of polysulfone (bisphenol-A-polysulfone, Westlake Plastics Company) were ultrasonically washed in an isopropyl alcohol / hexane mixture for 30 seconds and dried in air. High purity carbon tetrafluoride (99.7%, Air Products) and methane (99.7%, Air Products) gases were used for the various types of plasma treatment. Asymmetric polysulfone membranes were prepared as outlined in section 5.2. All treatments were carried out on the dense skin side of the asymmetric membrane.

The methane glow discharge treatment was carried out following the procedure outlined in section 2. 2. Subsequent CF_4 plasma treatment involved pumping down the vacuum system to base pressure before purging the system with CF_4. The plasma treatment then follows the procedure outlined in section 2. 2. Analysis by XPS and AFM was performed , section 2. 2, on the prepared samples.

FT-IR analysis involved depositing the plasma polymer onto a KBr disc. The plasma treatments were carried out over a longer period of time in order to improve sensitivity, typically 30 min for a methane plasma and 15 min for CF_4 treatment. A Mattson Polaris FTIR spectrometer was employed for analysis, 100 scans were accumulated at a resolution of 4 cm^{-1}.

Permeability experiments were carried out in accordance with section 5. 2. Typical plasma conditions for a permeability sample is a 30 minute CH_4 plasma followed by a 15 minute CF_4 plasma.

6. 3 RESULTS

6. 3. 1 XPS

The XP spectra of the clean untreated polymer was consistent with the parent structure of bisphenol-A-polysulfone (PSF)[22], figure 2(a), as discussed in section 2.2.1.

Plasma polymerization of methane results in the deposition of a hydrocarbon layer onto the polysulfone substrate with trace amounts (less than 2%) of oxygen and nitrogen incorporated into the film due to free radicals reacting with the atmosphere on transferral of the sample to the spectrometer[23,24]. Complete coverage by CH_4 plasma polymer was signified by the absence of any S(2p) signal showing from the polysulfone substrate and the alteration of the C(1s) spectrum to just a $\underline{C}_xH_y$ environment, figure 2(b). No change in the C(1s) envelope was found over the 5-50 W power range. This is not surprising since core level XPS does not detect hydrogen.

CF_4 plasma treatment of the deposited plasma polymer results in a dramatic change of the C(1s) envelope. Fluorinated moieties become the predominant groups with 12.8 ± 3.2 % $\underline{C}F_3$, 31.9 ± 3.1 % $\underline{C}F_2$, 16.9 ± 3 % $\underline{C}F_n$-CF_n, 9.1 ± 0.3 % $\underline{C}F$ and 8.1 ± 0.6 % C-$\underline{C}F_n$ present at the surface[25], figure 2(c). This gives rise to a F:C ratio of 1.08 ± 0.05. Once again no sulfur is observed indicating complete coverage of the substrate.

Variation in the power of the methane plasma (5-50 W), whilst retaining the CF_4 discharge power at 10 W gave rise to no changes in the elemental content at the surface nor the relative distribution of fluorine moieties. Similarly, the CF_4 discharge power was changed (10-50 W) did not

appear to influence the level of fluorination when the power of the methane glow discharge was kept constant at 20 W.

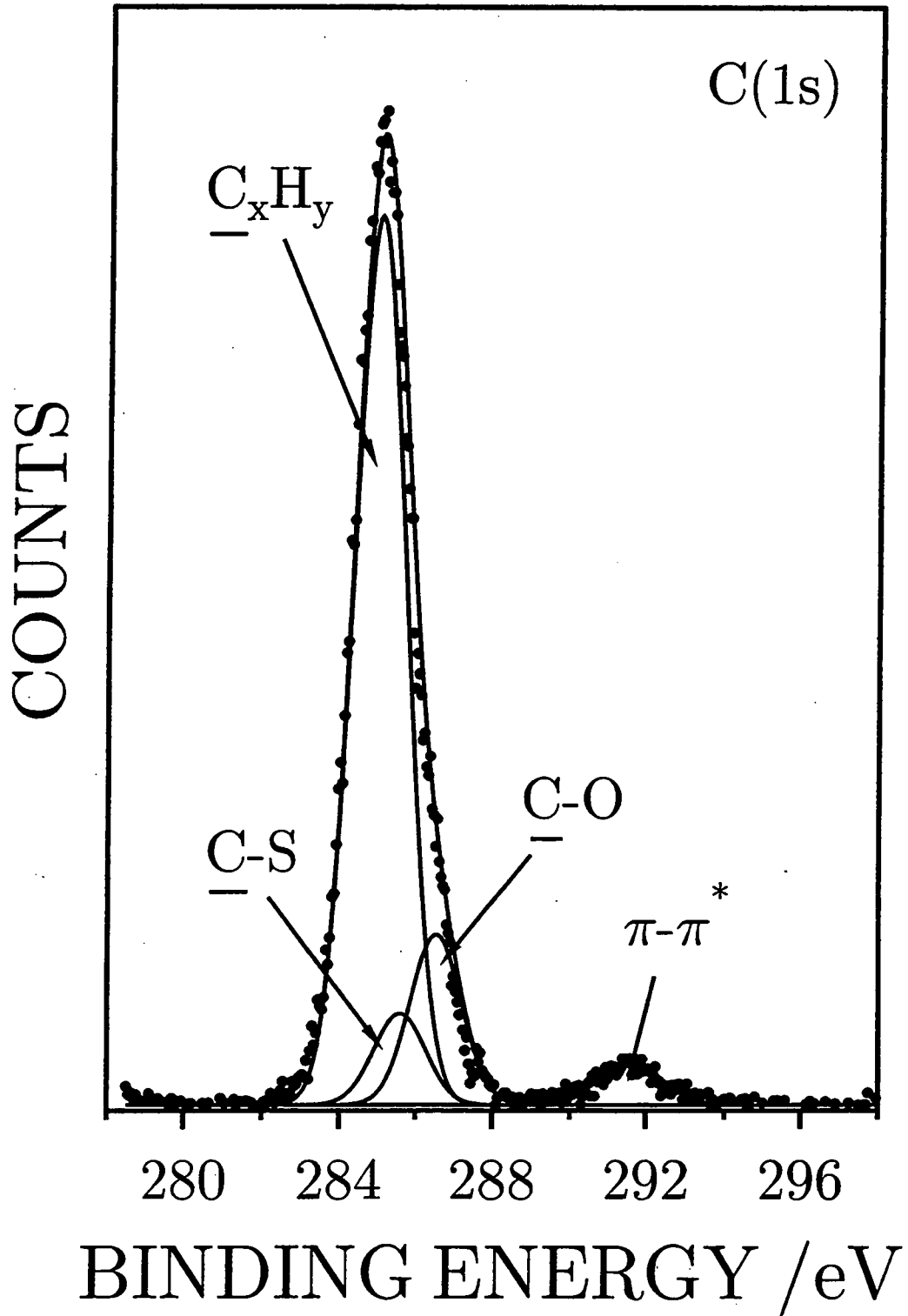Figure 2 (a): C(1s) XP spectra of clean polysulfone.

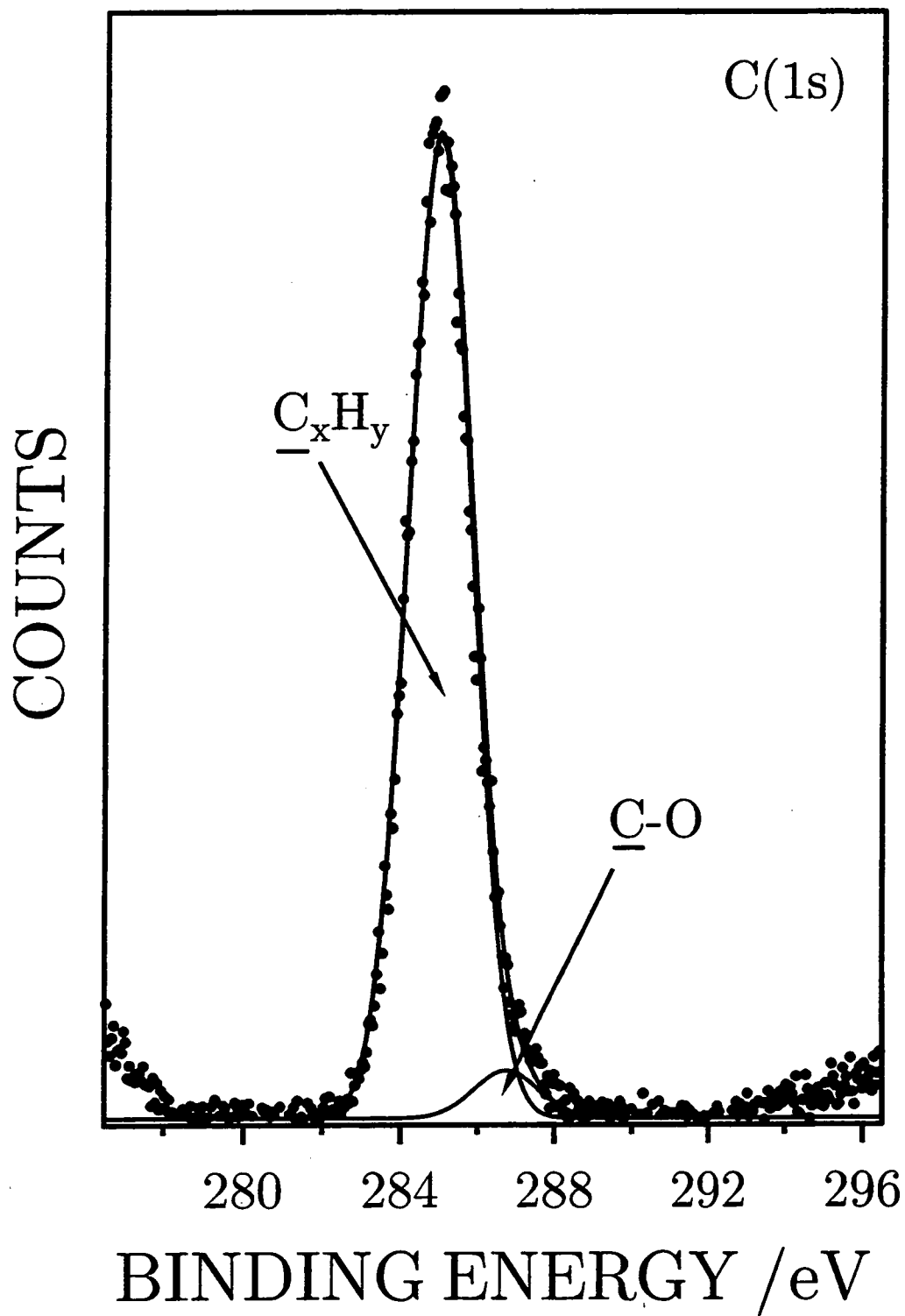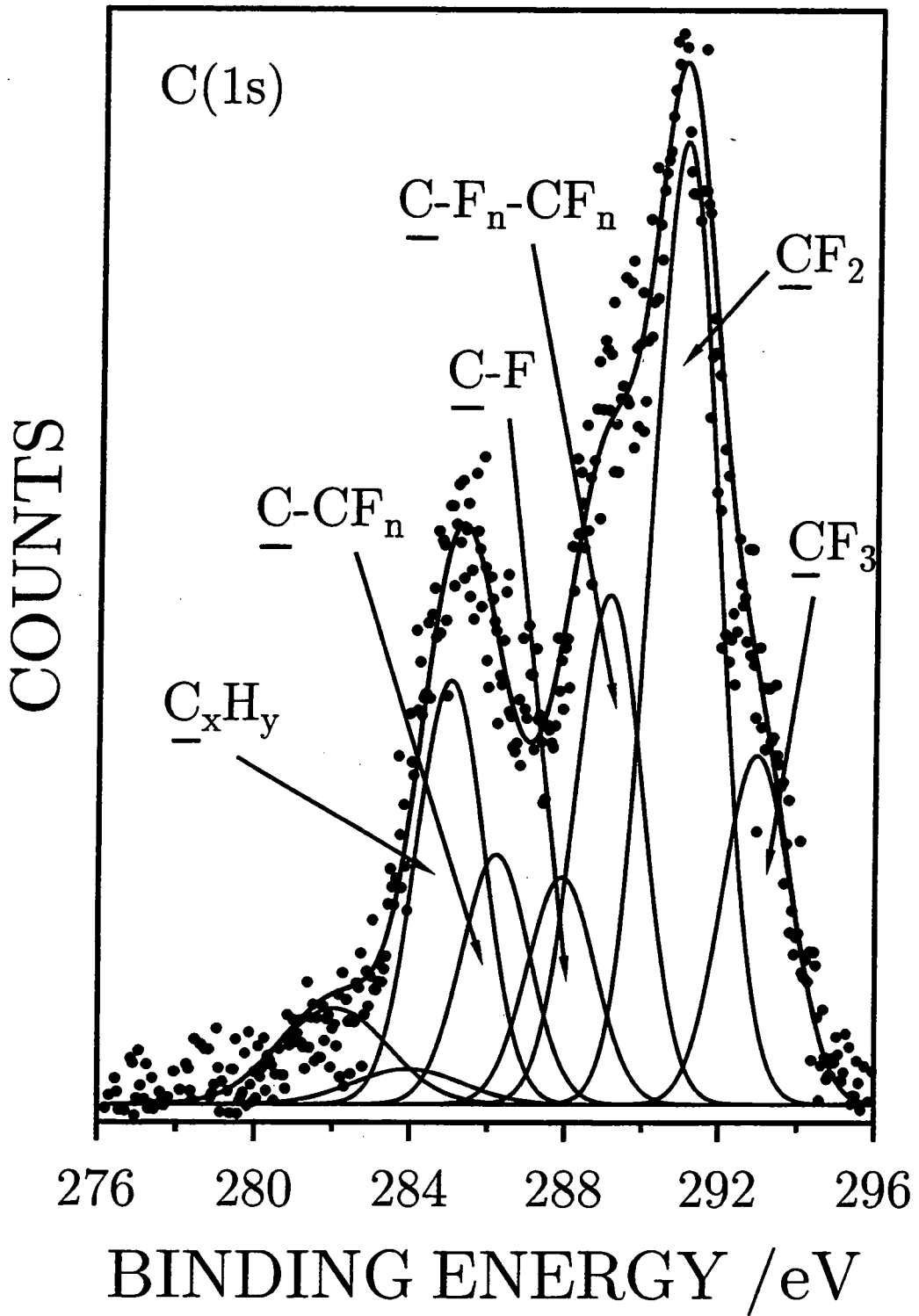Figure 2 (b): C(1s) XP spectra of CH_4 plasma polymer coated polysulfone (5 min, 20 W).

Figure 2 (c): CF$_4$ plasma treatment of 2(b).

6. 3. 2 FTIR

Methane plasma polymerization resulted in the deposition of a hydrocarbon layer. FTIR absorbances occurred at 2950 cm^{-1} (asymmetric CH_3 stretch), 2928 cm^{-1} (CH_2 asymmetric stretch), 2870 cm^{-1} (CH_3 symmetric stretch)[24,26,27,28], a broad peak centred around 1637 cm^{-1}($C=C$), 1460 cm^{-1}(CH_2 wagging or scissoring[29]) and 1377 cm^{-1} (CH_3 symmetric bending), figure 3(a). These infrared absorbances displayed no variation with increasing electrical discharge power (10 - 50 W), similar findings have been reported previously[30]. There was an additional weak absorbance band at 2349 cm^{-1} due to background CO_2 impurities present in the FTIR spectrometer during data aquisition.

CF$_4$ plasma treatment of the hydrocarbon plasma polymer layer produced a slight enhancement of the broad feature in the 1600-1700 cm^{-1} region, which overlaps with the following FTIR absorbances[31]: 1626 cm^{-1} (-CF=C< stretch in a crosslinked environment) and 1730 cm^{-1} (-CF=CF-stretch), figure 3(b). A difference in depth of analysis accounts for the much more dramatic change in the XPS spectra compared to the FTIR data[32]. Clearly, fluorination must only be occurring at the plasma polymer surface.

Figure 3: FTIR spectra of (a) CH$_4$ plasma polymer (30 min, 20 W); (b) CF$_4$ plasma treatment of (a) (15 min, 10 W).

(b) CF$_4$ / CH$_4$

(a) CH$_4$

Wavenumbers / cm^{-1}

500   1000   1500   2000   2500   3000
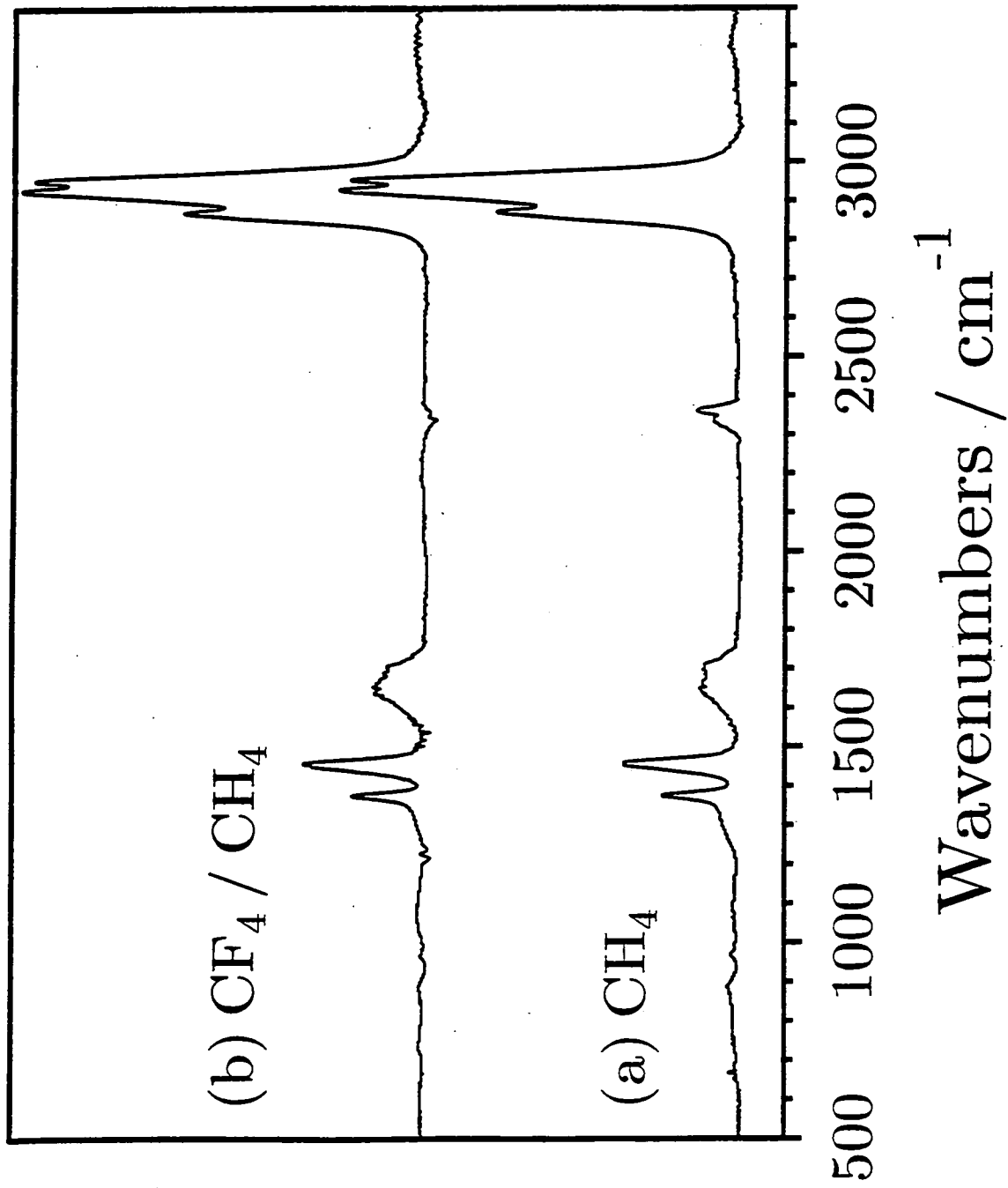
6. 3. 3 AFM

The dense side of an asymmetric polysulfone membrane has a compact structure. The AFM micrograph is shown in chapter five, figure 8a.

Plasma polymerization of methane produced a globular surface texture. An increase in methane glow discharge power causes the particle size to decrease, i.e. become more densely packed, figure 4. There also appears to be more defects at higher powers, figure 5 (a and b)

Post-treatment of the methane plasma polymer with a CF_4 glow discharge resulted in the unveiling of a much better defined globular surface texture which again reflects the decrease in particle size with increasing glow discharge power, illustrated in figure 5(c and d).

Figure 4: Variation of CH_4 plasma polymer particle size with glow discharge power.

Figure 5(a): AFM micrograph of 5 W CH$_4$ plasma polymer layer deposited for 30 min onto the dense side of an asymmetric polysulfone membrane.

x = 0.2 µm / div
z = 200 nm / div

µm

0.2 0.4 0.6 0.8

(a)

179

Figure 5(b): AFM micrograph of 5 W CH$_4$ plasma polymer layer deposited for 30 min onto the dense side of an asymmetric polysulfone membrane followed by a 10 W, 15 minute plasma treatment.

x = 1 µm / div
z = 1 µm / div

µm

1 2 3 4

(b)

Figure 5(c): AFM micrograph of 50 W CH$_4$ plasma polymer layer deposited for 30 min onto the dense side of an asymmetric polysulfone membrane.

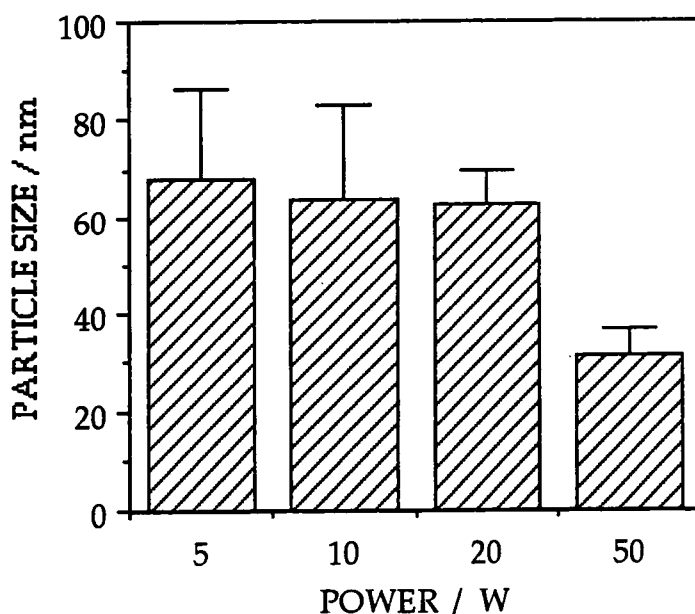x = 0.2 μm / div
z = 200 nm / div
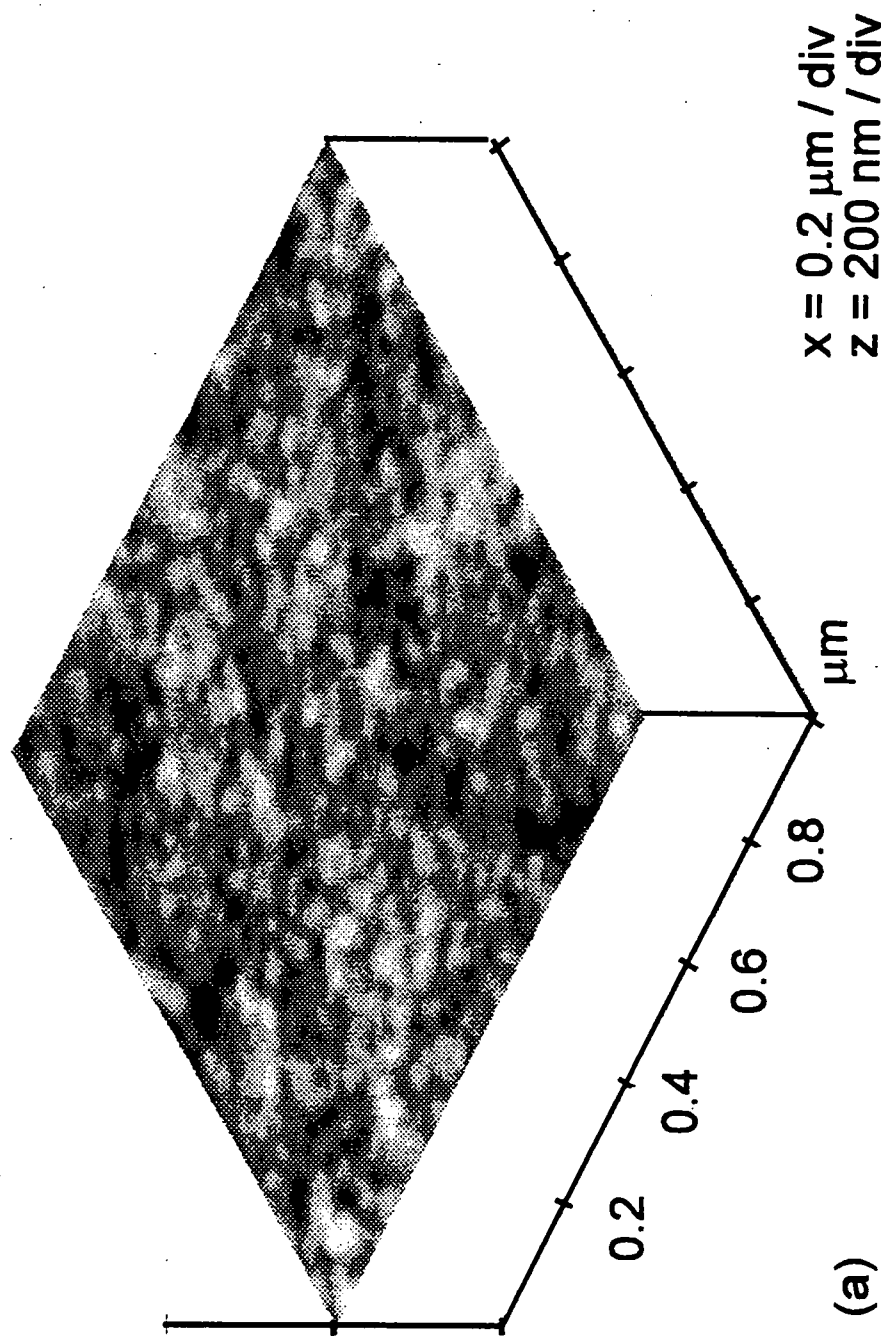
μm

0.2   0.4   0.6   0.8

(c)

181

Figure 5(d): AFM micrograph of 50 W CH₄ plasma polymer layer deposited for 30 min onto the dense side of an asymmetric polysulfone membrane followed by a 10 W, 15 minute plasma treatment.
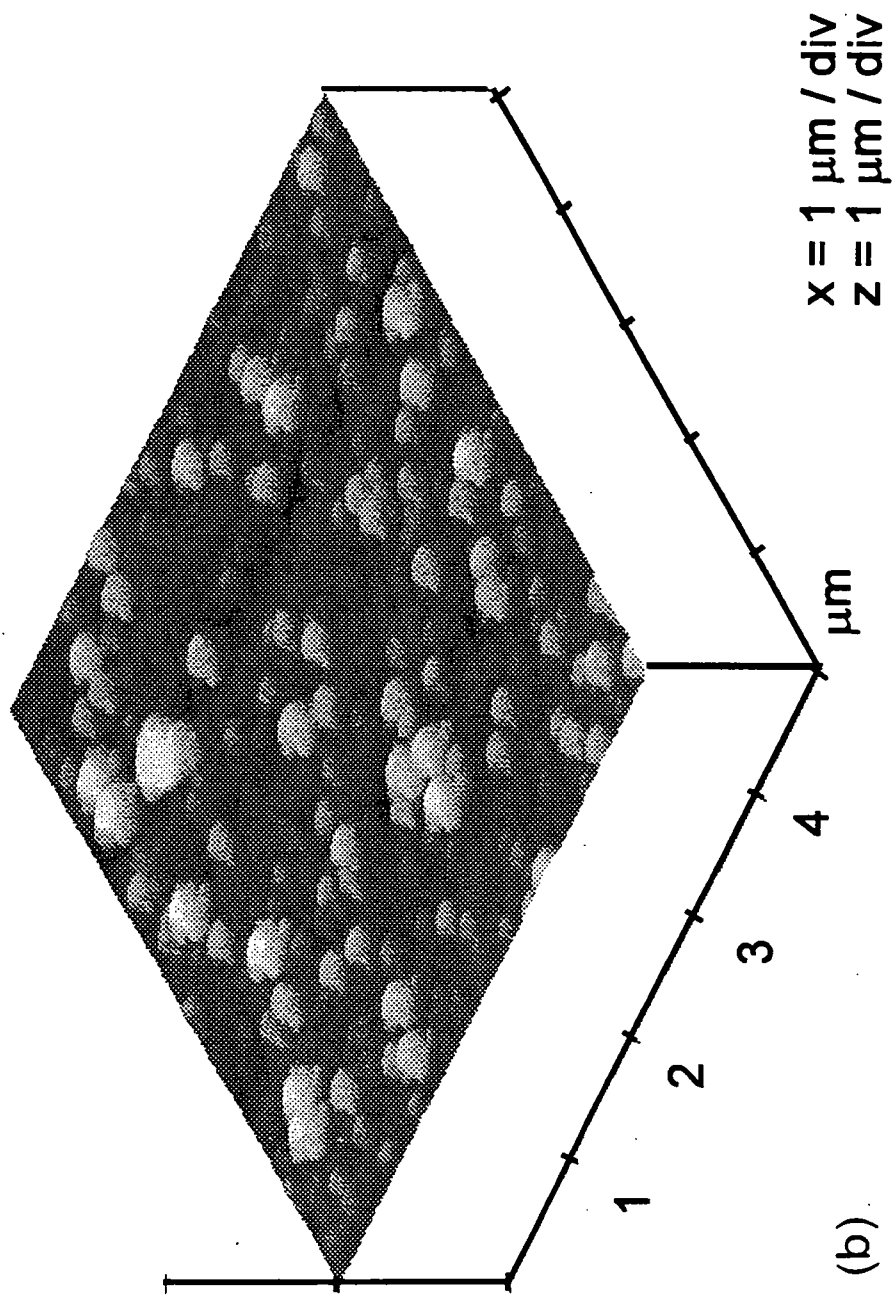
x = 1 μm / div
z = 1 μm / div

(d)

μm

182
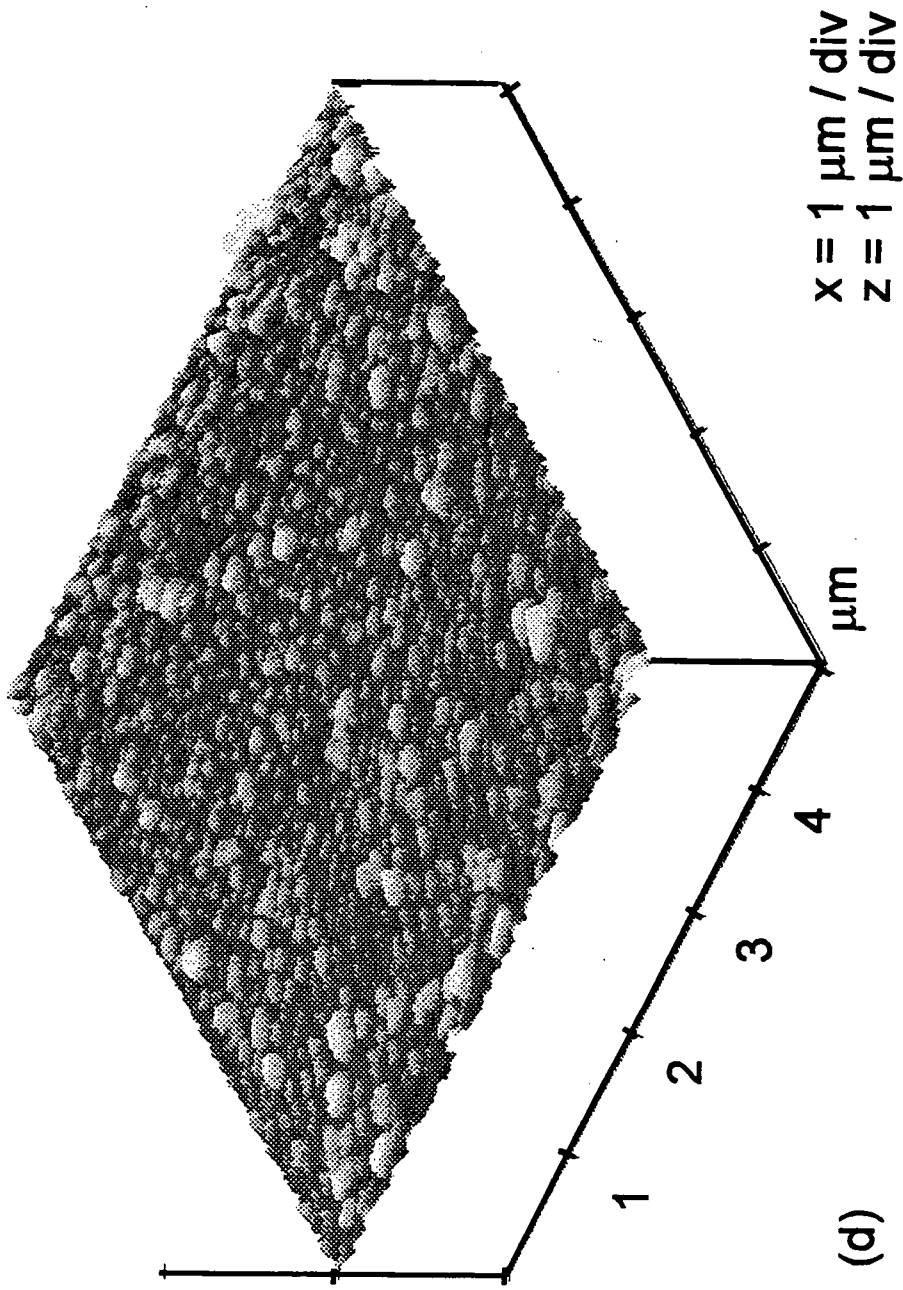
6. 3. 4 Permeability Measurements

An O_2/N_2 permselectivity of 3.09 ± 1.02 was measured for the untreated asymmetric polysulfone membrane. This compares with literature values of 4.7[33]. Both the N_2 and O_2 mean equilibrium permeant partial pressures increase with glow discharge power during CH_4 plasma polymerization onto the dense side of the asymmetric polysulfone membrane, figure 6(a), whilst the O_2/N_2 permselectivity is approximately halved with respect to the untreated substrate, figure 6(b).

CF_4 plasma treatment at 10 W for 15 min of a range of CH_4 plasma polymers deposited onto the dense side of the asymmetric membrane causes a decrease in permeant pressures relative to the untreated asymmetric membrane- and just CF_4 glow discharge modification of the asymmetric membrane, figure 7(a) This is accompanied by a shift in the O_2/N_2 selectivity back towards that of the untreated polysulfone membrane, figure 7(b).

Figure 6(a): Gas Permeation of CH₄ plasma polymer layer deposited for 30 min onto the dense side of an asymmetric polysulfone membrane.

184
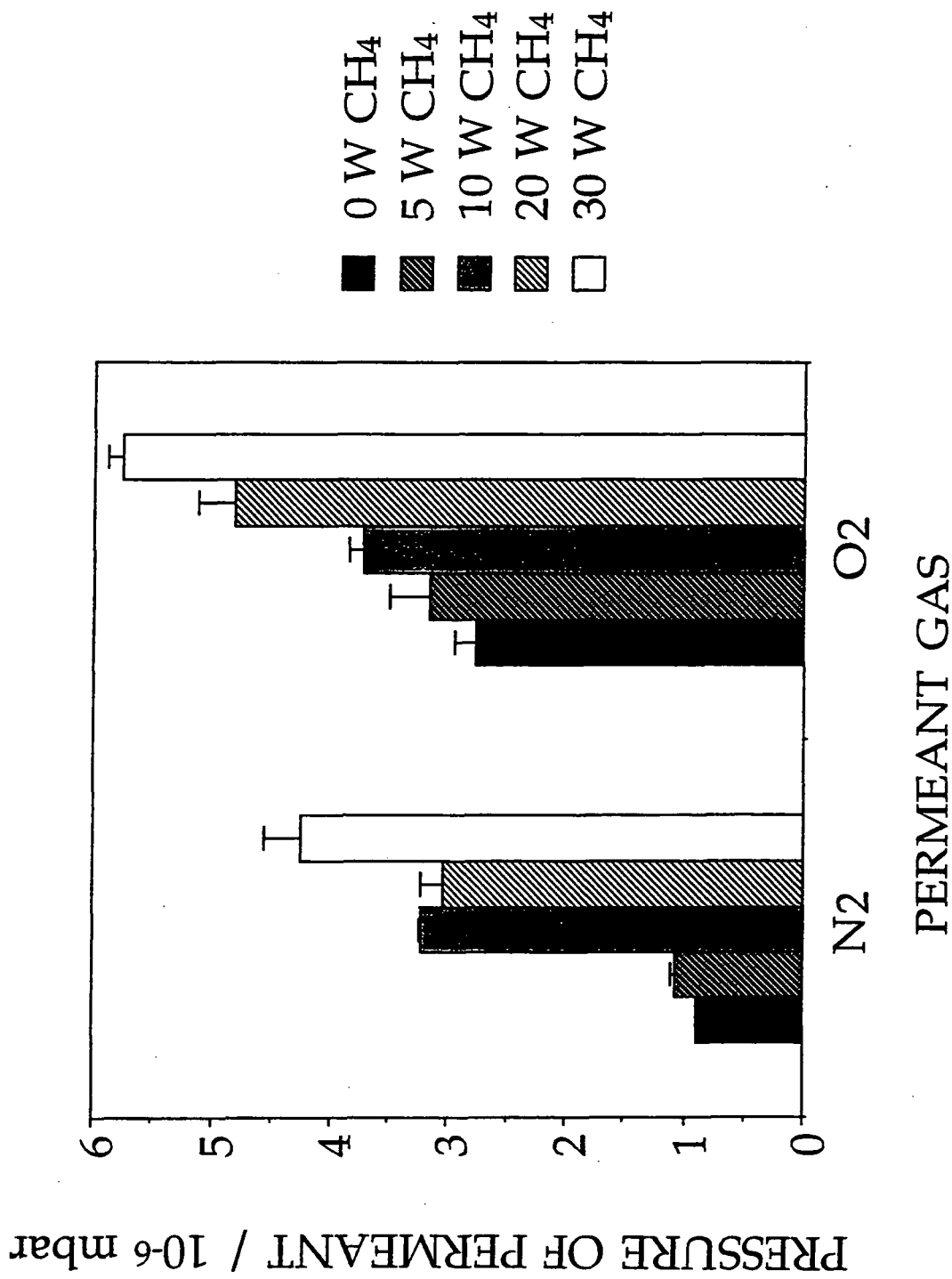
Figure 6(b): N_2/O_2 selectivity of a CH_4 plasma polymer layer deposited for 30 min onto the dense side of an asymmetric polysulfone membrane.
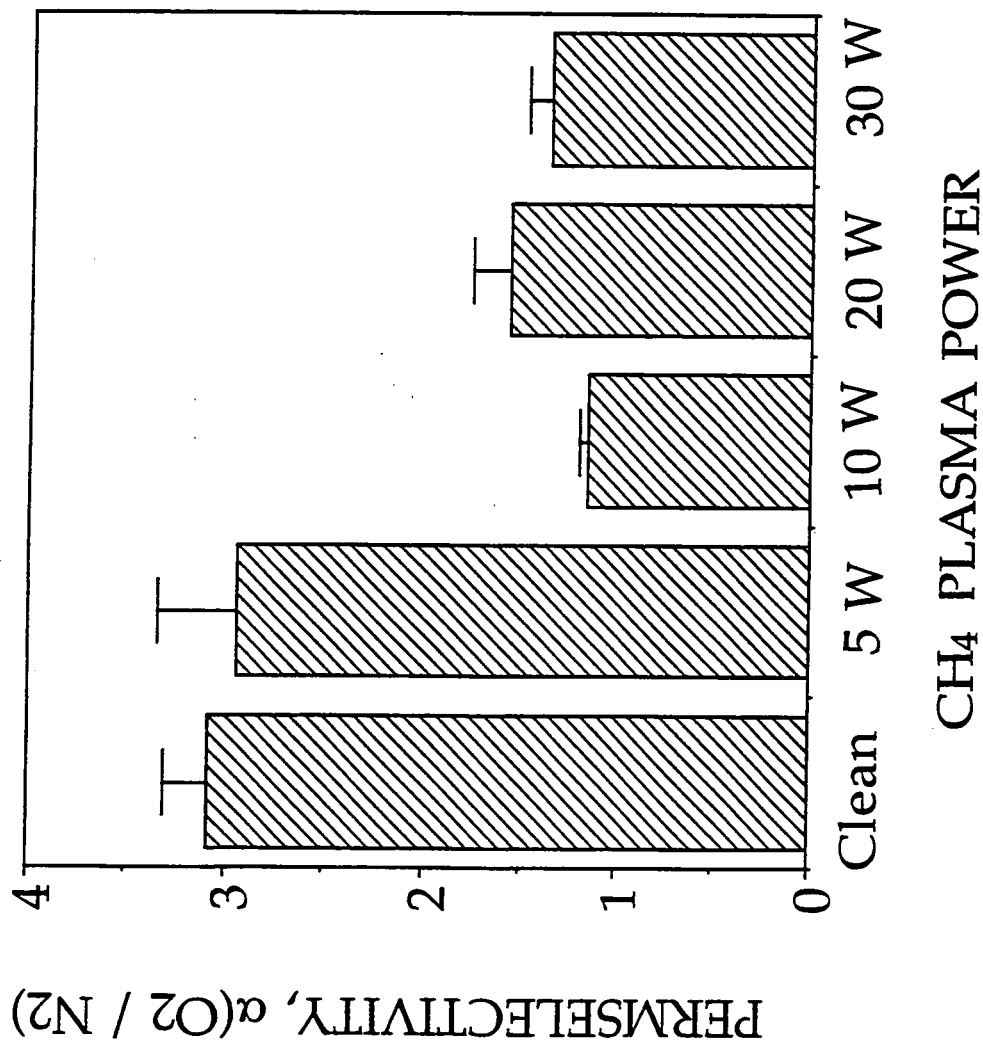
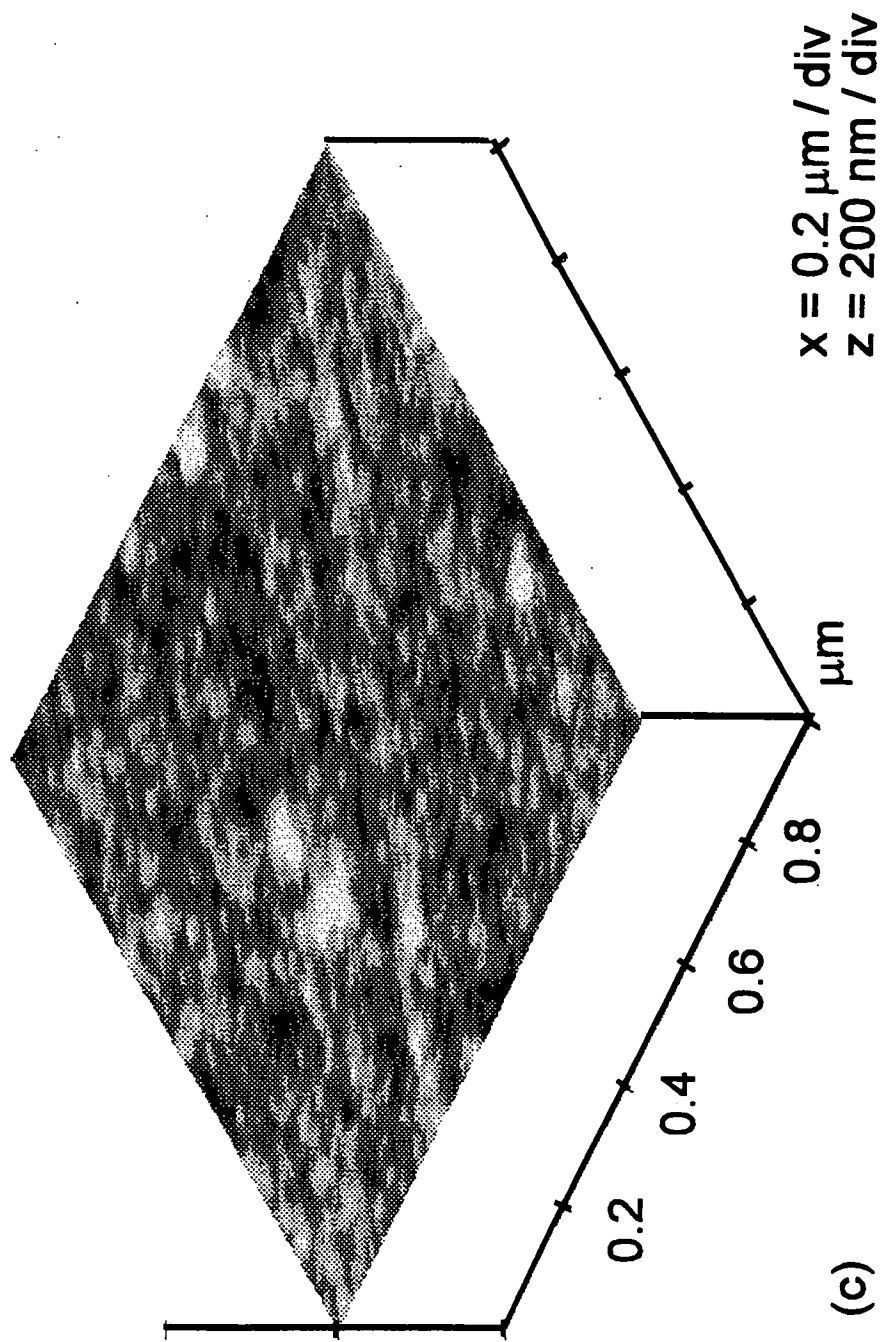Figure 7(a): Gas Permeation of CH$_4$ plasma polymer layer deposited for 30 min onto the dense side of an asymmetric polysulfone membrane which has been post treated with a CF$_4$ plasma for 15 min at 10 W.


186
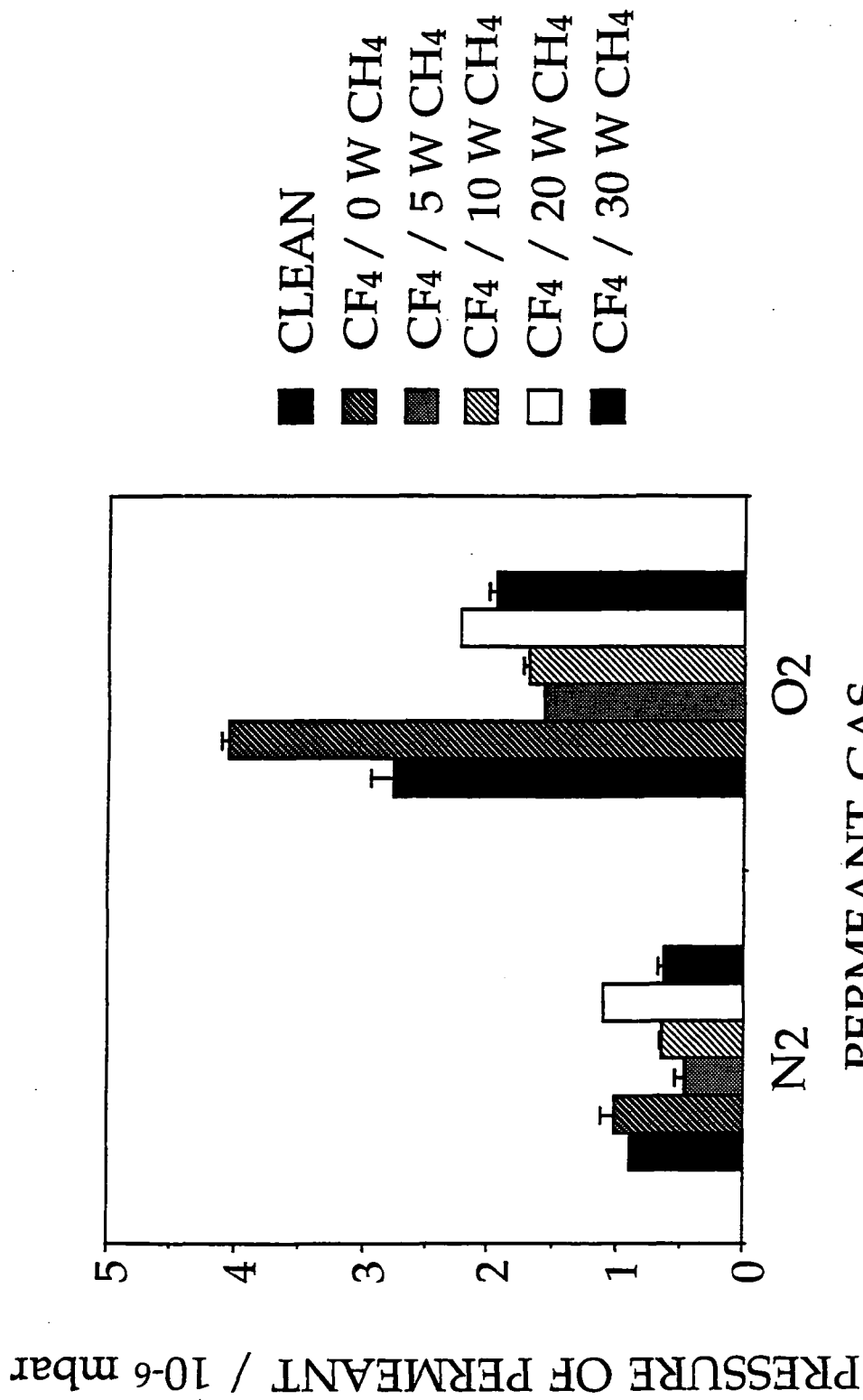
Figure 7(b): O2/N2 selectivity of a CH$_4$ plasma polymer layer deposited for 30 min onto the dense side of an asymmetric polysulfone membrane which has been post treated with a CF$_4$ plasma for 15 min at 10 W.

187
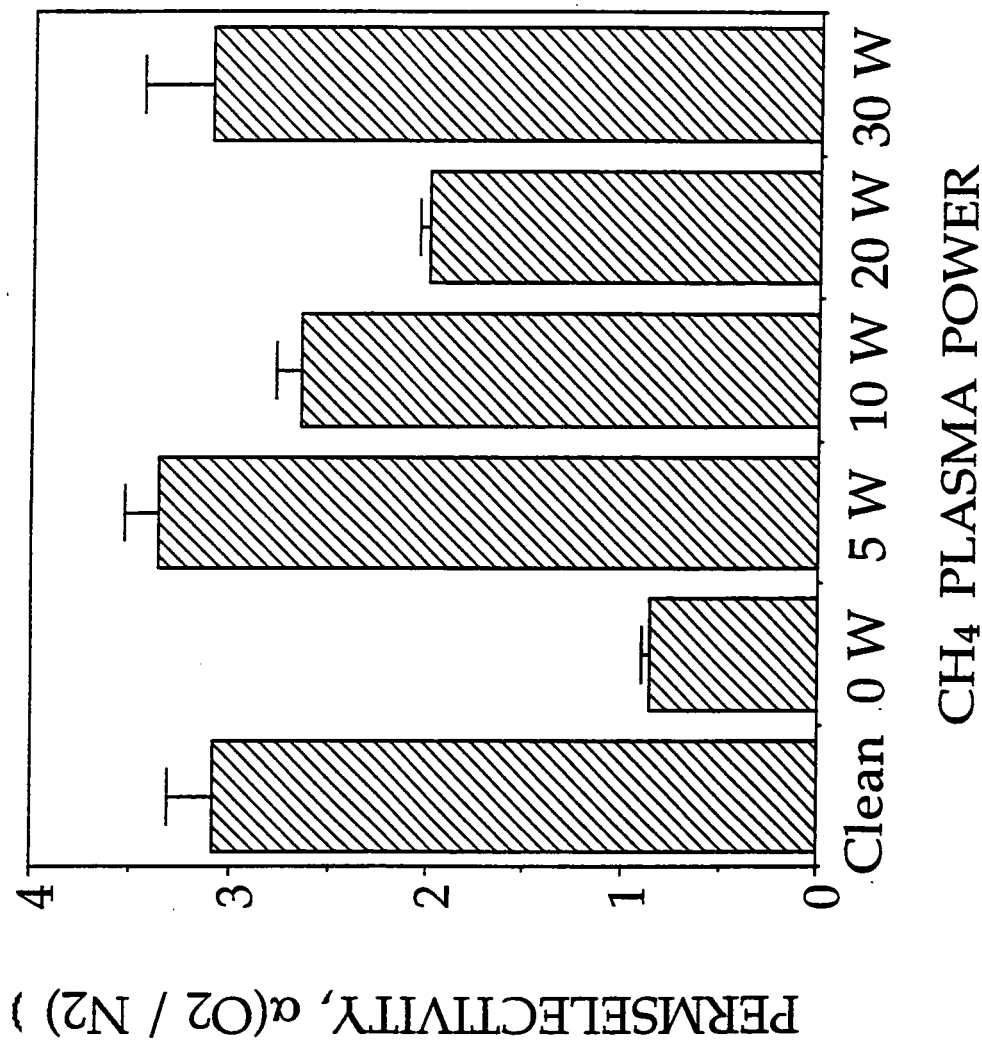
6. 4 DISCUSSION

There are numerous reaction pathways which can occur in a methane plasma to form many reactive intermediates such as CH_3, CH_2, CH and ionic species, however the CH_3 radical is considered to be the dominant deposition species. Figure 8 shows some of the possible reactions can occur in a methane plasma[34,35].

Figure 8: Schematic Diagram of the processes taking place in a CH_4 plasma[35].
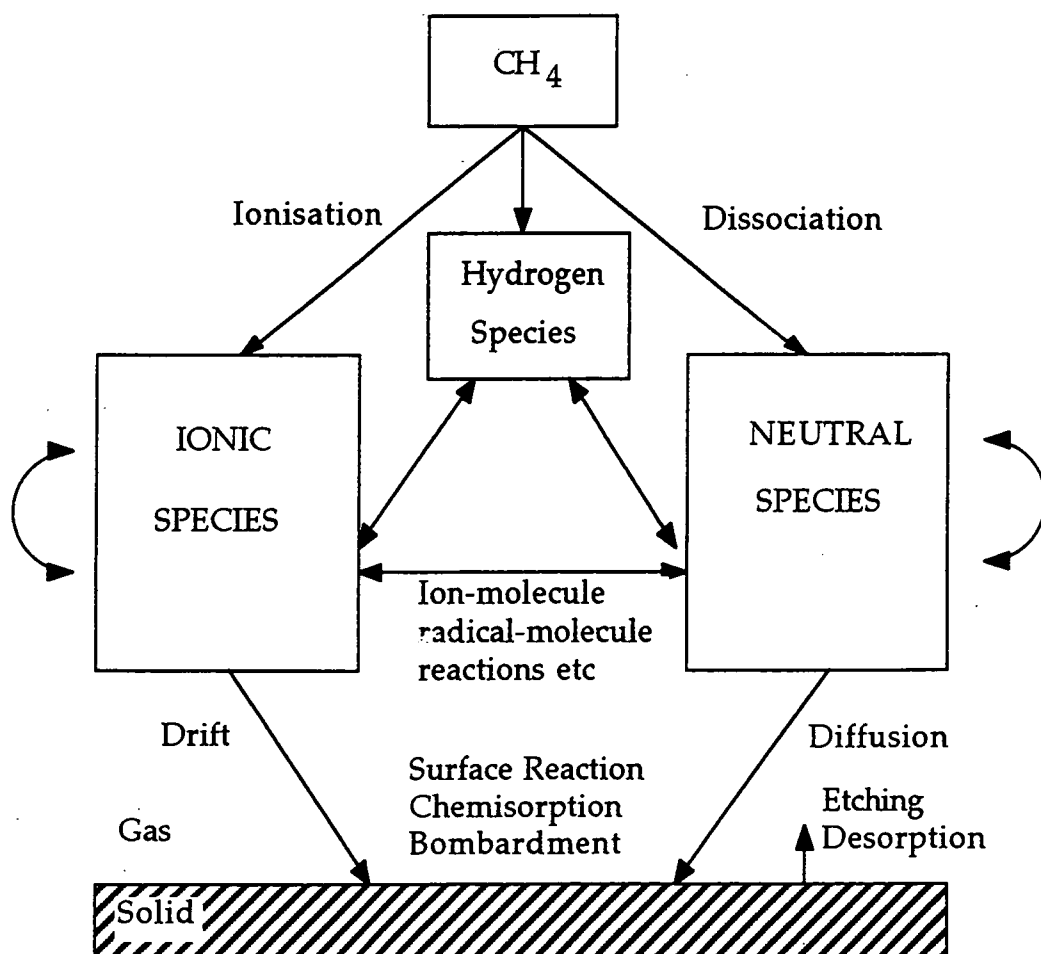
Depending upon the experimental conditions employed, either diamond-like-carbon or polymeric hydrocarbon materials can be

deposited[14,15,36]. The amorphous hydrocarbon films produced in this study were found to readily undergo fluorination by a CF4 glow discharge.

CF$_4$ is considered to be a non-polymerizable gas which does not form plasma polymer material, but instead grafts fluorine moieties to polymeric surfaces[18,19,37]. The most important species in a CF$_4$ plasma is the fluorine atom[38] resulting from the dissociation of the CF$_4$ molecule[39,40], equation 1.

$$CF_4 + e^- \xrightarrow{\hspace{2cm}} CF_3 + F + e^- \qquad (1)$$

The dissociation of CF$_4$ to give CF$_3$ can undergo further dissociation to form CF$_2$ and F. CF$_4$ itself can also dissociate to form CF$_2$ upon initial electron impact[41]. Grafting of fluorine moieties onto polymeric surfaces can be understood in terms of constituent fluorine atoms in the CF$_4$ plasma[38-40] undergoing hydrogen abstraction and substitution reactions at the hydrocarbon plasma polymer surface to produce CF, CF$_2$ and CF$_3$ functionalities[41]. The presence of the CF and tertiary C indicate a highly crosslinked network, whilst CF$_3$ moieties imply the end group of oligomers[36]. The fluorinated layer is fairly thin (< 1 μm) since it is absent during infrared analysis[42]. A C/H of approximately one has been reported in the literature for a methane plasma polymer deposit[24], which is consistent with the XPS F:C ratio found in this chapter if a substitution type mechanism of hydrogen replacement with fluorine is assumed.

The globular features observed at the surface of the methane plasma polymer can be attributed to particle formation during plasma polymerization[7,43-45]. These particles are formed in the gas phase and adsorb onto the polysulfone substrate, where they become embedded in the polymeric species being produced during surface reactions between incident oligomeric species on the substrate surface. Higher glow discharge input power leads to a shift in population of energetic electrons in the tail of the Maxwellian electron energy distribution, thereby providing a more

189

energetic plasma environment which can produce increased electron / ion densities[46]. Glow discharge polymerization of methane at higher powers results in a finer globular structure, which can be correlated to a greater number of potential nucleation centres for plasma polymerization, figure 5 (a and c). The observed change in surface texture of the methane plasma polymer layer after CF_4 plasma treatment can be attributed to the simultaneous fluorination of the embedded particles and etching of the surrounding polymeric layer, giving rise to the better defined globular particles, figures 5 (b and d).

Previous work has shown that plasma polymerization of CF_4 / monomer mixtures can lead to a significant improvement in O_2 and N_2 gas permselectivity and changes in permeability, depending upon the experimental conditions chosen[47,48]. Similar behaviour has been observed in the work carried out in this chapter, where the deposition and modification steps have been carried out consecutively. The increase in gas permeation observed by depositing a hydrocarbon plasma polymer onto an asymmetric polysulfone membrane is contrary to what one may expect, since a methane plasma polymer layer deposited at high glow discharge powers should produce a more cross-linked plasma polymer network, which in turn should further attenuate the gas permeation. The opposite trend is observed, figure 6(a). The observed increase in permeant pressure with CH_4 plasma power can be attributed to either greater intrinsic stress in the growing film, or higher permeant solubility[13]. Intrinsic stress arises from deposited plasma polymer film wedging inbetween existing chain segments[49]. Higher powers will lead to greater crosslinking which in turn causes more intrinsic stress[49] and therefore cracking[49] at the plasma polymer / polysulfone interface. The AFM images show the presence of more defects and irregularities at the surface at higher powers, figure 5(c).

CF_4 glow discharge fluorination of the CH_4 plasma polymer will effectively replace hydrogen atoms by fluorine atoms[17], thereby causing a

change in the polymeric network structure. The introduction of the polar fluorine groups results in stronger cohesive forces between the chains[50], which is manifested by a drop in the gas permeation characteristics of the composite membrane structure. Alternatively, if gas separation occurs by a molecular sieve mechanism (separation by gas size)[16] then greater crosslinking in the subsurface region may lead to restricted motion of the polymer segments which in turn will allow fewer permeants to pass through. Such effects would therefore reduce the diffusion velocity of the gas molecules across the membrane, however reduction in permeability could also be the result of a decrease in the solubility of the permeating gases[47] in the membrane.

6. 5 CONCLUSIONS

Plasma polymerization of CH_4 gas onto an asymmetric polysulfone gas separation membrane results in the deposition of an amorphous hydrocarbon coating which improves the gas permeation characteristics of the substrate but lowers the relative O_2/N_2 permselectivity. Subsequent CF_4 glow discharge treatment of these coatings leads to a drop in gas permeation to below that of the original polysulfone membrane accompanied by a slight enhancement in the O_2/N_2 gas permselectivity.

The changes in the permeability are possibly due to the extent of crosslinking in the plasma polymer at the surface of the polysulfone. The CF_4 treatment of the plasma polymer introduces fluorine moieties which may influence the permeation of gases through the membrane by restricting the available pathways.

Further work optimizing the plasma parameters, time and power, of the consecutive treatment should lead to better gas separation membranes.

6. 6 REFERENCES

1.   Csernica, J.; Prince, M., *Polymer*, **1993**, *34*, 2670.

2.   Eds. Osada, Y.; Nakagawa, T. *"Membrane Science and Technology"*, Marcel Dekker, 1992.

3.   Stancell, F.; Spencer, A. T. *J. Appl. Polym. Sci.*, **1972**, *16*, 1050

4.   Yasuda, H. *Appl. Polym. Symp.*, **1973**, 22, 241.

5.   Yasuda, K.; Uchimoto, Y.; Ogumi, Z.; Tekehara, Z. *J. Electrochem. Soc.*, **1994**, *141*, 2350.

6.   Grill, A. *"Cold Plasmas in Materials Fabrication"*, IEEE Press, 1994.

7.   Yasuda, H. *"Plasma Polymerization"*, Academic Press, 1985.

8.   Flosch, D.; Clarotti, G.; Geckkler, K. E.; Schue, F.; Gopel, W. *J. Memb. Sci.*, **1991**, *61*, 289.

9.   Poll, H. U.; Arritz, M.; Wickleder, K. H. *Eur. Polym. J.*, **1976**, *12*, 505.

10.   Brumlik, C. J.; Parthasarthy, A.; Chen, W. J.; Matrtin, C. R. *J. Electrochem. Soc.*, **1994**, *141*, 2273.

11.   Masukoka, T.; Iwatunbo, T.; Mizoguchi, K. *J. Appl. Polym. Sci.*, **1992**, *311*, 46.

12.   Ogumi, Z.; Ucimoto, Y.; Takehara, Z. *J. Electrochem. Soc.*, **1990**, *137*, 3319.

13.   Ho, C.; Yasuda, H. *J. Appl. Polym. Sci.*, **1990**, *39*, 1541.

14.   N. Inagaki, N.; Yasuda, H. *J. Appl. Polym. Sci.*, **1981**, *26*, 3333.

15.   Yasuda, H.; Sharma, A. A.; Yasuda, T. *J. Polym. Sci. Phys. Ed.*, **1981**, *19*, 1385.

16.   Inagaki. N.; Ohkubo, J. *J. Memb. Sci.*, **1986**, *27*, 63.

17.   Iriyama, Y.; Yasuda, T.; Cho, D. L.; Yasuda, H. *J. Appl. Polym. Sci.*, **1990**, *39*, 249.

18.   d' Agostino, R. Ed. *"Plasma Deposition, Treatment and Etching of Polymers"*, Academic Press, 1990, Chapter 2.

19. d' Agostino, R. Ed. *"Plasma Deposition, Treatment and Etching of Polymers"*, Academic Press, 1990, Chapter 1.

20. Egitto, F.; and L. Matienzo,L. *J. Vac. Sci. Technol.*, **1982**, *A10*, 3060, 1982.

21. Iriyama, Y.; Yasuda, H. *J. Polym. Sci. Chem. Ed.*, **1992**, *30*, 1731.

22. Beamson, G.; Briggs, D. *"High Resolution XPS of Organic Polymers: The Scienta ESCA300 Database"*, Wiley, 1992.

23. Inagaki, N.; Kawai, H. *J.Polym. Sci. Chem. Ed.*, **1986**, *24*, 3381.

24. Sharma, A. K.; Yasuda, H. *J. Appl. Polym. Sci.*, **1989**, *38*, 741.

25. Wells, R. K.; Ryan, M. E.; Badyal, J. P. S. *J. Phys. Chem*, **1993**, *97*, 12879.

26. Coltup, N. B.; Daly, L. H. Wilberley *"Introduction to Infra-Red and Raman Spectroscopy"*, Academic Press, 1990.

27. Silverstein, R. M.; Clayton Bassler, G.; Morrill, T. C. *"Spectrometric Identification of Organic Compunds"*, Wiley, 1991, Chapter 3.

28. Shimada, Y.; Mutsukura, N.; Machi,Y. *J. Appl. Phys*, **1992**, *71*, 4019

29. Shinohara, H.; Iwasaki, M.; Tsuyimara, S.; Wantanabe, K.; Okazaki, S. J. *Polym. Sci.*, **1072**, A1, *10*, 2129.

30. El Hossary, F. M., Fabian, D. F.; Webb, A. P. *Thin Solid Films*, **1990**, *192*, 201.

31. Ryan, M. E.; Fonesca, J. L. C.; Tasker, S.; Badyal, J. P. S. *J. Phys. Chem.*, **1995**, *99*, 7060.

32. Walls, J. M. *"Methods of Surface Anaysis"*, Cambridge University Press, 1989.

33. Fritzche, A. K.; Murphy, M.; Cruse, C. A,; Malon, R. F.; Kesting, R. E, *Gas Sep. Purif.*, **1989**, *3*, 106.

34. Tachibana, K.; Harima, H.; Wano, Y. *J. Phys D: Appl. Phys.*, **1984**, *17*, 1727.

35. Kline, L. E.; Partlow, W. D.; Beis, W. E. *J. Appl. Phys.*, **1985**, *65*, 70.

36. J. Wang, J.; Feing, D.; Wang, H.; Rembold, M.; Thommen, F. *J. Appl. Polym. Sci.*, **1993**, *50*, 585.

37. Cramarossos, F.; DeBenedictus, S. *Plasma Chem. Plasma Process.*, **1982**, *2*, 213.

38. Strobel, M.; Corn, S.; Lyons, C. S.; Korba, G. A. *J. Polym. Sci. Chem. Ed.*, **1985**, *23*, 1125.

39. Kay, E. Proc. Int Ion Congress ISIAT&IPAT, 1983.

40. Winters, H. F.; Inokuti, M.; *Physical Review*, **1982**, *25*, 3, 1420.

41. Plumb, I. C.; Ryan, K. R. *Plasma Chem. Plasma Process.*, **1986**, *6*, 3, 205.

42. Banwell, C. N. *"Fundamentals of Molecular Spectroscopy "*, 3rd Ed., McGraw Hill Book Company, 1983.

43. Grebowicz, J.; Pakula, T.; Wrobel, A. M.; Kryszewski, M. *Thin Solid Films*, **1980**, *65*, 351.

44. Li, G.; Tobin, J. A.; Denton, D. D. *Appl. Phys. Lett.*, **1994**, *64*, 560.

45. Kobayashi, H.; Bell, A. T.; Shen, M. *J. Appl. Polym. Sci.*, **1973**, *17*, 885.

46. Ferreira, C. M.; Loureiro, J. *J. Phys. D.*, **1984**, *17*, 1175.

47. Inagaki, N.; Tasaka, S.; Park, M. S. *J. Appl. Polym. Sci.*, **1990**, *40*, 143.

48. Inagaki, N.; Kobayashi, N.; Matsusima, M. *J. Membr. Sci.*, **1988**, *38*, 85.

49. Morinaka, A.; Asano, Y. *J. Appl. Polym. Sci*, **1982**, *27*, 2139.

50. Kesting, R. E. *"Synthetic Polymeric Membranes: A Structural Perspective"*, 2nd Ed., Wiley, 1985.

Chapter Seven

Conclusions

Chapter Seven

Conclusions

7. 1 INTRODUCTION

The performance of a gas separation membrane is dependent upon both chemical and physical properties. The dense skin layer of an asymmetric membrane is considered to be the region responsible for the permeability and permselectivity properties. Plasmas can be used to enhance the physicochemical nature of the surface and are therefore an ideal method of altering the permselectivity of a membrane.

7. 2 SUMMARY OF CONCLUSIONS

This thesis has investigated some fundamental plasma-polymer interactions, the results have then subsequently been used in the application of the plasma treatment of polysulfone gas separation membranes.

The treatment of dense polysulfone film by different gas plasma treatments was studied. The change in both the physical and chemical structure at the surface was dramatic. The inert gas plasmas resulted in the most pronounced topographical changes whilst tetrafluoromethane plasma treatment resulted in significant chemical changes. This work not only highlighted that different chemical species in a plasma result in different chemical surface structures but that the electromagnetic radiation component within a plasma may also contribute to some of the modification observed. Further work investigated this aspect and it was indeed found that the vacuum ultraviolet radiation does play a role in surface modification and that the modification is gas dependent.

Fluorination of several polymeric membranes has been shown to successfully enhance the separation of certain gas pairs[1,2]. In a plasma an inert CF_4 molecule is dissociated and can be considered to be a source of F atoms. Fluorination of a polymer surface using a plasma offers an efficient, "clean" alternative technique to conventional fluorination. Fluorination of a polysulfone membrane by a CF_4 plasma results in an increase in permeant pressure with little enhancement in oxygen/nitrogen selectivity except at very short treatment times and low powers. Such improvements in the membrane performance can be attributed to a number of factors. CF_4 plasmas can result in crosslinking at the surface skin layer which in turn will have an effect on the transport of permeating gases. Interaction between the permeant gas and surface chemical structure may also play a role in the transport properties. With more aggressive plasma treatment, etching or ablation of the membrane surface occurs resulting in destruction of the delicate skin layer of the asymmetric membrane which is manifested by a decrease in selectivity and an increase in the permeability. Changes in the membrane surface topography were observed whilst the surface chemical structure remained constant suggesting that the physical changes are responsible for the differences in gas transport properties. This illustrates the different effects of a plasma and the importance of both chemical and structural changes on a polymeric membrane and its relationship between permeability and permselectivity.

An alternative method of modification of a membrane surface is to deposit a polymer layer. The formation of the composite membrane will change the gas transport properties by blocking pores in the surface. A composite structure was achieved by depositing a methane plasma polymer onto the asymmetric polysulfone membrane, figure 1. The oxygen/nitrogen selectivity was not significantly enhanced.

Figure 1: Plasma treatment of membranes.
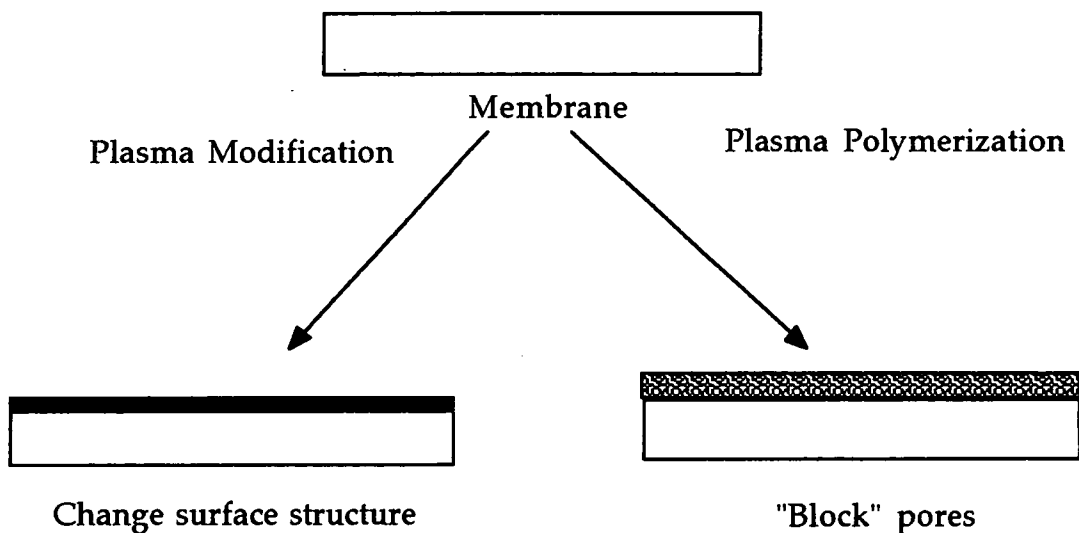
Ideally a single step process would be utilised in the modification of a membrane, however the two approaches described above did not achieve the enhancement in transport properties aimed for. The two approaches were combined resulting in the deposition of a methane plasma polymer which was subsequently fluorinated. This combination resulted in a slight improvement of the oxygen/nitrogen selectivity accompanied by a decrease in permeant pressure. This may be due to the positive effects of the methane plasma polymer plugging pores and defects in the skin layer and the fluorinated layer interacting with oxygen, enhancing its gas transport over nitrogen.

One of the major problems in dealing with asymmetric membranes is the difficulty in their formation. The production of the membrane involves numerous parameters making reproducibility even from the same casting solution difficult. However with the continuing research into the refinement of the phase-inversion casting technique[3], the formation of reproducible asymmetric membranes should be more readily obtainable.

Plasma treatment of membranes as a technique for the modification of membranes to improve the gas separation properties is a viable method.

With optimization of the plasma parameters, such as duration of treatment time and power level, the maximum gas selectivity of a particular membrane should be obtained. Coupled with the on-going "tuning" of membrane preparation, the target of achieving the ideal membrane is becoming closer.

7. 3 FUTURE WORK

7. 3. 1 Optimization of Plasma Parameters

The plasma parameters varied in this thesis were length of treatment time and the power, optimization of these parameters needs to be obtained, possibly using a chemometric approach for the production of the best membrane. The effect of pressure which the plasma is operated at is another variable which needs to be taken into account since this parameter will alter the characteristics of the plasma, for example the plasma density, which in turn will change the chemical and topographical features of the treated surface.

7. 3. 2 Plasma Feed Gas

Chapter two found that different feed gases used for the plasma had a dramatic effect upon the surface of the sample. The membranes investigated have been treated with CF_4 and CH_4 plasmas, however there is almost an unlimited number of different plasmas that can be used. One example to be considered would be inert gas plasma treatment of a membrane. Inert gas plasma treatment of polysulfone film resulted in dramatic topographical changes. Changes in the surface topography accompanied by any chemical changes could be exploited for the enhancement of asymmetric membrane performance.

7. 3. 3 Vacuum Ultraviolet Treatment

Results from chapter four indicated that the vacuum ultraviolet component within a plasma results in modification. This technique offers a less harsh modification environment when compared to the equivalent plasma treatment. The treatment of membranes by this method would predominantly offer to change the membrane performance by the physical structure.

7. 3. 4 Pulsed Plasmas

Pulsed plasmas are of growing interest because it enables the control of the rate of which radicals are generated and sufficient time for the radicals to react in the "off" cycle[4]. Such control would enable only specific functional groups to be deposited in plasma polymerization, in other words tailoring of the sample surface. This would be of great interest in the area of gas separation membranes since groups which interact specifically with particular permeating gases could be deposited. Pulsed plasmas also offer the advantage of less damage to the membrane upon treatment.

7. 4 REFERENCES

1. Mohr, J. M.; Paul., D. R.; Pinnau, I.; Koros, W. K. *J. Memb. Sci.*, **1991**, *56*, 77.

2. Le Roux, J. D.; Paul, D. R.; Kampa, J.; Lagow, R. J. *J. Memb. Sci.*, **1994**, *90*, 21.

3. Shilton, S. J.; Bell, G.; Ferguson, J. *Polymer*, **1994**, 35, 5327.

4. Hwa, W.; Zurawsky, W. P. *J. Polym. Sci. Chem. Ed.*, **1992**, *30*, 409.

Appendix

Courses, Seminars and Conferences Attended

University of Durham

Board of Studies in Chemistry

EXAMINED LECTURE COURSES

October to December 1992   General Laboratory Techniques

(Dr. Hampshire)

Spectroscopies (Dr. Halliday)

Electron Microscopy (Dr. Durose)

November to December 1992   Structure and Bonding in Solid

(Prof. Howard)

COLLOQUIA, LECTURES AND SEMINARS FROM INVITED SPEAKERS

1992

October 20   Dr. H. E. Bryndza, Du Pont Central Research

Synthesis, Reactions and Thermochemistry of Metal

(Alkyl) Cyanide Complexes and Their Impact on Olefin

Hydrocyanation Catalysis.

October 22   *The Ingold-Albert Lecture*

Prof. A. Davies, University College London

The Behaviour of Hydrogen as a Pseudometal.

October 28   Dr. J. K . Cockcroft, University of Durham

Recent Developments in Powder Diffraction.

November 5   Dr. C. J. Ludman, University of Durham
                    Explosions, A Demonstration Lecture.

November 18   Dr. R. Nix, Queen Mary College, London
                    Characterization of Heterogeneous Catalysts.

December 9   Dr. A. N. Burgess, ICI Runcorn
                    The Structure of Perfluorinated Ionomer Membranes.

1993

January 20   Dr. D. C. Clary, University of Cambridge
                    Energy Flow in Chemical Reactions.

March 3   Dr. K. J. P. Williams, B. P.
                    Raman Spectroscopy for Industrial Analysis.

May 13   *The Boys-Rahman Lecture*
                    Prof. J. A. Pople, Carnegie-Mellon University,
                    Pittsburgh, USA
                    Applications of Molecular Orbital Theory.

October 4   Prof. F. J. Feher, University of California, Irvine, USA
                    Chemistry in Solution versus Catalysis on Surfaces -
                    How Do We Bridge the Gap?

October 27   Dr. R. A. L. Jones, Cavendish Laboratory, Cambridge
                    Perambulating Polymers.

November 10   Prof. M. N. R. Ashfold, University of Bristol

High Resolution Photofragment Translational

Spectroscopy : A New Way to Watch Photodissociation.

November 17   Dr. A. Parker, Rutherford Appleton Laboratory, Didcot

Applications of Time Resolved Resonance Raman

Spectroscopy to Chemical and Biochemical Problems.

1994

January 26   Prof. J. Evans, University of Southampton

Shining Light on Catalysts.

February 2   Dr. A. Masters, University of Manchester

Modelling Water Without Using Pair Potentials.

February 16   Prof. K. H. Theopold, University of Delaware, USA

Paramagnetic Chromium Alkyls : Synthesis and

Reactivity.

February 23   Prof. P. M. Maitlis, University of Sheffield

Across the Border : From Homogeneous to

Heterogeneous Catalysis.

October 19   Prof. N. Bartlett, University of California

Some Aspects of Ag(II) and Ag(III) Chemistry.

November 16   Prof. M. I. Page, University of Huddersfield

Four Membered Rings and β-Lactamase.

November 23   Dr. J. Williams, University of Loughborough
                   New Approaches to Asymmetric Catalysis.

December 7   Prof. D. Briggs, ICI Wilton and University of Durham
                   Surface Mass Spectrometry.

1995

January 18   Dr. G. Rumbles, Imperial College, London
                   Real or Imaginary 3rd Order Non-Linear Optical
                   Materials.

February 1   Dr. T. Cosgrove, Bristol University
                   Polymers do it at Interfaces.

March 1   Dr. M. Rosseinsky, Oxford University
                   Fullerene Intercalation Chemistry.

April 26   Dr. M. Schroder, University of Edinburgh
                   Redox Active Macrocyclic Complexes: Rings, Stacks and
                   Liquid Crystals.

CONFERENCES ATTENDED

August 22 - 27 1993   11th International Symposium on Plasma Chemistry,
Loughborough University, England.

August 20 - 25 1995   12th International Symposium on Plasma Chemistry,
University of Minnesota, USA.